Pairs of geometric foliations of regular and singular surfaces

Joseph Michael Oliver

A Thesis presented for the degree of
Doctor of Philosophy

Pure Mathematics Research Group
Department of Mathematical Sciences
University of Durham
England

February 2010.

Pairs of geometric foliations of regular and singular surfaces

Joseph Michael Oliver

Submitted for the degree of Doctor of Philosophy
February 2010

Abstract

We examine some generic features of surfaces in the Euclidean 3-space $\mathbb{R}^3$ related to the Gauss map on the surface. We consider these features on smooth surfaces and on singular surfaces with a cross-cap singularity.

We study some symmetries between two classical pairs of foliations defined on smooth surfaces in $\mathbb{R}^3$: the asymptotic curves and the characteristic curves (called harmonic mean curvature lines in [41]). The asymptotic curves exist in hyperbolic regions of surfaces and have been well studied. The characteristic curves are in certain ways the analogy of the asymptotic curves in elliptic regions. In this thesis we extend this analogy. . We use We produce results on the characteristic curves mirroring those of Uribe-Vargas ([71]) on the asymptotic curves. By considering cross-ratios of Legendrian lines in the manifold of contact elements to the surface we show that certain properties of the characteristic curves are invariant under projective transformations, and examine their behaviour at cusps of Gauss.

We establish an analogy of the Beltrami-Enepper Theorem, which allows us to distinguish between the two characteristic foliations in a natural geometric way. We show that the local properties of characteristic curves may be used to prove certain global results concerning the elliptic regions of smooth surfaces.

Motivated by the study of the asymptotic, principal and characteristic curves on surfaces in $\mathbb{R}^3$, we construct a natural one-to-one correspondence between the set of non-degenerate binary differential equations (BDEs) and linear involutions on the real projective line. We show that one may construct pairs of BDEs that have

various symmetric properties using a single involution on $\mathbb{R}P^1$. We study the folded singularities of BDEs, and associate an affine invariant to such points. We show that one may associate a complex parameter to folded singularities that determines the relative positions of various curves of interest.

We show that the BDEs asymptotic, characteristic, and principal curves are related to other quadratic forms on surfaces. These include the BDE that defines the lines of arithmetic mean curvature which are studied in [39], and the third fundamental form of the surface. We define a new pair of foliations of a surface which we label the minimal orthogonal spherical image (MOSI) curves which are the integral curves of those tangent directions to a surface that have orthogonal images under the Gauss map, and are inclined at an extremal angle. We establish the configurations of the MOSI curves in a neighbourhood of umbilic points, parabolic points and cusps of Gauss.

We construct natural 1-parameter families of BDEs that interpolate between the BDEs we have studied, and establish relationships between these families.

We exhibit the existence of a curve of points of zero torsion of the characteristic curves, and a curve of points where the tangent plane to the surface is the osculating plane of a characteristic curve. We determine the behaviour of these curves near cusps of Gauss and umbilic points.

We study BDEs with coefficients that vanish simultaneously at an isolated point and with discriminant having an A_2-singularity at that point. We show that such BDEs can be grouped into three distinct types, and study the differences between these types in terms of their codimension and the linear parts of their coefficients. We establish the topological configurations of the solution curves in each case with codimension ≤ 4.

We study the asymptotic and characteristic curves in the neighbourhood of a parabolic cross-cap, that is, on a singular surface with a cross-cap singularity with a parabolic set having a cusp singularity at the singular point. We obtain the topological configurations of these foliations both in the domain of a parametrisation of such a surface, and on the surface itself. We construct a natural one-parameter family of surfaces with cross-cap singularities in which the parabolic cross-cap is

the transition from a hyperbolic cross-cap to an elliptic cross-cap. We study the bifurcations of the asymptotic and characteristic curves in this family.

Declaration

The work in this thesis is based on research carried out at the Pure Mathematics Group, the Department of Mathematical Sciences, University of Durham, England. No part of this thesis has been submitted elsewhere for any other degree or qualification and is all my own work unless referenced to the contrary in the text.

Acknowledgements

I am greatly indebted to Dr. Farid Tari for his inspiring, enthusiastic supervision and his friendship. I would also like to thank the other mathematicians in Durham who have always been happy to give help when it was needed, and all of my friends in the worldwide singularity theory community; in particular I would like to thank Raul Oset-Sinha for the invaluable advice he gave me during his visit to Durham.

My interest in mathematics is due in no small part to many wonderful teachers who I have been lucky enough work with, and I would like to acknowledge the part played in the development of this interest by Dr. Hilary Priestley at St. Anne's College Oxford, and Bob Jewitt at Queen Elizabeth High School, Hexham.

I would like to thank my Mum, my Dad, Judith, Rachel and Jen for their continued love and support.

As anyone who has undertaken a PhD knows, it is a hugely rewarding but emotionally exhausting experience, and its no exaggeration to say that this work would not have been possible without all of the fantastic people who have made my time in Durham so enjoyable.

It has been a real privilege to work in a department with such an excellent community spirit. There are times when a friendly conversation and a cup of coffee make a huge difference, and I would like to thank Pamela who never failed to provide either.

The best thing about being a postgraduate student is the opportunity it gives you to meet and spend time with, in your fellow students, a fantastic, interesting and diverse group of people. The practical help given is, of course, hugely appreciated, but the company, coffee and beer we've shared has made the whole thing worthwhile. Massive thanks, and best wishes, to my geometrical comrade-in-arms Femke, Danny,

Becky, Nathan, Ric, Ben, Becka, Jonathan, Andy, Ken, John, Kirsty, Luke, Scott, Mark, Rachel, Amani, James and Tan. Special thanks to Katie with whom I shared laughs, opinions, arguments and cricket commentary, not to mention an office, for over three years.

Thanks also to all of the members of the Hedgehog's Skin and 422 ceilidh bands for welcome musical distractions, and to the musicians of Durham who frequent the Dun Cow, the Elm Tree and the Shakespeare.

Finally much love and thanks to Alex, Martin, Rob, Abi, Ffion, Patrick and Elise for the great times we have spent doing silly things, to the amazing Durham University Folk Society, to my housemates Alice Mullen and Charlotte Spink for exuding calmness when it was required, to Lucy for agreeing with me, and to Maisie Greenwood whose energy, warmth and humanity is a constant source of inspiration.

Contents

Prologue

Geometry is one of the oldest branches of science: the first axiomatic study was carried out by Euclid in the third century BC. It is remarkable, therefore, that is still at the forefront of mathematical research today. Indeed, one could argue that all of mathematics stems from geometry, that is, from a need to understand the world around us.

It is even more remarkable that Euclidean geometry, that is, geometry based on Euclid's axioms, is still very much alive as an area of research. Two major developments in mathematics since Euclid's time have given the subject new impetus. The first was the invention of calculus by Newton and Leibniz in the seventeenth century. This gave mathematicians the tool they needed to understand curved objects. The second, over the last seventy years, was the development of singularity theory, a descendent of Newton's calculus.

Singularity theory is the framework within which to study *generic* geometric properties, that is, those properties that a curved object might typically have. Its study has led to a number of very classical objects in differential geometry being revisited and studied from a new angle. It has also made geometry more applicable to other scientific fields, for example, computer vision.

This thesis is a continuation of that process: an investigation of some generic properties of regular and singular surfaces in Euclidean space.

The aims of the thesis

In general a smooth surface in the Euclidean space $\mathbb{R}^3$ has open (possibly empty) hyperbolic and elliptic regions, where the Gaussian curvature K is respectively negative and positive, and a smooth curve where $K = 0$, known as the parabolic set.

Our interest is centred around two families of curves on smooth surfaces: the asymptotic curves and the characteristic curves. The asymptotic curves exist in the closure of the hyperbolic regions of surfaces, the characteristic curves exist in the closure of the elliptic regions of surfaces.

The asymptotic curves have been well studied, the characteristic curves less so, however a number of properties of the characteristic curves, discussed in Chapter 2, show them to be the analogue of the asymptotic curves in the elliptic region.

Much of the generic geometry of the non-elliptic regions of surfaces (discussed in Chapter 2) is related to the asymptotic curves. The similarities between the asymptotic curves and the characteristic curves suggest that the geometry of the elliptic region may be better understood by studying the characteristic curves.

The asymptotic and characteristic curves are given, in the domain of a parametrisation of a smooth surface, by certain *binary differential equations* (BDEs). These are implicit differential equations that may be written in the form

$$a(x,y)dy^2 + 2b(x,y)dxdy + c(x,y)dx^2 = 0,$$

where a, b, c are smooth functions. These equations have wide ranging applications in areas of mathematics including differential geometry, partial differential equations and control theory, and have been much studied. For a survey of work on BDEs see [68].

Whitney showed in [75] that a surface can have a stable singularity under smooth changes of coordinates in the source and target, that is, an isolated point at which is surface is not smooth. The singularity is known as a *cross-cap*. A model of a surface with a cross-cap singularity is shown in Figure 1.

As cross-cap points are the only stable singularities of immersed surfaces in $\mathbb{R}^3$, it is natural to seek to understand the differential geometry of surfaces in the neighbourhood of such points.

The aims of this Thesis are as follows:

1. to strengthen the case for the characteristic curves being justifiable objects of study, draw further parallels with asymptotic curve, and use them to understand the geometry of the elliptic region;

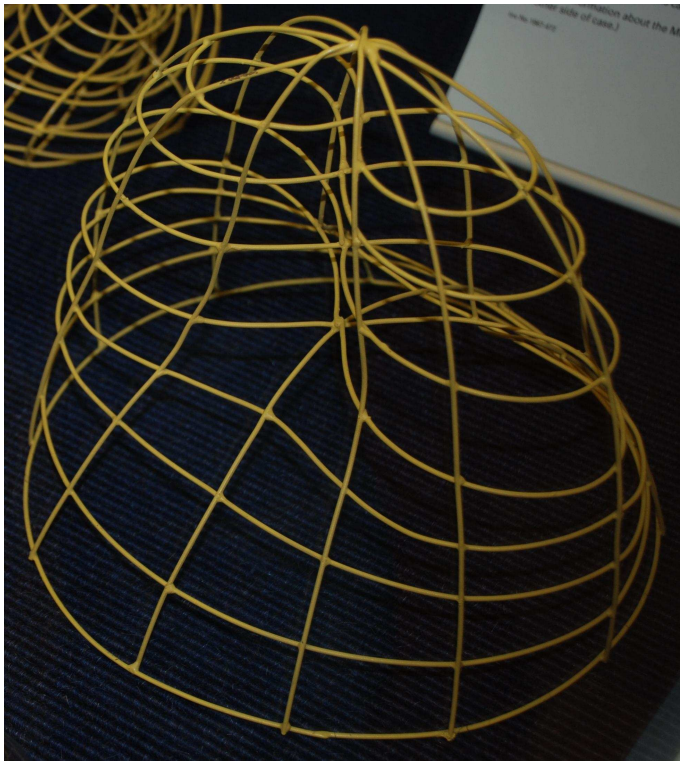

Figure 1: A wire model of a cross-cap in the Science Museum in London.

2. to understand further the geometry of the cross-cap connected to the asymptotic and characteristic curves;

3. to understand the types of differential equation that define the asymptotic and characteristic curves, and the relationships between them.

Our approach to the problems

Many of the generic features of surfaces in $\mathbb{R}^3$ that we consider can be defined and studied using two different approaches. The first is to use singularity theory directly by defining functions on such surfaces and classifying their singularities (see [46] for a survey of this use of singularity theory).

The alternative approach is to study foliations of smooth surfaces and related features by studying the differential equations that define these foliations. Many of the generic features of surfaces that we encounter may be alternatively characterised in terms of BDEs. For example, consider the contact of the surface with planes. The singularity theory approach involves considering the family of height functions

on the surface (see Section 1.2). Generally the height function is a submersion, however if the plane in question is the tangent plane to the surface the height function is singular. The singularity is generally an A_1-singularity (see Section 1.1), more specifically, and A_1^+-singularity if the point is elliptic and an A_1^--singularity if the point is hyperbolic. There are generally smooth curves of points on the surface where the tangent plane to the surface has more degenerate contact with the surface, namely the parabolic set, a height function having an A_2-singularity at such points. At isolated points on the parabolic set a height function may have an A_3-singularity, and the surface has even more degenerate contact with its tangent plane. These points are called *cusps of Gauss*. Alternatively these features of surfaces may also identified by studying the BDE of the asymptotic curves, which is given in Section 2.2. Hyperbolic (respectively elliptic) points are those points at which the asymptotic BDE has two (respectively zero) solution directions. The parabolic set and the cusps of Gauss are the discriminant and folded singularities (see Section 1.3) of the asymptotic BDE respectively.

It is often the case that more geometric information can be obtained using the differential equations approach. The cusps of Gauss are a good example. The height function approach shows that are two types of cusp of Gauss distinguished according to whether the singularity of the height function is of type A_3^+ or A_3^-. On the other hand, there are three generically occurring topological models of folded singularities of BDEs known as well-folded saddles, nodes and foci (see Section 1.3). As all three models can occur in the case of the asymptotic BDE at a cusp of Gauss, we obtain a finer classification of such points using the differential equations method.

The characteristic directions may be seen as an extreme example of this phenomenon. They have not yet been defined in terms of contact with any model-submanifold, and so all the information currently known about these curves stems from the study of the defining BDE.

In this thesis, therefore, we generally favour the differential equation approach, although we will occasionally revert to the classical methods.

An outline of the thesis

In Chapter 1 we review the methods and definitions required in the thesis. These include aspects of singularity theory, a rigorous definition of genericity, and techniques for the qualitative study of implicit differential equations. In Chapter 2 with give precise definitions of the curves of interest and the BDEs that define them, and review relevant existing results. We include a new interpretation of the notion of conjugacy.

In Chapter 3 we study the characteristic curves at cusps of Gauss, that is, at the folded singularities of the BDE (2.6). This work draws analogies with Uribe-Vargas' work on the asymptotic curves in [71]. We show that despite the characteristic curves themselves being invariant only under Euclidean transformations of the ambient space, certain associated features in the neighbourhood of a cusp of Gauss are preserved by projective transformations. We associate a projective invariant parameter to cusps of Gauss. We establish the configurations of various curves of interest at cusps of Gauss. We consider the Legendre transform of the characteristic BDE at these points. We provide a natural, geometric way to distinguish between the two characteristic curves through a non-umbilic elliptic point, and produce a result on the characteristic curves analogous to the Beltrami-Enepper Theorem for the asymptotic curves. We conclude the chapter with some results concerning elliptic discs on surfaces, an example of how the (local) study of the characteristic curves may be used to prove global results about elliptic regions of surface.

An alternative construction of the asymptotic and characteristic BDEs uses certain involutions on the real projective line. In Chapter 4 we generalise this idea, and some of our results from Chapter 3. This work lays the foundations for Chapter 5 where we show, by considering BDEs as points of the projective plane, that the asymptotic, principal and characteristic BDEs are connected to a number of other BDEs forms on the surface, which we study. We construct new 1-parameter families of BDEs on surfaces and show how they are related to each other.

In Chapter 6 we treat the characteristic curves as space curves in the ambient space $\mathbb{R}^3$ and consider their torsion. We exhibit the existence of smooth curves on the surface where the torsion of a characteristic curve vanishes, and further curves

where the tangent plane to the surface is the osculating plane of a characteristic curve.

The final three chapters concern the geometry of the cross-cap. The asymptotic BDE on a parabolic cross-cap has coefficients that all vanish simultaneously and a discriminant that has a cusp (A_2) singularity. Such BDEs have been studied previously, however, those encountered on the cross-cap are of a more degenerate type. We consider these BDEs in their own right in Chapter 7 and give a complete topological classification of cusp BDEs with codimension ≤ 4. In Chapter 8 we study the asymptotic and characteristic curves on a parabolic cross-cap and in Chapter 9 we study their bifurcation in a 1-parameter family of cross-caps.

Chapter 1

Methods

1.1 Singularity theory

We review the definitions and results from singularity theory that will be needed in the thesis.

1.1.1 Basic notions

Throughout the thesis *smooth* will always mean C^∞, that is, a map will be said to be smooth if it has continuous partial derivatives of all orders. We denote by $C^\infty(\mathbb{R}^n, \mathbb{R}^m)$ the set of smooth maps $\mathbb{R}^n \to \mathbb{R}^m$.

Jets, germs and the Whitney Topology

Definition 1.1.1 *The* k-jet space $J^k(n, m)$ *is the vector space of all polynomial maps of degree* k *from* $\mathbb{R}^n$ *to* $\mathbb{R}^m$.

We generally abbreviate $J^k(n, 1)$ to $J^k(n)$.

Definition 1.1.2 *Let* $f \in C^\infty(\mathbb{R}^n, \mathbb{R}^m)$. *The* k-jet, $j^k_p f$ *of* f *at a point* $p \in \mathbb{R}^n$ *is the Taylor expansion of* f *about the point* p *truncated at degree* k.

Definition 1.1.3 *Let* U, V *be open subsets of* $\mathbb{R}^n$ *with* $U \cap V \neq \emptyset$, *let*

$$\begin{aligned} f : U &\to \mathbb{R}^m \\ g : V &\to \mathbb{R}^m \end{aligned}$$

be smooth, and let $p \in U \cap V$. *We define an equivalence relation* $\sim$ *on* $C^\infty(U \cap V, \mathbb{R}^m)$ *by letting* $f \sim g$ *if and only if there is an open subset* $W \subset U \cap V$ *with* $p \in W$ *such that* $f = g$ *on* W. *The* $\sim$*-equivalence class of* f *is called the* germ at p *of* f, *and is denoted by*

$$f : \mathbb{R}, p \to \mathbb{R}.$$

All properties of germs will be checked on representatives so we will generally use the same notation for a germ and its representative.

In Definition 1.1.4 we consider the k-jet of a smooth function to be a point in a Euclidean space.

Definition 1.1.4 *Let* $\epsilon > 0$ *and let* $f : \mathbb{R}^m \to \mathbb{R}^n$ *be smooth. Let*

$$B^k_\epsilon(f) := \{g : \mathbb{R}^n \to \mathbb{R}^m || j^k_p f - j^k_p g| < \epsilon, \, \forall p \in \mathbb{R}^n\}.$$

The Whitney C^∞-topology *is the topology on* $C^\infty(\mathbb{R}^n, \mathbb{R}^m)$ *with base*

$$\{B^k_\epsilon(f) | \forall k \in \mathbb{N}, \forall \, \epsilon > 0, \forall f \in C^\infty(\mathbb{R}^m, \mathbb{R}^n)\}.$$

Remarks 1.1.5

1. *For any open subset* $U \subset \mathbb{R}^n$ *the Whitney topology induces a topology on* $C^\infty(U, \mathbb{R}^m)$, *the set of smooth maps* $U \to \mathbb{R}^m$. *In particular at any points* $p \in \mathbb{R}^n$ *and* $q \in \mathbb{R}^m$ *we have a topology on the set of germs at* p *of smooth maps* $\mathbb{R}^n, p \to \mathbb{R}^m, q$.

2. *The Whitney topology extends to smooth maps between manifolds, as locally a manifold is parametrised by an open subset of* $\mathbb{R}^n$.

The implicit function Theorem

We will make use of the following (standard) technical Theorem, so we include a statement for reference. A proof is given in, for example [6].

Theorem 1.1.6 *Let* $U \subset \mathbb{R}^n \times \mathbb{R}^m$ *be open, and let* $(0, 0) \in U$. *Let* $f : U \to \mathbb{R}$ *be a smooth function such that* $f(0, 0) = 0$ *and* $\partial f / \partial x_i \neq 0$ *for each* $i = n + 1..n + m$. *Then there exist open sets* $W_1 \subset \mathbb{R}^n$ *and* $W_2 \subset \mathbb{R}^m$ *with* $W_1 \times W_2 \subset U$, *and a unique smooth map* $g : W_2 \to \mathbb{R}^m$ *such that* $f(x, g(x)) = 0$ *for all* $x \in W_1$.

Singular map germs

Definition 1.1.7 *A map $f : \mathbb{R}^m \to \mathbb{R}^n$ has a singularity at a point p if its differential at p has less than maximal rank.*

For a basic reference on singular points of smooth maps we use [3].

Definition 1.1.8 *Two map-germs,*

$$f, g : \mathbb{R}^m, 0 \to \mathbb{R}^n, 0$$

are said to be $\mathcal{R}$-equivalent (respectively $\mathcal{L}$-equivalent, $\mathcal{A}$-equivalent) if there exists germs of diffeomorphisms

$$\phi : \mathbb{R}^m, 0 \to \mathbb{R}^m, 0$$

and

$$\psi : \mathbb{R}^n, 0 \to \mathbb{R}^m, 0$$

which preserve the origin and are such that $f \circ \phi = g$ (respectively $f = \psi \circ g$, $f \circ \phi = \psi \circ \phi$).

We give normal forms for the simplest singularities for reference in this thesis.

Example 1.1.1 *Let $f : \mathbb{R}^2, 0 \to \mathbb{R}$ be a function germ. Then f has an $A_k^{\pm}$-singularity if it is $\mathcal{R}$-equivalent to*

$$\pm x^2 \pm y^{k+1}$$

($k \geq 1$), and that f has a $D_k^{\pm}$-singularity if it is $\mathcal{R}$-equivalent to

$$x^2 y \pm y^{k-1}$$

($k \geq 4$).

Note that A_k^+- and A_k^--singularities are equivalent when k is even, as is the case with D_k^+- and D_k^--singularities. We shall refer to A_1-singularities as Morse singularities, A_2-singularities as cusp-singularities and A_3-singularities as swallowtail singularities.

Definition 1.1.9 *Let $f : \mathbb{R}^m, 0 \to \mathbb{R}^n, 0$ be a singular map germ. An* r-parameter unfolding *of f is a smooth map*

$$\begin{aligned} F : \mathbb{R}^m, 0 \times \mathbb{R}^r, 0 &\to \mathbb{R}^n \times \mathbb{R}^r, 0 \\ (x, u) &\mapsto (f(x, u), u) \end{aligned}$$

where $x \in \mathbb{R}^m$ and $u \in \mathbb{R}^r$, such that $f(x, 0) = f(x), \forall x \in \mathbb{R}^m$. The family of maps $f(x, u)$ is then referred to as an r-parameter deformation *of f.*

Definition 1.1.10 *If*

$$F : \mathbb{R}^m, 0 \times \mathbb{R}^r, 0 \to \mathbb{R} \times \mathbb{R}^r, 0$$

is an unfolding of a function germ $f : \mathbb{R}^m, 0 \to \mathbb{R}$, then the singular set *of F is*

$$\Sigma = \{(x, u) \in \mathbb{R}^m \times \mathbb{R}^r | \frac{\partial F}{\partial x}(x, u) = 0\},$$

the image of the critical set, $\mathcal{D} = F(\Sigma)$, is the discriminant set *of F and the* bifurcation set *of F is*

$$\mathcal{B} = \{u \in \mathbb{R}^r | \exists\, x \in \mathbb{R}^m \text{ s.t. } \frac{\partial F}{\partial x}(x, u) = \frac{\partial^2 F}{\partial x^2}(x, u) = 0\}.$$

Transversality

Let X and Y between smooth manifolds and let $g : X \to Y$ be a smooth map. Then at each point $x \in X$ we have the tangent map

$$\begin{aligned} Tg(x) : T_x X \to &\quad T_{g(x)} P \\ u \mapsto &\quad Dg(u). \end{aligned}$$

Definition 1.1.11 *If X, P are smooth manifolds, Y is a smooth submanifold of P, and $g : X \to Y$ is a smooth mapping, and if*

$$\mathrm{im}(Tg(x)) + T_{g(x)} Y = T_{g(x)} P$$

for all $x \in f^{-1}(Y)$, or if $\mathrm{im}(g) \cap Y = \emptyset$, then g is said to be transverse *to Y.*

Recall that a residual subset of a topological space is one whose compliment is nowhere dense, or equivalently one that is the countable intersection of open and dense subsets.

Theorem 1.1.12 *Let Q be a smooth submanifold of the jet space $J^k(n,m)$. Then the set of all smooth mappings $f : \mathbb{R}^n \to \mathbb{R}^m$ for which $j^k f$ is transverse to Q is residual in $C^\infty(\mathbb{R}^n, \mathbb{R}^m)$.*

1.2 Generic geometry

For a basic reference on generic geometry see [15, 43, 47, 73].

Genericity

Definition 1.2.1 *A property is generic for $C^\infty(\mathbb{R}^n, \mathbb{R}^m)$ if it defines a residual subset of $C^\infty(\mathbb{R}^n, \mathbb{R}^m)$.*

Theorem 1.1.12 (Thom's transversality Theorem) shows that the property that a map is transverse to any submanifold of a jet-space is generic. Equipped with this fact, Lemma 1.2.2 provides a powerful tool for studying generic properties of submanifolds.

Lemma 1.2.2 *Let R, P be smooth manifolds, and let $\phi : R \to P$ be a smooth map. If Q is a smooth submanifold of P with $\phi(R)$ transverse to Q, then $\phi^{-1}(Q)$ is a smooth submanifold of R with the same codimension as Q, or is empty.*

This thesis is concerned with smooth surfaces in the Euclidean space $\mathbb{R}^3$, and in particular their local geometry. As we will identify new geometric features of such surfaces, we require a method for establishing that they are generic. We follow the approach of Bruce in [9].

Given a smooth orientable surface $S \subset \mathbb{R}^3$, we may write S locally about some point p in *Monge form*

$$(x, y, f(x, y)).$$

If we are concerned with purely local properties, we may consider f to be the germ at p of a function and work in a single open neighbourhood U of p. Local geometric information about the surface is then given by the Monge function $f \in C^\infty(U, \mathbb{R})$ and its derivatives at p, so we work in the jet-space $J^k(2)$ for some k. Of course, there is the problem that the choice of coordinates is not unique.

We give S an orientation and let $\mathbf{n}(p)$ be the (positive) unit normal to S at the point p, $\mathbf{X}(p)$ be any smooth vector field on S, and choose a vector field $\mathbf{Y}(p)$ such that $\{\mathbf{X}(p), \mathbf{Y}(p), \mathbf{n}(p)\}$ is a right-handed orthonormal basis for $\mathbb{R}^3$ at each point $p \in S$. At any point p let the coordinate axes x, y, z lie along the tangents to $\mathbf{X}(p), \mathbf{Y}(p), \mathbf{n}(p)$ respectively, and parametrise the surface in Monge form $(x, y, f_p(x, y))$ at p, where f_p is a smooth function and $f_0 = f$. Note that f_p and its first derivatives vanish at p. We define the *k-jet-extension map* (or Monge-Taylor map)

$$\begin{aligned} \phi : \quad S &\to \quad J^k(2) \\ p &\mapsto \quad j^k f_p. \end{aligned}$$

It is clear that ϕ depends on the choice of vector field $\mathbf{X}$. The possible choices of (x, y)-axes at any point, however, are related by an $SO(2)$ change of coordinates, that is, by a rotation of T_pS about $\mathbf{n}(p)$, which leaves T_pS invariant. The group $SO(2)$ acts on $J^k(2)$ via the coefficients of the elements of $J^k(2)$. It follows that the transversality of ϕ at p to an $SO(2)$-invariant submanifold $V \subset J^k(2)$ is independent of the choice of vector field $\mathbf{X}$. For any $q \in J^k(2)$, the tangent space at q to the $SO(2)$-orbit of q is $\mathbb{R}.\{xq_y - yq_x\}$.

The method, then, is as follows. We parametrise a surface in Monge form with the origin at the point under consideration. We establish conditions on the k-jet of the Monge function for that point to have a particular geometric property, and use these conditions to define smooth submanifolds of the k-jet space. We establish the (open) conditions for the jet-extension map to be transverse to these submanifolds, and then apply Lemma 1.2.2 to establish the codimension of the set of points with such a property on the surface.

In order to carry out this process, we need to be able to calculate the image of the tangent map of the jet-extension map. Lemma 1.2.3 appears in [9] although the proof is not provided there.

Lemma 1.2.3 ([9]) *If $\phi : S \to J^k(2)$ is the k-jet extension map, then* $\mathrm{im}T\phi(0)$ *is spanned by*

$$\begin{aligned} v_x \;=\; & j^k(-f_{xx}(0,0)x - f_{xy}(0,0)y + f_x(x,y) \\ & -f_x(x,y)f(x,y)f_{xx}(0,0) - f_y(x,y)f(x,y)f_{xy}(0,0)), \end{aligned}$$

and

$$\begin{aligned} v_y &= j^k(-f_{xy}(0,0)x - f_{yy}(0,0)y + f_y(x,y) \\ &\quad -f_x(x,y)f(x,y)f_{xy}(0,0) - f_y(x,y)f(x,y)f_{yy}(0,0)). \end{aligned}$$

Proof: Let (x, y, z) be a coordinate system at the origin with the z-axis normal to the surface. The surface is parametrised in Monge form at the origin by

$$(x, y, f(x, y))$$

where $f(0,0) = f_x(0,0) = f_y(0,0) = 0$.

Let $p = (x_0, y_0, z_0)$ be point on the surface (that is, $z_0 = f(x_0, y_0)$). Let (X, Y, Z) be a right-handed co-ordinate system with origin at p. The surface is given in Monge form at p by $(X, Y, f_p(X, Y))$.

In what follows all partial derivatives of f are evaluated at (x_0, y_0).

The tangent space to the surface at p is spanned by $(1, 0, f_x)$ and $(0, 1, f_y)$, and the normal to the surface at p is parallel to $(-f_x, -f_y, 1)$. We choose the Z-axis to be normal to the surface at p, the X-axis to be parallel to $(1, 0, f_x)$, and the Y axis to be orthogonal to the X-and Z-axes such that they form a right handed system. The co-ordinates at p are related to those at the origin by

$$\begin{pmatrix} x \\ y \\ z \end{pmatrix} = \begin{pmatrix} 1 & -f_x f_y & -f_x \\ 0 & 1 + f_x^2 & -f_y \\ f_x & f_y & 1 \end{pmatrix} \begin{pmatrix} X + x_0 \\ Y + y_0 \\ Z + z_0 \end{pmatrix}. \tag{1.1}$$

From the first row of (1.1) we have that

$$x = (X + x_0) - f_x f_y (Y + y_0) - f_x (Z + z_0).$$

Setting $x = x_0$, differentiating this expression with respect to x_0 and y_0, and evaluating at $(x_0, y_0) = (0, 0)$ (observing that $Z(0,0) = 0$) we have that

$$\left(\frac{\partial X}{\partial x_0}\right) = \left(\frac{\partial X}{\partial y_0}\right) = 0$$

at $(x_0, y_0) = (0, 0)$. Similarly, from the second row of (1.1) we have that

$$y = (1 + f_x^2)(Y + y_0) - f_y (Z + z_0).$$

Setting $y = y_0$, differentiating this expression with respect to x_0 and y_0 and evaluating at the origin we have that

$$\left(\frac{\partial Y}{\partial x_0}\right) = \left(\frac{\partial Y}{\partial y_0}\right) = 0.$$

at $(x_0, y_0) = (0, 0)$.

From the third row of (1.1) we have

$$Z = z - z_0 - (X + x_0)f_x - (Y + y_0)f_y. \tag{1.2}$$

On the surface, however, we have that $z = f(x, y)$, that is,

$$z = f(X + x_0 - (Y + y_0)f_x f_y - (Z + z_0)f_x, (y + y_0)(1 + f_x^2) - (Z + z_0)f_y),$$

and $z_0 = f(x_0, y_0)$. Substituting these into (1.2) we have that

$$\begin{aligned} Z = \quad & f(X + x_0 - (Y + y_0)f_x f_y - (Z + f(x_0, y_0))f_x, \\ & (y + y_0)(1 + f_x^2) - (Z + f(x_0, y_0))f_y) \\ & -f(x_0, y_0) - (X + x_0)f_x - (Y + y_0)f_y. \end{aligned} \tag{1.3}$$

Observe now that since $Z = f_p(X, Y)$, $\mathrm{im}T\phi(0)$ is spanned by

$$j^k\left(\frac{\partial Z}{\partial x_0}\right), j^k\left(\frac{\partial Z}{\partial y_0}\right),$$

evaluated at $(x_0, y_0) = (0, 0)$. These may be found by differentiating (1.3) with respect to x_0 and y_0 and setting $(x_0, y_0) = (0, 0)$, and they are equal to the expressions given in the statement. □

The singularity theory approach

The study the generic differential geometry of smooth submanifolds using singularity theory involves considering the contact of these submanifolds with model submanifolds such as lines, planes, circles and spheres. This is achieved by defining families of functions or maps on the submanifolds of interest and classifying their critical points.

More visually, the discriminant and bifurcation sets of these families of functions may be viewed as geometric objects in their own right, whose singularities correspond to points where the contact with the test submanifold is more degenerate.

Although in this thesis we will largely use a different approach, as outlined in Section 1.3 below, it will be helpful to recall an example of this method that is important in the study of smooth surfaces.

Definition 1.2.4 *Let $S \subset \mathbb{R}^3$ be a smooth surface and let S^2 be the unit sphere in $\mathbb{R}^3$. The family of height functions on S is the family*

$$\begin{aligned} h : S \times S^2 &\to \mathbb{R}, \\ (p, u) &\mapsto p \cdot u \end{aligned}$$

where $\cdot$ denotes the usual inner product on $\mathbb{R}^3$.

We write h_u for the height function with u fixed. This is the projection of the surface to the line determined by u. The function h_u is used to measure the contact of the surface S with planes whose normal is u. The family defined by

$$\begin{aligned} H : S \times S^2 &\to \mathbb{R} \times S^2, \\ (p, u) &\mapsto (h(p, u), u) \end{aligned}$$

is an unfolding of any member of the family of height functions. It is trivial to show that h_u is singular if and only if u is normal to the surface, that is, the singular set of H consists of pairs $(p, \mathbf{n}_p)$ where $\mathbf{n}_p$ is a unit normal to the surface at p. The discriminant of H is the *dual surface* of S (the set of tangent planes to S).

Other examples of families of functions on surfaces include the *distance-squared functions* which measure the contact of the surface S with spheres (see, for example, [18, 59]). The bifurcation set of the family of distance squared functions is the *focal surface*. There is also the family of orthogonal projections of the surface to planes, which measures the contact of the surface with lines (see, for example, [9, 17, 19]).

1.3 Qualitative study of implicit differential equations

A first order implicit differential equation (IDE) is an equation of the form

$$F(x, y, p) = 0 \tag{1.4}$$

where F is a smooth function of $(x, y, p) \in \mathbb{R}^3$ with $p = dy/dx$.

At points where $F_p \neq 0$ the equation can be locally reduced to the form

$$\frac{dy}{dx} = g(x, y).$$

It thus defines just one direction in the plane, and can be studied using the theory of ordinary differential equations. If $F_p = 0$ then the equation may define locally more than one direction in the plane.

Suppose that at a given point $F = F_p = 0$ and $F_{pp} \neq 0$. In this case the equation may be written in some open neighbourhood of the point in the form

$$a(x, y)dy^2 + 2b(x, y)dxdy + c(x, y)dx^2 = 0, \tag{1.5}$$

where the coefficients a, b, c are smooth functions of $(x, y) \in \mathbb{R}^2$ that do not vanish simultaneously at any point in the neighbourhood. We extend this class of equation by including equations where the coefficients do all vanish simultaneously at a point. Equations of the form (1.5) are called *binary differential equations* (BDEs).

Let $\delta = b^2 - ac$. A BDE defines two distinct directions at points in the plane where $\delta > 0$, no directions at points when $\delta < 0$. The set

$$\Delta = \{(x, y) \in U | \delta(x, y) = 0\}$$

is called the *discriminant* of the BDE, and is generally a smooth curve. If the coefficients of the equation do not all vanish simultaneously at a given point we may assume locally that $a \neq 0$ and express the equation as a quadratic in $p = dy/dx$. In this case, the BDE defines a single direction at points on Δ (note that this is the case regardless of whether Δ is smooth). If all of the coefficients vanish simultaneously at a point then Δ is necessarily singular at that point and all directions in the plane are solutions at that point.

Away from its discriminant, a BDE determines either a pair of transverse foliations, $\mathcal{F}_i, i = 1, 2$, or no folitions. Hence all of the interesting features of the solution curves occur on the discriminant. If Δ is a smooth curve, then the solution curves form a family of cusps along this curve, except at points at which the unique solution direction is tangent to Δ. The configuration of the solutions of equation (1.5) refers to the triple $\{\Delta, \mathcal{F}_1, \mathcal{F}_2\}$.

Although the solution curves are singular at all points of the discriminant, we define a singularity of a BDE to be a point of the discriminant at which the unique solution is tangent to Δ (known as *folded singularities*), or a point at which the discriminant itself is singular. We are concerned only with isolated singularities, which we always assume, without loss of generality, to be at the origin.

We are interested in the *local* configurations of the integral curves, so we consider a, b, c in (1.5) as germs of smooth functions. Properties of germs are checked on representatives, and we use the same notation for a germ and its representative. We shall denote the germ of a BDE (1.5) by $\omega = (a, b, c)$.

Implicit differential equations on surfaces may be studied locally by parametrising the surface by an open subset of the plane and studying the BDE in that plane.

1.3.1 Classification

In this thesis we will classify BDEs up to topological equivalence. We consider two (germs of) BDEs, ω and τ to be topologically equivalent if there is a germ of a homeomorphism

$$\mathbb{R}^2, 0 \to \mathbb{R}^2, 0$$

that takes the integral curves of ω to those of τ.

We shall also occasionally consider smooth models for BDEs. Two (germs of) BDEs, ω and τ are said to be smoothly equivalent if there exist germs of a diffeomorphism

$$H : \mathbb{R}^2, 0 \to \mathbb{R}^2, 0$$

and a function not vanishing at zero

$$r : \mathbb{R}^2, 0 \to \mathbb{R}, 0$$

such that

$$\omega = rH^*\tau.$$

The cases distinguished according to whether the coefficients do or do not vanish simultaneously (often labelled type 1 and type 2 BDEs respectively) have crucial

differences, and must be treated separately. In particular, BDEs where the coefficients do not vanish simultaneously may have finite codimension in the set of all IDEs, and can be deformed in that set. Those BDEs with vanishing coefficients are of infinite codimension in the set of all IDEs, and are deformed in the set of all BDEs.

To a germ of a BDE $\omega(x,y)=(a,b,c)$, we associate the jet-extension map

$$\begin{aligned}\Phi:\ \mathbb{R}^2,0 &\to J^k(2,3)\\ (x,y) &\mapsto j^k\omega|_{(x,y)}.\end{aligned}$$

where

$$j^k\omega|_{(x,y)}=(j^ka(x,y),j^kb(x,y),j^kc(x,y)).$$

Let $\mathcal{G}_k$ be the group of $(k+1)$-jets of diffeomorphisms in (x,y) and multiplication by non-zero functions in (x,y). A singularity of a BDE with vanishing coefficients (respectively an IDE) is of codimension m if the conditions that define it yield a semi-algebraic set, V, of codimension $m+2$ (respectively $m+3$) in $J^k(2,3)$ for all $k\geq k_0$ for some k_0. The set V is supposed to be invariant under the natural action of the group $\mathcal{G}_k$.

1.3.2 The lifted field

An elegant, geometric approach to the study of IDEs (1.4) is given in [69] (see also [1]).

Consider $PT^*\mathbb{R}^2=\mathbb{R}^2\times\mathbb{R}P$, the manifold of contact elements to the plane (the projectivised cotangent bundle to $\mathbb{R}^2$). We take an affine chart $p=dy/dx$ for $\mathbb{R}P$, so the manifold of contact elements is $\mathbb{R}^3$ endowed with the canonical contact structure determined by the 1-form $dy-pdx$. The projection associated to the contact structure is

$$\begin{aligned}\pi:\mathbb{R}^3 &\to \mathbb{R}^2\\ (x,y,p) &\mapsto (x,y).\end{aligned}$$

If the coefficients of a BDE (1.5) do not vanish simultaneously we may assume $a\neq 0$ and write (1.5) as $F=0$ where

$$F(x,y,p)=a(x,y)p^2+2b(x,y)p+c(x,y),$$

and $p = dy/dx$. The set of directions defined by (1.5) form a surface

$$M = F^{-1}(0) \subset \mathbb{R}^3.$$

In general M is smooth, and the image of $\pi|_M$ is a two-fold covering of regions where $b^2 - ac > 0$. The critical set of $\pi|_M$ given by $F = F_p = 0$ is called the *criminant*. There is an involution σ on M that interchanges points with the same image under π.

The bivalued direction field given by (1.5) lifts to a single valued field ξ on M obtained by intersecting the contact planes with the tangent planes to M.

Lemma 1.3.1 ([8]) *A suitable lifted field is given by*

$$\xi = F_p \frac{\partial}{\partial x} + pF_p \frac{\partial}{\partial y} - (F_x + pF_y)\frac{\partial}{\partial p}.$$

Proof: Suppose that

$$\xi = A\frac{\partial}{\partial x} + B\frac{\partial}{\partial y} + C\frac{\partial}{\partial p},$$

for some smooth functions A,B,C. We require that $(dy - pdx)(\xi) = 0$. It follows that $B = pA$.

The normal to the surface M is given by (F_x, F_y, F_p). Since ξ is tangent to M we have that

$$(A, pA, C) \cdot (F_x, F_y, F_p) = 0,$$

that is, $CF_p = -A(F_x + pF_y)$. The result follows. □

The configuration of the solution curves of (1.5) at a point on the discriminant are determined by the pair (ξ, σ).

If the contact plane at a point is tangent to M then the lifted field vanishes, that is, has a singularity. This happens generically at isolated points, including at the lift of folded singularities. The projection of such points are called well-folded singularities if ξ has an elementary zero with separatrices transverse to the criminant and tangents not projecting to zero.

If the vector field ξ is regular then a smooth model (in the neighbourhood of a regular point on the discriminant) is given by

$$dy^2 - xdx^2 = 0$$

(see [26]). The integral curves are a family of cusps. A smooth model of in a neighbourhood of a well-folded singularities is given by

$$dy^2 - (y - \lambda x^2)dx^2 = 0$$

(see [27, 30]). We refer to the smooth modulus λ as the *index modulus* of the singularity.

There are three stable topological models: well-folded saddles ($\lambda < 0$), nodes ($0 < \lambda < 1/16$) and foci ($\lambda > 1/16$), occurring when the lifted field ξ has a saddle, node or focus respectively. These are illustrated in Figure 1.1. The index of the lifted field at the singular point is given by $\text{sign}(\lambda).1$.

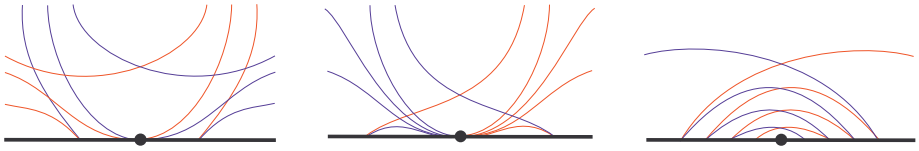

Figure 1.1: A well-folded saddle (left), well-folded node (centre) and well-folded focus (right).

The lifted field field method is illustrated in Figure 1.2.

The lifted field method may be extended to BDEs with vanishing coefficients (see for example [20]). In this case we consider the surface

$$\tilde{M} = \{(x, y, [\alpha : \beta]) \in \mathbb{R}^2, 0 \times \mathbb{R}P^1 | a\alpha^2 + 2b\alpha\beta + c\beta^2 = 0\}.$$

Observe that all directions are solutions where the coefficients vanish. We will consider BDEs for which this occurs at an isolated point which we we will always take to be the origin. The set $\pi^{-1}(0) = \{0\} \times \mathbb{R}P^1$ is called the *exceptional fibre*.

We use the term *criminant* for the closure of the set $\pi^{-1}(\Delta) \setminus (\{0\} \times \mathbb{R}P^1)$.

Consider the affine chart for $\mathbb{R}P^1$ $p = \beta/\alpha$ (we also consider the chart $q = \alpha/\beta$) and set

$$F(x, y, p) = a(x, y)p^2 + 2b(x, y)p + c(x, y).$$

The bi-valued direction field defined by the BDE in the plane lifts to the single field ξ on $\tilde{M}$ given in Lemma 1.3.1. The vector field ξ extends smoothly to the exceptional fibre, which is an integral curve of ξ.

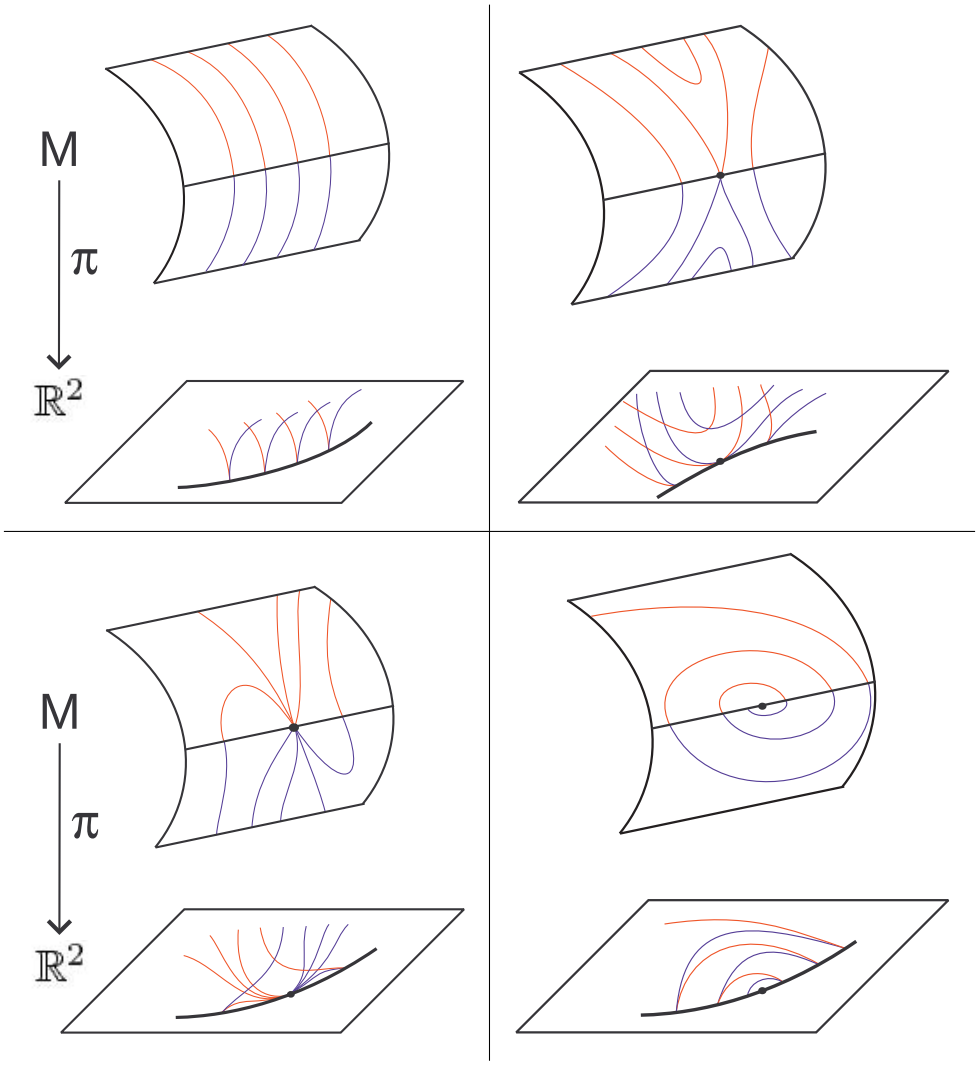

Figure 1.2: The lifted field method: the criminant (top left), a well-folded saddle (top right), a well-folded node (bottom left) and a well-folded focus (bottom right).

From Lemma 1.3.1 we have that zeros of ξ are given by

$$F = F_p = F_x + pF_y = 0. \tag{1.6}$$

When the BDE has an isolated singularity we may restrict attention to zeros of ξ on the exceptional fibre. Observe that $F(0,0,p) = F_p(0,0,p) = 0$. It follows that the zeros of ξ on the exceptional fibre are given by the roots of the cubic

$$\phi(p) = (F_x + pF_y)(0,0,p).$$

It shown in [20] that the surface $\tilde{M}$ is smooth if and only if δ has a Morse singularity. Furthermore, it is shown in [11] that if δ has an A_k-singularity then the

surface $\tilde{M}$ has an isolated A_{k-1}-singularity on the exceptional fibre and is smooth elsewhere. Thus, in the case of BDEs with discriminant having a cusp singularity, the surface $\tilde{M}$ has a Morse singularity. As the entire exceptional fibre $\{0\} \times \mathbb{R}P^1$ lies on the surface $\tilde{M}$ it follows that $\tilde{M}$ has an A_1^- (cone) singularity.

The term *separatrix* is used ambiguously in the study of IDEs; we make the following definition to avoid confusion.

Definition 1.3.2 *The images under the projection π of the stable, unstable and centre curves of a zero of the lifted field ξ are called the* separatrices *of the singularity.*

In the case of a folded saddle or node, the stable or unstable curves are the only integral curves passing through the singularity. They are smooth and transverse to each other and to the criminant. It follows (see Lemma 2.6 in [23]) that the separatrices are the only smooth curves passing through a folded singularity and that they are tangent to the discriminant. In the case of a saddle-node there is one stable or unstable manifold and a centre manifold tangent to the eigenvector associated to the zero eigenvalue.

Remark 1.3.3 *The ambiguity of the term separatrix arises from the fact that separatrices (in the sense of Definition 1.3.2) do not always separate distinct sectors. For example, in the case of a folded node, the projections of the weak separatrices of the node do not separate distinct sectors. Conversely, in certain cases (for example, cusp type 2 BDEs as defined in Chapter 7) there are curves that do separate distinct sectors that are not separatrices.*

1.3.3 Duality

Consider the conditions (1.6) for a zero of the lifted field ξ on the surface M. The condition $F = 0$ simply states that the zero lies on the surface, and the condition $F_p = 0$ states that the zero is on the criminant. The condition $F_x + pF_y = 0$ states that the zero is on the locus of inflections of the integral curves of the BDE. This may be seen by differentiating the expression $F(x, y, p) = 0$ with respect to x:

$$F_x + \frac{dy}{dx}F_y + \frac{dp}{dx}F_p = 0$$

The condition for an inflection is

$$\frac{d^2y}{dx^2} = 0,$$

but since $p = dy/dx$ this implies $dp/dx = 0$, that is, inflections occur when

$$F_x + pF_y = 0.$$

The Legendre transformation in $\mathbb{R}^3$ is given by

$$x = P, y = XP - Y, p = X.$$

The Legendre transformation of an IDE (1.4) is another IDE

$$G(X, Y, P) = F(P, XP - Y, X) = 0$$

(although the Legendre transformation of a BDE is not in general another BDE). The Legendre transformation of BDEs are studied in [8, 23, 65].

The integral curves of the Legendre transformation of an IDE are dual to those of the original IDE (see, for example, [1]). That is, if the plane is thought of as being part of the projective plane $\mathbb{R}P^2$, then the curve representing all the tangent lines to a solution of an IDE $F = 0$ is a solution curve of the Legendre transformation $G = 0$, and conversely. This fact is a result of the fact that the Legendre transformation of the 1-form $dy - pdx$ is (minus) the 1-form $dY - PdX$, so the Legendre transform preserves the contact structure on $\mathbb{R}^3$ used in the method of study described in Section 1.3.2.

It is shown in [23] that the dual of a well-folded singularity is another well-folded singularity, that is, such points are self-dual. Recall that the dual of an inflection is a cusp. Since we know that folded singularities lie on the discriminant, that is, the cusp set of the solution curves, and that this set is a smooth curve, it follows that there is a smooth curve of inflection points tangent to the cusp set (the discriminant curve) at a well-folded singularity.

Recall that the property that a curve has an inflection is preserved by affine changes of coordinates. The Legendre transform of an IDE is preserved up to affine equivalence by an affine change of coordinates. Therefore, when considering the Legendre transform, it is normal to consider affine normal forms for IDEs.

In [23] folded singularities are classified in terms of the relative positions of the discriminant (cusp set), the locus of inflections and any separatrix. It is shown that these curves are generically parabolae. It is shown that the two-jet of an IDE (1.4) may be transformed, by affine changes of coordinates, to the form

$$p^2 + uxp + y + \frac{v}{4}x^2 + w_1xy + w_2y^2 = 0. \tag{1.7}$$

The index modulus is given by

$$\lambda = \frac{v - u(u+1)}{4}.$$

The following codimension 1 phenomena are taken into account in the classification:

(a) the lifted field has a non-elementary singularity;

(b) the discriminant, locus of inflections or a separatrix has an inflection at the singularity;

(c) some pair of the discriminant, locus of inflections or separatrices have > 2-point contact.

It is shown that there are 18 different cases: 8 saddles, 7 nodes and 3 foci, distinguished by the values of u, v. The exceptional sets are:

1. $v = 0$: separatrices inflectional or singular and also inflection curve inflectional;
2. $v = u^2$: cusp set inflectional;
3. $v = u^2 - 1$: inflection curve inflectional;
4. $u + 1 = 0$: inflection curve singular;
5. $v = u(u+1)$: saddle / node change and also inflection curve and cusp set have > 2-point contact;
6. $v = u(u+1) + \frac{1}{4}$: focus / saddle node change;
7. $v = -2(u+1)$: the union of this set and 1 and 5 corresponds to inflection curve / separatrices having > 2-point contact.

In general no qualitative change occurs as we cross the line $u + 1 = 0$ although this set is exceptional in the sense that the inflection set is not a smooth curve. The exceptional sets and the configurations of the curves of interest are illustrated in Figure 1.3.

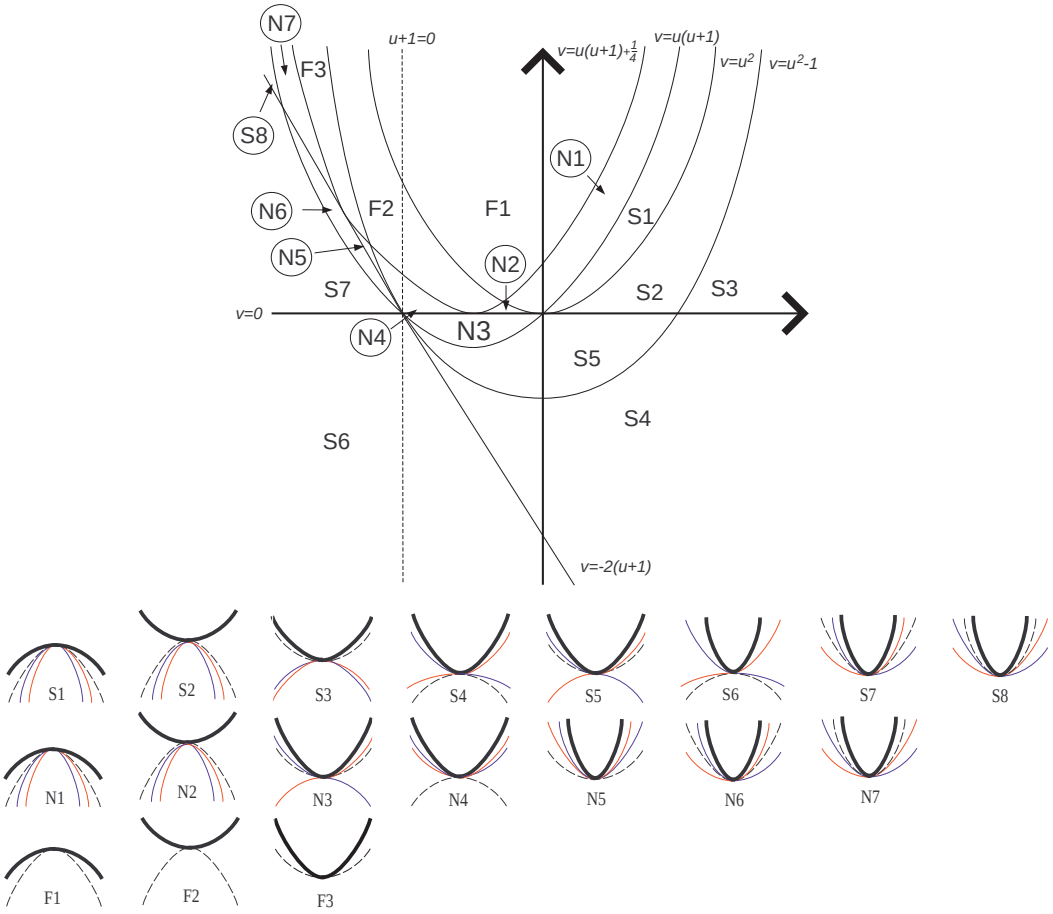

Figure 1.3: Partition of the (u, v)-plane.

It is also shown that the configurations at a well-folded singularity of an IDE with 2-jet affine equivalent to (1.7) and its dual are related by the involution

$$(u, v) \mapsto (-u - 1, v).$$

Remark 1.3.4 *Although the methods discussed here may be used to study BDEs on surfaces as well as in the plane, there is no reason why the Legendre transform or the locus of inflections should be of any significance, since the map from the parametrising plane to the surface is a diffeomorphism (that is, it does not preserve*

inflections). Curves on surfaces, however, have geodesic inflections*, which are the natural analogue of inflections. These are points where the curve crosses the plane spanned by its tangent line and the normal to the plane. It is shown in* [23] *that there is a curve of geodesic inflections at a folded singularity of a BDE on a surface, and that the two-jet of this curve coincides with that of the inflection curve in the parametrising plane. In other words, the same 18 cases occur.*

1.3.4 The blowing-up technique

Consider the case when the coefficients of the BDE all vanish simultaneously. The method of lifting the bi-valued direction field in the plane determined by a BDE to a single direction field on a surface $\tilde{M}$ may be used to establish the topological configurations of the integral curves of the BDE as long as the surface $\tilde{M}$ is smooth. The involution σ on $\tilde{M} \setminus (\{0\} \times \mathbb{R}P)$ which interchanges points with the same image under π is shown in [20, 66] to extend smoothly to $\tilde{M}$ when the coefficients a, b, c are smooth functions and the surface $\tilde{M}$ is smooth.

This method breaks down when $\tilde{M}$ is not smooth, as one needs to show that the involution σ extends smoothly to the whole of $\tilde{M}$ and this is not trivial.

An alternative method involves blowing-up the singularity, that is, making a coordinate change that replaces the singularity by a projective line (in practice, one simplifies calculations by considering charts for the projective line, leading to so-called directional blowing-up). The coordinate change is a diffeomorphism except at the origin. A explanation of the use of blowing-up methods in the study of vector fields (or BDEs) is given in [33].

Guíñez ([44]) used the blowing-up technique to study positive quadratic forms, that is, BDEs whose discriminant is an isolated point. The technique is extended by Tari in [64, 66] to cases where the discriminant is not an isolated point.

The BDE (1.5) may be written as the product of two 1-forms. Since we do not distinguish between non-zero multiples of BDEs, we may take these two 1-forms to be

$$ady + (b \pm \sqrt{b^2 - ac})dx.$$

The kernels of these 1-forms at each point of the plane determine the solution di-

rections, which are hence tangent to the vector fields

$$a\frac{\partial}{\partial x} + (-b + (-1)^i\sqrt{b^2 - ac})\frac{\partial}{\partial y}, i = 1, 2.$$

Following Guíñez's notation we denote by $\mathcal{F}_i(\omega)$, $i = 1, 2$ the two foliations by associated to the BDE (1.5). If ψ is a diffeomorphism and $\lambda(x, y)$ is a non vanishing real-valued function, then (see [44]) for $k = 1, 2$, we have that:

1. $\psi(\mathcal{F}_k(w)) = \mathcal{F}_k(\psi^*(\omega))$, if ψ is orientation preserving;
2. $\psi(\mathcal{F}_k(w)) = \mathcal{F}_{3-k}(\psi^*(\omega))$, if ψ is orientation reversing;
3. $\mathcal{F}_k(\lambda w) = \mathcal{F}_k(\omega)$, if $\lambda(x, y)$ is positive;
4. $\mathcal{F}_k(\lambda w) = \mathcal{F}_{3-k}(\omega)$, if $\lambda(x, y)$ is negative.

Example 1.3.1 *The most simple blowing-up is the standard polar blowing-up. We set*

$$(x, y) = (r\cos\theta, r\sin\theta).$$

In practice we use the x-direction blowing-up

$$x = u, y = uv$$

and the y-direction blowing-up

$$x = \tilde{u}\tilde{v}, y = \tilde{v}.$$

These are obtained by the changes of coordinates

$$(r, \theta) \mapsto (u, v) = (r\cos\theta, \tan\theta)$$

for $\theta \neq \pi/2, 3\pi/2$, and

$$(r, \theta) \mapsto (\tilde{u}, \tilde{v}) = (\cot\theta, r\sin\theta)$$

for $\theta \neq 0, \pi$ respectively. In the case of the y-direction blowing-up we consider only singularities at the origin, as all others will be detected by the x-direction blowing-up.

The x-direction (respectively y-direction) blowing-up is orientation preserving when $u > 0$ (respectively $\tilde{v} > 0$), and reversing when $u < 0$ (respectively $\tilde{v} < 0$). If a point (u_0, v_0) in the (u, v)-plane corresponds to a point with polar coordinates (r_0, θ_0), then the point $(-u_0, v_0)$ corresponds to the point $(r_0, \theta_0 + \pi)$. Similarly if a point $(\tilde{u}_1, \tilde{v}_1)$ corresponds to a point with polar coordinates (r_1, θ_1) then the point $(\tilde{u}_1, -\tilde{v}_1)$, corresponds to a point $(r_1, \theta_1 + \pi)$.

This method, while computational and less attractive than the contact geometrical approach described in Section 1.3.2, is effective when the BDEs have a discriminant having a worse-than-Morse singularity. We shall make use of it in Chapter 7, Chapter 8, and Chapter 9.

1.3.5 BDEs as points of the projective plane

We present now a way of considering BDEs that is used in [24]. Our aim is to understand the relationships between BDEs defined on surfaces that will be introduced in Chapter 2. Given a point $v \in \mathbb{R}^3$, where $v = (v_1, v_2, v_3)$, we denote by $[v] \in \mathbb{R}P^2$ the projectivisation $[v_1 : v_2 : v_3]$ of v.

Consider the set of BDEs with coefficients not all vanishing simultaneously. Such BDEs may be thought of as binary quadratic forms. As we do not distinguish between non-zero multiples of such forms, the set of BDEs with non-vanishing coefficients may be identified with the real projective plane $\mathbb{R}P^2$, where the BDE

$$\omega = ady^2 + 2bdxdy + cdx^2 = 0,$$

thought of as the form

$$ap^2 + 2bpq + cq^2$$

corresponds to the point $[a : b : c]$.

A conic Γ in $\mathbb{R}P^2$ is determined by a non-degenerate symmetric bilinear form $\mathcal{G}$ on $\mathbb{R}^3$:

$$\Gamma = \{[v] \in \mathbb{R}P^2 | \mathcal{G}(v, v) = 0\}.$$

Given any point $[v] \in \mathbb{R}P^2$, the *polar* of $[v]$ with respect to Γ is the set

$$\{[u] \in \mathbb{R}P^2 | \mathcal{G}(u, v) = 0\}.$$

As $\mathcal{G}$ is bilinear, the polar of any point $[v] \in \mathbb{R}P^2$ forms a line. Conversely, given any line in $\mathbb{R}P^2$, the polars of each point of the line intersect at a single point, which is called the polar of the line with respect to Γ.

The projective plane $\mathbb{R}P^2$ contains the conic Δ of singular forms given by $b^2 - ac$. We will consider pairs of forms and the pencils determined by them, which may be

thought of as lines in $\mathbb{R}P^2$. Any line in $\mathbb{R}P^2$ will have 0, 1 or 2 points on the conic of singular forms.

Three points in $\mathbb{R}P^2$ are said to form a *self-polar triangle* if the polar of any one of them is the line through the other two.

The following series of results follow from directly from the elementary geometry of the projective plane.

Proposition 1.3.1 ([24])

(a) *Let ω be a binary quadratic form with distinct real roots, determining a point in the projective plane $\mathbb{R}P^2$. The polar line of ω with respect to the conic of singular forms Δ consists of the line through the two forms which are the squares of the factors of ω. In other words, the tangents to the conic at these two points pass through ω. We refer to this intersection point as the polar form of the pencil. Conversely, given any pencil meeting the conic Δ, the corresponding polar form is the binary form whose factors are the repeated factors at the two singular members of the pencil.*

(b) *This polar form of the pencil is given by the classical Jacobian of any two of the forms in the pencil, that is, the 2×2 determinant of the matrix of partial derivatives of the forms with respect to p and q. The Jacobian is non-zero provided we have a genuine pencil, and is a square if and only if the forms have a factor in common.*

(c) *Fixing two forms*

$$\omega = ap^2 + bpq + cq^2$$
$$\Omega = Ap^2 + Bpq + Cq^2$$

we write $D(\alpha : \beta)$ for the discriminant of $\alpha\omega + \beta\Omega$; this is another binary quadratic form. We can write it as

$$D(\omega)\alpha^2 + E(\omega, \Omega)\alpha\beta + D(\Omega)\beta^2,$$

where $D(\omega) = b^2 - 4ac$, $D(\Omega) = B^2 - 4AC$, and $E(\omega, \Omega) = 2(bB - 2aC - 2Ac)$.

The associated polar point of the pencil, the Jacobian, determined by ω, Ω *is*

$$Jac(\omega,\Omega) = \begin{vmatrix} \partial\omega/\partial p & \partial\omega/\partial q \\ \partial\Omega/\partial p & \partial\Omega/\partial q \end{vmatrix} = (aB - Ab)p^2 + 2(aC - Ac)pq + (bC - Bc)q^2.$$

(d) *Pairs of forms with the term* $E(\omega,\Omega)$ *above zero are said to be* apolar. *This is equivalent to the condition that the corresponding four roots harmonically separate each other, or that the forms lie on each others polars with respect to the conic* Δ*, that is, are conjugate. The Jacobian of any two forms is apolar with respect to all the elements of the pencil determined by them.*

(e) *Three forms determine a self-polar triangle with respect to the conic* Δ *if and only if each is the Jacobian of the other two. There are a variety of ways of obtaining self-polar triples. Any form* ω *determines a polar line. Choose an arbitrary form say* Ω *on the line; this has a polar line which passes through* ω*. Consider the intersection point of these two polar lines; this gives a third form* μ*, with*

$$\{\omega,\ \Omega,\ \mu\}$$

self-polar. Any self-polar triple arises in this way. Also if ω, Ω *are conjugate, then the triple*

$$\{\omega,\ \Omega,\ Jac(\omega,\Omega)\}$$

is self-polar. Finally, if the vertices of a quadrangle lie on Δ*, then the diagonal triangle (the triangle whose vertices are intersections of the lines joining distinct pairs of distinct points) is self-polar.*

(f) *The discriminants, the invariant* E*, and the Jacobian of a pair of forms* ω,Ω *are related as follows:*

$$Jac^2(\omega,\Omega) - 4D(\Omega)\omega^2 - 4D(\omega)\Omega^2 + 4E(\omega,\Omega)\omega\Omega = 0.$$

Chapter 2

Geometrical background

In this chapter we define the geometric objects with which this thesis is concerned.

2.1 Elementary geometry of smooth surfaces

Given an oriented surface $S \subset \mathbb{R}^3$ with unit normal $\mathbf{n}(p)$ at each point $p \in S$ we have the Gauss map

$$\begin{aligned} N : S \to &\quad S^2 \\ p \mapsto &\quad \mathbf{n}(p). \end{aligned}$$

The Weingarten map (also known as the shape operator)

$$W_p = -dN(p) : T_pS \to T_{N(p)}S^2$$

is a self-adjoint operator, and can be thought of as an automorphism of T_pS.

The Gaussian curvature K is given by $K = \det(W_p)$ and the arithmetic mean curvature H is given by $H = \mathrm{tr}(W_p)/2$. The eigenvalues of W_p are the *principal curvatures* at p and are denoted κ_1 and κ_2, and the corresponding eigenvectors are the *principal directions*. Points where the principal curvatures are equal (and hence every direction is a principal direction) are called *umbilic points*.

The first and second fundamental forms of the surface are the quadratic forms on the tangent plane given by $\mathrm{I}(u, v) = u \cdot v$ and $\mathrm{II}(u, v) = u \cdot W_p(v)$ respectively.

If S is parametrised by $\mathbf{r}(x, y)$, with $(x, y) \in U$, where U is an open subset of $\mathbb{R}^2$, then the coefficients of the first (respectively second) fundamental form E, F, G

(respectively $l, m, n,$) are given by

$$E = \mathbf{r}_x \cdot \mathbf{r}_x, \quad F = \mathbf{r}_x \cdot \mathbf{r}_y, \quad G = \mathbf{r}_y \cdot \mathbf{r}_y,$$

$$l = W_p(\mathbf{r}_x) \cdot \mathbf{r}_x = \mathbf{r}_{xx} \cdot \mathbf{n}, \quad m = W_p(\mathbf{r}_x) \cdot \mathbf{r}_y = \mathbf{r}_{xy} \cdot \mathbf{n}, \quad n = W_p(\mathbf{r}_y) \cdot \mathbf{r}_y = \mathbf{r}_{yy} \cdot \mathbf{n}.$$

In terms of the coefficients of the first and second fundamental form the Gaussian and mean curvatures of the surface are given by

$$K = \frac{ln - m^2}{EG - F^2}, \qquad H = \frac{Gl + En - 2Fm}{2(EG - F^2)}.$$

The sectional curvature k_n at $p \in S$ in a direction $v \in T_pS$ is the curvature of the plane curve that is the intersection of S and the plane spanned by $\mathbf{n}(p)$ and v. The sectional curvature in a direction $v \in T_pS$ is given by the formula $k_n = \mathrm{II}(v, v)/\mathrm{I}(v, v)$, that is, if $(\cos\theta, \sin\theta)$ is a direction on a surface with respect to some choice of x and y-axes, then we have

$$k_n = \frac{l\cos^2\theta + 2m\cos\theta\sin\theta + n\sin^2\theta}{E\cos^2\theta + 2F\cos\theta\sin\theta + G\sin^2\theta}. \tag{2.1}$$

The geodesic torsion τ_g at $p \in S$ in a direction $v \in T_pS$ is the torsion of the geodesic passing through p in the direction v. The geodesic torsion in a direction $v \in T_pS$ is given by the formula $\tau_g = \mathrm{II}(v, v^\perp)/\mathrm{I}(v, v)$ where $v^\perp$ denotes a direction perpendicular to v, that is, if $(\cos\theta, \sin\theta)$ is a direction on a surface with respect to some choice of x and y-axes, then we have

$$\tau_g = \frac{l\cos\theta\sin\theta - m(\cos^2\theta - \sin^2\theta) - n\sin\theta\cos\theta}{E\cos^2\theta + 2F\cos\theta\sin\theta + G\sin^2\theta}. \tag{2.2}$$

A principal coordinate system is one where the x- and y-axes are always the principal directions. In a principal coordinate system we have

$$F = 0, \;\; m = 0, \;\; l = E\kappa_1, \;\; n = G\kappa_2.$$

We may also choose $E = G = 1$ at any given point. Then, at this point, we have

$$k_n = \kappa_1\cos^2\theta + \kappa_2\sin^2\theta, \;\; \tau_g = (\kappa_1 - \kappa_2)\sin\theta\cos\theta, \;\; K = \kappa_1\kappa_2, \;\; H = \frac{\kappa_1 + \kappa_2}{2}.$$

2.1.1 Generic properties of surfaces in $\mathbb{R}^3$

The flat geometry (that is, geometrical properties that may be defined in terms of contact with lines and / or planes) of smooth surfaces in $\mathbb{R}^3$ is considered in, for example, [9, 16, 17, 19, 58]. Such properties are preserved by affine changes of coordinates.

In general S has open hyperbolic and elliptic regions, where the Gaussian curvature K is respectively negative and positive, separated a smooth curve where $K = 0$, known as the parabolic set.

The hyperbolic (respectively elliptic) region is alternatively characterised as the set of points at which the height function in the direction of the unit normal to the surface has an A_1^-- (respectively A_1^+-) singularity. The parabolic set is the set of points at which the height function in the direction of the unit normal has an A_2-singularity. The height function in the normal direction generally has an A_3-singularity at isolated points on the parabolic set. These special points are known as cusps of Gauss, and they have many alternative characterisations; see [5]. The parabolic set corresponds to a cuspidal edge on the dual surface, and the cusps of Gauss correspond to swallowtail points on the dual surface.

The height function also has multi-local singularities. In particular, along smooth curves the tangent plane to the surface is also tangent to the surface at another point (such tangent planes are known as bitangent planes). The closure of the locus of points of contact with bitangent planes is known as the conodal curve (see, for example, [61]). The conodal curve is the locus of points where the height function has an A_1^2-singularity, and corresponds to a curve of transverse self-intersection points on the dual surface. The conodal curve is tangent to the parabolic set at a cusp of Gauss.

The geometry of smooth surfaces that is connected to contact with circles and spheres has been much studied, see for example [18, 49, 59]. In particular, umbilic points occur generically at isolated points in the elliptic region.

Throughout the thesis S will denote a smooth surface in $\mathbb{R}^3$. We will generally parametrise S in Monge form

$$(x, y, f(x, y))$$

and choose a principal coordinate system (that is, we choose the coordinate axes to be tangent to the lines of curvature at the origin). We will write

$$\begin{aligned} j^4 f(x,y) = \; & \frac{1}{2}(\kappa_1 x^2 + \kappa_2 y^2) + \frac{1}{6}(a_{30}x^3 + 3a_{31}x^2 y + 3a_{32}xy^2 + a_{33}y^3) \\ & + \frac{1}{24}(a_{40}x^4 + 4a_{41}x^3 y + 6a_{42}x^2 y^2 + 4a_{43}xy^3 + a_{44}y^4), \end{aligned} \tag{2.3}$$

where κ_1, κ_2 are the principal curvatures at the origin. Calculating the coefficients E, F, G, l, m, n of the first and second fundamental forms we have that

$$\begin{aligned} j^2 E = \; & 1 + \kappa_1 x^2, \\ j^2 F = \; & \kappa_1 \kappa_2 xy, \\ j^2 G = \; & 1 + \kappa_2 y^2, \\ j^2 l = \; & \kappa_1 + a_{30}x + a_{31}y + (\frac{1}{2}a_{40} - \kappa_1^3)x^2 + a_{41}xy + (\frac{1}{2}a_{42} - \kappa_1\kappa_2^2)y^2, \\ j^2 m = \; & a_{31}x + a_{32}y + \frac{1}{2}a_{41}x^2 + a_{42}xy + \frac{1}{2}a_{43}y^2, \\ j^2 n = \; & \kappa_2 + a_{32}x + a_{33}y + (\frac{1}{2}a_{42} - \kappa_2\kappa_1^2)x^2 + a_{43}xy + (\frac{1}{2}a_{44} - \kappa_2^3)y^2. \end{aligned}$$

Should the origin be a parabolic point, we will set $\kappa_1 = 0$, and should it be a cusp of Gauss we will set $\kappa_1 = a_{30} = 0$.

At umbilic points following Bruce ([18]) will write

$$j^3 f(x,y) = \frac{\kappa}{2}(x^2 + y^2) + \mathrm{Re}(z^3 + \beta z^2 z)$$

where $z = x + iy$ and β is a complex number.

2.1.2 Conjugate directions

Definition 2.1.1 *Two directions $v, \bar{v} \in T_pS$ are conjugate if $\mathrm{II}_p\ (v, \bar{v}) = 0$, where $\mathrm{II}_p(u, v) = W_p(u) \cdot v$.*

If $p \in S$ is a non-umbilic point then any direction $v \in T_pS$ has a unique conjugate direction $\bar{v}$.

Geometrically, one interprets conjugacy as follows. Given an (affine) conic section and a direction, then the lines parallel to the direction intersect the conic in either 0 or 2 points, or a single repeated point. When there are two distinct points of intersection, their midpoints are colinear, and determine the conjugate direction. For the ellipse $x^2/a^2 + y^2/b^2 = 1$ (respectively the hyperbola $x^2/a^2 - y^2/b^2 = 1$)

the directions parallel to the lines $y = ux$, $y = vx$ are conjugate if and only if $uv = -b^2/a^2$ (respectively $uv = b^2/a^2$).

At any point on a surface, the *Dupin indicatrix* is the conic approximation of the intersection of the surface with a small translation of the tangent plane in the normal direction. Note that at an elliptic point this translation needs to be in the right direction, at a hyperbolic point one may choose the direction arbitrarily, and at a parabolic point the Dupin indicatrix is the degenerate conic consisting of a pair of parallel lines. Two directions on a surface are conjugate in the sense of Definition 2.1.1 if and only if they are conjugate with respect to the Dupin indicatrix. The following remarks appear in [24].

Remarks 2.1.2 *1. The notion of conjugacy is invariant under affine and inversive transformations.*

2. If v and $\bar{v}$ are conjugate directions then $W_p(v)$ and $\bar{v}$ are orthogonal.

3. The angle between conjugate directions v, $\bar{v}$ at a point p and $W_p(v)$, $W_p(\bar{v})$ is equal (respectively supplementary) if p is a hyperbolic (respectively elliptic) point.

4. For any $v \in T_pS$ (excluding asymptotic directions at a parabolic point), the signed angle between v and $\bar{v}$ is α where

$$\sin\alpha = \frac{W_p(v)\cdot v}{|W_p(v)||v|}.$$

5. The sum of the radii of curvature in conjugate (non-asymptotic) directions is constant.

Further properties of conjugate directions are given in, for example, [24].

The alternative definition of conjugacy in the plane given in Proposition 2.1.1 does not appear to have been identified before.

Proposition 2.1.1 *Consider the plane $\mathbb{R}^2$ with the origin fixed, together with a fixed line at infinity. The origin is the polar of the line at infinity with respect to any hyperbola with asymptotes intersecting at the origin, or any ellipse with the origin as its centre.*

Given such a conic section, let l be a line through the origin. If l intersects the line at infinity at a point p then the polar line of p is parallel to the conjugate direction to l.

Proof: Consider a hyperbola with asymptotes intersecting at the origin. By a rotation of the coordinate axes we may take this to be the hyperbola

$$\frac{x^2}{a^2} - \frac{y^2}{b^2} = 1.$$

We include a line at infinity by choosing homogeneous coordinates $[x : y : z]$, the line at infinity being $z = 0$. The hyperbola is then given by

$$b^2x^2 - a^2y^2 = a^2b^2z^2.$$

Hence the hyperbola is the conic given by the set of points that are self-orthogonal with respect to the symmetric bilinear form that has matrix

$$\begin{pmatrix} -b^2 & 0 & 0 \\ 0 & a^2 & 0 \\ 0 & 0 & (ab)^2 \end{pmatrix}.$$

The origin, in the homogeneous coordinates, is $[0 : 0 : 1]$. The polar of the origin is the set of points $[\alpha : \beta : \gamma]$ where

$$\begin{pmatrix} \alpha & \beta & \gamma \end{pmatrix} \begin{pmatrix} -b^2 & 0 & 0 \\ 0 & a^2 & 0 \\ 0 & 0 & (ab)^2 \end{pmatrix} \begin{pmatrix} 0 \\ 0 \\ 1 \end{pmatrix} = 0,$$

that is, those points of the form $[1 : t : 0]$ for all $t \in \mathbb{R}$. This is the line at infinity, which establishes the first assertion.

Consider a direction in the plane. Suppose that the line through the origin in this direction is given by $y = ux$. In homogeneous coordinates this is the line $[x : ux : 1]$, that is, for $x \neq 0$, the line $[1 : u : 1/x]$, which meets the line at infinity at the point $[1 : u : 0]$. The polar of this point with respect to the conic is the set of points $[\tilde{\alpha} : \tilde{\beta} : \tilde{\gamma}]$ where

$$\begin{pmatrix} \tilde{\alpha} & \tilde{\beta} & \tilde{\gamma} \end{pmatrix} \begin{pmatrix} -b^2 & 0 & 0 \\ 0 & a^2 & 0 \\ 0 & 0 & (ab)^2 \end{pmatrix} \begin{pmatrix} 1 \\ u \\ 0 \end{pmatrix} = 0,$$

that is, those points of the form $[ua^2 : b^2 : sb^2]$ where $s \in \mathbb{R}$. This is the line through the origin given by $y = b^2x/ua^2$. This direction is conjugate to that parallel to the line $y = ux$, which establishes the second assertion.

The case that the conic is an ellipse centred at the origin follows by similar reasoning. □

Remark 2.1.3 *This definition breaks down when the conic is a parabola, as the polar of the line at infinity lies on the line at infinity. This is not a problem, however, when we are concerned with conjugate directions on a smooth surface, as the Dupin indicatrix is never a parabola.*

2.2 Foliations of smooth surfaces

There are three intimately related pairs of foliations on an embedded surface in the Euclidean space $\mathbb{R}^3$: the lines of curvature, the asymptotic curves and the characteristic curves (see for example [24]). It is this triple of pairs of foliations that the thesis is primarily concerned with. We give definitions of these pairs of foliations in this Section.

In all illustrations, following Porteous (see [59]), we shall distinguish between the two foliations in any given pair by drawing one in red curves and the other in blue curves.

2.2.1 The asymptotic curves, the characteristic curves and the lines of curvature

Lines of curvature

The lines of curvature are the integral curves of the principal directions, which were defined above as the eigenvectors of the Weingarten map. These directions may also be defined via conjugacy.

Definition 2.2.1 *The principal directions at a point are the unique pair of orthogonal conjugate directions.*

At any non-umbilic point there are two principal directions. At umbilic points all directions are principal.

Remarks 2.2.2 *1. The principal directions may be alternatively characterised as those directions in which the sectional curvature is extremal or those directions in which the geodesic torsion is zero.*

2. Principal directions may also be defined via contact with circles, see [49].

Proposition 2.2.1 *The lines of curvature are the integral curves of the BDE*

$$(Gm - Fn)dy^2 + (Gl - En)dxdy + (Fl - Em)dx^2 = 0. \tag{2.4}$$

The discriminant of (2.4) *is the umbilic points of the surface.*

The lines of curvature are defined everywhere away from umbilics and form an orthogonal net.

The configurations of the lines of curvature at umbilic points were first drawn by Darboux, and rigorous studies were carried out in [12, 62]. The coefficients of the principal BDE (2.4) all vanish at umbilic points, and the discriminant of (2.4) has an A_1^+-singularity (that is, a Morse isolated point singularity). There are three stable topological models of the integral curves of BDEs with discriminants of this type: star, monstar and lemon (see [20]). These are illustrated in Figure 2.1.

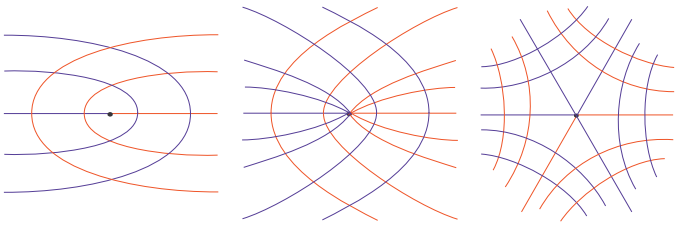

Figure 2.1: Integral curves of a BDE with vanishing coefficients and discriminant having an A_1-singularity: lemon (left), monstar (centre) and star (right).

If a surface is parametrised at an umbilic point in the form given in Section 2.1, then the singularity of the principal BDE (2.4) is of type star if the complex number β lies inside the circle $|\beta| = 3$, of type lemon if β is outside the hypercycloid $\beta = -3(2e^{i\theta} + e^{2i\theta})$, and of type monstar if β lies in the remaining regions of the complex plane. This partition of the complex plane is shown in Figure 2.2 (right).

Asymptotic curves

Definition 2.2.3 *An asymptotic direction is a self-conjugate direction. The asymptotic curves on a surface are the integral curves of the asymptotic directions.*

There are two real asymptotic directions at hyperbolic points, one repeated asymptotic direction at parabolic points, and no real asymptotic directions at elliptic points.

Remarks 2.2.4 *There are many alternative characterisations of the asymptotic directions; we adopt Definition 2.2.3 as it is most appropriate to the subsequent work in the thesis. The asymptotic directions may also be defined to be:*

1. *those directions in which the surface has zero sectional curvature.*
2. *those directions in which the geodesic torsion is equal to* $\sqrt{-K}$.
3. *those directions with tangent line having at least* 3*-point contact with the surface.*
4. *those directions in which the orthogonal projection of the surface to a plane has a cusp singularity (that is, it is* $\mathcal{A}$*-equivalent to* $(x, x^3 + xy)$ *([58])).*

Proposition 2.2.2 *The asymptotic curves are the integral curves of the BDE*

$$ndy^2 + 2mdydx + ldx^2 = 0. \tag{2.5}$$

The discriminant of (2.5) *is the parabolic set, and* (2.5) *has folded singularities at cusps of Gauss.*

The asymptotic curves form a pair of transverse foliations in the hyperbolic region and a family of cusps at the parabolic set, except at the cusps of Gauss, where the unique asymptotic direction is tangent to the parabolic set.

The geometry of the surface connected to contact with lines is studied in, for example, [9, 17, 19]. In particular, there are various other geometric features of the surface that are related to the asymptotic curves. As we have seen, one may characterise the hyperbolic region as the set of points at which two distinct asymptotic directions exist, the parabolic set as the set of points at which one repeated

asymptotic directions exists, and the elliptic region as the set of points at which no real asymptotic directions exist. Furthermore, the cusps of Gauss may be characterised as those isolated parabolic points at which the unique asymptotic direction is tangent to the parabolic set.

There is generically a smooth curve of points at which a line in an asymptotic tangent direction has at least 4-point contact with the surface. This is the *flecnodal curve*. This may be alternatively characterised as the locus of geodesic inflections of the asymptotic curves. Furthermore, it is shown in [23] that the pull-back to any parametrising plane of this curve is the inflection curve of the asymptotic BDE in that plane.

The flecnodal curve is tangent to the parabolic set at a cusp of Gauss. There are isolated points on the flecnodal curves called *biflecnodes* at which the asymptotic tangent line has 5-point contact with the surface. There are also isolated points in the hyperbolic region known as *hyperbonodes* where the flecnodal curve intersects itself, or alternatively, the surface has 4-point contact with a line in both asymptotic tangent directions (see, for example, [71]).

Remark 2.2.5 *The asymptotic curves are defined in terms of contact between the surface and lines, that is, flat test-submanifolds. Consequently they are a projective property of the surface, that is, they may be defined on a surface in a projective* 3*-space and are invariant under projective transformations. The same is true of all related features (the parabolic set, the flecnodal curves, the cusps of Gauss, biflecnodes and hyperbonodes). The conodal curve also has this property, as it is defined in terms of contact with planes.*

Characteristic curves

The asymptotic curves and the lines of curvature have been much studied. At non-umbilic elliptic points there is a well-defined pair directions known as the characteristic directions, that are in many ways analogous to the asymptotic curves, that have been much less studied. These curves are defined in [34, 51, 60], and studied more recently in [14, 24, 41, 42].

Definition 2.2.6 *The characteristic directions at a point are the unique pair of conjugate directions with extremal included angle.*

There are two real characteristic directions at non-umbilic elliptic points, one repeated characteristic direction at parabolic points, and no real characteristic directions at hyperbolic points. At umbilic points, all directions are characteristic.

Like the asymptotic curves, the characteristic directions may be alternatively defined via sectional curvature: they are those directions in which the sectional curvature is equal to H/K, the harmonic mean curvature of the surface (indeed, they are called harmonic mean curvature lines in [41]). There is not yet, however, a definition of the characteristic curves analogous to that of the asymptotic curves as those directions in which the surface has $\geq$ 3-point with its tangent line, that is, a direction defined via contact with a model-submanifold.

Proposition 2.2.3 *The BDE which gives the characteristic directions is*

$$\begin{aligned}(2m(Gm-Fn)-n(Gl-En))dy^2+\\ 2(m(Gl+En)-2Fln)dydx+\\ (l(Gl-En)-2m(Fl-Em))dx^2=0.\end{aligned} \tag{2.6}$$

The discriminant of (2.6) *is the parabolic set and umbilic points, and the singularities of* (2.6) *are the cusps of Gauss and umbilic points.*

The local behaviour of the characteristic curves at umbilic points is studied in [24], and global properties are considered in [41]

There are a number of properties of the characteristic curves that show that they are the analogue in the elliptic region of the asymptotic curves in the hyperbolic region.

Remarks 2.2.7 *Some elementary similarities between the asymptotic and characteristic curves include the following.*

1. *If (away from umbilic points) we choose a principal coordinate system, then the asymptotic BDE* (2.5) *becomes*

$$G\kappa_2 dy^2 + E\kappa_1 dx^2 = 0$$

and the characteristic BDE (2.6) *becomes*

$$G\kappa_2 dy^2 - E\kappa_1 dx^2 = 0,$$

that is, any any given point the asymptotic directions (respectively characteristic directions) are inclined at an angle of $\pm\tan^{-1}(\sqrt{-\kappa_1/\kappa_2})$ *(respectively* $\pm\tan^{-1}(\sqrt{\kappa_1/\kappa_2})$*) to a principal direction.*

2. *At parabolic points the single asymptotic and characteristic directions coincide and is a principal direction.*

3. *At a cusp of Gauss the value of the index moduli* λ *(see Section 1.3) of the asymptotic and characteristic BDEs* (2.5) *and* (2.6) *have opposite sign but equal absolute value* ([24])*. In particular if the asymptotic curves have a well-folded saddle then the characteristic curves have a well-folded node or focus, and vice-versa.*

The similarities between the asymptotic curves and the characteristic curves may be understood by considering their BDEs as points in the projective plane $\mathbb{R}P^2$. At any point the BDEs of the asymptotic and characteristic curves are apolar with respect to the pencil connecting them, and the polar of this pencil is the principal BDE, that is, these three BDEs form a self-polar triangle.

An important difference between the asymptotic curves and the characteristic curves is that the latter are not projectively invariant.

At umbilic points the coefficients of the characteristic BDE (2.6) vanish. The discriminant of (2.6) has an A_1^+-singularity. The configurations of the characteristic curves at umbilic points are established in [24].

If a surface is parametrised at an umbilic point in the form given in Section 2.1, then the singularity of the characteristic BDE (2.6) is of type star if the complex number β lies inside the circle $|\beta| = 3$, of type lemon if β is outside the hypercycloid $\beta = 3(2e^{i\theta} + e^{-2i\theta})$, and of type monstar if β lies in the remaining regions of the complex plane. This partition of the complex plane is shown in Figure 2.2 (left).

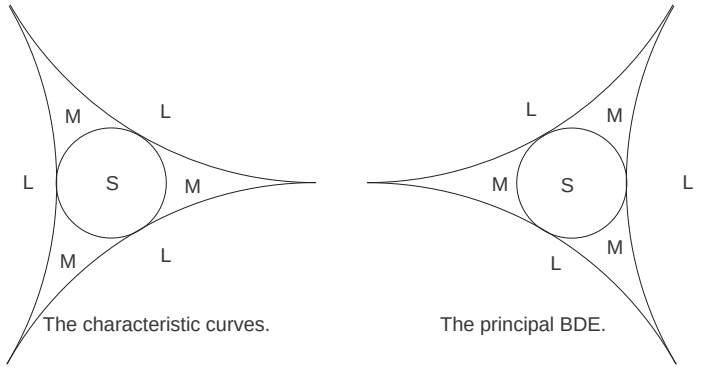

Figure 2.2: Partition of the β-plane: the characteristic BDE (left) and the principal BDE P (right).

2.2.2 The conjugate and reflected curve congruences

Further evidence that the characteristic curves are significant geometric objects worthy of further investigation is provided by two natural 1-parameter families of BDEs on surfaces, which are defined in [24, 36].

Observe that the notion of conjugacy gives rise to an involution C , the projectivised tangent plane to the surface at the point $p \in S$, $v \mapsto \bar{v}$. There is another involution on PT_pS, which we denote R, which is simply reflection in (either of) the principal directions. The convolution of C and R is another involution and $C \circ R = R \circ C$ ([24]). The asymptotic, principal and characteristic directions at each point p are the fixed points of the involutions C, R and $C \circ R$ respectively.

The conjugate curve congruence, C_α, is first defined in [36]. It consists of a natural 1-parameter family of BDEs that interpolates between asymptotic BDE and the principal BDE.

Definition 2.2.8 ([36]) *Let PTS denote the projective tangent bundle to S, and define $\Theta : PTS \to [-\frac{\pi}{2}, \frac{\pi}{2}]$ by $\Theta(p, v) = \alpha$ where α denotes the oriented angle between a direction v and the corresponding conjugate direction $\bar{v} = C(v)$. Note that Θ is not well defined at points corresponding to asymptotic directions at parabolic points. The conjugate congruence, for a fixed α, is defined to be $\Theta^{-1}(\alpha)$ which we denote $\mathcal{C}_\alpha$.*

If we consider BDEs as points in the projective plane $\mathbb{R}P^2$, the conjugate curve

congruence is a natural parametrisation of the pencil joining the asymptotic and principal BDEs. Observe that $\mathcal{C}_0$ is the set of all asymptotic directions and $\mathcal{C}_{\pm\frac{\pi}{2}}$.

Proposition 2.2.4 ([36]) *The conjugate curve congruence $\mathcal{C}_\alpha$ of a parametrised surface is given by the BDE*

$$\begin{aligned}(\sin\alpha(Gm-Fn)-n\cos\alpha\sqrt{EG-F^2})dy^2+\\ (\sin\alpha(Gl-En)-2m\cos\alpha\sqrt{EG-F^2})dydx+\\ (\sin\alpha(Fl-Em)-l\cos\alpha\sqrt{EG-F^2})dx^2=0.\end{aligned} \tag{2.7}$$

The discriminant of $\mathcal{C}_\alpha$, which we denote Δ_C^α, is given by

$$H^2(x,y)\sin^2\alpha - K(x,y) = 0,$$

where H is the mean curvature and K is the Gaussian curvature.

Away from umbilics the BDE $\mathcal{C}_\alpha$ can be written, with respect to a coordinate system given by the lines of curvature, by

$$G\kappa_2\cos\alpha dy^2 + \sqrt{EG}(\kappa_2-\kappa_1)\sin\alpha dydx + E\kappa_1\cos\alpha dx^2 = 0.$$

In [24] the congruence replacing C with $R\circ C$ is considered. This is a natural 1-parameter family of BDEs that interpolates between characteristic BDE and the principal BDE, that is, a natural parametrisation of the pencil in $\mathbb{R}P^2$ that joins the principal and characteristic BDEs.

Definition 2.2.9 ([24]) *Let $\Phi : PTS \to [-\frac{\pi}{2},\frac{\pi}{2}]$ by $\Phi(p,v)=\alpha$ where α denotes the oriented angle between a direction v and $R(\bar{v})(=R\circ C(v))$. Note that Φ is not well defined at umbilics. Then the reflected conjugate curve congruence, for a fixed α, is defined to be $\Phi^{-1}(\alpha)$ which we denote $\mathcal{R}_\alpha$.*

If we consider BDEs as points in the projective plane $\mathbb{R}P^2$, the conjugate curve congruence is a natural parametrisation of the pencil joining the asymptotic and principal BDEs. Observe that $\mathcal{R}_0$ is the set of all characteristic directions and $\mathcal{R}_{\pm\frac{\pi}{2}}$.

Proposition 2.2.5 ([24]) *The BDE of the reflected conjugate curve congruence on*

a parametrised surface is

$$\begin{aligned}((2m(Gm-Fn)-n(Gl-En))\cos\alpha-(Gm-Fn)\frac{2Fm-Gl-En}{\sqrt{EG-F^2}}\sin\alpha)dy^2+\\ (2(m(Gl+En)-2Fln)\cos\alpha-(Gl-En)\frac{2Fm-Gl-En}{\sqrt{EG-F^2}}\sin\alpha)dydx+\\ ((l(Gl-En)-2m(Fl-Em))\cos\alpha-(Fl-Em)\frac{2Fm-Gl-En}{\sqrt{EG-F^2}}\sin\alpha)dx^2=0.\end{aligned} \tag{2.8}$$

The discriminant consists umbilic points together with the set of

$$H^2(x,y)\sin^2\alpha+K(x,y)\cos^2\alpha=0,$$

which we denote by Δ_R^α.

Away from umbilics the equation for $\mathcal{R}_\alpha$ *is given, in the principal co-ordinate system, by*

$$G\kappa_2\cos\alpha dy^2-\sqrt{EG}(\kappa_2+\kappa_1)\sin\alpha dydx-E\kappa_1\cos\alpha dx^2=0.$$

When we consider BDEs as points in the projective plane $\mathbb{R}P^2$ these families correspond to natural parametrisations of the pencils of forms that join the asymptotic and principal BDEs (in the case of $\mathcal{C}_\alpha$) and characteristic and principal BDEs (in the case of $\mathcal{R}_\alpha$. There are symmetries between these families of BDEs and their integral curves, discussed in [24], which stem from the construction in $\mathbb{R}P^2$.

Properties of these two families of BDEs give further insight into the intimate relationship between the asymptotic curves, characteristic curves and the lines of curvature. Some of these are given in Remarks 2.2.10. Further properties are given in [24]. The singularities of these BDEs are studied in [14].

Remarks 2.2.10 *1. The discriminant curves* Δ_C^α *(respectively* Δ_R^α*) occur in the non-hyperbolic (respectively non-elliptic) region of the surface, and foliate this region. Furthermore* Δ_C^0 *and* Δ_R^0 *are the parabolic set,* $\Delta_C^{\pm\frac{\pi}{2}}$ *is the umbilic points, and* $\Delta_R^{\pm\frac{\pi}{2}}$ *is the curve* $H=0$*, that is the set of points where the arithmetic mean curvature of the surface vanishes.*

2. In general $\mathcal{C}_\alpha\neq\mathcal{C}_{-\alpha}$ *and* $\mathcal{R}_\alpha\neq\mathcal{R}_{-\alpha}$*, however* $\Delta_C^\alpha=\Delta_C^{-\alpha}$ *and* $\Delta_R^\alpha=\Delta_R^{-\alpha}$.

3. On Δ_C^α *(respectively* Δ_R^α*) the single direction defined by* $\mathcal{C}_\alpha$ *(respectively* $\mathcal{R}_\alpha$*) is one of the characteristic (respectively asymptotic) directions. The other*

characteristic (respectively asymptotic) direction at those points is the single direction defined by $\mathcal{C}_{-\alpha}$ (respectively $\mathcal{R}_{-\alpha}$).

Chapter 3

The characteristic curves on smooth surfaces

The folded singularities of the characteristic BDE are the cusps of Gauss. These isolated points on the parabolic set where the unique asymptotic direction is tangent to the parabolic set are aspects of the flat differential geometry of the surface. In this chapter we examine the behaviour of the characteristic curves in a neighbourhood of a cusp of Gauss. We show that certain properties of the characteristic curves in such a neighbourhood are invariant under projective transformations of $\mathbb{R}^3$, and associate a projective invariant to these points following Uribe-Vargas in [71].

3.1 Projective properties of cusps of Gauss

The asymptotic BDE (2.5) and characteristic BDE (2.6) give rise to three curves of interest on S at a cusp of Gauss: the parabolic set (which is the discriminant of equation (2.5) and part of the discriminant of equation (2.6)), and the mapping to S of the loci of inflections of the solution curves to the two BDEs (the flecnodal curve in the case of (2.5)).

A further curve of interest at a cusp of Gauss is the conodal curve, that is, the closure of the locus of points of contact of S with its bitangent planes (see Section 2.1).

We parametrise S in Monge form $(x, y, f(x, y))$ where f is as in (2.3), and choose

$\kappa_1 = 0$, $\kappa_2 \neq 0$ at parabolic points, and $a_{30} = 0$ at a cusp of Gauss.

Proposition 3.1.1 *Suppose that the origin is a cusp of Gauss. Then:*

(a) *the parabolic set is given by*

$$y = \frac{2a_{31}^2 - a_{40}\kappa_2}{2a_{31}\kappa_2}x^2 + h.o.t.;$$

(b) *the characteristic inflection curve is given by*

$$y = \frac{(4a_{31}^2 - a_{40}\kappa_2)(5a_{31}^2 - 2a_{40}\kappa_2)}{2a_{31}^3\kappa_2}x^2 + h.o.t.;$$

(c) *the flecnodal curve is given by*

$$y = \frac{a_{40}(3a_{31}^2 - 2a_{40}\kappa_2)}{18a_{31}^3}x^2 + h.o.t.;$$

(d) *the conodal curve is given by*

$$y = -\frac{a_{40}}{6a_{31}}x^2 + h.o.t..$$

Proof: As the origin is a cusp of Gauss, we can set $\kappa_1 = 0$ (the origin is a parabolic point) and $a_{30} = 0$ (the asymptotic direction at the origin is tangent to the parabolic set). We also assume $a_{31} \neq 0$ and $\kappa_2 \neq 0$, that is, the parabolic set is smooth and the origin is not a flat umbilic.

We set $p = dy/dx$ and write the characteristic BDE (2.6) as $\Omega(x, y, p) = 0$ and the asymptotic BDE (2.5) as $\Psi(x, y, p) = 0$. We have

$$\begin{aligned} j^2\Omega = \quad & \kappa_2^2p^2 + 2a_{31}\kappa_2xp + 2a_{32}\kappa_2yp - a_{31}\kappa_2y - \frac{1}{2}(a_{40}\kappa_2 - 4a_{31}^2)x^2 \\ & +(3a_{31}a_{32} - a_{41}\kappa_2)yx + (2a_{32}^2 - \frac{1}{2}a_{42}\kappa_2 + a_{31}^2 - a_{31}a_{33})y^2. \end{aligned}$$

Differentiating with respect to p we have

$$j^1\Omega_p = 2\kappa_2a_{31}x + 2\kappa_2^2p + 2a_{32}y\kappa_2.$$

Differentiating with respect to x and with respect to y we have

$$j^1(\Omega_x + p\Omega_y) = (-a_{40}\kappa_2 + 4a_{31}^2)x + a_{31}\kappa_2p + (-a_{41}\kappa_2 + 3a_{31}a_{32})y.$$

The criminant is given by $\Omega = \Omega_p = 0$. Eliminating p from these equations establishes (a).

Parts (b) and (c) follow in the same way, using the equations $\Omega = \Omega_x + p\Omega_y = 0$ and $\Psi = \Psi_x + p\Omega_y = 0$ respectively.

To prove (d) we choose two distinct points on S

$$\eta = (x, y, f(x, y))$$
$$\tilde{\eta} = (\tilde{x}, \tilde{y}, f(\tilde{x}, \tilde{y})).$$

The tangent planes $T_\eta S$ and $T_{\tilde{\eta}} S$ to the surface at these points have normals $(-f_x(x, y), -f_y(x, y), 1)$ and $(-f_x(\tilde{x}, \tilde{y}), -f_y(\tilde{x}, \tilde{y}), 1)$ respectively. Observe that $T_\eta S$ and $T_{\tilde{\eta}} S$ are parallel if and only if

$$f_x(x_1, y_1) = f_x(\tilde{x}, \tilde{y})$$
$$f_y(x_1, y_1) = f_y(\tilde{x}, \tilde{y}).$$

If in addition $\tilde{\eta} \in T_\eta S$ then $T_\eta S$ is a bitangent plane. This is the case if

$$f(x, y) = f(\tilde{x}, \tilde{y}) + (x - \tilde{x}) f_x(x, y) + (y - \tilde{y}) f_y(x, y).$$

Eliminating $\tilde{x}$, $\tilde{y}$ from these equations completes the proof. □

Recall the method of studying BDEs described in Section 1.3.2.

Given a curve γ on S, the Legendrian lift of γ to the manifold of contact elements to S (that is, the projectivised cotangent bundle PT^*S which we identify with $\mathbb{R}^3$, endowed with the contact structure given by the canonical form $dy - pdx$) consists of the contact elements to S tangent to γ. This is the unique curve in PT^*S that projects to γ under π and is tangent to the contact plane at every point.

In the parametrising plane the parabolic set, the locus of inflections of the characteristic BDE, the flecnodal and conodal curves are mutually tangent parabolae. Following Uribe-Vargas ([71]) we write their 2-jets as $y = c_P x^2$, $y = c_\chi x^2$, $y = c_\zeta x^2$, and $y = c_D x^2$ respectively. We denote their Legendrian lifts by L_P, L_χ, L_ζ and L_D, and the tangents at the origin to their Legendrian lifts by l_P, l_χ, l_ζ and l_D. We denote by l_g the contact element to the cusp of Gauss (the Legendrian lift of the origin, that is, the vertical line in the contact plane at that point). Observe that L_P is simply the criminant.

Remark 3.1.1 *It follows from Proposition 3.1.1 that $l_P, l_\zeta, l_\chi, l_D$ are generally all distinct. If $\kappa_2 a_{40} = 3a_{31}$ then they all coincide. This case is studied in* [71]*, but is non-generic; it is the collapse of two cusps of Gauss with opposite indices.*

Recall that the cross-ratio of four concurrent coplanar lines l_i, $i = 1..4$ with respective gradients c_i, $i = 1..4$ is given by

$$(l_1, l_2; l_3, l_4) = \frac{c_3 - c_1}{c_3 - c_2} \cdot \frac{c_4 - c_2}{c_4 - c_1}.$$

Observe, for example, that if l_2 has infinite gradient, then

$$(l_1, l_2; l_3, l_4) = \frac{c_3 - c_1}{c_4 - c_1}.$$

Theorem 3.1.2 *At a generic cusp of Gauss the cross-ratio of the Legendrian lines l_P, l_g, l_χ and l_ζ satisfies*

$$(l_P, l_g; l_\chi, l_\zeta) = -9.$$

Proof: The Legendrian lift of a curve in $\mathbb{R}^2$ given by $y = cx^2 + h.o.t.$ is tangent to the contact plane at the origin, and the gradient of its tangent line at the origin is $2c$.

Using Proposition 3.1.1 we have

$$(l_P, l_g; l_\chi, l_\zeta) = \frac{\dfrac{2a_{31}^2 - a_{40}\kappa_2}{2a_{31}\kappa_2} - \dfrac{20a_{31}^4 - 13a_{31}^2 a_{40}\kappa_2 + 2a_{40}^2\kappa_2^2}{2a_{31}^3\kappa_2}}{\dfrac{2a_{31}^2 - a_{40}\kappa_2}{2a_{31}\kappa_2} - \dfrac{a_{40}(3a_{31}^2 - 2a_{40}\kappa_2)}{18a_{31}^3}} = -9.$$

□

Recall that the parabolic set, the cusps of Gauss, and the flecnodal curve, being defined in terms of contact with flat model-submanifolds, are projectively invariant properties of the surface, but that the characteristic curves are not.

Remark 3.1.3 *Although there is no reason that inflections of the characteristic curves in the domain of a parametrisation should correspond to points of any significance on S, a curve with the same 2-jet as the locus of such points at a cusp of Gauss does have some meaning: as a consequence of Theorem 3.1.2 this 2-jet is projectively invariant, and is determined by the 2-jets of the flecnodal and parabolic curves.*

Definition 3.1.4 *We define the* characteristic cross ratio invariant *(ccr-invariant) of a cusp of Gauss by*

$$\rho_c = (l_\chi, l_P; l_D, l_g).$$

It follows from Theorem 3.1.2 that the ccr-invariant is a projective invariant and related to the cr-invariant ρ defined in [71] by the linear relation $\rho_c = 10 - 9\rho$. We have chosen this particular cross-ratio (among the six possible choices for these lines) to make the subsequent calculations simpler.

Proposition 3.1.2 *The ccr-invariant is given by* $\rho_c = 10 - \dfrac{3\kappa_2 a_{40}}{a_{31}^2}$.

Proof: Using Proposition 3.1.1 we have

$$\rho_c = (l_\chi, l_P; l_D, l_g) = \frac{-\dfrac{a_{40}}{6a_{31}} - \dfrac{20a_{31}^4 - 13a_{31}^2 a_{40}\kappa_2 + 2a_{40}^2\kappa_2^2}{2a_{31}^3\kappa_2}}{-\dfrac{a_{40}}{6a_{31}} - \dfrac{(2a_{31}^2 - a_{40}\kappa_2)}{2a_{31}\kappa_2}} = 10 - \frac{3\kappa_2 a_{40}}{a_{31}^2}.$$

□

Remark 3.1.5 *In the degenerate case when* $\kappa_2 a_{40} = 3a_{31}$ *the cross-ratios in Theorem 3.1.2 and Definition 3.1.4 are not well defined. As the limit of* ρ_c *of both cusps of Gauss at the collapse is equal to* 1*, we define* $\rho_c = 1$ *in this case. At any cusp of Gauss with ccr-invariant* ρ_c *we have that*

$$\lim_{\rho_c \to 1} (l_P, l_g; l_\chi, l_\zeta) = -9.$$

We now proceed to classify cusps of Gauss in terms of type of singularity of the characteristic BDE and the relative positions of special curves of interest. These results compliment those in [23, 71] on the asymptotic curves and the flecnodal curve.

Lemma 3.1.6 *The topological type of the singularity of the characteristic BDE is determined by the projective invariant* ρ_c*.*

Proof: The topological type of the singularity of the characteristic BDE is given by the type of singularity of the lifted field ξ. Using the expressions for $j^1\Omega_p$ and $j^1\Omega_x + p\Omega_y$ given in the proof of Proposition 3.1.1, the linear part of ξ is

$$2(\kappa_2^2 p + a_{31}\kappa_2 x)\frac{\partial}{\partial x} - (a_{31}\kappa_2 p - (a_{40}\kappa_2 - 4a_{31}^2)x)\frac{\partial}{\partial p}.$$

By a linear change of coordinates in the (x, p)-plane and multiplication by a non-zero scalar this may be transformed to

$$2(p-2x)\frac{\partial}{\partial x} + (p - \frac{(5 - 2a_{40}\kappa_2/a_{31}^2)}{(3 - a_{40}\kappa_2/a_{31}^2)}x)\frac{\partial}{\partial p}.$$

It is clear that the type of singularity depends only on the value of $a_{40}\kappa_2/a_{31}^2$, that is, on the value of the projective invariant ρ_c. □

Lemma 3.1.7 *At a cusp of Gauss, we may make projective transformations and parametrise the surface by* $(x, y, f(x, y))$ *where*

$$j^4 f(x,y) = \frac{y^2}{2} - x^2 y + \frac{(10-\rho_c)x^4}{18}.$$

Proof: Platanova ([58]) showed that $j^4 f(x, y)$ is projectively equivalent to

$$\frac{y^2}{2} - x^2 y + \lambda x^4.$$

It is immediate from Proposition 3.1.2 that $\rho_c = 10 - 18\lambda$. □

Theorem 3.1.8 *At a cusp of Gauss with ccr-invariant* ρ_c*, the characteristic curves have a well-folded singularity if* $\rho_c, \neq 1, 11/8$*. The singularity is a well-folded saddle if* $\rho_c < 1$*, a well-folded node if* $1 < \rho_c < 11/8$ *and a well-folded focus if* $\rho_c > 11/8$*.*

Proof: We parametrise the surface in Monge form and use the projective normal form given in Lemma 3.1.7. We calculate the coefficients E, F, G, l, m, n of the first and second fundamental forms. We have that

$$\begin{aligned} j^2E &= 1, & j^2l &= -2y + \frac{20-2\rho_c}{3}x^2, \\ j^2F &= 0, & j^2m &= -2x, \\ j^2G &= 1+y^2, & j^2n &= 1-y^2. \end{aligned}$$

We calculate the coefficients of the characteristic BDE (2.6). We set $p = dy/dx$ and write (2.6) as $\Omega(x, y, p) = 0$, then we have

$$j^2\Omega(x,y,p) = p^2 - 4xp + 2y + 4y^2 + \frac{2(2+\rho_c)}{3}x^2.$$

The linear part of the projection to the (x, p)-plane of the lifted field ξ associated to the characteristic BDE is

$$2(p-2x)\frac{\partial}{\partial x} + 2(p - \frac{2(2+\rho_c)}{3}x)\frac{\partial}{\partial p}.$$

We calculate the eigenvalues of this linear vector field at the origin. They are found to be

$$-1 \pm \frac{\sqrt{11 - 8\rho_c}}{\sqrt{3}},$$

which are distinct and non-zero provided that $\rho_c \neq 1, 11/8$. The singularity of ξ is a saddle (real eigenvalues of opposite sign) when $\rho_c < 1$, a node (real eigenvalues of the same sign) when $1 < \rho_c < 11/8$ and a focus (complex conjugate eigenvalues) when $\rho_c > 11/8$. □

Remark 3.1.9 *Combining Theorem 3.1.8 with Theorem 5 in* [71] *(see also Proposition 2.5 in* [24]*), we have in Figure 3.1, the four generic combinations of the (topological) type of singularity of the asymptotic curves and characteristic curves at a cusp of Gauss.*

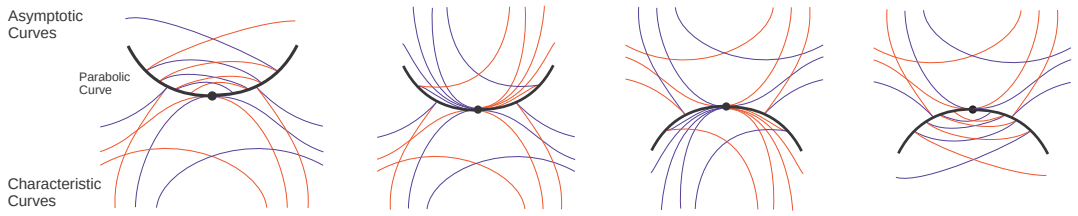

Figure 3.1: The asymptotic and characteristic curves at a cusp of Gauss.

Theorem 3.1.10 *There are seven possible configurations of the parabolic set, conodal curve, and the inflection curve of the characteristic BDE at a cusp of Gauss, distinguished by the value of ρ_c. These are illustrated in Figure 3.2.*

Proof: We adopt the projective normal form given in Lemma 3.1.7 and write the characteristic BDE (2.6) as $\Omega(x, y, p) = 0$ where $p = dy/dy$. Using Proposition 3.1.1 the parabolic set is given by

$$y = \frac{(4 - \rho_c)}{3}x^2 + h.o.t.,$$

the inflection curve of the characteristic BDE is given by

$$y = \frac{(2 + \rho_c)(5 - 2\rho_c)}{9}x^2 + h.o.t.,$$

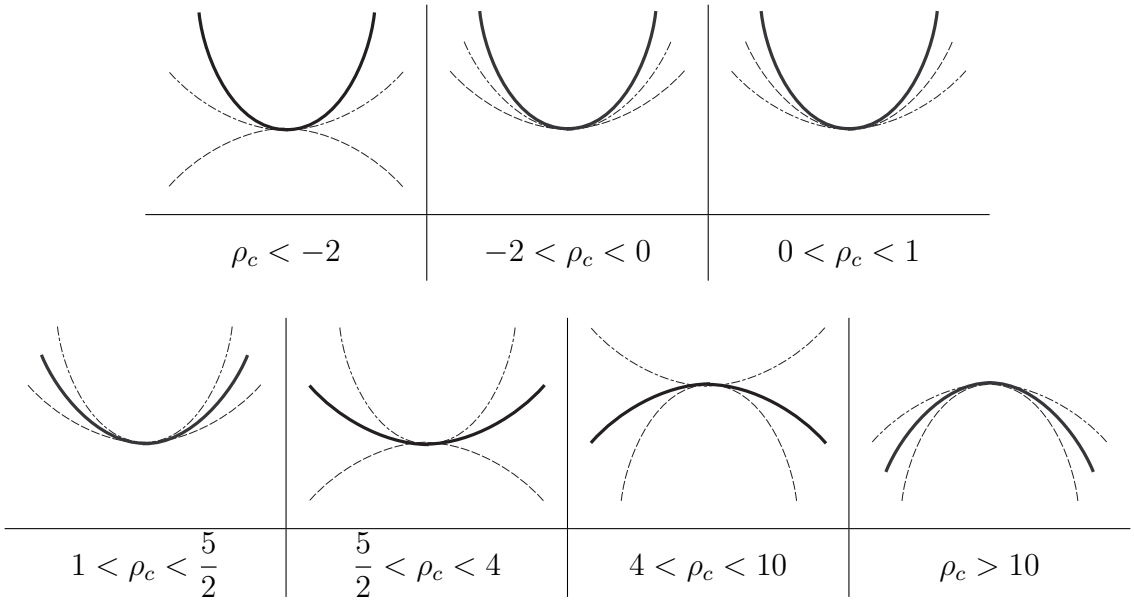

Figure 3.2: The parabolic set (thick), inflection curve of the characteristic BDE (dotted), and conodal curve (dot-dashed) at a cusp of Gauss.

and the conodal curve is given by

$$y = \frac{10 - \rho_c}{9} x^2 + h.o.t..$$

The inflection curve is always regular as the tangent to the curve in $\mathbb{R}^3$ given by $\Omega = \Omega_x + p\Omega_y = 0$ is transverse to the line $y = x = 0$ for all values of ρ_c.

These expressions show that when $\rho_c = 1$, all the curves of interest have greater than 2-point contact when considered pairwise. The conodal curve and locus of inflections also have greater than 2-point contact when $\rho_c = 0$.

The parabolic set is inflectional if $\rho_c = 4$, the locus of inflections is inflectional if $\rho_c = 5/2$ or $\rho_c = -2$, and the conodal curve is inflectional if $\rho_c = 10$.

The proof is completed by considering the 2-jets of the curves of interest when ρ_c takes a value of in each of the open intervals bounded by the given exceptional values. □

Further curves of interest at a cusp of Gauss are the separatrices of the singularity. Recall Definition 1.3.2.

Lemma 3.1.11 *The relative positions of the parabolic set and the separatrices and inflection curve of the characteristic BDE at a cusp of Gauss are invariant under*

projective transformations.

Proof: The relative positions of the curves of interest at a cusp of Gauss are given by the ratios of their 2-jets at that point. To second order the separatrices are parabolae tangent to the parabolic set, so they may be written in the form

$$y = c_\sigma x^2 + h.o.t..$$

Substituting this into the equation $\Omega(x, y, p) = 0$ we find that

$$c_\sigma = \frac{-3 \pm \sqrt{(8\kappa_2 a_{40} - 23a_{31}^2)}}{8\kappa_2}.$$

We label these two values $c_{\sigma+}$ and $c_{\sigma-}$. The proof is completed by using Proposition 3.1.1 to show that the ratio of any two elements of the set $\{c_P, c_\chi, c_{\sigma+}, c_{\sigma-}\}$ depends only on the value of $\kappa_2 a_{40}/a_{31}^2$, that is, on the value of ρ_c. □

Proposition 3.1.3 *There are six possible configurations of the parabolic set, locus of inflections and separatrices associated to the characteristic BDE at a cusp of Gauss. These are are invariant under affine transformations of* $\mathbb{R}^3$ *and distinguished by the value of* ρ_c *as illustrated in Figure 3.3.*

Proof: We adopt the projective normal form given in Lemma 3.1.7. The separatrices are given by

$$y = \frac{3}{4} \pm \frac{\sqrt{33 - 24\rho_c}}{12} x^2 + h.o.t.$$

Recall that the parabolic set is given by

$$y = \frac{(4 - \rho_c)}{3} x^2 + h.o.t.,$$

and the inflection curve of the characteristic BDE is given by

$$y = \frac{(2 + \rho_c)(5 - 2\rho_c)}{9} x^2 + h.o.t.$$

Using these expression we have that the following exceptional values of ρ_c correspond to the given codimension 1 phenomena:

1. The separatrices are inflectional or singular when $\rho_c = -2$.

2. The parabolic set is inflectional if $\rho_c = 4$.

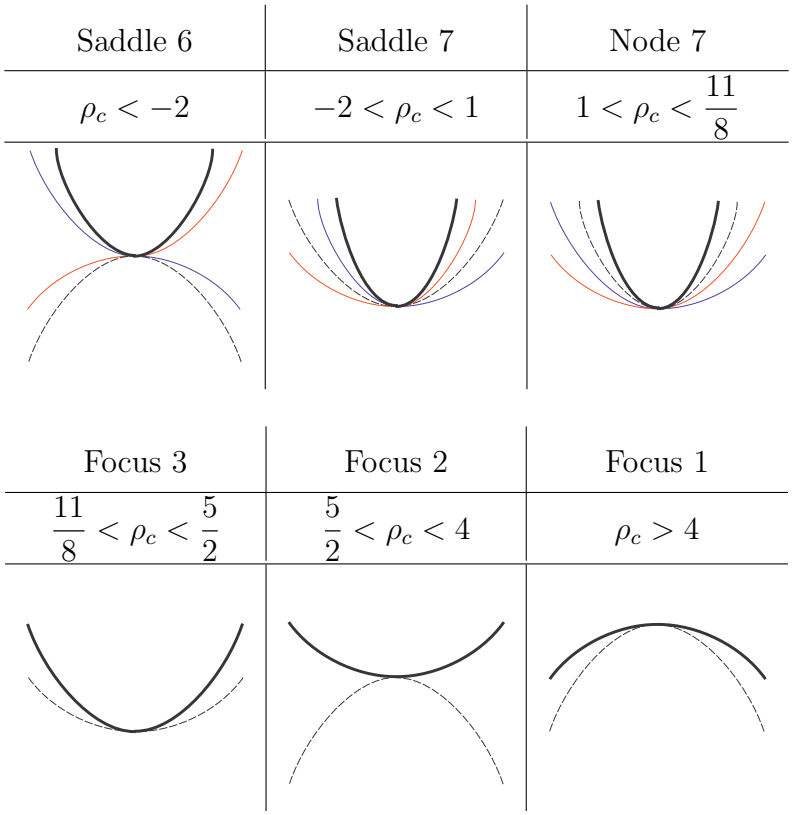

Figure 3.3: Configurations of the parabolic curve (thick curves), locus of inflections (broken curves) and separatrices (thin curves) at a cusp of Gauss. The label given to each configuration refers to the labels given to the 18 configurations established in [23], see Section 1.3.3.

3. The locus of inflections is inflectional if $\rho_c = -2, 5/2$.

4. The singularity of the lifted field changes from a saddle to a node at $\rho_c = 1$.

5. The parabolic and locus of inflection curves have greater than two-point contact if $\rho_c = 1$.

6. The type of singularity changes from a node to a focus at $\rho_c = 11/8$.

7. The locus of inflections and separatrices have greater than two-point contact if $\rho_c = 1$ or $\rho_c = -2$.

The proposition is established by choosing a value of ρ_c in each of the open intervals bounded by these exceptional values and calculating the 2-jet of the parabolic set, inflection curve and any separatrices. □

3.2 The Legendre transformation of the characteristic BDE

We have seen that the inflections of the characteristic curves are of some geometric interest, at least in the neighbourhood of a cusp of Gauss. It follows that the Legendre transform of the characteristic BDE (2.6) is also of interest.

The property that a curve has an inflection is affine invariant, however we have seen that the relative positions of the curves of interest (cusp set, inflection set and separatrices) are invariant under projective changes of coordinates. We may thus use the normal form given in Lemma 3.1.7.

Proposition 3.2.1 *There are six possible configurations of the cusp set, locus of inflections and separatrices associated to the dual curves of the integral curves of the characteristic BDE at a cusp of Gauss. These are distinguished by the value of* ρ_c *as illustrated in Figure 3.4.*

Proof: We consider the characteristic BDE (2.6) at a cusp of Gauss parametrised in the projective normal form given in Lemma 3.1.7. We write this equation as $F(x, y, p) = 0$ where $p = dy/dx$ and apply the Legendre transformation as given in Section 1.3.3. The Proposition is then established by calculating the appropriate 2-jets in a manner similar to the proof of Proposition 3.1.1 and arguing as in the proof of Proposition 3.1.3. □

It is a well known in singularity theory that projections from the plane to the plane generally have fold singularities along smooth curves and cusp singularities, known as Whitney-pleats, at isolated points where two fold curves meet (see for example [47]).

When we consider the surface M associated to the asymptotic or characteristic BDE the fold curves of the natural projection π are the Legendrian lift of the parabolic set. For smooth surfaces the parabolic set is generally a smooth curve so we do not expect Whitney-pleat singularities in general. The Legendre transform of these BDEs, however, may have such points.

When we consider the Legendre transformation of the characteristic BDE at a

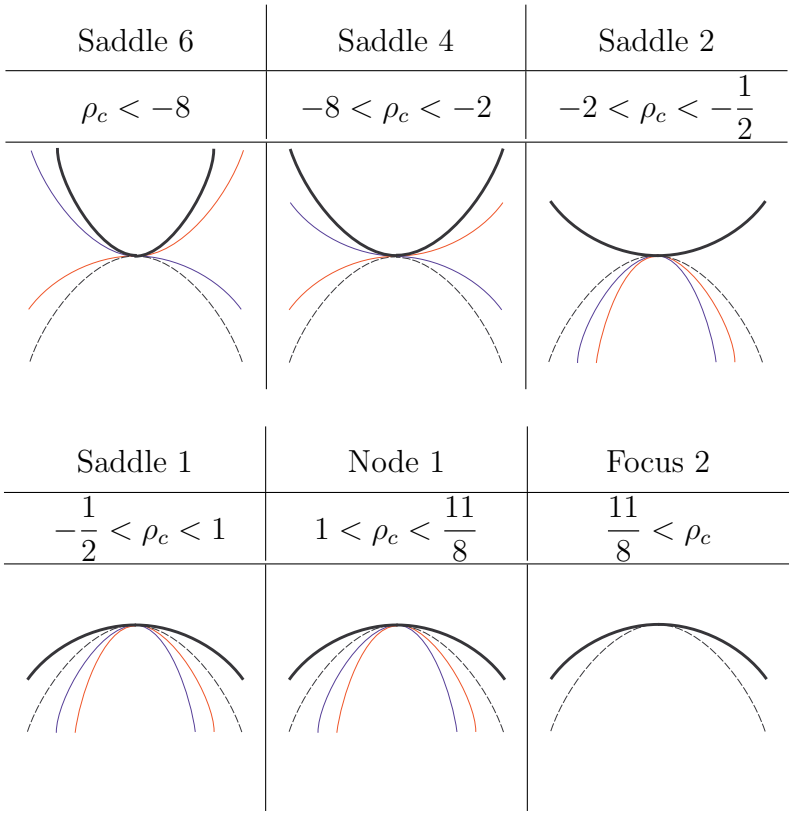

Figure 3.4: Configurations of the discriminant (thick curves), locus of inflections (broken curves) and separatrices (thin curves) of the Legendre transform of the characteristic BDE at a cusp of Gauss. The label given to each configuration refers to the labels given to the 18 configurations established in [23], see Section 1.3.3.

cusp of Gauss, the projection π has a Whitney-pleat (that is, a cusp) singularity at the origin when $\rho_c = -2$, that is, when the inflection set is inflectional. This is symmetric with a result on the asymptotic curves identified by Uribe-Vargas in [72]: the Legendre transformation of the asymptotic BDE at a cusp of Gauss has a Whitney-pleat when the flecnodal curve is inflectional. Furthermore, hyperbolic points where the Legendre transform of the asymptotic BDE has a Whitney-pleat are shown to be biflecnodes, that is, points where the tangent line in the asymptotic direction has 5-point contact with the surface. Such points are generic features of surfaces (cusps of Gauss with an inflectional flecnodal curve are not, they have codimension 1 so occur in 1-parameter families of surfaces).

It follows from our results that elliptic points where the Legendre transformation

of the characteristic BDE has a Whitney-pleat may also be of interest. We label such points *characteristic bi-inflections*. It follows that a codimension 1 cusp of Gauss with $\rho_c = -2$ may be thought of as the superposition of a generic cusp of Gauss and a characteristic bi-inflection.

3.3 Left and right characteristic curves

The rate of turning, per unit length of arc as we move along any curve on S, of the tangent plane to S is $\mathbf{n}'$, where $'$ denotes differentiation with respect to arc length along the curve. This is given by $-\kappa_n \mathbf{t} + \tau_g(\mathbf{t} \wedge \mathbf{n})$, where κ_n and τ_g are respectively the sectional curvature and geodesic torsion, and $\mathbf{t}$ is the unit tangent to the curve (see for example [34]).

The Beltrami-Enepper Theorem states that the respective torsions (as space curves) of the two asymptotic curves through a hyperbolic point are $\pm\sqrt{-K}$, or equivalently $\tau^2 = -K$ (see, for example, [70]). For an asymptotic curve the torsion and geodesic torsion are equal and the sectional curvature is zero. Therefore, one can re-write the Beltrami-Enepper formula in the form

$$\kappa_n^2 + \tau_g^2 = -K.$$

This reformation shows that the Theorem 3.3.1 is the analogous result for the characteristic curves.

Theorem 3.3.1 *Let κ_n and τ_g be the sectional curvature and geodesic torsion in a particular direction on a surface. The direction is a characteristic direction if and only if*

$$\kappa_n^2 + \tau_g^2 = K.$$

Proof: Let κ_2, κ_1 be the principal curvatures at a point on a surface. At an elliptic point we may assume, without loss of generality, that $\kappa_1 > 0$ and $\kappa_2 > 0$. A curve tangent to a direction making an angle ϕ with the principal direction with sectional curvature κ_1 at a point has sectional curvature given by

$$\kappa_n = \kappa_1 \cos^2 \phi + \kappa_2 \sin^2 \phi$$

and geodesic torsion given by

$$\tau_g = \cos\phi \sin\phi(\kappa_2 - \kappa_1).$$

The characteristic directions ϕ satisfy

$$\begin{aligned} \cos\phi = & \pm\sqrt{\frac{\kappa_2}{\kappa_2+\kappa_1}}, \\ \sin\phi = & \sqrt{\frac{\kappa_1}{\kappa_2+\kappa_1}}. \end{aligned}$$

The result follows. □

Corollary 3.3.2 *The magnitude of the rate of turning of the tangent plane along a characteristic (respectively asymptotic) curve is equal to $\sqrt{K}$ (respectively $\sqrt{-K}$).*

Definition 3.3.3 *A curve on a surface is said to be a left (respectively right) curve if its geodesic torsion is negative (respectively positive).*

Definition 3.3.3 is consistent with the terminology in [71] as torsion and geodesic torsion are equal for the asymptotic curves.

A corollary of Theorem 3.3.1 is that at any elliptic point one characteristic curve is a left curve and the other is a right curve (the geodesic torsion of the characteristic curves through an elliptic point must have opposite sign as they are separated by a principal direction). The left (respectively right) characteristic curves at the origin have slope $\sqrt{\kappa_1/\kappa_2}$ (respectively $-\sqrt{\kappa_1/\kappa_2}$).

Definition 3.3.4 *The left (respectively right) branch of the inflection curve is the set of points corresponding to an inflection of a left (respectively right) characteristic curve.*

A change from the left branch to the right branch occurs as the inflection curve passes through a generic cusp of Gauss, and as the Legendrian curve L_χ is transverse to the criminant at a well-folded singularity. Similar to that in [71] for the flecnodal curve, there is a natural way to locate the left and right branches at a cusp of Gauss.

Proposition 3.3.1 *At a cusp of Gauss choose an orthonormal right-handed coordinate system with the x-axis tangent to the parabolic set and the elliptic region locally*

in the region $z > 0, y > 0$. Then left and right branches of the inflection curve of the characteristic BDE correspond locally to the negative and positive x-axis respectively if and only if the singularity of the characteristic curves has positive index. The opposite correspondence holds when the singularity has negative index.

Proof: We choose a principal coordinate system at a non-umbilic elliptic point. Let $(x, y_i(x))$ be the parametrisation in the plane of a solution to the characteristic BDE (2.6) with slope $(-1)^i\sqrt{\kappa_1/\kappa_2}$ at the origin (that is, $j^1y_i = (-1)^i\sqrt{\kappa_1/\kappa_2}x$).

Let $p_i = dy_i/dx$, $i = 1, 2$. Observe that in a neighbourhood of the origin $p_2 > p_1$. Since $c_P > c_\chi$, the slope of the Legendrian line l_P at the origin in the (x, p)-plane is always greater than that of l_χ. Hence locally the half space $x > 0$ (respectively $x < 0$) contains the left (respectively right) branch of the inflection curve.

From Proposition 3.1.1 the elliptic domain lies in $y > 0$ when $\rho_c < 1$, which from Theorem 3.1.10 is when the index of the lifted field of the characteristic BDE is equal to -1.

When $\rho_c > 1$ we make the coordinate change $(x, y, z) \mapsto (-x, -y, z)$ to obtain the required coordinate system, after which the half space $x < 0$ (respectively $x > 0$) contains the left (respectively right) branch of the inflection curve. In this case the index of the lifted field of the characteristic BDE is equal to $+1$. □

Remark 3.3.5 *Combining Proposition 3.3.1 with Theorem 8 in* [71] *we have in Figure 3.5 the two possible configurations of the flecnodal curve and the inflection curve of the characteristic BDE at a cusp of Gauss.*

3.4 Elliptic discs of smooth surfaces

Definition 3.4.1 *An elliptic disc is an elliptic region of a smooth surface bounded by a smooth simple closed parabolic curve.*

Hyperbolic discs (hyperbolic regions bounded by smooth simple closed parabolic curves) are considered by Uribe-Vargas in [71], where the asymptotic curves are used to prove global results concerning the number and type of cusps of Gauss on the parabolic curve bounding the disc. The local properties of the characteristic curves

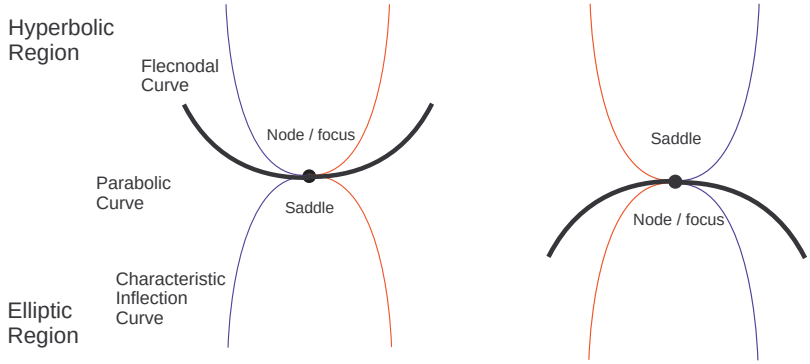

Figure 3.5: The left (blue) and right (red) branches of the flecnodal curve and the inflection curve of the characteristic BDE at a cusp of Gauss with $\rho_c < 1$ (left) and $\rho_c > 1$ (right).

we have established allow us to prove similar results concerning elliptic discs on smooth surfaces. A key fact used in [71] is that the singularities of the asymptotic BDE (2.5) all lie on the parabolic set. The characteristic BDE (2.6), however, may have singularities in the elliptic region, namely at umbilic points. This presents problems when adapting the results in [71], so we restrict ourselves here to the study of elliptic discs containing no umbilic points.

Proposition 3.4.1 *The sum of the indices of the singularities of the characteristic curves at the cusps of Gauss on a parabolic curve bounding an elliptic disc with no umbilic points is equal to* $+1$.

Proof: We write the characteristic BDE (2.6) as

$$\Omega(x, y, p) = 0$$

where $p = dy/dx$. As there are no umbilic points and the elliptic region is a disc, the surface $M \subset \mathbb{R}^3$ given by $\Omega = 0$ is smoothly equivalent to a sphere.

Consider the vector field ξ on M. As M is a compact surface without boundary of genus 0, the sum of the indices of all singular points of ξ is 2 by the Poincaré-Hopf Theorem, so the sum of the indices of the folded singularities is 1. □

Corollary 3.4.2 *The parabolic curve bounding an elliptic disc that contains no umbilic points has a positive even number of cusps of Gauss.*

The following partially answers a problem set in [71].

Corollary 3.4.3 *If an elliptic disc contains no umbilic points and the characteristic curves have nodes or foci at all cusps of Gauss on the parabolic curve bounding the disc, then there are only two cusps of Gauss.*

Remarks 3.4.4 *1. The case that the parabolic set is an isolated point (that is, the discriminant of the asymptotic BDE* (2.5) *has an* A_1^+ *singularity) has codimension 1. If a surface with such a parabolic set is perturbed within a generic* 1*-parameter family of surfaces, a simple, closed parabolic curve appears in the bifurcation. Thus although closed parabolic curves are generic (that is, stable) features of surfaces, a natural context in which to study elliptic and hyperbolic discs is within* 1*-parameter families of surfaces.*

2. It is clear that the number and type of cusps of Gauss on the parabolic set bounding an elliptic disc is partly governed by the number and type of the umbilic points on the disc, and that information on the nature of this governance may be obtained by studying the characteristic curves. Observe that the set $\Omega = 0$ *is then a surface in* $\mathbb{R}^2 \times \mathbb{R}P^1$ *that is smooth if all umbilic points are generic, but is not generally orientable.*

Chapter 4

Linear involutions on the real projective line

In this Chapter we temporarily leave the geometry of surfaces in $\mathbb{R}^3$ and consider binary differential equations on surfaces in their own right.

Our motivation is two-fold. We begin by considering the relationship between linear involutions on $\mathbb{R}P^1$ and families of BDEs on surfaces, using the method of considering BDEs as points in $\mathbb{R}P^2$. The asymptotic (2.5), characteristic (2.6) and principal (2.4) BDEs and the related families $\mathcal{C}_\alpha$ (2.7) and $\mathcal{R}_\alpha$ (2.8) may be constructed using such involutions (see [24]). We seek to generalise this method to general linear involutions on $\mathbb{R}P^1$. This work lays the foundation for Chapter 5, where we exhibit BDEs on surfaces that do not appear to have been considered previously

Secondly we aim to generalise the results of Chapter 3, and show that we may assign an affine invariant to well-folded singularities of BDEs in the plane. The affine properties of such points are completely determined by this invariant and the index modulus λ.

We begin by recalling some simple facts concerning the geometry of the projective plane $\mathbb{R}P^2$.

Let $\Gamma \subset \mathbb{R}P^2$ be a conic associated to a symmetric bilinear form $\mathcal{G}$ on $\mathbb{R}^3$. The polar line of a point $P \in \mathbb{R}P^2$ with respect to Γ is denoted by $\hat{P}$ (conversely, given any projective line $\hat{Q} \in \mathbb{R}P^2$, we denote its polar point by Q).

We denote by $\mathbb{R}P^2_{\Gamma^+}$ (respectively $\mathbb{R}P^2_{\Gamma^-}$) those points $[v] \in \mathbb{R}P^2$ with $\mathcal{G}(v,v) > 0$ (respectively $\mathcal{G}(v,v) < 0$). Clearly $\{\mathbb{R}P^2_{\Gamma^+}, \mathbb{R}P^2_{\Gamma^-}, \Gamma\}$ forms a partition of $\mathbb{R}P^2$.

The set of all projective lines in $\mathbb{R}P^2$ (that is, the Grassmannian $G_2(\mathbb{R}^3)$) may be similarly partitioned into three disjoint sets using Γ: those lines that intersect Γ at two distinct points, those that are tangent to Γ and those that do not intersect Γ. We define

$$\begin{aligned} G_2(\mathbb{R}^3)_{\Gamma^+} = &\ \{\hat{P} \in G_2(\mathbb{R}^3) || \hat{P} \cap \Gamma| = 2\} \\ G_2(\mathbb{R}^3)_{\Gamma^0} = &\ \{\hat{P} \in G_2(\mathbb{R}^3) || \hat{P} \cap \Gamma| = 1\} \\ G_2(\mathbb{R}^3)_{\Gamma^-} = &\ \{\hat{P} \in G_2(\mathbb{R}^3) | \hat{P} \cap \Gamma| = 0\}. \end{aligned}$$

Lemma 4.0.5 follows trivially from the definition of polarity with respect to a given conic.

Lemma 4.0.5 **(a)** *$P \in \mathbb{R}P^2_{\Gamma^+}$ if and only if $\hat{P} \in G_2(\mathbb{R}^3)_{\Gamma^+}$,*

(b) *$P \in \mathbb{R}P^2_{\Gamma^-}$ if and only if $\hat{P} \in G_2(\mathbb{R}^3)_{\Gamma^-}$,*

(c) *$\hat{P} \in G_2(\mathbb{R}^3)_{\Gamma^0}$ if and only if $P \in \hat{P} \cap \Gamma$.*

Consider a projective line $\hat{P} \in G_2(\mathbb{R}^3)_{\Gamma^+} \cup G_2(\mathbb{R}^3)_{\Gamma^-}$. Given any point $[v] \in \hat{P}$, there is a unique point $\sigma_{P\Gamma}([v]) \in \hat{P}$ such that $[v]$ and $\sigma_{P\Gamma}([v])$ are apolar with respect to Γ, that is, the set $\{[v], \sigma_{P\Gamma}([v]), P\}$ forms a self-polar triangle. It is clear that the map

$$\begin{aligned} \sigma_P : \hat{P} \to &\ \hat{P} \\ [v] \mapsto &\ \sigma_{P\Gamma}([v]) \end{aligned}$$

defines an involution on $\hat{P}$.

Lemma 4.0.6 *Let $\hat{P} \in G_2(\mathbb{R}^3)_{\Gamma^+}$ and let $[v] \in \hat{P}$. If $[v] \in \mathbb{R}P^2_{\Gamma^+}$ then $\sigma_{P\Gamma}([v]) \in \mathbb{R}P^2_{\Gamma^-}$, if $[v] \in \mathbb{R}P^2_{\Gamma^-}$ then $\sigma_{P\Gamma}([v]) \in \mathbb{R}P^2_{\Gamma^+}$, and if $[v] \in \Gamma$ then $\sigma_{P\Gamma}([v]) = [v]$.*

Proof: Observe that $\sigma_{P\Gamma}([v])$ is the polar of the pencil joining $[v]$ and P with respect to the conic Γ. We denote this pencil by $\widehat{\sigma_{P\Gamma}([v])}$.

As $\hat{P} \in G_2(\mathbb{R}^3)_{\Gamma^+}$, it follows from Lemma 4.0.5 **(a)** that $P \in \mathbb{R}P^2_{\Gamma^+}$. If $[v] \in \mathbb{R}P^2_{\Gamma^-}$ then $\widehat{\sigma_{P\Gamma}([v])} \in G_2(\mathbb{R}^3)_{\Gamma^+}$. Then by Lemma 4.0.5 **(a)** again we have that $\sigma_{P\Gamma}([v]) \in \mathbb{R}P^2_{\Gamma^+}$.

The other assertions follow by similar reasoning. □

Recall also that polarity with respect to any conic is preserved by projective transformations.

In what follows we shall adopt the notation $\hat{P}$ for the polar of a point $P \in \mathbb{R}P^2$ with respect to the conic Δ.

4.1 Quadratic forms constructed from involutions

4.1.1 Linear involutions on $\mathbb{R}P^1$

A linear involution on the real projective line $\mathbb{R}P^1$ is a projective linear map

$$\sigma : \mathbb{R}P^1 \to \mathbb{R}P^1$$

such that $(\sigma \circ \sigma)([v]) = [v]$ for all $[v] \in \mathbb{R}P^1$. The set of all linear involutions on the real projective line is a subset of the projective general linear group $PGL(2, \mathbb{R})$: it is the induced action on $\mathbb{R}P^1$ of the subset so the general linear group $GL(2, \mathbb{R})$ whose elements are linear transformations $T : \mathbb{R}^2 \to \mathbb{R}^2$ such that $T^2 = \mu I$ for some constant $\mu \neq 0$. We denote by Id the identity involution given by $[v] \mapsto [v]$ for all $[v] \in \mathbb{R}P^1$. This involution corresponds to linear transformations that are themselves multiples of the identity. We denote the compliment of Id in the set of all linear involutions on $\mathbb{R}P^1$ by $PLI(2, \mathbb{R})$.

Remark 4.1.1 *The composition of two linear involutions is not necessarily another involution, hence $PLI(2, \mathbb{R})$ does not form a group under composition of involutions.*

A linear transformation $T : \mathbb{R}^2 \to \mathbb{R}^2$ that is not a multiple of the identity but is such that T^2 is a multiple of the identity if and only it is given by a matrix of the form

$$\begin{pmatrix} a & b \\ c & -a \end{pmatrix}$$

where $a^2 + bc \neq 0$. Two matrices of this form define the same involution if and only if one is a non-zero multiple of the other. It follows that we may identify $PLI(2, \mathbb{R})$ with the compliment of the conic $a^2 + bc = 0$ in the real projective plane $\mathbb{R}P^2$, by considering the above matrix to be the point $[a : b : c]$. We denote by $\tilde{\Delta}$ the conic in $\mathbb{R}P^2$ given by $a^2 + bc = 0$.

Given a linear involution

$$\begin{aligned} \sigma : \mathbb{R}P^1 \to & \quad \mathbb{R}P^1 \\ [\alpha : \beta] \mapsto & \quad [a\alpha + b\beta : c\alpha - a\beta] \end{aligned}$$

we denote by Σ the matrix

$$\begin{pmatrix} a & b \\ c & -a \end{pmatrix}$$

of the associated linear transformation.

The set $PLI(2,\mathbb{R})$ has two simply connected components. We define

$$\begin{aligned} PLI_+(2,\mathbb{R}) &:= \{\sigma \in PLI(2,\mathbb{R}) | \det\Sigma > 0\} \\ PLI_-(2,\mathbb{R}) &:= \{\sigma \in PLI(2,\mathbb{R}) | \det\Sigma < 0\}. \end{aligned}$$

Given a direction $[v] \in \mathbb{R}P^1$, we denote by $[v^*] \in \mathbb{R}P^{1*}$ the projectivised one-form that is associated to $[v]$ (that is, if $[v] = [v_1 : v_2], [v^*] = v_1 p - v_2 q$. Let $\sigma \in PLI(2,\mathbb{R})$, and let $\omega([v]) = [v^*].\sigma([v])^*$. As the product of two 1-forms, $\omega([v])$ is a binary quadratic form which we may consider to be a point in $\mathbb{R}P^2$. We shall consider the locus of this point as the direction $[v]$ varies. We need the following result from elementary geometry.

Lemma 4.1.2 *Let a, b, c be real numbers with $a^2 + bc \neq 0$. The set*

$$\{(\cos\theta(a\cos\theta + b\sin\theta), -(b\sin^2\theta + c\cos^2\theta), \sin\theta(c\cos\theta - a\sin\theta)) \subset \mathbb{R}^3 | \theta \in [0,\pi]\}$$

is an ellipse in a plane through the origin. The ellipse encloses the origin if and only if $a^2 + bc < 0$.

Proof: We set

$$v(\theta) = \begin{pmatrix} \cos\theta(a\cos\theta + b\sin\theta) \\ -(b\sin^2\theta + c\cos^2\theta) \\ \sin\theta(c\cos\theta - a\sin\theta) \end{pmatrix}$$

Observe that

$$v(\theta) = \frac{1}{2}\begin{pmatrix} a + a\cos 2\theta + b\sin 2\theta \\ (b-c)\cos 2\theta - b - c \\ a\cos 2\theta + c\sin 2\theta - a \end{pmatrix}.$$

We apply the rotation about a line through the origin that is given by the matrix

$$\frac{1}{\sqrt{a^2+b^2}\sqrt{a^2+b^2+c^2}}\begin{pmatrix} a^2+b^2 & -ca & cb \\ c\sqrt{a^2+b^2} & a\sqrt{a^2+b^2} & -b\sqrt{a^2+b^2} \\ 0 & b\sqrt{a^2+b^2+c^2} & a\sqrt{a^2+b^2+c^2} \end{pmatrix},$$

followed by a dilation centred on the origin with scale factor

$$2\sqrt{a^2+b^2}.$$

The image of v under these transformations is

$$\begin{pmatrix} \sqrt{a^2+b^2+c^2}a \\ 0 \\ -a^2-b^2-bc \end{pmatrix} + \cos 2\theta \begin{pmatrix} a\sqrt{a^2+b^2+c^2} \\ 0 \\ b^2-bc+a^2 \end{pmatrix} + \sin 2\theta \begin{pmatrix} b\sqrt{a^2+b^2+c^2} \\ 0 \\ ac \end{pmatrix}.$$

This is an ellipse in a plane containing the origin, which we denote by $\tilde{v}(\theta)$. As the transformation we used was linear and preserved the origin, $v(\theta)$ is also an ellipse in a plane containing the origin.

The curve $\tilde{v}$ encloses the origin if and only if there are no values of θ such that $\tilde{v}$ and $\tilde{v}'$ are linearly dependent. Differentiating we have that

$$\tilde{v} \times \tilde{v}' = \sqrt{a^2+b^2+c^2}(a^2+b^2)\begin{pmatrix} 0 \\ (c+b)\cos 2\theta - 2a\sin 2\theta + c - b \\ 0 \end{pmatrix}.$$

The equation

$$(c+b)\cos 2\theta - 2a\sin 2\theta + c - b = 0$$

is satisfied by some real θ if and only if $a^2+bc > 0$. □

Let $\mathcal{T}$ be the projective transformation

$$\begin{aligned} \mathcal{T} : \mathbb{R}P^2 &\to \mathbb{R}P^2 \\ [a:b:c] &\mapsto [b:2a:-c]. \end{aligned}$$

Theorem 4.1.3 (a) *Let $\sigma \in PLI_+(2,\mathbb{R})$. Then the set $\{\omega([v])|[v] \in \mathbb{R}P^1\}$ form a line $\hat{L} \in G_2(\mathbb{R}^3)_{\Delta^-}$ when quadratic forms are considered as points in the projective plane.*

(b) *Let $\sigma \in PLI_{-}(2,\mathbb{R})$. Then there exists a line $\hat{L} \in G_2(\mathbb{R}^3)_{\Delta^+}$ such that set $\{\omega([v])|[v] \in \mathbb{R}P^1\} = \hat{L} \cap (\mathbb{R}P^2_{\Delta^+} \cup \Delta)$, when quadratic forms are considered as points in the projective plane.*

(c) *The polar of the pencil $\hat{L}$ with respect to the conic Δ is $\mathcal{T}(\sigma)$.*

Proof: Let

$$\Sigma = \begin{pmatrix} a & b \\ c & -a \end{pmatrix}$$

where $a^2 + bc \neq 0$. Observe that $\sigma \in PLI_{-}(2,\mathbb{R})$ (respectively $\sigma \in PLI_{+}(2,\mathbb{R})$) if $a^2 + b > 0$ (respectively $a^2 + b < 0$). Let $[v] = [\cos\theta : \sin\theta]$ (we choose $\theta \in [0,\pi]$) so

$$v = \begin{pmatrix} \cos\theta \\ \sin\theta \end{pmatrix}.$$

It follows that $[v^*] = \cos\theta p - \sin\theta q$. We have that

$$\Sigma v = \begin{pmatrix} a\cos\theta + b\sin\theta \\ c\cos\theta - a\sin\theta \end{pmatrix}.$$

It follows that $\sigma([v])^* = (a\cos\theta + b\sin\theta)p + (a\sin\theta - c\cos\theta)q$.

The quadratic form $\omega([v])$ is given by

$$\begin{aligned} \omega([v]) = &\ (\cos\theta p - \sin\theta q)((a\cos\theta + b\sin\theta)p + (a\sin\theta - c\cos\theta)q) \\ = &\ Ap^2 + Bpq + Cq^2, \end{aligned}$$

where

$$\begin{aligned} A = &\ \cos\theta(a\cos\theta + b\sin\theta) \\ B = &\ -(c\cos^2\theta + b\sin^2\theta) \\ C = &\ \sin\theta(c\cos\theta - a\sin\theta), \end{aligned}$$

that is, $\{\omega([v])|[v] \in \mathbb{R}P^1\} = [A : B : C]$.

Suppose that $\sigma \in PLI_{+}(2,\mathbb{R})$. By Lemma 4.1.2 the set $(A,B,C)(\theta)$ is a closed, convex, planar curve in a plane including the origin, and encloses the origin. It follows that $[A : B : C]$ is a line $\hat{L} \in G_2(\mathbb{R}^3)_{\Delta^-}$. This establishes part **(a)**.

Suppose now that $\sigma \in PLI_{-}(2,\mathbb{R})$. By Lemma 4.1.2 the set $(A,B,C)(\theta)$ is an ellipse in a plane including the origin, but does not enclose the origin. It follows

that $[A:B:C]$ is a segment of a line $\hat{L} \in G_2(\mathbb{R}^3)_{\Delta^+}$. By construction $[A:B:C]$ for any fixed θ is a quadratic form defining two real directions, so

$$[A:B:C] \subset \hat{L} \cap (\mathbb{R}P^2_{\Delta^+} \cup \Delta).$$

Finally observe that $\omega([v]) \in \Delta$ if and only if $[v] = \sigma([v])$, that is, if and only if θ satisfies $p/q = \tan\theta$ and $p/q = (c - a\tan\theta)/(a + b\tan\theta)$. It follows that θ satisfies

$$b\tan^2\theta + 2a\tan\theta - c = 0.$$

Since $a^2 + bc > 0$ this equation has two distinct real solutions for $\tan\theta$.

As $[A:B:C]$ is connected, it follows that $[A:B:C] = \hat{L} \cap (\mathbb{R}P^2_{\Delta^+} \cup \Delta)$. This establishes part **(b)**.

To calculate the polar of $\hat{L}$ with respect to the conic Δ of degenerate forms we choose two distinct points on $\omega([v])$. We set $v_0 = (1,0)$, $v_1 = (0,1)$. Then

$$\omega(v_0) = ap^2 - cpq,$$
$$\omega(v_1) = -bpq - aq^2$$

(note that when $a = 0$ these points coincide and we must make a different choice of v_0, v_1). The polar of the line of which $\omega([v])$ forms part is given by the determinant

$$\begin{vmatrix} \dfrac{\partial(\omega(v_0))}{\partial p} & \dfrac{\partial(\omega(v_0))}{\partial q} \\ \dfrac{\partial(\omega(v_1))}{\partial p} & \dfrac{\partial(\omega(v_1))}{\partial q} \end{vmatrix} = \begin{vmatrix} 2ap - cq & -cp \\ -bq & -bp - 2aq \end{vmatrix} = -2a(bp^2 + 2aqp - cq^2).$$

This establishes part **(c)**. □

Corollary 4.1.4 **(a)** $\mathcal{T}(PLI_-(2,\mathbb{R}^2)) = \mathbb{R}P^2_{\Delta^-}$,

(b) $\mathcal{T}(PLI_+(2,\mathbb{R}^2)) = \mathbb{R}P^2_{\Delta^+}$

(c) $\mathcal{T}(\tilde{\Delta}) = \Delta$.

Proof: This follows directly from Theorem 4.1.3 and Lemma 4.0.5. □

It follows that when $\sigma \in PLI_-(2,\mathbb{R})$ (respectively $\sigma \in PLI_+(2,\mathbb{R})$) the binary quadratic form $\mathcal{T}(\sigma)$ defines no (respectively two) real directions.

Proposition 4.1.1 *Let $\sigma \in PLI(2,\mathbb{R})$ be a linear involution. Then*

(a) *σ has two distinct fixed points (respectively no fixed points) if $\sigma \in PLI_-(2,\mathbb{R})$ (respectively $\sigma \in PLI_+(2,\mathbb{R})$),*

(b) *when $\sigma \in PLI_-(2,\mathbb{R})$ the binary quadratic form $\mathcal{T}(\sigma)$ is the product of a pair of forms associated to the fixed points of σ.*

Proof: Part **(a)** is trivial: fixed points of an involution σ are given by eigenvectors of the associated matrix Σ. Since $\mathrm{tr}\Sigma = 0$, the eigenvalues t of Σ are given by the equation

$$t^2 = -\det\Sigma.$$

If $\det\Sigma < 0$ then Σ has two distinct eigenvalues and hence two linearly independent eigenvectors. If $\det\Sigma > 0$ then Σ has no real eigenvalues and hence no real eigenvectors.

Following the notation of the proof of Theorem 4.1.3, the quadratic form

$$bp^2 - 2aqp - cq^2$$

is the product of the two 1-forms associated to the vectors w_1 and w_2 where

$$w_i = (b, -a + (-1)^i\sqrt{a^2+bc}).$$

Applying the involution we have that

$$\sigma(w_1) = [ab - ba - b\sqrt{a^2+bc} : bc + a^2 - a\sqrt{a^2+bc}] = [b : -a - \sqrt{a^2+bc}] = w_1.$$

Similarly $w_2 = \sigma(w_2)$. □

As we are considering involutions on the projective line, it is natural to consider the effect of projective transformations of this line on such involutions.

Lemma 4.1.5 *Projective changes of coordinates in $\mathbb{R}P^1$ induce projective transformations of $PLI(2,\mathbb{R})$ that preserves the sets $PLI_+(2,\mathbb{R})$, $PLI_-(2,\mathbb{R})$ and $\tilde{\Delta}$ when $PLI(2,\mathbb{R})$ is identified with $\mathbb{R}P^2$.*

Proof: We let σ be the linear involution with associated matrix

$$\Sigma = \begin{pmatrix} a & b \\ c & -a \end{pmatrix}.$$

A projective change of coordinates in $\mathbb{R}P^1$ is the induced action on $\mathbb{R}P^1$ of a non-degenerate linear transformation on $\mathbb{R}^2$. Let $\mathcal{H}$ be the matrix of such a linear transformation. Then if Σ is the matrix of a linear transformation associated to some $\sigma \in PLI(2,\mathbb{R})$ with respect to some chart. The matrix of a linear transformation associated $\sigma \in PLI(2,\mathbb{R})$ with respect to the transformed chart is $\mathcal{H}^{-1}\Sigma\mathcal{H}$.

We set

$$\mathcal{H} = \begin{pmatrix} \alpha & \beta \\ \gamma & \delta \end{pmatrix}.$$

We calculate $\mathcal{H}^{-1}\Sigma\mathcal{H}$. Identifying σ with the point $[a : b : c] \in \mathbb{R}P^2$ we have that the induced transformation is given by

$$[a : b : c] \mapsto [(\beta\gamma + \alpha\delta)a + \delta\gamma b - \beta\alpha c : 2\beta\delta a + \delta^2 b - \beta^2 c : -2\alpha\gamma a - \gamma^2 b + \alpha^2 c],$$

that is, a projective transformation of $\mathbb{R}P^2$.

Observe finally that

$$((\beta\gamma+\alpha\delta)a+\delta\gamma b-\beta\alpha c)^2+(2\beta\delta a+\delta^2 b-\beta^2 c)(-2\alpha\gamma a-\gamma^2 b+\alpha^2 c) = (\alpha\delta-\beta\gamma)^2(a^2+bc).$$

It follows that the induced projective transformation preserves the sets $PLI_+(2,\mathbb{R})$, $PLI_-(2,\mathbb{R})$ and $\tilde{\Delta}$. □

Allowing such changes of coordinates allows us to construct normal forms for elements of $PLI(2,\mathbb{R})$.

Lemma 4.1.6 *Let $\sigma \in PLI_+(2,\mathbb{R})$ (respectively $PLI_-(2,\mathbb{R})$). Then σ is equivalent to $[x : y] \mapsto [y : x]$ (respectively $[x : y] \mapsto [y : -x]$) under projective changes of coordinates in $\mathbb{R}P^1$.*

Proof: We let σ be the linear involution with associated matrix

$$\Sigma = \begin{pmatrix} a & b \\ c & -a \end{pmatrix}.$$

We make a projective change of of coordinates in $\mathbb{R}P^1$ associated to a linear transformation with matrix $\mathcal{H}$.

If $\sigma \in PLI_-$ we set

$$\mathcal{H} = \begin{pmatrix} a^2+bc & a\sqrt{a^2+bc}+b \\ \sqrt{a^2+bc} & c\sqrt{a^2+bc}-a \end{pmatrix}.$$

We then have

$$\mathcal{H}^{-1}\Sigma\mathcal{H} = \sqrt{a^2+bc}\begin{pmatrix} 0 & 1 \\ 1 & 0 \end{pmatrix}.$$

If $\sigma \in PLI_+$ we set

$$\mathcal{H} = \begin{pmatrix} \dfrac{c\sqrt{-a^2-cb}-2a}{c\sqrt{-a^2-cb}} & \dfrac{cb-2a^2+ac\sqrt{-a^2-cb}}{(a^2+cb)c} \\ \dfrac{1}{\sqrt{-a^2-cb}} & \dfrac{c\sqrt{-a^2-cb}-a}{a^2+cb} \end{pmatrix}.$$

We then have

$$\mathcal{H}^{-1}\Sigma\mathcal{H} = \sqrt{-a^2-bc}\begin{pmatrix} 0 & 1 \\ -1 & 0 \end{pmatrix}.$$

The results follow. □

4.1.2 Pairs of involutions

As remarked (4.1.1), $PLI(2,\mathbb{R})$ is not closed under composition. In fact the composition of two involutions σ_1 and σ_2 is another involution if and only if the two involutions commute:

$$\begin{aligned}
(\sigma_1\circ\sigma_2)\circ(\sigma_1\circ\sigma_2) = \mathrm{Id} \Leftrightarrow\ & (\sigma_2\circ\sigma_1)\circ(\sigma_1\circ\sigma_2)\circ(\sigma_1\circ\sigma_2) = \sigma_2\circ\sigma_1 \\
\Leftrightarrow\ & (\sigma_1\circ\sigma_2)\circ\sigma_1\circ(\sigma_2\circ\sigma_2)\circ\sigma_1 = \sigma_2\circ\sigma_1 \\
\Leftrightarrow\ & (\sigma_1\circ\sigma_2)\circ\sigma_1\circ\mathrm{Id}\circ\sigma_1 = \sigma_2\circ\sigma_1 \\
\Leftrightarrow\ & (\sigma_1\circ\sigma_2)\circ(\sigma_1\circ\sigma_1) = \sigma_2\circ\sigma_1 \\
\Leftrightarrow\ & (\sigma_1\circ\sigma_2)\circ\mathrm{Id} = \sigma_2\circ\sigma_1. \\
\Leftrightarrow\ & (\sigma_1\circ\sigma_2) = \sigma_2\circ\sigma_1.
\end{aligned}$$

Proposition 4.1.2 *Given a linear involution $\sigma \in PLI(2,\mathbb{R})$ the set of involutions that commute with σ is the polar line of σ with respect to the conic $\tilde{\Delta}$ when $PLI(2,\mathbb{R})$ is identified with $\mathbb{R}P^2$.*

Proof: Let

$$\Sigma = \begin{pmatrix} a & b \\ c & -a \end{pmatrix}$$

be the matrix of an associated linear transformation to σ. Let suppose that

$$\tilde{\Sigma} = \begin{pmatrix} \tilde{a} & \tilde{b} \\ \tilde{c} & -\tilde{a} \end{pmatrix}$$

is a matrix associated to an involution that commutes with σ. It follows that $\Sigma\tilde{\Sigma}$ also gives rise to an involution. Calculating we have that

$$\Sigma\tilde{\Sigma} = \begin{pmatrix} a\tilde{a} + b\tilde{c} & a\tilde{b} - \tilde{a}b \\ c\tilde{a} - \tilde{c}a & c\tilde{b} + a\tilde{a} \end{pmatrix}.$$

This matrix gives rise to an involution if and only if $a\tilde{a} + b\tilde{c} = -(c\tilde{b} + a\tilde{a})$, that is, if and only if $2a\tilde{a} + b\tilde{c} + c\tilde{b} = 0$. The set of points $[\tilde{a} : \tilde{b} : \tilde{c}] \in \mathbb{R}P^2$ satisfying this (linear) condition form a line.

The conic $\tilde{\Delta}$ is given by the bilinear form that has matrix

$$\begin{pmatrix} 1 & 0 & 0 \\ 0 & 0 & 1/2 \\ 0 & 1/2 & 0 \end{pmatrix}.$$

The result follows by observing that

$$\begin{pmatrix} \tilde{a} & \tilde{b} & \tilde{c} \end{pmatrix} \begin{pmatrix} 1 & 0 & 0 \\ 0 & 0 & 1/2 \\ 0 & 1/2 & 0 \end{pmatrix} \begin{pmatrix} a \\ b \\ c \end{pmatrix} = 0$$

if and only if $2a\tilde{a} + b\tilde{c} + c\tilde{b} = 0$. □

Corollary 4.1.7 *Let $\sigma_1, \sigma_2 \in PLI(2, \mathbb{R})$ be distinct linear involutions such that $\sigma_1 \circ \sigma_2 = \sigma_2 \circ \sigma_1$. Then σ_1, σ_2 and $\sigma_1 \circ \sigma_2$ form a self-polar triangle with respect to the conic $\tilde{\Delta}$.*

Proof: This follows directly from Proposition 4.1.2 and Lemma 4.0.6. □

Remarks 4.1.8

1. *As $\mathcal{T}(\tilde{\Delta}) = \Delta$ the three quadratic forms corresponding to the fixed points of $\sigma_1, \sigma_2, \sigma_1 \circ \sigma_2$ form a self-polar triangle with respect to Δ, since projective transformations preserve polarity with respect to conics.*

2. *The set $\{\mathrm{Id}, \sigma_1, \sigma_2, \sigma_1 \circ \sigma_2\}$ forms a group under composition which is trivially isomorphic to the Klein 4-group.*

Recall the involution $\sigma_{P\Gamma}$ on any line $\hat{P} \subset \mathbb{R}P^2$ induced by a conic Γ.

Proposition 4.1.3 *Let σ_1, σ_2 be involutions and let $\hat{P} \subset \mathbb{R}P^2$ be the line joining σ_1 and σ_2. Then*

(a) *$\sigma_1 \circ \sigma_2 \circ \sigma_1$ is a further involution;*

(b) *$\sigma_1 \circ \sigma_2 \circ \sigma_1 \in \hat{P}$;*

(c) *$\sigma_1 \circ \sigma_2 \circ \sigma_1$ is the projective harmonic conjugate of σ_2 with respect to σ_1 and $\sigma_{L\tilde{\Delta}}(\sigma_1)$.*

Proof: Assertion **(a)** is trivial:

$$\begin{aligned}(\sigma_1 \circ \sigma_2 \circ \sigma_1) \circ (\sigma_1 \circ \sigma_2 \circ \sigma_1) &= (\sigma_1 \circ \sigma_2) \circ (\sigma_1 \circ \sigma_1) \circ (\sigma_2 \circ \sigma_1) \\ &= (\sigma_1 \circ \sigma_2) \circ (\sigma_2 \circ \sigma_1) \\ &= \sigma_1 \circ (\sigma_2 \circ \sigma_2) \circ \sigma_1 \\ &= \sigma_1 \circ \sigma_1 \\ &= \mathrm{Id}.\end{aligned}$$

We may, by Lemma 4.1.6, choose σ_1 to be given by $[x : y] \mapsto [y : \pm x]$. Let σ_2 be the involution given by $[x : y] \mapsto [ax + by : cx - ay]$. It follows that the involution $\sigma_1 \circ \sigma_2 \circ \sigma_1$ is

$$[x : y] \mapsto [\mp ax + cy : bx \pm ay].$$

It is clear that $[0 : 1 : \pm 1], [a : b : c], [\mp a : c : b]$ (that is, the points in $\mathbb{R}P^2$ corresponding to σ_1, σ_2 and $\sigma_1 \circ \sigma_2 \circ \sigma_1$) are colinear, which establishes **(b)**.

A calculation shows that $\sigma_{P\tilde{\Delta}}(\sigma_1)$ is the involution

$$[x : y] \mapsto [2ax + (b \mp c)y : x(b \mp c) - 2ay].$$

As a point in $\mathbb{R}P^2$ this is $[2a : b \mp c : b \mp c]$.

The cross-ratio of four colinear points in the real projective plane $\mathbb{R}P^2$ written in the form $[X : Y : Z]$ is equal to the cross ratio of the corresponding complex numbers $X/Y + iZ/Y$.

Calculating the cross-ratio of $[0 : 1 : \pm 1], [a : b : c], [\mp a : c : b]$ and $[2a : b \mp c : b \mp c]$ we have

$$\left(\frac{a/b + ic/b \mp i}{a/b + ic/b - 2a/(b \mp c) - i}\right)\left(\frac{-2a/(b \mp c) - i \mp a/c + ib/c}{\mp a/c + ib/c \mp i}\right) = -1.$$

This establishes **(c)**. □

4.2 Self polar triples of binary differential equations on surfaces

If, in the construction of binary quadratic forms from linear involutions on $\mathbb{R}P^1$ described in Section 4.1.1, we replace the direction $[v] \in \mathbb{R}P^1$ with a smooth direction field on a surface $S \subset \mathbb{R}^3$, we may construct a BDE on the surface using involutions on each projectivised tangent plane varying smoothly with the surface.

The first fundamental form of S (which we will refer to as the metric) on the surface is of course a binary quadratic form on the surface in its own right,

$$Eq^2 + 2Fpq + Gp^2. \tag{4.1}$$

It may therefore be considered to be a point in $\mathbb{R}P^2$ which we will denote by L. Since the first fundamental form is positive definite, $L \in \mathbb{R}P^2_{\Delta^+}$ at all points of the surface. It follows from Lemma 4.0.5 that $\hat{L} \in G_2(\mathbb{R}^3)_{\Gamma^+}$ and hence the quadratic form corresponding to each point of $\hat{L}$ defines two real directions. These directions are orthogonal (with respect to the metric L).

As it is a binary quadratic form, the metric is determined by an involution. Applying the projective transformation $\mathcal{T}^{-1}$ to L we find that the corresponding involution is given by

$$[x : y] \mapsto [Fx + Gy : -Ex - Fy].$$

This is the involution that maps each direction to that which is orthogonal to it (with respect to the metric. We denote this involution by O. It is clear that $O \in PLI_+(2, \mathbb{R})$.

As an involution varies on the surface, there may be points where it becomes degenerate (in the notation of the previous section, $a^2 + bc = 0$). The set of such points is the discriminant of the corresponding BDE. As the projective transformation $\mathcal{T}$ extends across such points, we may extend the BDE to these points.

Let $\sigma \in PLI(2, \mathbb{R})$ with $\sigma \neq O$. Then the polars of σ and O with respect to the conic $\tilde{\Delta}$ intersect at a single point. We denote the linear involution corresponding to this point by R_σ. By Proposition 4.1.2 we have that σ, R_σ commute and that

$\sigma \circ R_\sigma \in PLI(2, \mathbb{R})$. Finally by Corollary 4.1.7 we have that $\mathcal{T}(\{\sigma, R_\sigma, \sigma \circ R_\sigma\})$ is a self-polar triangle of BDEs.

Proposition 4.2.1 *Amongst pairs of directions* $([v], \sigma([v]))$*, the solutions of the form* $\mathcal{T}(R_\sigma \circ \sigma)$ *are those that have extremal included angle.*

Proof: Without loss of generality, we may assume that at any given point the solutions of $\mathcal{T}(R_\sigma)$ are the coordinate directions, that is, $\mathcal{T}(R_\sigma)$ is the form pq, and that the metric is the form $p^2 + q^2$. The involution R_σ is given by

$$\begin{aligned} R_\sigma : \mathbb{R}P^1 &\to \mathbb{R}P^1 \\ [x : y] &\mapsto [x : -y] \end{aligned}$$

As a point in $\mathbb{R}P^2$ then, the involution R_σ is the point $[1 : 0 : -1]$. As σ lies in the polar of R_σ, we have that

$$\begin{aligned} \sigma : \mathbb{R}P^1 &\to \mathbb{R}P^1 \\ [x : y] &\mapsto [by : cx] \end{aligned}$$

for some $b, c \in \mathbb{R}$. The involution $R_\sigma \circ \sigma$ is therefore

$$\begin{aligned} R_\sigma \circ \sigma : \mathbb{R}P^1 &\to \mathbb{R}P^1 \\ [x : y] &\mapsto [by : -cx]. \end{aligned}$$

The BDE $\mathcal{T}(R_\sigma \circ \sigma)$ is therefore

$$by^2 + cdx^2.$$

Consider a direction

$$[\cos\theta : \sin\theta] \in \mathbb{R}P^1.$$

If α denotes the angle between $[\cos\theta : \sin\theta]$ and $\sigma([\cos\theta : \sin\theta])$ then α satisfies

$$\cos^2\alpha = \frac{(b+c)\sin\theta\cos\theta}{b^2\sin^2\theta + c^2\cos^2\theta}.$$

We differentiate with respect to θ and equate $d\alpha/d\theta$ to zero, and find that α is extremal if and only if θ satisfies

$$b\cos^2\theta + c\sin^2\theta = 0,$$

that is, if $[\cos\theta : \sin\theta]$ is a solution of $\mathcal{T}(R_\sigma \circ \sigma)$. □

The asymptotic, characteristic and principal curves on a smooth surface may, away from umbilic points, be constructed in this way using a single involution, namely conjugation: the involution $C \in PLI(2,\mathbb{R})$ that maps a direction to its conjugate direction. Umbilic points are isolated points where the involution (conjugation) coincides with the involution O. At hyperbolic points $C \in PLI_+(2,\mathbb{R})$ and at elliptic points $C \in PLI_-(2,\mathbb{R})$. The asymptotic BDE is given by $\mathcal{T}(C)$, the principal BDE by $\mathcal{T}(R_C)$ and the characteristic BDE by $\mathcal{T}(C \circ R_C)$.

Remark 4.2.1 *The constructions discussed in this section have used only the metric L and a smoothly varying involution on each projectivised tangent plane. Our results may thus be generalised to any Riemmannian manifold endowed with such an involution.*

4.2.1 Configurations of solution curves

Many of the symmetries between the asymptotic and characteristic curves are shared between pairs of BDEs $\mathcal{T}(\sigma)$ and $\mathcal{T}(R_\sigma \circ \sigma)$ constructed as in the previous section. Our aim is to exploit these in order to generalise some of the results from Chapter 3. We require the following Lemma.

Lemma 4.2.2 *Let ω_1 and ω_2 be BDEs with the same discriminant Δ. Suppose that Δ is a smooth curve, that on Δ the BDEs define the same single direction, and that in a neighbourhood of Δ the solution curves exist on opposite sides of Δ. If ω_1 has a well-folded singularity at a point on Δ, then ω_2 has a well-folded singularity with opposite index at the same point.*

Proof: Suppose that ω_1 has a well-folded singularity at a point on Δ. We assume that the point under consideration is the origin. We make smooth changes of coordinates and write ω_1 as

$$dy^2 - (y - \lambda_1 x^2)dx^2 = 0 \tag{4.2}$$

for some constant $\lambda_1 \neq 0, 1/16$ ([30]). Consider the affine chart $p = dy/dx$. The discriminant of (4.2) is the curve $y = \lambda_1 x^2$.

Observe that the condition that the BDEs define the same direction on Δ is equivalent to the BDEs having the same criminant projecting to Δ. The criminant of (4.2) is the curve

$$(0, \lambda_1 x^2, 0).$$

We write ω_2 as

$$a(x,y)p^2 + 2b(x,y)p + c(x,y) = 0. \tag{4.3}$$

The criminant of (4.3) lies on the surface $ap + b = 0$. Hence if ω_2 has the same criminant as ω_1 then $b = 0$ on Δ. We may then write

$$b = (y - \lambda_1 x^2)\tilde{b}(x,y)$$

where $\tilde{b}(x,y)$ is a smooth function which is non-zero in a neighbourhood of Δ.

We may write

$$c(x,y) = (y - \lambda_1 x^2)\tilde{c}(x,y)$$

for some smooth function $\tilde{c}$ which is non-zero in a neighbourhood of the discriminant. Furthermore the discriminant of (4.3) is the curve $y = \lambda_1 x^2$, so $a(x,y) \neq 0$ in a neighbourhood of the discriminant. We may then assume $a = 1$.

We thus have that ω_2 may be written as

$$p^2 + (y - \lambda_1 x^2)(2p\tilde{b} + \tilde{c}) = 0, \tag{4.4}$$

which has a well-folded singularity at the origin.

The discriminant of (4.4) is

$$((y - \lambda_1 x^2)\tilde{b}^2 - \tilde{c})(y - \lambda_1 x^2).$$

In a neighbourhood of the discriminant we have

$$\tilde{c} > (y - \lambda_1 x^2)\tilde{b}^2$$

since the solution curves exist on opposite sides of the discriminant to those of ω_1. Hence $\tilde{c}(0,0) > 0$.

The index modulus of (4.4) is

$$\lambda_2 = -\frac{\lambda_1}{\tilde{c}(0,0)}.$$

This clearly has opposite sign to λ_1. □

Let ω be a BDE determined by an involution $\sigma \in PLI(2,\mathbb{R})$, that is, let

$$\omega = \mathcal{T}(\sigma).$$

Let $\omega_p = \mathcal{T}(R_\sigma)$ and let $\tilde{\omega} = \mathcal{T}(R_\sigma \circ \sigma)$.

Proposition 4.2.2 **(a)** *The BDE ω has a solution direction in common with $\omega^\perp$ if and only if $\omega \in \Delta$.*

(b) *If $\omega \in \Delta$ then $\tilde{\omega} = \omega$.*

(c) *The BDE $\omega^\perp$ has solutions at all points of the surface. At points where ω has two (respectively no) solutions the BDE $\tilde{\omega}$ has no (respectively two) solutions.*

Proof: As $L \in \mathbb{R}P^2_{\Delta^-}$ and $\omega^\perp \in \hat{L}$ we have that $\omega^\perp \in \mathbb{R}P^2_{\Delta^+}$ by Lemma 4.0.5. The set of forms with solution directions in common with $\omega^\perp$ comprises the two lines in $G_2(\mathbb{R}^3)_{\Delta^0} =$ that intersect at $\omega^\perp$. The points of tangency of these lines with Δ lie on $\hat{\omega^\perp}$. By construction $\omega \in \hat{\omega^\perp}$, so ω has a direction in common with $\omega^\perp$ if and only if $\omega \in \Delta$.

Since $\tilde{\omega} = \sigma_{\omega^\perp}(\omega)$ parts **(b)** and **(c)** follows directly from Lemma 4.0.6. □

Corollary 4.2.3 *The well-folded singularities of the BDEs ω and $\tilde{\omega}$ coincide and have opposite index.*

Proof: This is a combination of Lemma 4.2.2 and Proposition 4.2.2 **(b)**. □

Remark 4.2.4 *If ω lies on the polar of the metric L then the directions defined by ω are a rotation through $\pi/4$ of those defined by $\omega^\perp$, and $\tilde{\omega} = L$.*

Proposition 4.2.3 *If the BDE ω has a folded singularity at the origin and has 2-jet affine equivalent to*

$$p^2 + uxp + y + \frac{v}{4}x^2 + w_1xy + w_2y^2. \tag{4.5}$$

then the BDE $\tilde{\omega}$ has 2-jet affine-equivalent to

$$p^2 - uxp + y + (\frac{u^2}{2} - \frac{v}{4})x^2 + w_1xy + (w_2 - 1)y^2. \tag{4.6}$$

Proof: We first construct the BDE $\omega^{\perp}$. We may write the metric L as

$$p^2 + 2l_2(x,y)pq + (1 + l_3(x,y))q^2,$$

where l_2 and l_3 are smooth functions with $j^2 l_2 = j^3 l_3 = 0$. We write the BDE ω as

$$p^2 + (ux + s_2(x,y))pq + (y + \frac{v}{4}x^2 + w_1xy + w_2y^2 + s_3(x,y))q^2$$

where s_2 and s_3 are smooth functions with $j^1 s_2 = j^2 s_3 = 0$. The BDE $\omega^{\perp}$ is the polar of the pencil connecting L and ω. It follows that

$$\omega^{\perp} = \begin{vmatrix} 2p + 2l_2q & 2l_2p + 2(1 + l_3)q \\ 2p + (ux + s_2)q & (ux + s_2)p + 2(y + \frac{v}{4}x^2 + w_1xy + w_2y^2 + s_3)q \end{vmatrix}.$$

We write the BDE $\omega^{\perp}$ as

$$\begin{aligned}&(2l_2 - ux - s_2)dy^2 + 2(1 - y + l_3 - \frac{v}{4}x^2 - w_1xy - w_2y^2 - s_3)dxdy \\ &+((1 + l_3)(ux + s_2) - 2l_2(y + \frac{v}{4}x^2 - w_1xy - w_2y^2 + s_3))dx^2 = 0.\end{aligned}$$

The BDE $\tilde{\omega}$ is the polar of the pencil joining the BDE $\omega^{\perp}$ and the BDE ω. It follows that

$$\tilde{\omega} = Jac(\omega, \omega^{\perp}).$$

We calculate this determinant. The BDE $\tilde{\omega}$ is

$$ady^2 + 2bdydx + cdx^2$$

where

$$\begin{aligned}
a = \;& -8l_2ux - 8l_2s_2 + 4u^2x^2 + 8uxs_2 + 4s_2^2 + 8 - 8y + 8l_3 - 2vx^2 - 8s_3, \\
b = \;& 4s_3ux + 4yux + vx^3u - 4l_2vx^2 + vx^2s_2 + 4l_3ux + 4ys_2 \\
& +4l_3s_2 + 4s_3s_2 - 16l_2y - 16l_2s_3 + 4ux + 4s_2 \\
& +8l_2w_1xy - 4w_1ux^2y - 4w_1s_2xy - 4w_2uxy^2 + 8w_2l_2y^2 - 4w_2s_2y^2, \\
c = \;& -8y - 2vx^2 - 8s_3 + 8y^2 + 4yvx^2 + 16ys_3 - 8l_3y - 2l_3vx^2 - 8l_3s_3 \\
& +\frac{1}{2}v^2x^4 + 4vx^2s_3 + 8s_3^2 + 4u^2x^2 + 8uxs_2 + 4s_2^2 \\
& +4l_3u^2x^2 + 8l_3uxs_2 + 4l_3s_2^2 - 8l_2yux - 8l_2ys_2 - 2l_2vx^3u \\
& -2l_2vx^2s_2 - 8l_2s_3ux - 8l_2s_3s_2 \\
& -8w_1xy^2 + 8l_3w_1xy - 2vw_1x^3y - 8w_1s_3xy + 8w_1xy \\
& -2w_2vx^2y^2 - 8w_2y^3 - 8w_2s_3y^2 + 8w_2y^2 + 8w_2l_3y^2.
\end{aligned}$$

Since $a(0,0) \neq 0$ we may set $p = dy/dx$ and write the BDE $\tilde{\omega}$ as

$$\tilde{F}(x, y, p) = 0$$

where

$$j^2\tilde{F}(x, y, p) = -8p^2 - 8uxp + 8y + 8w_1xy + (8w_2 - 8)y^2 + (2v - 4u^2)x^2.$$

We make the linear change of coordinates

$$(x, y) \mapsto (x, -y)$$

and divide by -8 to complete the proof. □

4.2.2 The ocr-invariant

The affine properties of a well-folded singularity of a BDE ω that are used in the classification in [23] are determined by the values of u and v in the 2-jet of ω at the singularity. The corresponding parameters for the BDE $\tilde{\omega}$ are, by Proposition 4.2.3, $-u$ and $2u^2 - v$. The map $(u, v) \mapsto (-u, 2u^2 - v)$ defines an involution on the (u, v)-plane which preserves the sets

$$v = u^2$$

(the discriminant is inflectional) and

$$v = u(u + 1)$$

(saddle-node change and inflection set / discriminant having $>$ 2-point contact).

We now associate an invariant to a folded singularity of a BDE using the contact elements to the discriminant and inflectional curves, following the approach used to define the ccr-invariant in Chapter 3.

Definition 4.2.5 *The ocr-invariant ρ of a well-folded singularity of a BDE ω is defined to be the cross-ratio of the the tangents to the contact elements to the discriminant of ω, the loci of inflections of the solution curves of ω and $\tilde{\omega}$ and the fibre of the projection π over the singularity.*

Unlike the ccr-invariant defined in Chapter 3, the ocr-invariant ρ is not a projective invariant of the surface, merely an affine invariant.

Proposition 4.2.4 **(a)** *The ocr-invariant ρ of a well-folded singularity of a BDE ω with 2-jet affine-equivalent to*

$$p^2 + uxp + y + \frac{v}{4}x^2 + w_1xy + w_2y^2$$

is given by

$$\rho = -\frac{(u-1)^2}{(u+1)^2}.$$

(b) *Suppose that a well-folded singularity of the BDE ω has index modulus λ and ocr-invariant ρ. Then the well-folded singularity of the BDE $\tilde{\omega}$ has index modulus $-\lambda$ and ocr-invariant $1/\rho$.*

Proof: We set

$$j^2F(x,y,p) = p^2 + uxp + y + \frac{v}{4}x^2 + w_1xy + w_2y^2.$$

Then the surface $F_p(x,y,p) = 0$ is given by $p = -ux/2$. Substituting this into the equation $F = 0$ we have that the discriminant curve is given by

$$y = \frac{(u^2 - v)}{2}x^2 + h.o.t.$$

The surface $F_x + pF_y = 0$ is given by

$$(u+1)p = -\frac{v}{2}x + h.o.t.$$

Substituting this into the equation $F = 0$ we have that the inflection curve associated to the BDE ω is

$$y = \frac{v(-v + u^2 - 1)}{4(u+1)^2}x^2 + h.o.t.$$

Using the involution $(u,v) \mapsto (-u, 2u^2 - v)$ we have that the inflection curve associated to the BDE $\tilde{\omega}$ is

$$y = \frac{(2u^2 - v)(u^2 + 1 - v)}{4(u-1)^2}x^2 + h.o.t.$$

We use these 2-jets to calculate the required cross-ratio and establish part **(a)**.

The well-folded singularity at the origin of the BDE

$$p^2 + uxp + y + \frac{v}{4}x^2 + w_1xy + w_2y^2 = 0$$

has index modulus

$$\lambda = (v - u(u+1))/4$$

and ocr-invariant

$$\rho = -(u-1)^2/(u+1)^2.$$

Applying the involution $(u, v) \mapsto (-u, 2u^2 - v)$ we have

$$\frac{(v - u(u+1))}{4} \mapsto \frac{(-v + u(u+1))}{4}.$$

Similarly we have

$$\frac{-(u-1)^2}{(u+1)^2} \mapsto \frac{-(u+1)^2}{(u-1)^2}.$$

This establishes part **(b)**. □

As explained in Section 1.3, the configurations of the cusp and inflection sets of a BDE at a folded singularity are determined by the values of u and v in the 2-jet of the equation. We establish now the relationship between the ocr-invariant and these configurations. Recall that the cusp and inflection sets are generically parabolae meeting tangentially at the singularity. We are interested in how these parabolae nest.

The ocr-invariant is not defined on the sets $u = -1$ where the inflection set of the BDE ω is singular, and $u = 1$ where the inflection set of the BDE $\tilde{\omega}$ is singular. We refer to the region $u \in (-1, 1)$ (respectively the region $u \in (\infty, -1) \cup (1, \infty)$) as region 1 (respectively region 2). The map restriction of the map

$$\begin{aligned} \mathbb{R} &\to \mathbb{R} \\ u &\mapsto \rho(u) \end{aligned}$$

is a bijection on each of region 1 and region 2. Observe also that each of these regions is closed under the action of the involution $(u, v) \mapsto (-u, 2u^2 - v)$

To any well-folded singularity of a BDE we associate the complex number

$$z = \sqrt{-\rho}e^{2i \arctan(16\lambda)}$$

(we choose $\arctan(16\lambda) \in (-\pi/2, \pi/2)$ and the positive square root). Consider the complex valued function

$$\begin{aligned} f : \mathbb{R}^2 &\to \mathbb{C} \\ (u, v) &\mapsto z. \end{aligned}$$

Observe that $f(1, v) = 0$ and $f(-1, v)$ has infinite modulus. The closure of the restriction of f to either region 1 or region 2 is the entire complex plane which may be compactified by adding a point at infinity, and that such a restriction of f defines a smooth bijection.

Proposition 4.2.5 (a) *The configurations of the solution curves and relative positions of the cusp and inflection sets of a BDE ω at a well-folded singularity are given by the complex parameter z associated to the singularity.*

(b) *Let* $\arg(z) = \theta$ *and* $|z| = r$. *Codimension 1 phenomena are given by the following exceptional sets in the complex plane:*

	Region 1	*Region 2*
saddle/node	$\theta = 0$	$\theta = \pi$
node/focus	$\theta = \pi/2$	$\theta = \pi/2$
focus/saddle	$\theta = \pm\pi$	$\theta = \pm\pi$
cusp set inflectional	$(r+1)\tan\frac{\theta}{2} = 4(r-1)$	$(r-1)\tan\frac{\theta}{2} = 4(r+1)$
inflection set inflectional	$\tan\frac{\theta}{2}(r+1) = -8$ $\tan\frac{\theta}{2}(1+r)^2 = 8(r-1)$	$\tan\frac{\theta}{2}(r-1) = 8$ $\tan\frac{\theta}{2}(1-r)^2 = -8(1+r)$
cusp set singular	$\theta = \pm\pi$	$r = 1$
inflection set singular	$r = \infty$	$r = 1$ $r = \infty$

The relative positions of the cusp and inflection curves are constant in the open regions of the complex plane bounded by these curves. This partition of the complex plane and the corresponding configurations of the curves of interest are shown in Figure 4.1.

(c) *The corresponding configurations at the singularity of the BDE $\tilde{\omega}$ are given by the complex number $1/z$.*

Proof: Part **(a)** is trivial: the parameters u and v determine both z and the relative positions of the cusp and inflection curves.

When $u \in (-1, 1)$ we have that

$$r = \frac{1-u}{1+u}$$

and

$$\theta = 2\arctan(4(v - u(u+1)).$$

It follows that

$$u = \frac{1-r}{1+r}$$

and

$$v = \frac{\tan\frac{\theta}{2}}{4} + 2\frac{1-r}{(1+r)^2}.$$

It is clear that a saddle / node change ($\lambda = 0$) occurs when $\theta = 0$, a node / focus change ($\lambda = 1/16$) occurs when $\theta = \pi/2$, and that at $\theta = \pm\pi$ there is a change in the sign of λ through infinity.

We use the expressions for the 2-jets of the cusp and inflection curves obtained in the proof of Proposition 4.2.4. The cusp set is inflectional when $v = u^2$. Substituting the expressions for u and v in terms of r and θ we have that the cusp set is inflectional when

$$(r-1)\tan\theta = 4(r+1).$$

Similarly the inflection set is inflectional when $v = 0$ or $v = u^2 - 1$, that is, when

$$\tan\frac{\theta}{2}(1+r)^2 = 8(r-1)$$

or

$$\tan\frac{\theta}{2}(r+1) = -8.$$

The cusp set is singular only on the line at infinity in the (u, v)-plane. It is clear that $v = \infty$ corresponds to the set $\theta \pm \pi$. The inflection set is singular on this line, and also at $u = 1$, that is, when $r = \infty$.

When $u \in (\infty, -1) \cup (1, \infty)$ we have that

$$r = \frac{u-1}{1+u}$$

and

$$\theta = 2\arctan(4(v - u(u+1)).$$

Similar calculations to those above establish the exceptional sets.

Part (**b**) is then established by choosing values of r and θ in each of the open regions bounded by the exceptional sets and calculating the required 2-jets.

Part **(c)** follows immediately from Proposition 4.2.4 **(b)**. □

Remarks 4.2.6 *1. Each complex number z (that does not lie in an exceptional set) corresponds to two smoothly equivalent well-folded singularities, that is, a complex number z does not uniquely determine a configuration.*

2. A finer classification of folded singularities may be obtained by including the separatrices of the singularities in our study.

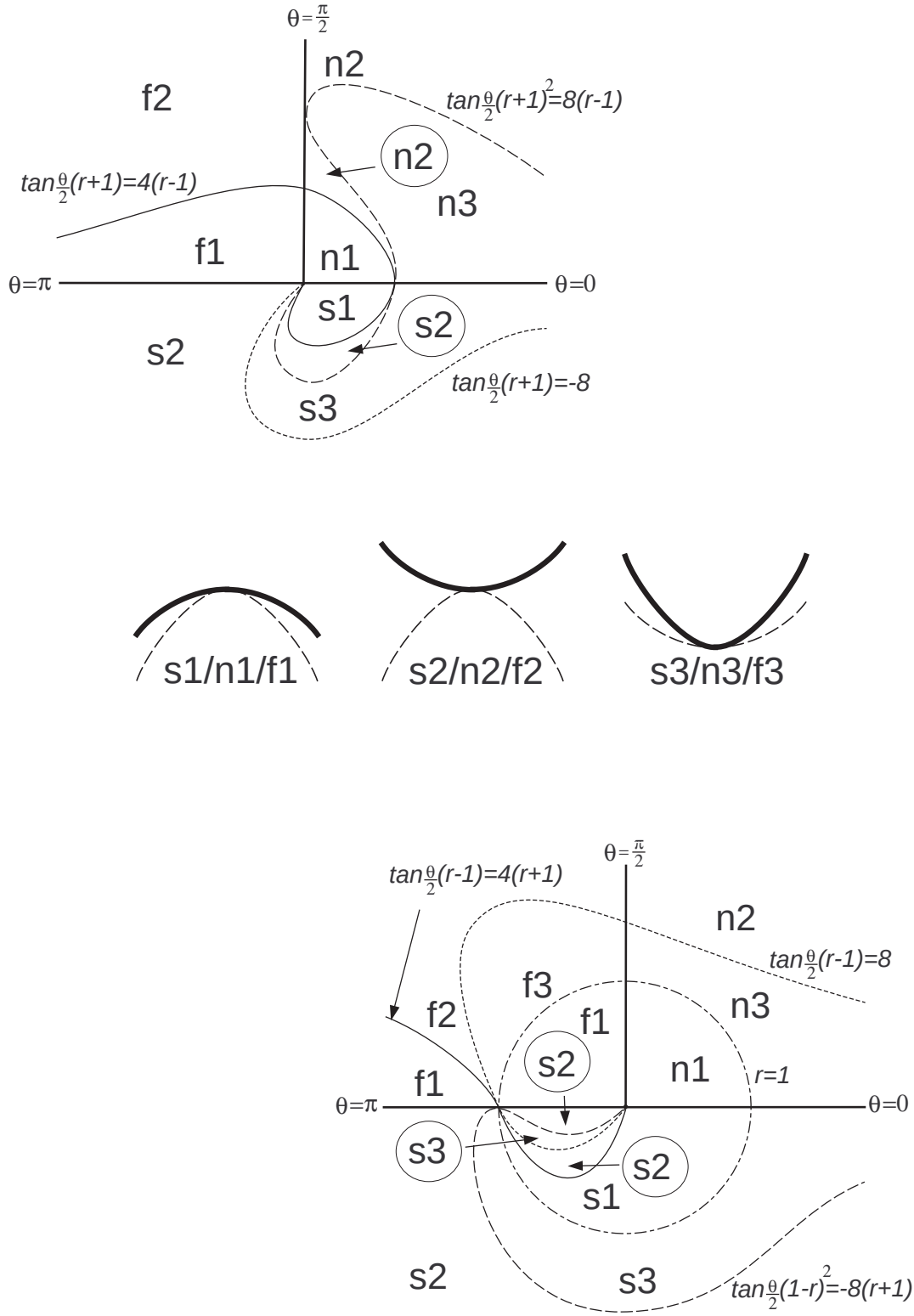

Figure 4.1: Partitions of the z-plane: region 1 (left) and region 2 (right), and configurations of the cusp set (thick curves) and inflection set (broken curves).

Chapter 5

Polarity and pencils of quadratic forms

In this chapter we show that, in addition to the asymptotic (2.5), characteristic (2.6) and principal (2.4) BDEs, certain other BDEs on surfaces are objects worthy of further investigation. We gain further insight into the intimate connections between the asymptotic, characteristic and principal BDEs. Drawing upon the work in Chapter 4 concerning involutions of the real projective line, we prove that the asymptotic, characteristic and principal BDEs are related to another well-studied BDE on the surface, namely that of the arithmetic mean curvature lines, and also to a new BDE that we define in Section 5.1.3.

We also consider the pencils of forms that connect the BDEs of interest, and show that there are natural parametrisations of these pencils which are related to one another in a particularly nice way.

The geometric concepts of asymptotic curves, lines of curvature and characteristic curves on surfaces in $\mathbb{R}^3$ are all derived from the first fundamental form (that is, the metric) and the shape operator (the Weingarten map), which is a self-adjoint operator on the tangent space. The new BDEs defined in this chapter are also all derived from the metric and the shape operator. It follows that one may define these BDEs on any Riemmannian manifold endowed with a self-adjoint operator, although their meaning in that more general context may be different.

We will use the labels shown in Table 5.1 for the binary quadratic forms on

surfaces in which we are interested (these will be defined during the course of the chapter).

Metric (4.1)	L
Asymptotic BDE (2.5)	A
Characteristic BDE (2.6)	Ch
Principal BDE (2.4)	P
BDE of the lines of arithmetic mean curvature (5.1)	Me
Third fundamental form (5.3)	B
BDE of the MOSI curves (5.4)	T

Table 5.1: Binary quadratic forms on surfaces.

As in Chapter 4, we shall use the symbol $\hat{Q}$ to denote the polar line of a point $Q \in \mathbb{R}P^2$.

5.1 Quadratic forms on surfaces

5.1.1 Arithmetic mean curvature lines

The lines of arithmetic mean curvature (the integral curves of those directions on a surface in which the sectional curvature is equal to H, the arithmetic mean curvature of the surface) are studied in [39, 42].

Proposition 5.1.1 **(a)** ([39]) *The BDE of the lines of arithmetic mean curvature is*

$$\begin{aligned}(nEG - 2nF^2 - G^2l + 2GFm)dy^2 \\ +2(2mEG - FGl - FEn)dxdy \\ +(lEG - 2lF^2 - E^2n + 2EFm)dx^2 = 0.\end{aligned} \tag{5.1}$$

(b) *The discriminant of* (5.1) *consists of umbilic points.*

(c) *Away from umbilic points the BDE may be written, with respect to a principal coordinate system as*

$$Gdy^2 - Edx^2 = 0.$$

(d) *The geodesic torsion in the direction of the lines of arithmetic mean curvature is equal to*

$$\pm\frac{(\kappa_1-\kappa_2)}{2}.$$

Proof: The first assertion is established in [39] by setting

$$\frac{\mathrm{II}([dx:dy],[dx:dy])}{\mathrm{I}([dx:dy],[dx:dy])}=H,$$

where I (respectively II) denotes the first (respectively second) fundamental form, and where H is the expression for the arithmetic mean curvature in terms of the coefficients of the first and second fundamental forms given in Section 2.1.

A simple calculation shows that the discriminant of the the BDE (5.1) is

$$4(EG-F^2)(n^2E^2+4Em^2G-2EnGl-4EmnF+l^2G^2-4mFlG+4F^2ln),$$

which vanishes only at umbilic points.

To obtain the BDE (5.1) with respect to a principal coordinate system we set $F=m=0$, $l=E\kappa_1$ and $n=G\kappa_2$.

The final assertion follows from the formulae in Section 2.1. □

We denote the BDE of the lines of arithmetic mean curvature by Me. Away from umbilic points, the lines of arithmetic mean curvature form an orthogonal net, and are inclined at an angle of $\pm\pi/4$ to the principal directions. It is clear, therefore, that the BDEs defining the lines of arithmetic mean curvature and the lines of curvature are related.

Proposition 5.1.2 *Considered as a point in the projective plane $\mathbb{R}P^2$, the BDE Me is the polar of the pencil joining the metric L and the principal BDE P, that is, these three forms constitute a self-polar triangle.*

Proof: Consider the quadratic forms corresponding to the principal BDE P and the metric L. We calculate $Jac(L,P)$, which is given by

$$\begin{vmatrix} 2Eq+2Fp & 2Fq+2Gp \\ 2(Fl-Em)q+(Gl-En)p & (Gl-En)q+(Gm-Fn)p \end{vmatrix}.$$

This is equal to

$$\begin{aligned} 2(nEG - 2nF^2 - G^2l + 2GFm)p^2 \\ +4(2mEG - FGl - FEn)pq \\ +2(lEG - 2lF^2 - E^2n + 2EFm)q^2 = 0, \end{aligned}$$

which corresponds to the same point in the projective plane $\mathbb{R}P^2$ as the BDE Me. □

Remark 5.1.1 *Given that the lines of arithmetic mean curvature form an orthogonal net, Proposition 5.1.2 follows immediately from Proposition 1.3.1* **(d)**.

Consider the projective space PT_pS of all tangent directions through a point p on S which is neither an umbilic nor parabolic point. Clearly this is simply the real projective line $\mathbb{R}P^1$. Recall the projective transformation

$$\begin{aligned} \mathcal{T} : \mathbb{R}P^2 &\to \mathbb{R}P^2 \\ [a : b : c] &\mapsto [b : 2a : -c]. \end{aligned}$$

defined in Chapter 4 that relates linear involutions of the real projective line to binary differential equations on surfaces.

Recall also the linear involution R on PT_pS that reflects in (either of) the principal directions, and the linear involution O that rotates each direction through $\pi/2$.

Corollary 5.1.2 (a) *The BDE P of the lines of curvature is given by $\mathcal{T}(R)$.*

(b) *The BDE Me of the lines of arithmetic mean curvature is given by $\mathcal{T}(R \circ O)$.*

Proof: The principal directions are clearly the fixed points of the linear involution R, so assertion **(a)** follows from Theorem 4.1.3. By construction (see Section 4.2), the metric L is given by $\mathcal{T}(O)$. Assertion **(b)** then follows from Proposition 5.1.2 and Corollary 4.1.7. □

5.1.2 The third fundamental form

The third fundamental form is a quadratic form on a surface that has not been much studied, as it is determined by the first and second fundamental forms. Our results in

Chapter 4 gives further insight into the relationship between these quadratic forms, and show that the third fundamental form is related to the characteristic curves.

Definition 5.1.3 *The third fundamental form at a point p of a surface S is the quadratic form on T_pS given by $\mathrm{III}(u,v) = W_p(u)\cdot W_p(v)$ where W_p is the Weingarten map.*

The third fundamental form of a surface is the metric on the spherical image (the image of the surface under the Gauss map). It follows that the corresponding linear involution is $C \circ O \circ C$ (recall from Proposition 4.1.3 part **(a)** that, given any two linear involutions σ_1, σ_2 on the real projective line, $\sigma_1 \circ \sigma_2 \circ \sigma_1$ is also a linear involution).

Proposition 5.1.3 *Given a parametrisation*

$$\mathbf{r} : U \to S,$$

the third fundamental form is represented with respect to the coordinate system $\{\mathbf{r}_x, \mathbf{r}_y\}$ by the matrix

$$\frac{1}{EG-F^2}\begin{pmatrix} (2Fml - Em^2 - Gl^2) & (Fln + Fm^2 - Gml - Emn) \\ (Fln + Fm^2 - Gml - Emn) & (2Fnm - Gm^2 - En^2) \end{pmatrix}.$$

Away from umbilic points, if we choose a principal coordinate then this matrix is

$$\begin{pmatrix} E\kappa_1^2 & 0 \\ 0 & G\kappa_2^2 \end{pmatrix}.$$

Proof: The first fundamental form is represented by the symmetric matrix

$$\mathcal{M}_{\mathrm{I}} = \begin{pmatrix} E & F \\ F & G \end{pmatrix}.$$

The second fundamental form is represented by the symmetric matrix

$$\mathcal{M}_{\mathrm{II}} = \begin{pmatrix} l & m \\ m & n \end{pmatrix}.$$

The third fundamental form is represented by the matrix $\mathcal{M}_{\mathrm{III}}$ where

$$\mathcal{M}_{\mathrm{III}} = \mathcal{M}_{\mathrm{II}}\mathcal{M}_{\mathrm{I}}^{-1}\mathcal{M}_{\mathrm{II}}. \tag{5.2}$$

(see [45]). We obtain the matrix of the third fundamental form by the appropriate multiplication of matrices.

Away from umbilic points, we substitute

$$F = m = 0, \;\; l = E\kappa_1, \;\; n = G\kappa_2$$

to obtain the third fundamental form in a principal coordinate system. □

When considered as a point in $\mathbb{R}P^2$ we do not distinguish between non-zero multiples of forms. The third fundamental form and the quadratic form B given by

$$(2Fml - Em^2 - Gl^2)q^2 + 2(Fln + Fm^2 - Gml - Emn)pq + (2Fnm - Gm^2 - En^2)p^2 \tag{5.3}$$

are represented by the same point in $\mathbb{R}P^2$.

In the principal coordinate system this reduces to

$$E\kappa_1^2 q^2 + G\kappa_2^2 p^2.$$

Remark 5.1.4 *The matrices of the first, second and third fundamental forms on a surface are also related, away from umbilic points, by the equation*

$$\mathcal{M}_{\mathrm{III}} = 2H\mathcal{M}_{\mathrm{II}} - K\mathcal{M}_{\mathrm{I}}.$$

This is obtained by applying the Cayley-Hamilton Theorem to the Weingarten map.

5.1.3 The minimal orthogonal spherical image curves

As the matrix of the third fundamental form is a linear combination of those of the first and second fundamental forms, the quadratic form B, considered as a point in $\mathbb{R}P^2$, lies on the pencil joining the asymptotic BDE A and the metric L. As this pencil is the polar of the principal BDE P the third fundamental form B and P are apolar on the pencil that joins them. It follows that there is a further BDE $T = Jac(P, B)$, making (P, B, T) a self-polar triple.

The results in Chapter 4 explain the geometric significance of this BDE. By Theorem 4.1.3, the polar $\hat{B}$, of the third fundamental form B is the set of BDEs with

solution directions $[u], [v]$ satisfying $B(u, v) = 0$ or alternatively $(C \circ O \circ C)(u) = v$. The images of such directions under the Gauss map are orthogonal directions on the spherical image.

Definition 5.1.5 *The* minimal orthogonal spherical image directions *(MOSI directions) are the unique pair of tangent directions to S that have orthogonal images under the Weingarten map and that are inclined at a minimal angle at each point of S. The* MOSI curves *are the integral curves of the MOSI directions.*

It follows from Proposition 4.2.1 that the MOSI curves (as defined in Definition 5.1.5) are indeed given by the BDE completing a self-polar triple with the principal BDE and the third fundamental form (that is, $T = Jac(P, B)$), and satisfy

$$(R \circ C \circ O \circ C)(v) = v.$$

Remark 5.1.6 *The BDE P lies at the intersection of those pencils corresponding to BDEs with orthogonal solutions and BDEs with solutions having orthogonal spherical images. We thus have the following alternative characterisation of the principal directions on a smooth surface in $\mathbb{R}^3$: they are the only pair of orthogonal tangent directions to the surface that map to orthogonal directions on S^2 under the Weingarten map.*

Proposition 5.1.4 (a) *The BDE T of the MOSI curves is*

$$a_T dy^2 + 2b_T dxdy + c_T dx^2 = 0 \tag{5.4}$$

where

$$\begin{aligned}
a_T = \;& 3Gm^2En - 2FnmGl - 2FGm^3 + G^2m^2l - 4Fn^2mE \\
& + 2F^2n^2l + 2m^2F^2n - En^2Gl + E^2n^3 \\
b_T = \;& 2Gm^3E + G^2ml^2 - 3Gm^2Fl - 3Fnm^2E \\
& - FnGl^2 + 4F^2nml - Fn^2lE + E^2n^2m \\
c_T = \;& 3lGEm^2 + l^3G^2 - 4l^2GmF + E^2nm^2 - EnGl^2 \\
& - 2EnmFl + 2F^2l^2n + 2F^2lm^2 - 2Em^3F.
\end{aligned}$$

(b) *The discriminant of T consists of the parabolic set and umbilic points.*

(c) *Away from umbilic points the BDE T can be written with respect to a principal coordinate system as*

$$G\kappa_2^2 dy^2 - E\kappa_1^2 dx^2 = 0. \tag{5.5}$$

Proof: The quadratic form T is the Jacobian of the principal BDE and the third fundamental form B. We establish the BDE T by calculating the appropriate determinant.

Calculating $b_T^2 - a_T c_T$, we have that the discriminant of T is

$$(ln-m^2)^2(EG-F^2)(n^2E^2+4EGm^2-2EGnl-4EnmF+l^2G^2-4lmFG+4lnF^2),$$

which vanishes at parabolic and umbilic points.

In a principal coordinate system we have $F = m = 0$ and $l = E\kappa_1$, $n = G\kappa_2$. The simplified form follows. □

The following Theorem provides further evidence that the characteristic curves and the MOSI curves are significant geometric objects.

Theorem 5.1.7 (a) *The third fundamental form B is the projective harmonic conjugate of the metric L with respect to the asymptotic BDE A and the characteristic BDE Ch.*

(b) *The BDE T of the MOSI curves is the projective harmonic conjugate of the BDE of the lines of arithmetic mean curvature Me with respect to A and Ch.*

Proof: We use the projective transformation $\mathcal{T}$ on the set of linear involutions of the projective line identified with $\mathbb{R}P^2$. The asymptotic BDE A is given by $\mathcal{T}(C)$, the characteristic BDE Ch is given by $\mathcal{T}(R \circ C)$, the metric is given by $\mathcal{T}(O)$ and the third fundamental form is given by $\mathcal{T}(C \circ O \circ C)$.

By Theorem 4.1.3 **(c)**, the involution $C \circ O \circ C$, considered as a point in $\mathbb{R}P^2$ is the projective harmonic conjugate of O with respect to C and $C \circ R$, and assertion **(a)** follows since projective transformations preserve the cross-ratio of 4 colinear points.

Assertion **(b)** follows by the same method, with $R \circ O$ replacing O, since by Corollary 5.1.2 the BDE Me of the lines of arithmetic mean curvature is given by $\mathcal{T}(R \circ O)$. □

In conclusion then, we have six colinear forms, namely Me, A, Ch, T, B and L, the common line being the polar of the principal BDE, comprising three pairs of apolar points (and thus three self-polar triangles involving the principal BDE). This is illustrated in Figure 5.1 (in this picture the point in question is a hyperbolic point).

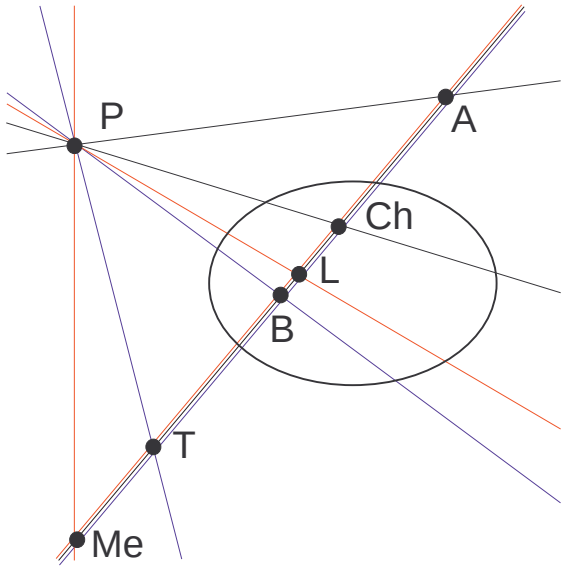

Figure 5.1: Self-polar triples of BDEs: $\{P, L, Me\}$ (red), $\{P, A, Ch\}$ (black), and $\{P, B, T\}$ (blue).

5.2 Configurations of the MOSI curves

The MOSI curves defined by BDE T (5.4) do not appear to have been considered before. Some elementary geometric properties of the MOSI curves are given in Proposition 5.2.1.

Proposition 5.2.1 **(a)** *The sectional curvature in MOSI directions is*

$$\frac{KH}{2H^2 - K}.$$

(b) *The geodesic torsion in the MOSI directions is*

$$\pm\frac{K\sqrt{H^2 - K}}{2(2H^2 - K)}.$$

Proof: We choose a principal coordinate system. The solutions make an angle $\pm\theta$ with the coordinate axes where

$$\cos\theta = \frac{\kappa_2}{\sqrt{\kappa_2^2+\kappa_1^2}}, \quad \sin\theta = \frac{\kappa_1}{\sqrt{\kappa_2^2+\kappa_1^2}}.$$

The results follow by using the formulae for the sectional curvature (2.1) and geodesic torsion (2.2). □

Remark 5.2.1 *The MOSI curves are an example of a mean curvature foliation as defined by Garcia and Sotomayor in* [42]*, that is, the sectional curvature is given by a smooth function* $\tilde{k_n}(H,K)$ *satisfying* $(\tilde{k_n}-H)^2 \leq (H^2-K)$ *on the region* $H^2 \geq K \geq 0$*, and* $\tilde{k_n}(tH,t^2K) = t\tilde{k_n}(H,K)$ *for each* $t \geq 0$*.*

Away from its discriminant, the BDE (5.4) defines a pair of transverse foliations. We examine here its behaviour near points on the discriminant, that is, near umbilic points and the parabolic set.

5.2.1 Configurations at umbilic points

The BDEs of the lines of curvature lines of curvature (2.4), characteristic curves (2.6), the MOSI curves (5.4) and the lines of arithmetic mean curvature (5.1) are all singular at umbilic points. The configuration of the lines of arithmetic mean curvature was established in [39].

In each case the discriminant has a Morse (A_1^+)-singularity. Recall the three stable topological models of the integral curves of BDEs with discriminants of this type: star, monstar and lemon, which are illustrated in Figure 2.1. Each of the three generic topological configurations can occur in the cases of the BDEs of the arithmetic mean curvature lines, the lines of curvature and the characteristic curves. In fact, the configurations of the lines of arithmetic mean curvature at an umbilic point are topologically equivalent to those of the characteristic curves.

We consider here the configurations of the MOSI curves at an umbilic point. We parametrise S at an umbilic point in the way given in Section 2.1, that is, in the form $(x,y,f(x,y))$ where

$$j^3f(x,y) = \frac{\kappa}{2}(x^2+y^2) + \mathrm{Re}(z^3+\beta z^2 z)$$

where $z = x + iy$ and β is a complex number.

Proposition 5.2.2 *At an umbilic point the coefficients of the BDE T of the MOSI curves all vanish and the discriminant generally has a Morse (A_1^+) singularity. The umbilic of type star if β is inside the circle $|\beta| = 3$, of type lemon if β is outside the hypercycloid $\beta = 3(2e^{i\theta} + 2e^{-i\theta})$ and of type monstar in the remaining regions of the complex plane; see Figure 5.2.*

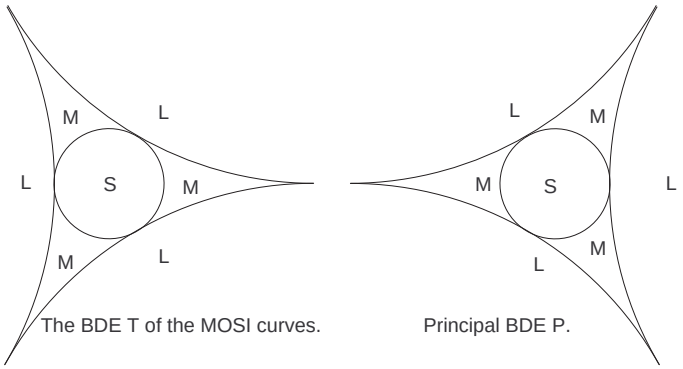

Figure 5.2: Partition of the β-plane: the BDE T of the MOSI curves (left) and the principal BDE P (right).

Proof: At an umbilic point we have that $m^2 \neq ln$, so the discriminant of the BDE T (5.4) is given by

$$\Delta_T = n^2E^2 - 2EGnl + 4EGm^2 - 4EnFm + l^2G^2 - 4lmFG + 4lnF^2.$$

We write $\beta = a + ib$ where $a, b \in \mathbb{R}$. We calculate the coefficients of the first and second fundamental forms. We have that

$$j^2\Delta = -16\kappa^2((b^2 + 9 + a^2 + 6a)x^2 + 12bxy + (-6a + a^2 + 9 + b^2)y^2).$$

This has a Morse singularity provided that

$$(b^2 + a^2 - 9)^2 \neq 0,$$

that is, provided that β does not lie on the circle $|\beta| = 3$.

We use the lifted field method described in Section 1.3.2. It is shown in, for example, [20], that the topological type depends only on the number and type of

the singularities of the lifted field ξ. Hence we must identify the exceptional sets in the β-plane where these change.

We consider the affine chart $p = dy/dy$ (we also consider the affine chart $q = dx/dy$). We write the BDE (5.4) as $F(x, y, p) = 0$. Consider the cubic

$$\phi = (F_x + pF_y)(0, 0, p).$$

We have that

$$\phi(p) = 4\kappa^2(a + 3) - 4b\kappa^2 p + 4\kappa^2(a - 9)p^2.$$

This has only simple roots provided that ϕ and $\phi'(p)$ have no common roots. This occurs if and only if

$$2b^2a^2 + 72b^2a + 162b^2 + a^4 - 24a^3 + 162a^2 - 2187 + b^4 \neq 0$$

(this condition is obtained by calculating the resultant of $\phi(p)$ and $\phi'(p)$). We substitute $a = r\cos\theta, b = r\sin\theta$ into this expression and find that ϕ has only simple roots provided β does not lie on the hypercycloid $\beta = 3(2e^{i\theta} + 2e^{-i\theta})$.

Finally, observe that one eigenvalue of the lifted field ξ at a singular point is given by $-\phi'(p)$, and we have seen that this is non-zero at the roots of ϕ provided that β does not lie on the given hypercycloid. The other eigenvalue is given by the quadratic

$$\alpha_1(p) = -8\kappa^2(bp^2 + 6p + b)$$

(see for example [20]). It follows that the lifted field ξ has no zero eigenvalues provided α_1 and ϕ have no common roots. This is the case provided that $|\beta| \neq 3$ (this is established by calculating res$\{\phi(p), \alpha_1)\}$).

The exceptional sets where the topological type changes are thus the given circle and hypercycloid. The topological type of each BDE is established by choosing a value of β in each of the open regions bounded by the exceptional sets and calculating the types of the zeros of ξ. □

Remark 5.2.2 *The MOSI curves at umbilic points are topologically equivalent to the lines of arithmetic mean curvature and to the characteristic curves at umbilic points.*

5.2.2 Configurations at the parabolic set

Proposition 5.2.3 **(a)** *The unique MOSI direction at parabolic points coincides with the unique asymptotic direction, and is thus tangent to the parabolic set only at cusps of Gauss.*

(b) *The discriminant of the BDE T of the MOSI curves is singular at all parabolic points.*

Proof: We adopt the usual Monge form parametrisation $(x, y, f(x, y))$ and set $\kappa_1 = 0$ at a parabolic point. We calculate the coefficients of the first and second fundamental forms. Writing the BDE T as $F(x, y, p) = 0$ we have that

$$\begin{aligned} j^2F = \; & \kappa_2^3p^2 + (-2a_{31}a_{30}\kappa_2 + 2a_{32}a_{31}\kappa_2)yx + 2\kappa_2^2a_{31}px + (a_{31}^2\kappa_2 - a_{30}^2\kappa_2)x^2 \\ & +(a_{32}^2\kappa_2 - a_{31}^2\kappa_2)y^2 + 2\kappa_2^2a_{32}yp. \end{aligned}$$

It is clear that at $x = y = 0$ the BDE reduces to $p^2 = 0$, that is, the solution direction is given by the y-axis, which is the unique asymptotic direction at the origin.

We calculate the discriminant $\Delta_T = b_T^2 - a_tc_T$. We have that

$$j^2\Delta_T = \kappa_2^4(a_{30}x + a_{31}y)^2,$$

so clearly

$$\frac{\partial\Delta_T}{\partial x} = \frac{\partial\Delta_T}{\partial y} = 0$$

at parabolic points. □

Remark 5.2.3 *Proposition 5.2.3* **(a)** *in fact follows directly from the relationship between the BDEs T, P and A identified in Theorem 5.1.7.*

As the BDE T has a non-isolated singularity it is of infinite codimension in the set of IDEs (and the set of BDEs), and so our previous methods of study do not work.

Lemma 5.2.4 *A BDE with coefficients that do not vanish, and discriminant the square of a smooth function is smoothly equivalent to*

$$dy^2 - (g(x, y))^2dx^2 = 0 \tag{5.6}$$

for some smooth function g. The solution curves are a pair of smooth foliations that are transverse at points where $g \neq 0$ and mutually tangent at points where $g = 0$.

Proof: We may suppose that $a \equiv 1$ and that $b^2 - c = (h(x,y))^2$ some smooth function h. We make changes of coordinates of the form

$$x = X, y = \phi(X, Y)$$

for some function ϕ where $\phi_Y \neq 0$ in a neighbourhood of the origin. We have that $dx = dX, dy = \phi_X dX + \phi_Y dY$. We write $b(X, \phi) = B$ and $c(X, \phi) = C$. The BDE becomes

$$\phi_Y^2 dY^2 + 2(\phi_X \phi_Y + B\phi_Y)dXdY + (\phi_X^2 + 2B\phi_X + C)dX^2 = 0.$$

Since $\phi_Y \neq 0$ it is enough to solve the partial differential equation $\phi_X = -B$. For each fixed Y this is an ODE in X. If we demand $\phi(0, Y) = Y$ then this ODE has a unique smooth solution that depends smoothly on the initial value Y.

The original BDE then becomes

$$\phi_Y^2 dY^2 + (-B^2 + C)dX^2 = 0.$$

Observe that $C - B^2 = (h(X, \phi))^2$. We set $g(X, Y) = (h(X, \phi)/\phi_Y)^2$ and divide the equation by ϕ_Y^2 to complete the proof. □

Proposition 5.2.4 *The MOSI curves extend smoothly across the parabolic set. The two foliations are tangent to one another at parabolic points.*

Proof: Since at parabolic points we have that

$$EG - F^2 \neq 0$$

and

$$n^2E^2 + 4EGm^2 - 2EGnl - 4EnmF + l^2G^2 - 4lmFG + 4lnF^2 \neq 0,$$

it follows that the integral curves of the BDE T in a neighbourhood parabolic set are the same as those of the BDE $\tilde{T}$ obtained by multiplying the BDE T (5.4) by the smooth function

$$\sqrt{(EG - F^2)(n^2E^2 + 4EGm^2 - 2EGnl - 4EnmF + l^2G^2 - 4lmFG + 4lnF^2)}.$$

The discriminant of the BDE $\tilde{T}$ is $(ln - m^2)^2$.

We apply Lemma 5.2.4. Equations of the form (5.6) are the product of two 1-forms

$$dy \pm gdx,$$

giving rise to two smooth foliations that are tangent to one another on the discriminant curve $g(x, y) = 0$. □

Pairs of foliations of the plane are studied in, for example, [52]. We use Theorem 5.2.5, established there, to draw the configurations of the MOSI curves at the parabolic set. Given a pair of foliations associated to a pair of 1-forms, (α, β), in the plane, we use the term *discriminant* for the locus of points where β is a multiple of α.

Theorem 5.2.5 ([52]) *Let (α, β) be a pair of germs, at the origin, of regular 1-forms in the plane. If the discriminant Δ of the pair (α, β) is a regular curve then (α, β) is topologically equivalent to*

(a) *$(dy, d(y - x^2))$, if the contact of Δ with the leaf of α (and β) at the origin is odd;*

(b) *$(dy, d(y + xy - x^3))$, if the contact of Δ with the leaf of α (and β) at the origin is even.*

It turns out that the topological configuration of the integral curves of T at a cusp of Gauss depends only on the index of characteristic (or asymptotic) folded singularity at the cusp of Gauss.

Proposition 5.2.5 (a) *Away from cusps of Gauss the MOSI curves have 2-point contact with each other and 1-point contact with the parabolic set. A topological model is given by the pair of one-forms*

$$(dy, d(y - x^2)).$$

The integral curves are as shown in Figure 5.3.

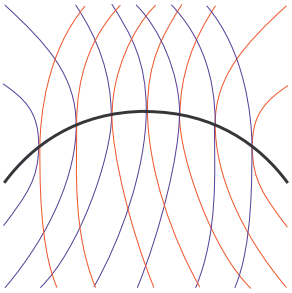

Figure 5.3: The MOSI curves at the parabolic set.

(b) *At cusps of Gauss both MOSI curves generically have* 2*-point with the parabolic set. A topological model is given the pair of 1-forms*

$$(dy, d(y + xy - x^3)).$$

There are two possibilities distinguished according to the value of ρ_c*. The integral curves are as shown in Figure 5.4.*

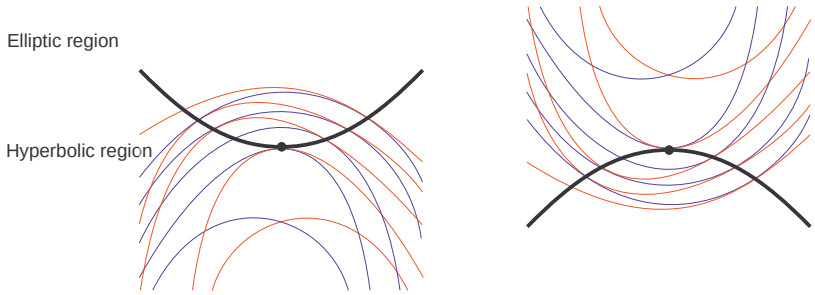

Figure 5.4: The MOSI curves a cusp of Gauss: $\rho_c < 1$ (left) and $\rho_c > 1$ (right).

Proof: We adopt the usual Monge form parametrisation at a parabolic point. The parabolic set is smooth, and tangent to the line

$$a_{30}x + a_{31}y = 0.$$

By Proposition 5.2.4, the integral curves of (5.4) through the origin are smooth. They are tangent to the y-axis, so we may write them (in the parametrising plane) in the form $y = y_i(x)$ for $i = 1, 2$, where

$$j^3 y_i = \alpha_{i1}x^2 + \alpha_{i2}x^3.$$

We substitute these expressions into (5.4) (setting $dx = 1, dy = dy_i/dx$). Equating second order terms to zero we find that

$$\alpha_{i1} = -\frac{a_{31} + (-1)^i a_{30}}{2\kappa_2}.$$

Thus we see that when $a_{30} \neq 0$ the two curves have 2-point contact with each other and 1-point contact with the discriminant (the parabolic set). We apply Theorem 5.2.5 **(a)** to establish assertion **(a)**.

When the origin is a cusp of Gauss we have $a_{30} = 0$, and so $\alpha_{11} = \alpha_{21} = -a_{31}/2\kappa_2$. We return to the equation. The third order terms vanish identically, hence we equate fourth order terms and solve for α_{i2}. We find that

$$\alpha_{i2} = -\frac{(-1)^i a_{40}\kappa_2 - 3(-1)^i a_{31}^2 - 3a_{32}a_{31} + a_{41}\kappa_2}{6\kappa_2^2}.$$

It follows that the two curves have 3-point contact with each other and 2-point contact with the discriminant. We apply Theorem 5.2.5 **(b)** to establish the topological configurations at a cusp of Gauss.

From Proposition 3.1.1 we know that at a cusp of Gauss the parabolic set is given by

$$y = \frac{2a_{31}^2 - a_{40}\kappa_2}{2a_{31}\kappa_2}x^2 + h.o.t.$$

It follows that the solution curves of T that pass through the cusp of Gauss have > 2-point contact with the parabolic set at a cusp of Gauss if

$$\frac{2a_{31}^2 - a_{40}\kappa_2}{2a_{31}\kappa_2} = -\frac{a_{31}}{2\kappa_2},$$

that is, if $\rho_c = 1$. We complete the proof by adopting the projective normal form for the surface given in Proposition 3.1.7, choosing a value of ρ_c in each of the intervals separated by the exceptional value 1 and establishing whether the integral curves of T through the origin lie locally in the elliptic or hyperbolic region. □

Remark 5.2.6 *The relative positions of the MOSI curves through a cusp of Gauss and the parabolic set is invariant under projective transformations. When the surface is sent, via projective transformations, to the normal form given in Proposition 3.1.7, the 2-jet of the parametrisation of the MOSI curves through the cusp of Gauss is simply*

$$y = x^2.$$

This coincides with the separating 2-jet *as defined in* [71]. *This is a curve of significance on the dual surface, suggesting that the MOSI curves may be defined in terms of the flat geometry of the surface.*

5.3 Pencils of BDEs

We now use the linear involutions C, R and O to define families of BDEs that parametrise the pencils joining P to T, Me and B, following the ideas in [24, 36] that are used to define the families $\mathcal{C}_\alpha$ and $\mathcal{R}_\alpha$ described in Chapter 2.

To simplify the notation, we label the coefficients of the BDE of the lines of curvature (2.4) a_P, b_P, c_P, and the coefficients of the third fundamental form $a_B, 2b_B, c_B$ respectively. Explicitly, we set

$$\begin{aligned} a_P &= Gm - Fn, \quad & a_B &= n(2Fm - En) - Gm^2, \\ b_P &= Gl - En, \quad & b_B &= F(ln + m^2) - m(Gl + En), \\ c_P &= Fl - Em, \quad & c_B &= l(2Fm - Gl) - Em^2. \end{aligned}$$

Recall also the formulae for the Gaussian and arithmetic mean curvatures given in Section 2.1:

$$K = \frac{ln - m^2}{EG - F^2}, \;\; H = \frac{Gl + En - 2Fm}{2(EG - F^2)}.$$

The coefficients of the characteristic BDE (2.6) (respectively the BDE of the lines of arithmetic mean curvature (5.1)) are similarly labelled $a_{Ch}, 2b_{Ch}, c_{Ch}$ (respectively $a_{Me}, 2b_{Me}, c_{Me}$). Observe that, as the characteristic BDE (respectively the BDE of the lines of arithmetic mean curvature) is the polar of the pencil connecting the asymptotic and principal BDEs (respectively the principal BDE and the metric), that is $Ch = Jac(P, A)$ (respectively $Me = Jac(P, L)$ we have that

$$a_{Ch} = 2ma_P - nb_P, \;\; b_{Ch} = 2(nc_P - la_P), \;\; c_{Ch} = lb_P - 2mc_P, \tag{5.7}$$

$$a_{Me} = 2Fa_P - Gb_P, \;\; b_{Me} = Ea_P - Gc_P, \;\; c_{Me} = Eb_P - 2Fc_P. \tag{5.8}$$

Similarly, observe that

$$a_T = 2a_Pb_B - a_Bb_P, \;\; b_T = (a_Pc_B - a_Bc_P), \;\; c_T = b_Pc_B - 2b_Bc_P. \tag{5.9}$$

The pencil of BDEs with orthogonal solution directions is the polar of the metric. The corresponding involution is O. A natural parametrisation of this pencil is obtained by considering those directions v that make an oriented angle α with $(O \circ R)(v)$ for each fixed $\alpha \in [-\frac{\pi}{2}, \frac{\pi}{2}]$.

Definition 5.3.1 *Let PTS denote the projectivised tangent bundle to S, and define*

$$\begin{aligned} \Xi : PTS &\to [-\tfrac{\pi}{2}, \tfrac{\pi}{2}] \\ (p, v) &\mapsto \alpha \end{aligned}$$

where α denotes the signed angle between v and $(O \circ R)(v)$. The orthogonal curve congruence*, denoted $\mathcal{O}_\alpha$, for a fixed α, is defined to be $\Xi^{-1}(\alpha)$.*

We use the projective transformation $\mathcal{T}$ to establish the BDE of the orthogonal curve congruence.

Theorem 5.3.2 **(a)** *The orthogonal curve congruence $\mathcal{O}_\alpha$ is given by the BDE*

$$\begin{aligned} &(a_M \sin\alpha - 2\sqrt{EG - F^2} a_P \cos\alpha) dy^2 \\ &+2(b_M \sin\alpha - \sqrt{EG - F^2} b_P \cos\alpha) dx dy \\ &+(c_M \sin\alpha - 2\sqrt{EG - F^2} c_P \cos\alpha) dx^2 = 0. \end{aligned} \tag{5.10}$$

(b) *The set of all principal directions is $\mathcal{O}_0$ and the the set of all arithmetic mean curvature directions is $\mathcal{O}_{\pm\frac{\pi}{2}}$, so $\mathcal{O}_\alpha$ joins the principal BDE P to the BDE of the lines of arithmetic mean curvature Me.*

(c) *Away from umbilic points the BDE $\mathcal{O}_\alpha$ can be written with respect to a principal coordinate system as*

$$G\cos\alpha dy^2 + 2\sqrt{GE}\sin\alpha dx dy - E\cos\alpha dx^2 = 0. \tag{5.11}$$

(d) *The discriminant of $\mathcal{O}_\alpha$ consists of the umbilic points.*

Proof: The involution O is given by $\mathcal{T}^{-1}(L)$ where L is the point

$$[E : 2F : G] \in \mathbb{R}P^2$$

which represents the metric (see Section 4.2).

As the principal directions are the fixed points of the involution R, it follows from Theorem 4.1.3 that the involution R is given by $\mathcal{T}^{-1}(P)$ where P is the point $[Gm - Fn : Gl - En : Fl - Em] \in \mathbb{R}P^2$ which represents principal BDE.

Calculating, it follows that O is given by

$$\begin{aligned} O : \mathbb{R}P^1 &\to \mathbb{R}P^1 \\ [x : y] &\mapsto [Fx + Gy : -Ex - Fy], \end{aligned}$$

and the involution R is given by

$$\begin{aligned} R : \mathbb{R}P^1 &\to \mathbb{R}P^1 \\ [x : y] &\mapsto [(Gl - En)x + 2(Fl - Em)y : 2(Fn - Gm)x + (En - Gl)y]. \end{aligned}$$

Composing we have that the involution $O \circ R$ is given by

$$\begin{aligned} O \circ R : \mathbb{R}P^1 \to &\ \mathbb{R}P^1 \\ [x : y] \mapsto &\ [(2mEG - GFl - FEn)x + (nEG - 2nF^2 - G^2l + 2GFm)y : \\ &\ (2lF^2 - lEG + E^2n - 2FEm)x - (2mEG - GFl - FEn)y]. \end{aligned}$$

This involution is associated to the linear transformation of $\mathbb{R}^2$ that has matrix

$$\mathcal{M}_1 = \begin{pmatrix} 2mEG - GFl - FEn & nEG - 2nF^2 - G^2l + 2GFm \\ 2lF^2 - lEG + E^2n - 2FEm & -2mEG + GFl + FEn \end{pmatrix}.$$

Consider a direction $[v] \in PT_pS$ tangent to the surface S at a point p. We apply the involution $O \circ R$. If α denotes the signed angle between $[v]$ and $O \circ R([v])$ then we have

$$\cos\alpha = \frac{\mathrm{I}(v, \mathcal{M}_1 v)}{\sqrt{\mathrm{I}(v, v)\mathrm{I}(\mathcal{M}_1 v, \mathcal{M}_1 v)}}. \tag{5.12}$$

The involution O is associated to the linear transformation of $\mathbb{R}^2$ that has matrix

$$\mathcal{M}_2 = \begin{pmatrix} -F & -G \\ E & F \end{pmatrix}.$$

Observe that since $\cos(\frac{\pi}{2} - \alpha) = \sin(\alpha)$ and $O([v])$ is orthogonal to $[v]$, the angle α satisfies

$$\sin\alpha = \frac{\mathrm{I}(\mathcal{M}_1 v, \mathcal{M}_2 v)}{\sqrt{\mathrm{I}(\mathcal{M}_1 v, \mathcal{M}_1 v)\mathrm{I}(\mathcal{M}_2 v, \mathcal{M}_2 v)}}. \tag{5.13}$$

Eliminating $\mathrm{I}(\mathcal{M}_1 v, \mathcal{M}_1 v)$ from equation (5.12) and equation (5.13) we have that

$$\mathrm{I}(v, \mathcal{M}_1 v)\sqrt{\mathrm{I}(\mathcal{M}_2 v, \mathcal{M}_2 v)}\sin\alpha - \mathrm{I}(\mathcal{M}_1 v, \mathcal{M}_2 v)\sqrt{\mathrm{I}(v, v)}\cos\alpha = 0. \tag{5.14}$$

Now for any vectors $u_1, u_2 \in T_pS$, we have that

$$\mathrm{I}(u_1, u_2) = u_1^T \mathcal{M}_{\mathrm{I}} u_2$$

where $\mathcal{M}_{\mathrm{I}}$ is the matrix of the first fundamental form used in the proof of Proposition 5.1.3. We set

$$v = \begin{pmatrix} dx \\ dy \end{pmatrix}.$$

We then have that

$$\begin{aligned}
\mathrm{I}(v, \mathcal{M}_1 v) = \; & 2(EG - F^2)((Em - Fl)dx^2 \\
& +(En - Gl)dydx + (Fn - Gm)dy^2), \\
\mathrm{I}(\mathcal{M}_1 v, \mathcal{M}_2 v) = \; & (EG - F^2)((2lF^2 - lEG + E^2 n - 2FEm)dx^2 \\
& +2(EnF - 2mEG + GFl)dydx \\
& +(2nF^2 + G^2 l - nEG - 2GFm))dy^2, \\
\mathrm{I}(\mathcal{M}_2 v, \mathcal{M}_2 v) = \; & (EG - F^2)(Edx^2 + 2Fdydx + Gdy^2, \\
\mathrm{I}(v, v) = \; & Edx^2 + 2Fdydx + Gdy^2.
\end{aligned}$$

We substitute these expressions into equation (5.14) to complete the proof of part **(a)**.

Part **(b)** is trivial. One obtains the equation in a principal coordinate system by setting $m = F = 0$, $l = Ek_1$ and $n = Gk_2$, which establishes part **(c)**.

The discriminant of (5.10) is

$$\Delta_M^\alpha = (EG - F^2)(n^2E^2 - 2EGln + 4EGm^2 - 4EnFm + l^2G^2 - 4lFmG + 4lF^2n).$$

The second factor is equal to $4(H^2 - K^2)(EF - F^2)^2$ (see Section 2.1) which vanishes only at umbilic points. This establishes part **(d)**. □

The pencil $\hat{B}$ that joins the BDEs P and T comprises, by Theorem 4.1.3, those BDEs with solutions that have orthogonal spherical images.

Definition 5.3.3 *Let PTS denote the projectivised tangent bundle to S, and define*

$$\begin{aligned}
\Upsilon : PTS &\to [-\tfrac{\pi}{2}, \tfrac{\pi}{2}] \\
(p, v) &\mapsto \alpha
\end{aligned}$$

where α denotes the signed angle between v and $(R \circ C \circ O \circ C)(v)$. The orthogonal spherical image congruence*, denoted $\mathcal{T}_\alpha$, for a fixed α, is defined to be $\Upsilon^{-1}(\alpha)$.*

Theorem 5.3.4 (a) *The orthogonal spherical image congruence $\mathcal{T}_\alpha$ is given by the BDE*

$$\begin{aligned}&(2K(EG-F^2)^{\frac{3}{2}}a_P\cos\alpha+a_T\sin\alpha)dy^2\\&+2(K(EG-F^2)^{\frac{3}{2}}b_P\cos\alpha+b_T\sin\alpha)dxdy\\&+(2K(EG-F^2)^{\frac{3}{2}}c_P\cos\alpha+c_T\sin\alpha)dx^2=0,\end{aligned}\tag{5.15}$$

(b) *The set of all principal directions is $\mathcal{T}_0$ and the the set of all MOSI directions is $\mathcal{T}_{\pm\frac{\pi}{2}}$, so $\mathcal{T}_\alpha$ joins the principal BDE P to the BDE of the MOSI curves T.*

(c) *Away from umbilic points the BDE $\mathcal{T}_\alpha$ can be written with respect to a principal coordinate system as*

$$G\sin\alpha\kappa_2^2dy^2-2\kappa_1\kappa_2\sqrt{EG}\cos\alpha dxdy-\sin\alpha\kappa_1^2Edx^2=0.\tag{5.16}$$

(d) *The discriminant of $\mathcal{T}_\alpha$ consists of the parabolic set and umbilic points.*

Proof: This proof is similar to that of Theorem 5.3.2 and is omitted. □

Of course, the pencils joining the BDE P to the BDEs Me and T may be parametrised in other ways, leading to different 1-parameter families. Theorem 5.3.5 shows that, amongst possible parametrisations, we have made a very natural choice.

Theorem 5.3.5 (a) *For any given (fixed) $\alpha\in(-\frac{\pi}{2},\frac{\pi}{2})$, the BDE $\mathcal{T}_\alpha$ is the polar of the pencil connecting the BDEs $\mathcal{C}_\alpha$ and $\mathcal{R}_\alpha$.*

(b) *For any given (fixed) $\alpha\in(-\frac{\pi}{2},\frac{\pi}{2})$, the BDE $\mathcal{O}_\alpha$ is the polar of the pencil connecting the BDEs $\mathcal{C}_\alpha$ and $\mathcal{R}_{-\alpha}$.*

Proof: We fix α and calculate the Jacobian of the BDEs $\mathcal{C}_\alpha$ (2.7) and $\mathcal{R}_\alpha$ (2.8), which we now write as

$$\begin{aligned}(a_P\sin\alpha-n\cos\alpha\sqrt{EG-F^2})dy^2+\\(b_P\sin\alpha-2m\cos\alpha\sqrt{EG-F^2})dydx+\\(c_P\sin\alpha-l\cos\alpha\sqrt{EG-F^2})dx^2=0\end{aligned}\tag{5.17}$$

and

$$\begin{aligned}(a_{Ch}\cos\alpha+2a_PH\sqrt{EG-F^2}\sin\alpha)dy^2+\\2(b_{Ch}\cos\alpha+b_PH\sqrt{EG-F^2}\sin\alpha)dydx+\\(c_{Ch}\cos\alpha+2c_{Ch}H\sqrt{EG-F^2}\sin\alpha)dx^2=0.\end{aligned}\tag{5.18}$$

respectively. We find that this is equal to $4\cos\alpha\mathcal{T}_\alpha$, where $\mathcal{T}_\alpha$ is the BDE (5.15). Thus when $\cos\alpha \neq 0$ the BDE $\mathcal{T}_\alpha$ is the polar of the pencil connecting the BDEs $\mathcal{C}_\alpha$ and $\mathcal{R}_\alpha$. This establishes assertion **(a)**.

Assertion **(b)** follows by a similar calculation. □

Remarks 5.3.6 *1. The BDEs $\mathcal{C}_\alpha$ and $\mathcal{R}_\alpha$ (respectively $\mathcal{C}_\alpha$ and $\mathcal{R}_{-\alpha}$) are not in general apolar on the pencils that connect them, that is, $\{\mathcal{C}_\alpha, \mathcal{R}_\alpha, \mathcal{T}_\alpha\}$ (respectively $\{\mathcal{C}_\alpha, \mathcal{R}_{-\alpha}, \mathcal{O}_\alpha\}$) is not in general a self-polar triangle.*

2. When $\alpha = \pi/2$ the BDEs $\mathcal{C}_\alpha$, $\mathcal{R}_\alpha$ and $\mathcal{O}_\alpha$ coincide and are the principal BDE (2.4). It follows that there is no pencil joining them, and $Jac(\mathcal{C}_\alpha, \mathcal{R}_\alpha) = Jac(\mathcal{C}_\alpha, \mathcal{R}_{-\alpha}) = 0$. Observe, from the proof of Theorem 5.3.5, however, that

$$\lim_{\alpha\to\pm\pi/2} \frac{Jac(\mathcal{C}_\alpha, \mathcal{R}_\alpha)}{\cos\alpha} = \mathcal{T}_{\frac{\pi}{2}} = T$$

and

$$\lim_{\alpha\to\pm\pi/2} \frac{Jac(\mathcal{C}_\alpha, \mathcal{R}_{-\alpha})}{\cos\alpha} = \mathcal{O}_{\frac{\pi}{2}} = Me.$$

We thus have that $\hat{B} = \{T_\alpha | \alpha \in [-\frac{\pi}{2}, \frac{\pi}{2}]\}$ is the closure of the set

$$\{Jac(\mathcal{C}_\alpha, \mathcal{R}_\alpha) | (\alpha \in (-\frac{\pi}{2}, \frac{\pi}{2})\},$$

and $\hat{L} = \{O_\alpha | \alpha \in [-\frac{\pi}{2}, \frac{\pi}{2}]\}$ is the closure of the set

$$\{Jac(\mathcal{C}_\alpha, \mathcal{R}_{-\alpha}) | (\alpha \in (-\frac{\pi}{2}, \frac{\pi}{2})\}.$$

One may also consider $\hat{M}$ and $\hat{T}$, the polar lines of the BDEs M and T respectively. These are the pencils joining the principal BDE P to the metric L, and the principal BDE P to the third fundamental form B.

The solutions to BDEs in the pencil connecting the third fundamental form and the principal BDE are orthogonal to their images under the Weingarten map.

Definition 5.3.7 *Let PTS denote the projectivised tangent bundle to S, and define*

$$\begin{aligned} \Gamma : PTS &\to [-\tfrac{\pi}{2}, \tfrac{\pi}{2}] \\ (p, v) &\mapsto \alpha \end{aligned}$$

where α denotes the signed angle between v and $(C \circ O \circ C)(v)$. The orthogonal conjugate curve congruence*, denoted $\mathcal{B}_\alpha$, for a fixed α, is defined to be $\Gamma^{-1}(\alpha)$.*

Theorem 5.3.8 **(a)** *The BDE $\mathcal{B}_\alpha$ is*

$$\begin{aligned}&(a_B\cos\alpha - H\sqrt{EG-F^2}a_P\sin\alpha)dy^2\\&+(2b_B\cos\alpha - H\sqrt{EG-F^2}b_P\sin\alpha)dxdy\\&+(c_B\cos\alpha - H\sqrt{EG-F^2}c_P\sin\alpha)dx^2 = 0.\end{aligned} \tag{5.19}$$

(b) *The set of all principal directions is $\mathcal{B}_{\pm\frac{\pi}{2}}$ and $\mathcal{B}_0 = B$, so $\mathcal{B}_\alpha$ joins the principal BDE P to the third fundamental form B.*

(c) *Away from umbilic points the BDE $\mathcal{B}_\alpha$ can be written with respect to a principal coordinate system as*

$$G\kappa_2^2\cos\alpha dy^2 + \sqrt{EG}(\kappa_1^2-\kappa_2^2)\sin\alpha dxdy + E\kappa_1^2\cos\alpha dx^2 = 0. \tag{5.20}$$

(d) *The discriminant of $\mathcal{B}_\alpha$ consists of the sets given by*

$$K\cos\alpha \pm H\sqrt{H^2-K}\sin\alpha = 0$$

which we denote by $\Delta^\alpha_{\mathcal{B}\pm}$.

Proof: This proof is similar to that of Theorem 5.3.2 and is omitted. □

Remarks 5.3.9 *1. While it is clear from the equation* (5.19) *that, in general, $\mathcal{B}_\alpha \neq \mathcal{B}_{-\alpha}$, these two BDEs do have the same discriminant, since $\Delta^\alpha_{\mathcal{B}+} = \Delta^{-\alpha}_{\mathcal{B}-}$.*

2. The sets $\Delta^0_{\mathcal{B}\pm}$ are the parabolic set, the sets $\Delta^{\frac{\pi}{2}}_{\mathcal{B}\pm}$ consist of the umbilic points together with the curve given by $H = 0$.

3. The discriminant curves $\Delta^\alpha_{\mathcal{B}\pm}$ foliate the surface.

It is less obvious what the parametrisation of the pencil connecting the metric and the principal BDE (that is, $\hat{M}$, the polar line of the BDE of the lines of arithmetic mean curvature) should be. We show that one possibility, obtained demanding that if θ is the angle that the solution directions makes with a (particular) principal direction be proportional to $H\sqrt{H^2-K}/K$, turns out to be particularly natural.

If θ is the angle between the solution direction and a choice of principal direction, we set

$$\sin 2\theta = \tan\alpha\frac{H\sqrt{H^2-K}}{K}.$$

Observe that this gives rise to a real value of θ if any only if

$$\tan\alpha \in [-\frac{K}{H\sqrt{H^2-K}}, \frac{K}{H\sqrt{H^2-K}}],$$

and that $\tan\alpha = \pm K/H\sqrt{H^2-K}$ if and only if $\theta = \pi/4$, that is, if the solution direction is an arithmetic mean curvature direction.

Definition 5.3.10 *Let PTS denote the projectivised tangent bundle to S, and define*

$$\begin{aligned}\Lambda : PTS &\to [-\tfrac{\pi}{2}, \tfrac{\pi}{2}]\\ (p,v) &\mapsto \alpha\end{aligned}$$

with α given by $\sin 2\theta = \tan\alpha H\sqrt{H^2-K}/K$ where θ is the angle between v and the principal direction associated to the principal curvature κ_1. We define $\mathcal{L}_\alpha$, for a fixed α, to be $\Lambda^{-1}(\alpha)$.

Theorem 5.3.11 (a) *The BDE $\mathcal{L}_\alpha$ is*

$$\begin{aligned}&(Ha_P\sin\alpha + GK\sqrt{EG-F^2}\cos\alpha)dy^2\\ &+(Hb_P\sin\alpha + 2FK\sqrt{EG-F^2}\cos\alpha)dxdy\\ &+Hc_P\sin\alpha + EK\sqrt{EG-F^2}\cos\alpha)dx^2 = 0.\end{aligned} \tag{5.21}$$

(b) *The set of all principal directions is $\mathcal{L}_{\pm\frac{\pi}{2}}$ and $\mathcal{L}_0 = L$, so $\mathcal{B}_\alpha$ joins the principal BDE P to the metric L.*

(c) *Away from umbilic points the BDE $\mathcal{L}_\alpha$ can be written with respect to a principal coordinate system as*

$$\kappa_1\kappa_2 G\cos\alpha dy^2 + (\kappa_2^2-\kappa_1^2)\frac{\sqrt{GE}}{2}\sin\alpha dxdy + \kappa_1\kappa_2 E\cos\alpha dx^2 = 0. \tag{5.22}$$

(d) *The discriminant of $\mathcal{L}_\alpha$ consists of the sets $\Delta^\alpha_{\mathcal{B}\pm}$.*

Proof: This proof is similar to that of Theorem 5.3.2 and is omitted. □

Recall the involution $\sigma_{P\Gamma}$ on any line $\hat{P} \subset \mathbb{R}P^2$ induced by a conic Γ, that was defined a the start of Chapter 4. Recall also Lemma 4.0.6.

Considering the involution on the lines $\hat{A}$ and $\hat{Ch}$ induced by the conic Δ allows us to prove a result analogous to Theorem 5.3.5.

Theorem 5.3.12 **(a)** *For any given (fixed) α, the BDE $\mathcal{L}_\alpha$ is the polar of the pencil containing the BDEs $\sigma_{Ch}(\mathcal{C}_\alpha)$ and $\sigma_A(\mathcal{R}_\alpha)$.*

(b) *For any given (fixed) α, the BDE $\mathcal{B}_\alpha$ is the polar of the pencil containing the BDEs $\sigma_{Ch}(\mathcal{C}_\alpha)$ and $\sigma_A(\mathcal{R}_{-\alpha})$.*

Proof: The polar of the pencil $\mathcal{R}$ is the asymptotic BDE A. Given some fixed α, we therefore have that $\sigma_A(\mathcal{R}_\alpha)$ is the Jacobian of the BDEs $\mathcal{R}_\alpha$ and A. We find that this is the BDE

$$\begin{aligned}(a_{Ch}H\sqrt{EG-F^2}\cos\alpha - 2Ka_P\sin\alpha)dy^2\\ +2(b_{Ch}H\sqrt{EG-F^2}\cos\alpha - Kb_P\sin\alpha)dxdy\\ +(c_{Ch}H\sqrt{EG-F^2}\cos\alpha - 2Kc_P\sin\alpha)dx^2 = 0.\end{aligned} \tag{5.23}$$

A calculation of the Jacobian of the BDEs $\mathcal{C}_\alpha$ (5.17) and $\sigma_A(\mathcal{R}_\alpha)$ (5.23) shows that the polar of the pencil connecting these two BDEs is the BDE $\mathcal{B}_\alpha$.

The second assertion follows by similar calculations. □

Remark 5.3.13 *When $\alpha = \pi/2$ the BDEs $\sigma_{\mathcal{C}}(\mathcal{C}_\alpha)$, $\sigma_{\mathcal{R}}(\mathcal{R}_\alpha)$ and $\sigma_{\mathcal{R}}(\mathcal{R}_{-\alpha})$ coincide and are the principal BDE* (2.4)*. For similar reasons to those used in Remarks 5.3.6 2. we have that $\hat{Me} = \{L_\alpha | \alpha \in [-\frac{\pi}{2}, \frac{\pi}{2}]\}$ is the closure of the set*

$$\{Jac(\sigma_{\mathcal{C}}(\mathcal{C}_\alpha), \sigma_{\mathcal{R}}(\mathcal{R}_\alpha))|(\alpha \in (-\frac{\pi}{2}, \frac{\pi}{2})\},$$

and $\hat{T} = \{B_\alpha | \alpha \in [-\frac{\pi}{2}, \frac{\pi}{2}]\}$ is the closure of the set

$$\{Jac(\sigma_{\mathcal{C}}(\mathcal{C}_\alpha), \sigma_{\mathcal{R}}(\mathcal{R}_{-\alpha}))|(\alpha \in (-\frac{\pi}{2}, \frac{\pi}{2})\}.$$

We conclude the chapter will an observation concerning special points of surfaces.

Remark 5.3.14 *We have seen that the curve $H = 0$ is significant: it forms part of the discriminant of the BDEs $\mathcal{R}_{\pm\frac{\pi}{2}}, \mathcal{B}_{\pm\frac{\pi}{2}}$, and $\mathcal{L}_{\pm\frac{\pi}{2}}$. On this the asymptotic directions are orthogonal to one another (in fact they coincide with the arithmetic mean curvature directions), and one cannot canonically order the principal directions. Since at such points the asymptotic BDE A, the BDE of the lines of arithmetic mean curvature Me and the BDE of the MOSI curves T coincide, all pairs of orthogonal directions on the surface are mapped to orthogonal directions on the spherical*

image, and the characterisation of the principal directions given in Remark 5.1.6 breaks down.

This set in some ways plays a role in the hyperbolic region similar to that played by the umbilic points in the elliptic region. For example, an umbilic point my be seen as a point at which the shape operator is a multiple of the identity operator, that is, A and L coincide in the projective plane, whereas at points where $H = 0$ it is the characteristic BDE Ch that coincides with L (so that, as we have seen, A coincides with Me). This similarity may be further understood by considering the alternative definition of conjugacy given in Proposition 2.1.1. An umbilic point the Dupin indicatrix is a circle; at a point where $H = 0$ the Dupin indicatrix is a rectangular hyperbola, however, a circle centred at the origin is a rectangular hyperbola when viewed from (any) point on the line at infinity.

Chapter 6

The characteristic curves as space curves in $\mathbb{R}^3$

In this chapter we consider the characteristic curves on a smooth surface as space curves in $\mathbb{R}^3$. In Chapter 3 we were able to produce a result on the characteristic curves analogous to the Beltrami-Enepper Theorem on the asymptotic curves. The key observation was that the torsion of the two asymptotic curves through each hyperbolic point is equal to their geodesic torsion. This is not the case for the two characteristic curves through an elliptic point. We consider the torsion of the characteristic curves in this chapter.

6.1 The torsion of the characteristic curves

The torsion τ of a smooth parametrised curve γ in $\mathbb{R}^3$ is given by

$$\tau = \frac{(\gamma' \wedge \gamma'') \cdot \gamma'''}{|\gamma'' \wedge \gamma'|^2} \tag{6.1}$$

where $(')$ denotes differentiation with respect to the parameter.

We parametrise S in Monge form $(x, y, f(x, y))$ with f as in (2.3). We write the BDE of the characteristic curves on S (2.6) as $\Omega(x, y, p) = 0$ where $p = dy/dx$.

Assume that the origin is a non-umbilic elliptic point. Without loss of generality we assume $\kappa_2 > \kappa_1 \geq 0$. We calculate expressions for the coefficients of the first

and second fundamental form at the origin. The integral curves of the characteristic BDE through the origin are smooth, so we may set

$$y_i(x) = (-1)^i(\sqrt{\frac{\kappa_1}{\kappa_2}})x + \alpha_i x^2 + \beta_i x^3 + h.o.t.,$$

for some α_i, β_i, $i = 1, 2$. Let $\Omega_i = \Omega(x, y, dy_i/dx)$. We calculate $j^2\Omega_i(x)$. By setting first (respectively second) order terms to zero, we find α_i (respectively β_i), $i = 1, 2$. Considered as space curves in $\mathbb{R}^3$, the characteristic curves are parametrised as:

$$\gamma_i(x) = (x, y_i(x), f(x, y_i(x))), i = 1, 2.$$

We find (using Maple) that the torsion at the origin of the characteristic curve γ_i is given by

$$\tau_i = \frac{\sqrt{K}A + (-1)^i K^3 B}{\sqrt{K}\Gamma + (-1)^i \Lambda}, i = 1, 2,$$

where

$$\begin{aligned}
A = \;& 32\kappa_1^4\kappa_2^4(\kappa_1 - \kappa_2) \\
& +\kappa_1((17\kappa_1^2 + 22\kappa_1\kappa_2 + 9\kappa_2^2)\kappa_2^2 a_{31}^2 \\
& +2(5\kappa_1^2 - 14\kappa_1\kappa_2 - 7\kappa_2^2)\kappa_1\kappa_2 a_{31}a_{33} - 7(\kappa_1 - \kappa_2)^2\kappa_1^2 a_{33}^2) \\
& -\kappa_2((17\kappa_1^2 + 22\kappa_1\kappa_2 + 9\kappa_2^2)\kappa_2^2 a_{32}^2 \\
& +2(5\kappa_1^2 - 14\kappa_1\kappa_2 - 7\kappa_2^2)\kappa_1\kappa_2 a_{32}a_{30} - 7(\kappa_1 - \kappa_2)^2\kappa_2^2 a_{30}^2) \\
& +4\kappa_1\kappa_2(\kappa_1^2(\kappa_1 - \kappa_2)^2 a_{44} + 4\kappa_1\kappa_2(\kappa_1^2 - \kappa_2^2)a_{42} - \kappa_2^2(\kappa_1 - \kappa_2)^2 a_{40}),
\end{aligned}$$

$$B = \; 16(2a_{30}a_{31} - 2a_{32}a_{33} - a_{41}(\kappa_1 - \kappa_2) - a_{43}(\kappa_1 - \kappa_2)),$$

$$\Gamma = \; 2(\kappa_2 a_{30}(\kappa_1 - \kappa_2) + \kappa_1 a_{32}(\kappa_1 + 3\kappa_2))(\kappa_2 a_{31}(\kappa_2 + 3\kappa_1) - \kappa_1 a_{33}(\kappa_1 - \kappa_2)),$$

$$\begin{aligned}
\Lambda = \;& 16\kappa_1^3\kappa_2^3(\kappa_1 + \kappa_2)(\kappa_1 - \kappa_2)^2 + \kappa_2(\kappa_2 a_{30}(\kappa_1 - \kappa_2) + \kappa_1 a_{32}(\kappa_1 + 3\kappa_2))^2 \\
& +\kappa_1(\kappa_2 a_{31}(\kappa_2 + 3\kappa_1) - \kappa_1 a_{33}(\kappa_1 - \kappa_2))^2.
\end{aligned}$$

It is clear that $\tau_1\tau_2$ depends on the value of the coefficients of $j^4 f$ and can be positive, negative or zero, that is, the respective torsions of the two characteristic curves through a point may have the same or different signs, and may also vanish.

The results in this chapter are proved using the transversality method given in [9] (see also [73]) outlined in Section 1.2.2, and we include here only the key facts. Detailed calculations, carried out using Maple, are generally omitted.

At any point p we parametrise the surface in Monge form $(x, y, f_p(x, y))$ at p, where f_p is a smooth function and $f_0 = f$. We define the jet-extension map

$$\begin{aligned} \phi : S \to & \quad J^4(2) \\ p \mapsto & \quad j^4 f_p. \end{aligned} \tag{6.2}$$

The differential map to ϕ is denoted by $T_p\phi : T_pS \to T_{\phi(p)}J^4(2)$. Recall the basis $\{v_x, v_y\}$ for $\mathrm{im}(T_0\phi)$ given in Lemma 1.2.3.

Let $\mathcal{L} = J^4(2)/SO(2)$. A polynomial $q \in J^4(2)$, where

$$q(x,y) = \frac{1}{2}\sum_{i=0}^{2}\begin{pmatrix} 2 \\ i \end{pmatrix} a_{2i}y^i x^{2-i} + \frac{1}{6}\sum_{i=0}^{3}\begin{pmatrix} 3 \\ i \end{pmatrix} a_{3i}y^i x^{3-i} + \frac{1}{24}\sum_{i=0}^{4}\begin{pmatrix} 4 \\ i \end{pmatrix} a_{4i}y^i x^{4-i},$$

is $SO(2)$-equivalent to a polynomial r with $a_{21} = 0$, that is, we may identify $\mathcal{L}$ with the hyperplane $a_{21} = 0$.

We define a function

$$\begin{aligned} h : \mathcal{L} \to & \quad \mathbb{R} \\ r \mapsto & \quad \frac{(A^2 - K^5B^2)K}{K\Gamma^2 - \Lambda^2} \end{aligned} \tag{6.3}$$

where $K = a_{20}a_{22}$ and A, B, Γ, Λ are evaluated with $\kappa_1 = a_{20}$ and $\kappa_2 = a_{22}$. Let $\mathcal{V} \subset \mathcal{L}$ be the set given by $h^{-1}(0)$, and let $V \subset J^4(2)$ be the $SO(2)$-orbit of $\mathcal{V}$. It is clear that V is an $SO(2)$-invariant set with codimension 1 in $J^4(2)$.

Let ∇ denote the gradient vector field on smooth hypersurfaces in $J^4(2)$ (which is identified with $\mathbb{R}^{12}$ via the coordinates a_{ji}). The tangent space to V at a point $r \in \mathcal{V}$ is given by $\mathbb{R}.\{xr_y - yr_x\} \oplus T\mathcal{V}$, where $T\mathcal{V}$ is the tangent space to $\mathcal{V}$, that is, the orthogonal compliment of ∇h in $J^4(2)$.

We define a regular stratification $\mathcal{S} = \{S_H, S_E, S_P, S_G, S_U\}$ of $J^4(2)$, where $q(x, y) \in J^4(2)$ is in S_H (respectively S_E, S_P, S_G, S_U) if the point $(0, 0, 0)$ is a hyperbolic point (respectively parabolic point not a cusp of Gauss, non-umbilic elliptic point, cusp of Gauss, umbilic point) of the smooth surface parametrised by $(x, y, q(x, y))$. The codimensions of S_H, S_E, S_P, S_G, S_U in $J^4(2)$ are respectively $0, 0, 1, 2$ and 2, and S_P, S_G, S_U are in the closure of S_E. The intersection of V with S_H, S_E, S_U and S_P are denoted by V_H, V_E, V_U and V_P as appropriate, and form a regular stratification of V into smooth submanifolds.

Proposition 6.1.1 *The torsion of a characteristic curve approaches zero as the curve approaches a generic parabolic point. Near such points the characteristic curves have torsion of opposite sign.*

Proof: The set S_P may be taken to be the $SO(2)$-orbit of the subset of $\mathcal{L}$ given by $a_{20} = 0$, $a_{30} \neq 0$. It is clear that $S_P \subset V$, that is, $V_P = S_P$. Calculations show that $\mathbb{R}.\{xf_y - yf_x\}$ does not generally lie in $\mathbb{R}.\{v_x, v_y\}$ when $a_{20} = 0$, and $\nabla a_{20} \cdot v_x = a_{30}/2$, which does not vanish in S_P, hence ϕ is transverse to V_P. The first assertion follows since the function h (6.3) is smooth at points in a neighbourhood of S_P. The second assertion is proved by observing that $\partial h/\partial a_{20} < 0$ in S_P. □

Proposition 6.1.2 *The torsion of the characteristic curves does not vanish in a neighbourhood of a generic umbilic point.*

Proof: The set S_U is given by $a_{21} = 0, a_{20} = a_{22}$. Consider the function h (6.3). Calculations show that $\nabla h \cdot v_x$ and $\nabla h \cdot v_y$ do not in general vanish simultaneously and that $\mathbb{R}.\{xf_y - yf_x\}$ does not lie in $\mathbb{R}.\{v_x, v_y\}$ when $a_{20} = a_{22}$, that is, V_U is generally transverse to ϕ. The function h does not vanish identically on S_U, hence V_U has codimension 3, so $\phi^{-1}(V_U)$ is generally empty. As h is smooth at points in S_U, there is a neighbourhood Q of any generic point of S_U in which h does not vanish. In $\phi^{-1}(Q)$, a neighbourhood of a generic umbilic, the torsion of the characteristic curves does not vanish. □

At an umbilic point we may write

$$j^3 f(x, y) = \frac{\kappa}{2}(x^2 + y^2) + \mathrm{Re}(z^3 + \beta z^2 z)$$

where $z = x + iy$ and β is a complex number ([18]).

Proposition 6.1.3 *The two characteristic curves passing through any point in a neighbourhood of an umbilic point have torsion of the same (respectively opposite) sign if β lies in a region labelled + (respectively −) in Figure 6.1. These regions are bounded by the lines*

$$\arg(3\beta - \bar{\beta} - 6) = \pm\frac{\pi}{4}$$

and

$$\arg(5\beta - \bar{\beta} + 14) = \pm\frac{\pi}{4},$$

shown in solid lines.

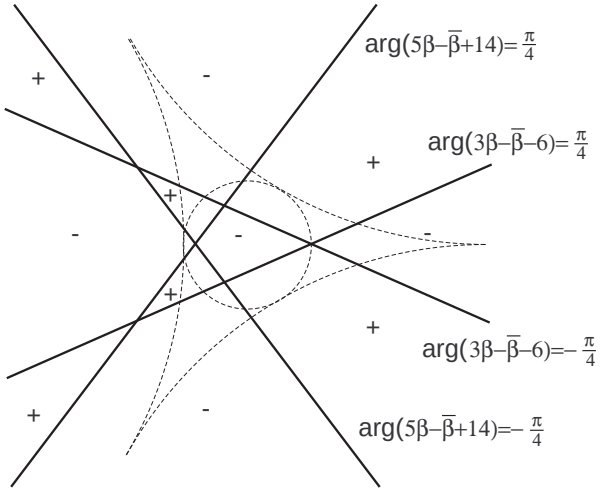

Figure 6.1: Partitions of the β plane into regions where the torsion of the two characteristic curves through each point in a neighbourhood of an umbilic point with complex parameter β have the same (+) or different (-) sign. The regions are divided by the solid lines.

Proof: The sign of the torsion at points in a neighbourhood of S_U are given by that of the function h (6.3) at points in S_U as h is smooth on S_U. A calculation shows that

$$h = -9K^2 \frac{\mathrm{Re}(3\beta - \bar{\beta} - 6)^2)}{\mathrm{Re}(5\beta - \bar{\beta} + 14)^2)}.$$

The exceptional sets in the complex plane where h changes sign are thus those where $(3\beta - \bar{\beta} - 6)$ or $5\beta - \bar{\beta} + 14$ have an argument of $\pm\pi/4$. The proof is completed by calculating the sign of h for a value of β in each of the open regions defined by these lines. □

Remark 6.1.1 *As described in Section 2.2, there are three generic topological configurations of the characteristic curves at an umbilic point, distinguished by the position of β with respect to the circle $|\beta| = 3$ and the hypercycloid $\beta = 2(2e^{i\theta} + 2e^{-2i\theta})$* ([24]). *These sets are shown in dashed lines in Figure 6.1.*

We now consider the set of points where the torsion of a characteristic curve vanishes.

Theorem 6.1.2 *There are generically smooth or empty curves in the elliptic region on which the curves of one characteristic foliation have zero torsion and isolated points in the elliptic region where the curves of both foliations have zero torsion.*

Proof: The set of points at which a characteristic curve vanishes is $\phi^{-1}(V_E)$. The set V_E is the $SO(2)$-orbit of the subset of the hyperplane $a_{21} = 0$ given by

$$A^2 - K^5 B^2 = 0.$$

As $\mathbb{R}.\{xf_y - yf_x\}$ does not generally lie in $\mathbb{R}.\{v_x, v_y\}$ and $\nabla(A^2 - K^5B^2) \cdot v_x$ and $\nabla(A^2 - K^5B^2) \cdot v_y$ do not in general vanish simultaneously, ϕ is generally transverse to V. The codimension of V_E in $J^4(2)$ is 1, hence by Lemma 1.2.2 $\phi^{-1}(V_E \cap \mathrm{im}(\phi))$ is a smooth curve or is empty.

The set of points where the torsion of both characteristic curves vanishes is given by $\phi^{-1}(W \cap \mathrm{im}(\phi))$ where $W \subset J^4(2)$ is the $SO(2)$-orbit of the subset of $\mathcal{L}$ given by $A = B = 0$. Calculations show that ∇A and ∇B are generally linearly independent, so the codimension of W in $J^4(2)$ is 2, and that $\nabla A \cdot v_x$, $\nabla A \cdot v_y$, $\nabla B \cdot v_x$ and $\nabla B \cdot v_y$ do not in general vanish simultaneously, that is ϕ is generally transverse to W. By Lemma 1.2.2 $\phi^{-1}(W \cap \mathrm{im}(\phi))$ is a smooth submanifold of S of codimension 2 (an isolated point), or is empty. □

Definition 6.1.3 *The* characteristic zero torsion curve *is the closure of the locus of points where a characteristic curve has zero torsion. The left (respectively right) branch of the characteristic zero torsion curve consists of the points of zero torsion of the left (respectively right) characteristic curves.*

It is immediate from Proposition 6.1.2 that the characteristic zero torsion curve does not pass through umbilic points. We now consider its behaviour near parabolic points.

Proposition 6.1.4 *The characteristic zero torsion curve meets the parabolic set at a cusp of Gauss with ccr-invariant ρ_c if $\rho_c < 13/4$. At such points the left and right branches of the characteristic zero torsion curve are C^2 curves tangent to the parabolic set and divide a neighbourhood of a cusp of Gauss as shown in Figure 6.2*

(right). In a neighbourhood of a cusp of Gauss with $\rho_c > 13/4$ the torsion of the characteristic curves have opposite sign.

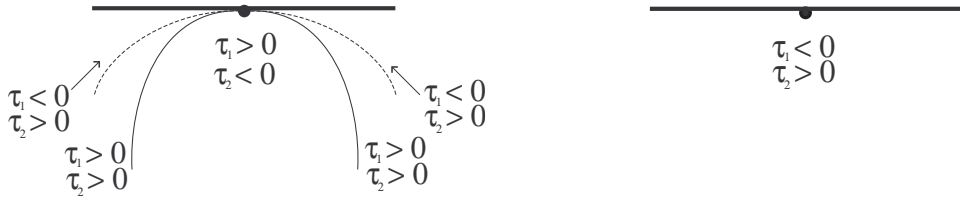

Figure 6.2: The left (solid curve) and right (broken curve) branches of the characteristic zero torsion curve at a cusp of Gauss, $\rho_c < 13/4$ (left) and $\rho_c > 13/4$ (right). The thick line is the parabolic set.

Proof: The set S_G may be taken to be the $SO(2)$-orbit of the set given by $a_{20} = a_{21} = a_{30} = 0$. The characteristic zero torsion curve is given by $\phi^{-1}(\overline{V_E})$ where $\overline{V_E}$ is the closure of V_E. The set V_E is given by

$$A^2 - K^5 B^2 = 0.$$

A calculation shows that

$$A^2 - K^5 B^2 = -\frac{49 a_{22}^{10} a_{30}^4}{16}$$

when $a_{20} = 0$, hence in general $S_G \subset \overline{V_E}$.

Observe that the expressions $A \pm K^{5/2}$ are C^2 functions of a_{20} and a_{30}. In S_E the varieties corresponding to left and right branches of the characteristic zero torsion curve are given by $A - K^{5/2}B = 0$ and $A + K^{5/2}B = 0$ respectively. In a neighbourhood of S_G these equations can be written as

$$a_{22}^4(4a_{40}a_{22} - 9a_{31}^2)a_{20} = 7a_{22}^5 a_{30}^2 + O(a_{20}^3),$$

that is, the varieties are tangent to $S_P \cup S_G$, and lie locally in S_E (respectively S_H) when $4\rho_c - 13$ is negative (respectively positive), using Proposition 3.1.2. It follows that the branches of the characteristic zero torsion curve are tangent to the parabolic set at cusps of Gauss with $\rho_c > 13/4$.

The relative positions of the two branches are established by considering higher order terms in a_{20}, a_{30} in $A \pm K^{5/2}B$. As $S_G \subset \overline{S_P}$ the final assertion follows from Proposition 6.1.1. □

6.2 Osculating planes of the characteristic curves

Let θ be the angle between the principal normal to a curve on a surface parametrised by arc length s and $\mathbf{n}$, the unit normal to the surface. Then at any point of the curve we have Bonnet's formula:

$$\tau_g = \tau - \frac{d\theta}{ds},$$

where τ and τ_g are respectively the torsion and geodesic torsion of the curve. It follows that the osculating plane of a curve on the surface is equal to the tangent plane of the surface if and only if the torsion and geodesic torsion of the curve are the same.

The Beltrami-Enepper Theorem is a consequence, therefore, of the fact that the osculating plane of the asymptotic curves is the tangent plane to the surface.

Recall that the geodesic torsions of the characteristic curves through an elliptic point are

$$\pm\frac{\sqrt{\kappa_1\kappa_2}(\kappa_2-\kappa_1)}{(\kappa_2+\kappa_1)}.$$

Points at which the osculating plane of a characteristic curve are equal to the tangent plane to the surface are located by equating these expressions to those for the torsion of the characteristic curves given in Section 6.1, that is, by setting

$$\pm\frac{\sqrt{\kappa_1\kappa_2}(\kappa_2-\kappa_1)}{(\kappa_2+\kappa_1)} = \frac{\sqrt{K}A \pm K^3B}{\sqrt{K}\Gamma + \pm\Lambda}.$$

Let the geodesic torsion of a the characteristic curve with torsion τ_i be τ_{gi}, where $i = 1, 2$. The difference between the torsion and the geodesic torsion of a characteristic curve at a non-umbilic elliptic point is given by

$$\tau_i - \tau_{gi} = \frac{\sqrt{K}A + (-1)^i K^3 B}{\sqrt{K}\Gamma + (-1)^i\Lambda} - \sqrt{K}\frac{(\kappa_1-\kappa_2)}{(\kappa_1+\kappa_2)}, i = 1, 2.$$

We consider $(\tau_1 - \tau_{g1})(\tau_2 - \tau_{g2})$. As in Section 6.1 we define a function

$$\begin{aligned} \tilde{h} : \mathcal{L} &\to \mathbb{R} \\ \tilde{q} &\mapsto h + 2K\frac{(a_{22}-a_{20})(K^3B\Gamma - \Lambda A)}{(a_{22}+a_{20})(K\Gamma^2-\Lambda^2)} - K\frac{(a_{22}-a_{20})^2}{(a_{22}+a_{20})^2}. \end{aligned} \tag{6.4}$$

where $K = a_{20}a_{22}$ and A, B, Γ, Λ are evaluated with $\kappa_1 = a_{20}$ and $\kappa_2 = a_{22}$.

Let $\tilde{\mathcal{V}} \subset \mathcal{L}$ be the set given by $\tilde{h}^{-1}(0)$, and let $\tilde{V} \subset J^4(2)$ be the $SO(2)$-orbit of $\tilde{\mathcal{V}}$. The intersection of $\tilde{V}$ with S_E, S_G and S_P are denoted by $\tilde{V_E}$, $\tilde{V_G}$ and $\tilde{V_P}$ respectively.

The proofs of the remaining results in this section use the same methods as the corresponding results in Section 6.1, so details are omitted.

Theorem 6.2.1 *There are generically smooth or empty curves in the elliptic region along which the osculating plane of a characteristic curve is the tangent plane of the surface. There are isolated points in the elliptic region at which the tangent plane to the surface is the osculating plane of both the characteristic curves.*

Proof: The result follows using the method of Theorem 6.1.2 with $\tilde{h}$ (6.4) replacing the function h (6.3). □

Definition 6.2.2 *The* characteristic geodesic torsion curve *is the locus of points at which the tangent plane to the surface is the osculating plane of a characteristic curve. The left (respectively right) branch of the characteristic geodesic torsion curve consists of the points at which the tangent plane to the surface is the osculating plane of a left (respectively right) characteristic curve.*

Proposition 6.2.1 *There is a neighbourhood of a generic umbilic point in which the torsion and geodesic torsion of the characteristic curves through each point are not in general equal.*

Proof: Observe that the geodesic torsion of the characteristic curves through a point approaches zero as the point approaches an umbilic. The result follows using the same method as Proposition 6.1.2. □

It follows immediately from Proposition 6.2.1 that the characteristic geodesic torsion curve does not pass through umbilic points in general.

It is clear that the torsion and geodesic torsion of a characteristic curve approaches zero as the curve approaches parabolic points. We examine now the behaviour of the characteristic geodesic torsion curve near the parabolic set.

Proposition 6.2.2 **(a)** *There are two characteristic geodesic torsion curves (a left branch and a right branch) which are of class C^1 and tangent to the parabolic set at a cusp of Gauss with ccr-invariant ρ_c if $\rho_c < 33/8$.*

(b) *The relative positions of the characteristic geodesic torsion curve and the characteristic zero torsion curve at a cusp of Gauss are as shown in Figure 6.3.*

(c) *When $\rho_c = -2$ the characteristic geodesic torsion curve and the characteristic zero torsion curve have degenerate contact. When $\rho_c = 4$ the left and right branches of the characteristic geodesic torsion curve have degenerate contact. No change in the relative positions of these curves occurs at these values of ρ_c.*

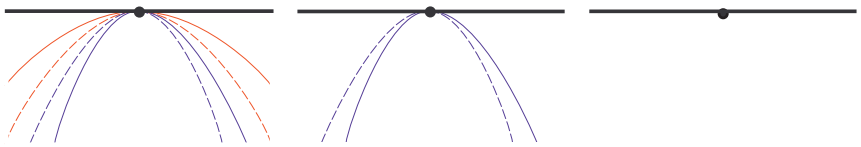

Figure 6.3: Relative positions of the characteristic geodesic torsion curves (blue) and characteristic zero torsion curves (red) at a cusp of Gauss with ccr-invariant $\rho_c \in (-\infty, -2) \cup (-2, \frac{13}{4})$ (left), $\rho_c \in (\frac{13}{4}, \frac{33}{8}) \setminus \{4\}$ (centre), and $\rho_c > \frac{33}{8}$ (right). In each case the left branch is shown in solid curves and the right branch is shown in broken curves. The thick black line is the parabolic set.

Proof: Recall that the set S_G may be taken to be the $SO(2)$-orbit of the set given by $a_{20} = a_{21} = a_{30} = 0$. The characteristic geodesic torsion curve is given by $\phi^{-1}(\overline{\tilde{V}_E})$ where $\overline{\tilde{V}_E}$ is the closure of $\tilde{V}_E$ and ϕ is the jet-extension map (6.2). The set $\tilde{V}_E$ is given by

$$(A^2 - K^5B^2)(a_{22} + a_{20})^2 + (2(a_{22}^2 - a_{20}^2))(K^3B\Gamma - \Lambda A) - (a_{22} - a_{20})^2(K\Gamma^2 - \Lambda^2).$$

A calculation shows that when $a_{20} = 0$ the set $\tilde{V}_E$ is given by $-9a_{22}^{12}a_{30}^4 = 0$ hence in general $S_G \subset \overline{V_E}$.

We consider the varieties in $\mathcal{L}$ that correspond to the left and right branches of the characteristic geodesic torsion curve (these form a partition of $\tilde{V}_E$). These are given respectively by

$$\tau_i - \tau_{gi} = \frac{\sqrt{K}A + (-1)^i K^3 B}{\sqrt{K}\Gamma + (-1)^i \Lambda} - \sqrt{K}\frac{(a_{20} - a_{21})}{(a_{20} + a_{21})}$$

$i = 1, 2$. Using the expressions for A, B, Γ, Λ given in Section 6.1 we have that these varieties are given by

$$\begin{aligned}(-4a_{31}^2 + 2a_{22}^2 a_{40})a_{20} - \sqrt{a_{22}^3}a_{31}\sqrt{a_{20}}a_{30} - 3a_{22}^2 a_{30}^2 + h.o.t. &= 0,\\ -(-4a_{31}^2 + 2a_{22}^2 a_{40})a_{20} - \sqrt{a_{22}^3}a_{31}\sqrt{a_{20}}a_{30} + 3a_{22}^2 a_{30}^2 + h.o.t. &= 0,\end{aligned}$$

in a neighbourhood of S_G.

We make the substitution $a_{20} = b^2$ and restrict our attention to the region $b \geq 0$. The sets of interest are then given by

$$\begin{aligned}(-4a_{31}^2 + 2a_{22}^2 a_{40})b^2 - \sqrt{a_{22}^3}a_{31}ba_{30} - 3a_{22}^2 a_{30}^2 + O(b^2, a_{30}^3) &= 0,\\ -(-4a_{31}^2 + 2a_{22}^2 a_{40})a_{20} - \sqrt{a_{22}^3}a_{31}\sqrt{a_{20}}a_{30} + 3a_{22}^2 a_{30}^2 + O(b^2, a_{30}^3). &= 0.\end{aligned} \tag{6.5}$$

These sets have Morse singularities at the origin: an A_1^+- (respectively A_1^--) singularity when $-47a_{31}^2 + 24a_{22}a_{40} > 0$ respectively $-47a_{31}^2 + 24a_{22}a_{40} > 0$). By Proposition 3.1.2 we have that $-47a_{31}^2 + 24a_{22}a_{40} > 0$ if and only if $\rho_c < 33/8$.

When the singularity is A_1^- we decompose the quadratic expressions in b and a_{30} (6.5) into linear factors. By the implicit function Theorem 1.1.6, the varieties corresponding to the characteristic geodesic torsion curve are then expressible in the form

$$b = ua_{30} + h.o.t$$

for some $u_i(a_{22}, a_{31}, a_{40})$ $i = 1, 2$. Observe that if we substitute $b = \sqrt{\kappa_2}$ these varieties are given by $\sqrt{\kappa_1} = u_i a_{30} + h.o.t$, that is, they are of class C^1 and tangent to the set $S_P \cup S_G$. Assertion **(a)** then follows as the jet-extension map ϕ is a diffeomorphism.

Recall from the proof of Proposition 6.1.4 that the varieties corresponding to the zero torsion curves in a neighbourhood S_G are both given by

$$(4a_{40}a_{22} - 9a_{31}^2)a_{20} = 7a_{22}a_{30}^2 + O(a_{20}^3).$$

We substitute $a_{20} = b^2$ into this expression to obtain

$$(4a_{40}a_{22} - 9a_{31}^2)b^2 = 7a_{22}a_{30}^2 + O(a_{20}^3). \tag{6.6}$$

Observe that this set now has a Morse singularity at the origin: an A_1^+- (respectively A_1^--) singularity when $-9a_{31}^2 + 4a_{22}a_{40} > 0$ (respectively $-9a_{31}^2 + 4a_{22}a_{40} > 0$). We decompose the quadratic expression (6.6) into linear factors.

Assertions **(b)** and **(c)** are established by comparing these linear factors and those obtained from the expressions (6.5). Codimension one phenomena occur when any pair of these linear factors coincide or when the singularities of the relevant varieties are worse than Morse. Calculations show that instances of these phenomena are given by the value of $a_{40}a_{22}/a_{31}^2$, that is, on the value of the ccr-invariant ρ_c.

The exceptional values are $\rho_c = -2$ (a pair of linear factors corresponding to the characteristic geodesic torsion curves coincide), $\rho_c = 4$ (a linear factor corresponding to a characteristic geodesic torsion curve coincides with a linear factor corresponding to the characteristic zero torsion curve), $\rho_c = 13/4$ (the variety corresponding to the characteristic zero torsion curves has a worse than Morse singularity) and $\rho_c = 33/8$ (the variety corresponding to the characteristic geodesic torsion curves has a worse than Morse singularity).

The proof is completed by choosing a value of ρ_c in each of the open intervals bounded by the exceptional values, and calculating expressions for the varieties in $\mathcal{L}$ corresponding to each curve. □

Chapter 7

BDEs with discriminant having a cusp singularity

In this chapter we again leave the differential geometry of surfaces and study binary differential equations in their own right, in preparation for the study of pairs of foliations on singular surfaces in Chapter 8 and Chapter 9.

We consider BDEs (1.5) with coefficients all vanishing at an isolated point where the discriminant has an A_2- (cusp) singularity. We refer to such equations as cusp BDEs.

We show that cusp BDEs are generally of one of three types. A normal form for the 1-jet of BDEs of each is established. We also show that there are certain degenerate cusp BDEs that are not of any of the three types. We give a complete topological classification of cusp BDEs with codimension ≤ 4. The results are summarised in Theorem 7.0.3.

Theorem 7.0.3 *A BDE with discriminant having a local A_2-singularity with vanishing coefficients at the singular point and with codimension ≤ 4 is locally topologically equivalent to one of the normal forms in Table 7.1.*

Remark 7.0.4 *There are no topologically stable singularities of BDEs with vanishing coefficients: the discriminant is necessarily singular, and a generic deformation in the set of all BDEs removes this singularity. It follows that generic deformations must be born in mind when considering topological equivalence (indeed a topological*

Cusp Type	Codimension	Topological Normal Forms	Figure
1	2	$(y, -x + y, y^2); (y, x + 2y, y^2)$ $(y, x + y, y^2)$	Figure 7.1
	3	$(y, x + \sqrt{2}y, y^2)$	Figure 7.2
2	3	$(x, -2y, x^2); (x, -y, x^2)$ $(x, -2y/3, x^2); (x, -y/4, x^2)$ (x, y, x^2)	Figure 7.4
	4	$(x, -3y/2 + x^2, x^2); (x, -3y/4, x^2)$	Figure 7.10
3	4	$(x + y, -y/2, x^2)$	Figure 7.15

Table 7.1: Cusp BDEs with codimension ≤ 4.

classification of cusp BDEs would be of little interest otherwise, since the discriminant itself is homeomorphic to a straight line). Consequently, although certain BDEs with different normal forms in Table 7.1 are topologically equivalent (see Section 7.2), we consider them to be distinct as their deformations in generic families may not be equivalent. Furthermore, there are certain geometric differences between the solution curves, which we highlight in Section 7.3.

We also study in this chapter certain BDEs with discriminant having a $Y^1_{1,2}$-singularity, as such BDEs arise in the study of the characteristic curves on a parabolic cross-cap in Chapter 6.

Remark 7.0.5 *A BDE with coefficients that do not vanish simultaneously may also have a discriminant with an A_2-singularity. These are studied in* [63].

7.1 The three types of cusp BDE

We will always assume that the point under consideration is the origin.

We use the method of lifting the bi-valued direction field defined by the BDE in the plane to a single vector field on a surface that is described in Section1.3. We consider the surface

$$\tilde{M} = \{(x, y, [\alpha : \beta]) \in \mathbb{R}^2, 0 \times \mathbb{R}P^1 | a\alpha^2 + 2b\alpha\beta + c\beta^2 = 0\}$$

associated to the BDE (1.5). When the discriminant has an A_2-singularity the surface $\tilde{M}$ has a Morse singularity at a point on the exceptional fibre ([11]).

Consider the affine chart for $\mathbb{R}P^1$, $p = \beta/\alpha$ (we also consider the chart $q = \alpha/\beta$) and write equation (1.5) as

$$F(x, y, p) = a(x, y)p^2 + 2b(x, y)p + c(x, y) = 0. \tag{7.1}$$

Recall that a suitable lifted field on the smooth part of $\tilde{M}$ is

$$\xi = F_p \frac{\partial}{\partial x} + pF_p \frac{\partial}{\partial y} - (F_x + pF_y)\frac{\partial}{\partial p}.$$

The lifted field ξ extends smoothly to the regular part of the exceptional fibre, and the exceptional fibre is an integral curve of ξ. We consider the zeros of ξ on the exceptional fibre, which are the roots of the cubic

$$\phi(p) = (F_x + pF_y)(0, 0, p) = 0. \tag{7.2}$$

At a singular point of $\tilde{M}$, $F_x = F_y = 0$, so ϕ has a root at such a point.

Definition 7.1.1 *A BDE with discriminant having an A_2-singularity at the origin is said to be of cusp type $1, 2$ or 3 according to whether the root of ϕ at the singular point of the surface $\tilde{M}$ is simple, double or triple.*

Remark 7.1.2 *There exist cusp BDEs for which the lifted field ξ (and hence the cubic ϕ) vanishes along the whole of the exceptional fibre. We refer to these as degenerate cusp BDEs, and study the cases of lowest codimension in Section 7.4.*

Proposition 7.1.1 *For a cusp BDE the singularity of the surface $\tilde{M}$ lies on the criminant if and only if the BDE is not of cusp type 1.*

Proof: Consider the affine chart for $\mathbb{R}P^1$, $p = dy/dx$ and write equation (1.5) in the form (7.1). As the surface $\tilde{M}$ has a Morse singularity ([11]), the Hessian of F is non-degenerate. Since $F_{pp} = 0$ on the exceptional fibre, we have that

$$(F_{xp}, F_{yp}) \neq (0, 0).$$

We assume (by making a linear change of coordinates if necessary) without loss of generality that $F_{yp} \neq 0$ in a neighbourhood of the intersection of the criminant and

the exceptional fibre (observe that a liner change of coordinates will not alter the fact that $F_{pp} = 0$ since the coefficients of the BDE all vanish at the origin).

Suppose that the criminant is parametrised by $(x(t), y(t), p(t))$. Then

$$(x', y', p') \cdot (F_{px}, F_{py}, F_{pp}) = 0$$

since the criminant lies in the surface $F_p = 0$. Since $F_{pp} = 0$ on the exceptional fibre and $p = y'/x'$ it follows that the intersection of the criminant and the exceptional fibre satisfies $(F_{xp} + pF_{yp})(0, 0, p) = 0$.

Consider the cubic ϕ. Differentiating we have

$$\phi'(p) = F_{xp}(0, 0, p) + F_y(0, 0, p) + pF_{yp}(0, 0, p),$$

so the intersection of the criminant and the exceptional fibre is a root of $\phi'(p) = 0$ if and only if it is a root of $F_y(0, 0, p) = 0$. Hence the intersection of the criminant and the exceptional fibre is a root of $\phi(p) = 0$ of order ≥ 2 if and only if it is a common root of $F_y(0, 0, p) = 0$ and $F_x(0, 0, p) = 0$, that is, if it occurs at the singular point of the surface $\tilde{M}$. □

Proposition 7.1.2 *A BDE of cusp type m has codimension at least $(m + 1)$.*

Proof: We work in $J^k(2, 3)$ where $k \geq 2$. Let $\tilde{V}$ be the variety of BDEs with discriminant having a worse-than-Morse singularity, which is given by

$$a(0, 0) = b(0, 0) = c(0, 0) = (\delta_{xy}^2 - \delta_{xx}\delta_{yy})(0, 0) = 0.$$

If the discriminant δ has an A_2-singularity then the second derivatives of δ with respect to x and y do not all vanish at the origin. Since cusp BDEs lie in $\tilde{V}$ it follows that $(\delta_{xx}, \delta_{yy}) \neq 0$. By making a linear change of coordinates if necessary, we assume without loss of generality $\delta_{yy} \neq 0$.

We complete the construction of the semi-algebraic set V of cusp BDEs by observing the discriminant now has a genuine A_2-singularity provide that $\delta_{xx}x + \delta_{xy}y$ is not a factor of the cubic terms in the 3-jet at the origin of δ. This is the case provided

$$\delta_{yyy}\delta_{xy}^3 - 3\delta_{xyy}\delta_{xy}^2\delta_{yy} + 3\delta_{xyy}\delta_{xy}\delta_{yy}^2 - \delta_{xxx}\delta_{yy}^3 \neq 0.$$

Consider the affine chart for $\mathbb{R}P^1$, $p = dy/dx$ (we also consider the affine chart $q = dx/dy$), and write equation (1.5) in the form (7.1). Recall the cubic ϕ (7.2). Observe that

$$\phi(p) = a_y(0,0)p^3 + (a_x + 2b_y)(0,0)p^2 + (b_x + 2c_y)(0,0)p + c_x(0,0).$$

Let $V_m \subset V$ be the set defining BDEs of cusp type m, where $m = 1, 2, 3$.

The limiting tangent direction to the cusp is $(-\delta_{yy}, \delta_{xy})$, that is, the criminant intersects the exceptional fibre at $p = -\delta_{xy}/\delta_{yy}$. By applying Proposition 7.1.1 we have that V_1 consists of those BDEs in V with

$$\phi\left(\frac{-\delta_{xy}}{\delta_{yy}}\right) \neq 0.$$

The set V_2 consists of those BDEs in V with

$$\phi\left(\frac{-\delta_{xy}}{\delta_{yy}}\right) = 0, \;\; \phi''\left(\frac{-\delta_{xy}}{\delta_{yy}}\right) \neq 0.$$

The set V_3 consists of those BDEs in V with

$$\phi\left(\frac{-\delta_{xy}}{\delta_{yy}}\right) = \phi''\left(\frac{-\delta_{xy}}{\delta_{yy}}\right) = 0, \;\; \phi'''\left(\frac{-\delta_{xy}}{\delta_{yy}}\right) \neq 0.$$

The set $V \setminus (V_1 \cup V_2 \cup V_3)$ consists of degenerate cusp BDEs.

The hyperplanes in $J^k(2,3)$ defined by each of the conditions

$$a(0,0) = 0, \; b(0,0) = 0 \; c(0,0) = 0$$

clearly intersect transversely, hence their intersection is a plane of codimension 3. Observe that these conditions on the constant terms in the k-jets at the origin of a, b, c, whereas

$$(\delta_{xy}^2 - \delta_{xx}\delta_{yy})(0,0) = 0$$

is a condition on the first order terms in the k-jets of a, b, c. It follows that the variety defined by this condition is transverse to the plane $a(0,0) = b(0,0) = c(0,0) = 0$, and hence that V is a semi-algebraic set of codimension 4.

Let ∇ denote the gradient vector field on $J^k(2,3)$. By calculating

$$\nabla\left(\phi\left(\frac{-\delta_{xy}}{\delta_{yy}}\right)\right) \text{ and } \nabla\left(\phi''\left(\frac{-\delta_{xy}}{\delta_{yy}}\right)\right) = 0$$

it may be shown that the varieties defined by the conditions

$$\phi\left(\frac{-\delta_{xy}}{\delta_{yy}}\right)=0 \text{ and } \phi''\left(\frac{-\delta_{xy}}{\delta_{yy}}\right)=0$$

are transverse to V and to each other. It then follows that V_m, $m=1,2,3$ is a semi-algebraic set of codimension $m+3$ as required. Details of this (lengthy, though straightforward) calculation are omitted. □

Proposition 7.1.3 *The* 1*-jet of the coefficients of a cusp BDE is linearly equivalent to one of the following normal forms.*

(i)	$(y, \epsilon x + b_{11}y, 0)$	*(cusp type 1) where* $\epsilon = \pm 1$,
(ii)	$(x, b_{11}y, 0)$	*(cusp type 2) where* $b_{11} \neq 0, -1/2$,
(iii)	$(x+y, -y/2, 0)$	*(cusp type 3),*
(iv)	$(x, -y/2, 0)$	*(degenerate cusp BDEs).*

Proof: The reduction of the 1-jets of BDEs to normal forms is carried out in [22]. We include here only the key facts. We write

$$j^2a = a_{10}x + a_{11}y + a_{20}x^2 + a_{21}xy + a_{22}y^2$$
$$j^2b = b_{10}x + b_{11}y + b_{20}x^2 + b_{21}xy + b_{22}y^2$$
$$j^2c = c_{10}x + c_{11}y + c_{20}x^2 + c_{21}xy + c_{22}y^2.$$

If the discriminant has a worse-than-Morse singularity then (by linear changes of coordinates if necessary) we may assume

$$c_{10} = c_{11} = 0.$$

We also have

$$b_{10}a_{11} - b_{11}a_{10} \neq 0$$

(otherwise the singularity of the discriminant is worse than A_2).

Consider the affine chart for $\mathbb{R}P^1$, $p = dy/dx$ (we also consider the affine chart $q = dx/dy$). The surface $\tilde{M}$ is singular at $x = y = p = 0$ and regular elsewhere in a neighbourhood of the exceptional fibre $x = y = 0$.

The cubic $\phi(p)$ is given by

$$\phi(p) = (F_x + pF_y)(0,0,p) = 2b_{10}p + (2b_{11} + a_{10})p^2 + a_{11}p^3.$$

Differentiating we have $\phi'(0) = 2b_{10}$ and $\phi''(0) = 2(2b_{11} + a_{10})$.

If $b_{10} \neq 0$ we have a cusp type 1 BDE. Since $b_{10}a_{11} - b_{11}a_{10} \neq 0$ we may make further linear changes of coordinates to set $a_{10} = 0, a_{11} = 1, b_{10} = \pm 1$. The discriminant has an A_2-singularity if $c_{22} \neq 0$.

If $b_{10} = 0$ we have a cusp type 2 BDE provided $2b_{11} + a_{10} \neq 0$. Since we have that $b_{10}a_{11} - b_{11}a_{10} \neq 0$, we have $b_{11}a_{10} \neq 0$. We make further linear changes of coordinates to set $a_{11} = 0$ and $a_{10} = 1$ (we then have that $b_{11} \neq -1/2$). The discriminant has an A_2-singularity if $c_{20} \neq 0$.

If $b_{10} = 2b_{11} + a_{10} = 0$ we have a cusp type 3 BDE provided $a_{11} \neq 0$. We make further linear changes of coordinates to set $a_{10} = a_{11} = 1$. We then have $b_{11} = -1/2$. The discriminant has an A_2-singularity if $c_{20} \neq 0$.

If $b_{10} = 2b_{11} + a_{10} = a_{11} = 0$ the lifted field vanishes everywhere on the exceptional fibre. The discriminant has an A_2-singularity if $b_{11}a_{10}c_{20} \neq 0$. We make further linear changes of coordinates to set $a_{11} = 1$, hence $b_{11} = -1/2$. □

7.2 Topological normal forms

The smooth normal forms for the 1-jets of cusp BDEs established in Proposition 7.1.3 contain moduli which may not be removed by smooth changes of coordinates. It follows that there are no discrete local models under smooth equivalence. We classify cusp BDEs up to topological equivalence as defined in Section 1.3.1.

The lifted field method may not be used to establish the topological configurations of the integral curves of cusp BDEs as the surface $\tilde{M}$ is not smooth. Therefore we use the blowing-up technique described in Section 1.3.

Two blowing-ups are required to establish topological configurations of the integral curves of cusp type two BDEs and cusp type three BDEs. The first is the standard polar blowing-up described in Example 1.3.1.

The second blowing-up is made at the point where the blown-up discriminant meets the exceptional fibre, which we may take to be at $u = 0$, $v = 0$. We use the quasi-homogeneous polar blowing-up $(u, v) = (r^2 \cos\theta, r \sin\theta)$. Our use of this more complicated blowing-up saves work, as the resulting vector fields have only

elementary singularities in most of the cases we consider.

In practice we use the v-direction blowing-up $u = st^2, v = t$, obtained by the change of coordinates $(r, \theta) \mapsto (s, t) = (\cot\theta \csc\theta, r\tan\theta)$. We also consider the u-direction blowings-up $u = \pm\tilde{t}^2, v = \tilde{s}\tilde{t}$, and look for singularities at $\tilde{s} = \tilde{t} = 0$.

Remarks 7.2.1 *1. The first x-direction (respectively y-direction) blowing-up is orientation preserving when $u > 0$ (respectively $\tilde{v} > 0$), and reversing when $u < 0$ (respectively $\tilde{v} < 0$).*

2. If a point (u_0, v_0) in the (u, v)-plane corresponds to a point with polar coordinates (r_0, θ_0), then the point $(-u_0, v_0)$ corresponds to the point $(r_0, \theta_0 + \pi)$. Similarly if a point $(\tilde{u}_1, \tilde{v}_1)$ corresponds to a point with polar coordinates (r_1, θ_1) then the point $(\tilde{u}_1, -\tilde{v}_1)$, corresponds to a point $(r_1, \theta_1 + \pi)$.

3. The second (v-direction) blowing-up is orientation preserving when $t \neq 0$.

4. If a point (s_0, t_0) in the (s, t)-plane corresponds to a point with polar coordinates (r_0, θ_0), then the point $(-s_0, t_0)$ corresponds to the point $(r_0, -\theta_0)$.

A full proof of Theorem 7.2.4 is given. The other results are proved using a similar method and we include only the key points. We use the appropriate normal forms of the 1-jets of the coefficients from Proposition 7.1.3 throughout. In all illustrations the foliation $\mathcal{F}_1$ (respectively $\mathcal{F}_2$) and its blowings-up are solid (respectively broken) curves. The thick black curves are the discriminants.

7.2.1 Cusp type 1 BDEs

Cusp type 1 BDEs with codimension 2 are studied in [66]. The cubic ϕ (7.2) has either two or no roots at regular points of the exceptional fibre. Such BDEs are stable when deformed within the set of cusp BDEs.

Theorem 7.2.2 ([66]) *Suppose that the discriminant of a BDE has a cusp singularity. Then the BDE is generically locally topologically equivalent to one of the following normal forms.*

(i) $(y, -x + y, y^2)$ *Figure 7.1, left,*

(ii) $(y, x + 2y, y^2)$ *Figure 7.1, center,*

(iii) $(y, x + y, y^2)$ *Figure 7.1, right,*

The topological type is determined by the 2-jets of the coefficients of the BDE.

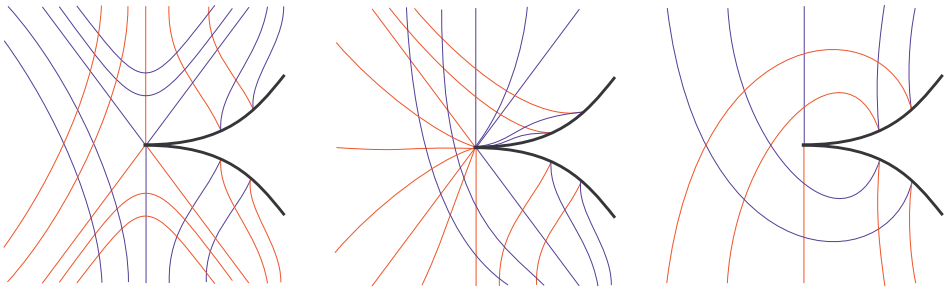

Figure 7.1: The integral curves of cusp type 1 BDEs.

For a cusp type 1 BDE the cubic ϕ may have double root at a regular point of the exceptional fibre. Such BDEs have codimension 3.

Theorem 7.2.3 *A BDE of cusp type 1 with the cubic ϕ having a double root is locally topologically equivalent to $(y, x + \sqrt{2}y, y^2)$. The configuration of the integral curves are as shown in Figure 7.2. The topological type is determined by the 2-jets of the coefficients of the BDE.*

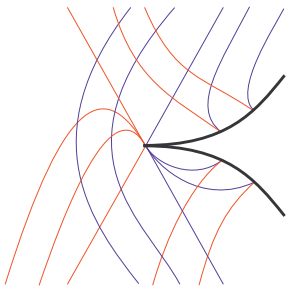

Figure 7.2: The integral curves of the cusp type 1 BDE $(y, x + \sqrt{2}y, y^2)$.

Proof: We adopt the normal form for the 1-jet of the coefficients of a cusp type 1 BDE given in Proposition 7.1.3. The cubic ϕ is determined by the 1-jet of the coefficients, and is given by

$$\phi(p) = p^3 + 2b_{11}p^2 \pm 2p.$$

The surface $\tilde{M}$ is singular at $x = y = p = 0$. Hence ϕ has a double root at a regular point of the exceptional fibre if the quadratic $p^2 + 2b_{11}p \pm 2$ has a double root. This occurs when $b_{11}^2 = 2$. By making the change of coordinates

$$(x, y) \mapsto (x, -y)$$

if necessary we take $b_{11} = \sqrt{2}$.

A single x-direction blowing-up is sufficient to establish the topological configurations of the integral curves. The blown-up discriminant is a parabola tangent to the exceptional fibre at the point $u = 0, v = -\sqrt{2}/2$. One blown-up vector field is regular in a neighbourhood of the exceptional fibre, the other has a saddle singularity at the point $u = 0, v = 0$ and a saddle-node singularity at the point $u = 0, v = -\sqrt{2}$, equivalent to

$$u\frac{\partial}{\partial u} + (v + \sqrt{2})^2\frac{\partial}{\partial v}.$$

□

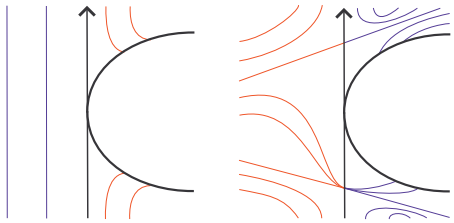

Figure 7.3: The integral curves of Y_1 (left) and Y_2 (right) for a cusp type one BDE with $b_{11}^2 = 2$.

7.2.2 Cusp type 2 BDEs

We now establish topological models for cusp type 2 BDEs. As the modulus b_{11} appearing in the 1-jet varies, topological changes occur when the type or relative position of the singularities occurring on the exceptional fibres change. We begin by identifying the values where changes occur and establishing the configurations when b_{11} lies in each of the open intervals that they define.

Theorem 7.2.4 *A BDE of cusp type 2 with* $b_{11} \neq -3/2, -3/4, -1/2, 0$ *is locally topologically equivalent to*

$$xdy^2 + 2b_{11}ydxdy + x^2dx^2 = 0.$$

The exceptional values bound open intervals where the topological type is constant. The integral curves are shown in Figure 7.4.

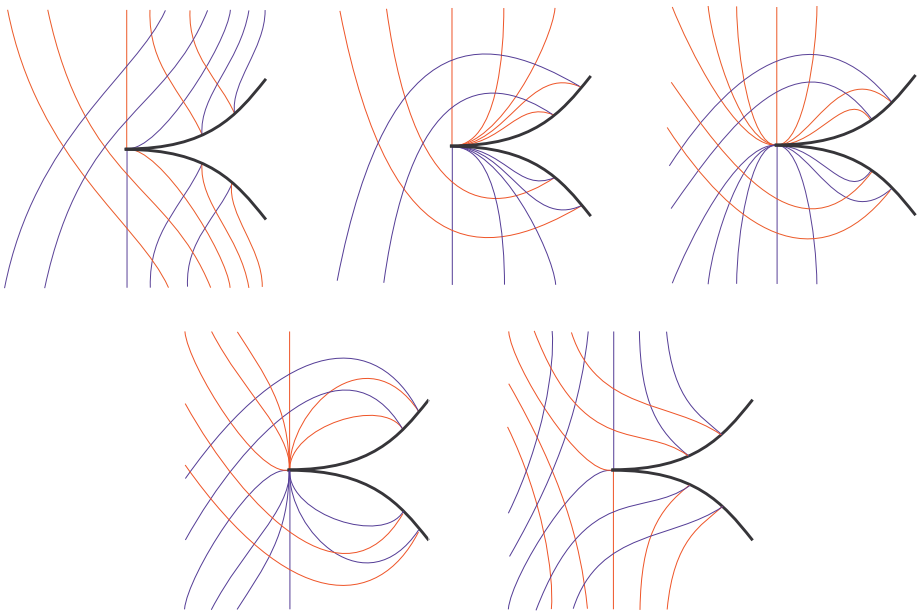

Figure 7.4: The integral curves of a BDE of cusp type 2 with b_{11} a fixed value in the intervals (left to right) $(-\infty, -\frac{3}{2}), (-\frac{3}{2}, -\frac{3}{4})$, and $(-\frac{3}{4}, -\frac{1}{2})$ (top pictures), and $(-\frac{1}{2}, 0)$ and $(0, \infty)$ (bottom pictures).

Proof: We write

$$\omega = (a, b, c) = (x + H_a(x, y), b_{11}y + H_b(x, y), H_c(x, y)),$$

where the H_a, H_b and H_c are germs of smooth functions with zero 1-jets at the origin and $b_{11} \neq -1/2, 0$. We set

$$\begin{aligned} j^2H_a &= a_{20}x^2 + a_{21}xy + a_{22}y^2, \\ j^2H_b &= b_{20}x^2 + b_{21}xy + b_{22}y^2, \\ j^2H_c &= c_{20}x^2 + c_{21}xy + c_{22}y^2. \end{aligned}$$

(a) Blowing-up in the x-direction.

We set $x = u, y = uv$. We write

$$H_a(u, uv) = u^2 K_a(u, v), \;\; H_b(u, uv) = u^2 K_b(u, v), \;\; H_c(u, uv) = u^2 K_c(u, v)$$

where K_a, K_b, K_c are smooth functions. Observe that

$$\begin{aligned} dy^2 = &\;\; u^2 dv^2 + 2uvdudv + v^2 du^2 \\ dxdy = &\;\; udvdu + vdu^2 \\ dx^2 = &\;\; du^2. \end{aligned}$$

The blown-up BDE is therefore $(u, v)^* \omega = u\omega_1$, where

$$\omega_1 = (u^2 A, uB, C)$$

with

$$\begin{aligned} A &= 1 + uK_a, \\ B &= (1 + b_{11})v + uvK_a + uK_b, \\ C &= (1 + 2b_{11})v^2 + uv^2 K_a + 2uvK_b + uK_c. \end{aligned}$$

The quadratic form ω_1 is a product of two 1-forms with associated vector fields

$$X_i = u^2 A \frac{\partial}{\partial u} + (-uB + (-1)^i \sqrt{u^2(B^2 - AC)}) \frac{\partial}{\partial v}, i = 1, 2.$$

We can factor out a term u from X_i and consider the vector fields

$$Y_i = uA \frac{\partial}{\partial u} + (-B + (-1)^i \sqrt{B^2 - AC}) \frac{\partial}{\partial v}, i = 1, 2,$$

in a neighbourhood of the exceptional fibre $u = 0$. Both Y_1 and Y_2 are singular at $u = v = 0$ and regular elsewhere on the exceptional fibre. As the origin is at the intersection of the exceptional fibre and the blown-up discriminant $B^2 - AC = 0$, neither vector field Y_i is smooth there. We make a further blowing-up.

Second blowing-up.

We consider the BDE ω_1 and set $u = st^2, v = t$. We write

$$K_a(st^2, t) = \bar{K_a}(s, t), \;\; K_b(st^2, t) = \bar{K_b}(s, t), \;\; K_c(st^2, t) = \bar{K_c}(s, t).$$

Observe that $\bar{K_c}(s,0) = c_{20}$. The blown-up BDE is

$$(s,t)^*\omega_1 = t^4\omega_2,$$

with $\omega_2 = (t^2\bar{A}, st\bar{B}, s^2\bar{C})$, where

$$\begin{aligned}
\bar{A}(s,t) &= (1+2b_{11}) + s(t^2\bar{K_a} + 2t\bar{K_b} + \bar{K_c}),\\
\bar{B}(s,t) &= (3+5b_{11}) + s(3t^2\bar{K_a} + 5t\bar{K_b} + 2\bar{K_c}),\\
\bar{C}(s,t) &= (9+12b_{11}) + s(9t^2\bar{K_a} + 12t\bar{K_b} + 4\bar{K_c}).
\end{aligned}$$

The blown-up discriminant is $\bar{\delta} = \bar{B}^2 - \bar{A}\bar{C}$. We have $j^1\bar{\delta} = b_{11}^2 - sc_{20}$, so the discriminant intersects the exceptional fibre $t = 0$ transversely at $s = b_{11}^2/c_{20}$. The quadratic form ω_2 is a product of two 1-forms with associated vector fields

$$\bar{X_i} = t^2\bar{A}\frac{\partial}{\partial t} + (-ts\bar{B} + (-1)^i\sqrt{s^2t^2(\bar{B}^2 - \bar{A}\bar{C})})\frac{\partial}{\partial s}, i = 1,2.$$

We factor out a term t in X_i and consider the vector fields

$$\bar{Y_i} = t\bar{A}\frac{\partial}{\partial t} + (-s\bar{B} + s(-1)^i\sqrt{(\bar{B}^2 - \bar{A}\bar{C})})\frac{\partial}{\partial s}, i = 1,2.$$

We study the vector fields $\bar{Y_i}, i = 1,2$ in a neighbourhood of the exceptional fibre $t = 0$. Observe that both Y_1 and Y_2 are regular at the intersection of the exceptional fibre $t = 0$ and the blown-up discriminant $\bar{\delta} = 0$, and are transverse to the blown-up discriminant there. We have

$$\bar{Y_i}(s,0) = s(-(3+5b_{11}+2c_{20}s) + (-1)^i\sqrt{(b_{11}^2 - c_{20}s)})\frac{\partial}{\partial s}, i = 1,2.$$

Both $\bar{Y_1}$ and $\bar{Y_2}$ are singular at the origin, and $\bar{Y_1}$ (respectively $\bar{Y_2}$) is also singular at $t = 0, s = \alpha$ where $\alpha = -3(3+4b_{11})/(4c_{20})$ when $b_{11} > -3/2$ (respectively $b_{11} < -3/2$). Observe that $\alpha > 0$ when $b_{11} < -3/4$ and $\alpha < 0$ otherwise. We calculate $j^1\bar{Y_i}(0,0)$ and $j^1\bar{Y_i}(\alpha,0)$, where $i = 1,2$. The type of singularity at each point as b_{11} varies is shown in Table 7.2.

We have divided by a factor of st^5. Hence the integral curves of the vector field $\bar{Y_i}$ are the blowings-up of $\mathcal{F}_i$ when $st > 0$ and the blowings-up of $\mathcal{F}_{3-i}$ when $st < 0$. The integral curves of $\bar{Y_1}$ and $\bar{Y_2}$ in a neighbourhood of the exceptional fibre $t = 0$ are shown in Figure 7.5.

	$(0,0)$		$(\alpha,0)$	
b_{11}	$\bar{Y}_1$	$\bar{Y}_2$	$\bar{Y}_1$	$\bar{Y}_2$
$(-\infty,-3/2)$	Saddle	Saddle	Regular	Saddle
$(-3/2,-3/4)$	Saddle	Saddle	Node	Regular
$(-3/4,-1/2)$	Node	Saddle	Saddle	Regular
$(-1/2,0)$	Saddle	Saddle	Saddle	Regular
$(0,\infty)$	Saddle	Saddle	Saddle	Regular

Table 7.2: Singularities of the vector fields $\bar{Y}_1$ and $\bar{Y}_2$ for cusp type 2 BDEs.

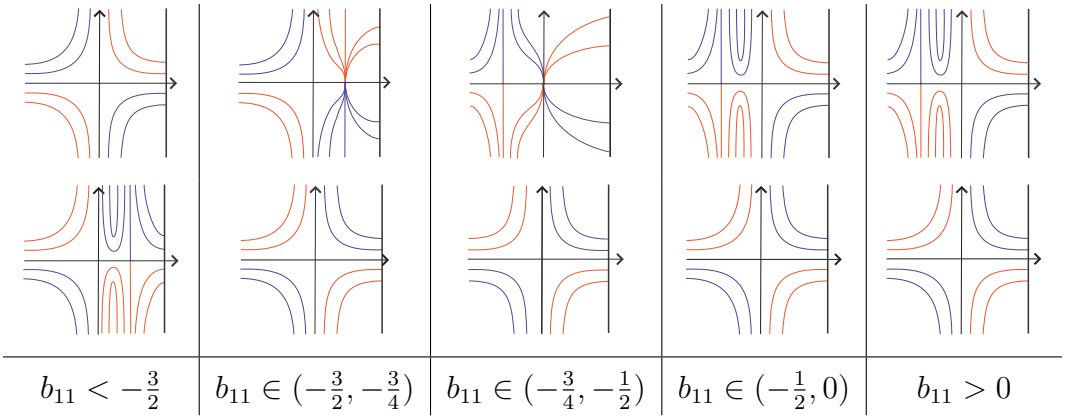

Figure 7.5: The integral curves of the vector fields $\bar{Y}_1$ (top) and $\bar{Y}_2$ (bottom) for cusp type 2 BDEs.

Blowing down.

Blowing down we have the integral curves of the first x-direction blowing-up, that is, the integral curves of the vector fields Y_1 and Y_2. The first blowing-up is orientation preserving when $u > 0$ and orientation reversing when $u < 0$, and we have divided by a factor of u^2. Hence the integral curves of the vector field Y_i are the blowings-up of $\mathcal{F}_i$ when $u > 0$ and the blowings-up of $\mathcal{F}_{3-i}$ when $u < 0$. These are shown in Figure 7.6.

(b) Blowing-up in the y-direction.

Consider the directional blowing-up $x = \tilde{u}\tilde{v}, y = \tilde{v}$. We set

$$H_a(\tilde{u}\tilde{v},\tilde{v}) = \tilde{v}^2 P_a(\tilde{u},\tilde{v}), H_b(\tilde{u}\tilde{v},\tilde{v}) = \tilde{v}^2 P_b(\tilde{u},\tilde{v}), H_c(\tilde{u}\tilde{v},\tilde{v}) = \tilde{v}^2 P_c(\tilde{u},\tilde{v}),$$

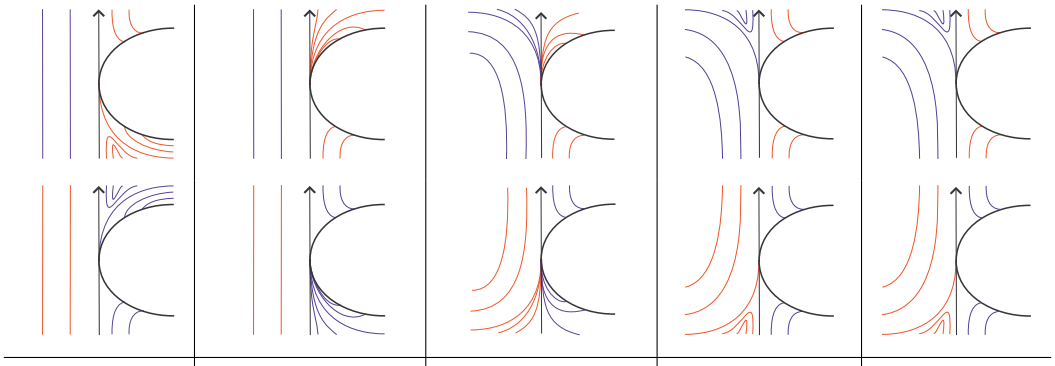

Figure 7.6: The integral curves of the vector fields Y_1 (top pictures) and Y_2 (bottom pictures) for cusp type 2 BDEs.

where P_a, P_b, P_c are smooth functions. The blown-up BDE is $(\tilde{u}, \tilde{v})^*\omega = \tilde{v}\tilde{\omega}_1$, where

$$\tilde{\omega}_1 = (\tilde{v}^2\tilde{A}, 2\tilde{v}\tilde{B}, \tilde{C}),$$

with

$$\begin{aligned}\tilde{A} &= \tilde{v}P_c \\ \tilde{B} &= (b_{11} + \tilde{v}P_b + \tilde{u}\tilde{v}P_c) \\ \tilde{C} &= (1 + 2b_{11})\tilde{u} + \tilde{v}P_a + 2\tilde{u}\tilde{v}P_b + \tilde{v}\tilde{u}^2P_c.\end{aligned}$$

We decompose $\tilde{\omega_1}$ into 1-forms, factor out a term $\tilde{v}$ and consider the vector fields

$$\tilde{Y}_i = \tilde{v}\tilde{A}\frac{\partial}{\partial\tilde{v}} + (-\tilde{B} + (-1)^i\sqrt{(\tilde{B}^2 - \tilde{A}\tilde{C})})\frac{\partial}{\partial\tilde{u}}, i = 1, 2,$$

in a neighbourhood of the exceptional fibre. At the origin, when $b_{11} < 0$, Y_1 is singular and Y_2 is regular. This is interchanged when $b_{11} > 0$.

The singular vector field is

$$\tilde{Y}_j = \tilde{v}\tilde{A}\frac{\partial}{\partial\tilde{v}} + (-\frac{\tilde{A}\tilde{C}}{2\tilde{B}} + \tilde{A}^2g(u, v))\frac{\partial}{\partial\tilde{u}},$$

where $j = 1$ if $b_{11} < 0$, $j = 2$ if $b_{11} > 0$, and $g(u, v)$ is the germ of some smooth function with zero 1-jet at the origin. This is singular on the set $\tilde{A}(\tilde{u}, \tilde{v}) = 0$ which (since $c_{20} \neq 0$) is generally a smooth curve. At the origin

$$j^1(\tilde{Y}_j/\tilde{A}) = \tilde{v}\frac{\partial}{\partial\tilde{v}} - \frac{((1 + 2b_{11})\tilde{u} - a_{22}\tilde{v})}{2b_{11}}\frac{\partial}{\partial\tilde{u}}.$$

Hence the type of singularity is as shown in Table 7.3.

b_{11}	$\tilde{Y}_1$	$\tilde{Y}_2$
$(-\infty, -1/2)$	Saddle	Regular
$(-1/2, 0)$	Node	Regular
$(0, \infty)$	Regular	Saddle

Table 7.3: Singularities of the vector fields $\tilde{Y}_1$ and $\tilde{Y}_2$ for cusp type 2 BDEs.

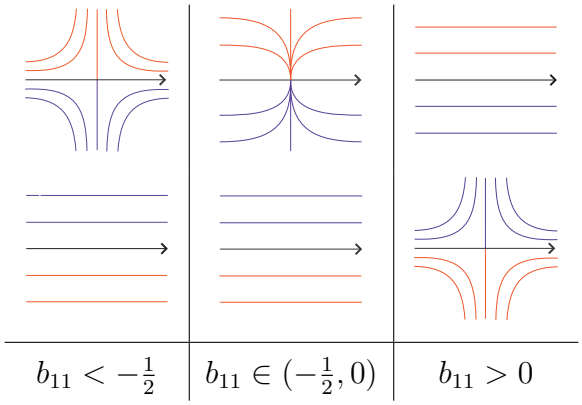

Figure 7.7: The integral curves of the vector fields $\tilde{Y}_1$ (top pictures) and $\tilde{Y}_2$ (bottom pictures) for cusp type 2 BDEs.

The y-direction blowing-up is is orientation preserving when $\tilde{v} > 0$ and orientation reversing when $\tilde{v} < 0$, and we have divided by a factor of $\tilde{v}^2$. Hence the integral curves of the vector field Y_i are the blowings-up of $\mathcal{F}_i$ when $\tilde{v} > 0$ and the blowings-up of $\mathcal{F}_{3-i}$ when $\tilde{v} < 0$. The integral curves of $\tilde{Y}_1$ and $\tilde{Y}_2$ in a neighbourhood of the exceptional fibre $\tilde{v} = 0$ are shown in Figure 7.7.

(c) Blowing-down.

We combine the x-direction and y-direction blowings-up into a polar blowing-up, and blow down. The full polar blowing-ups are shown in Figure 7.8 (upper pictures) and the integral curves are shown in Figure 7.8 (lower pictures).

(d) The equivalence homeomorphism.

The next step is to show that any two BDEs with these configurations are topologically equivalent. We give a proof in the case $b_{11} \in (-3/2, -3/4)$, the other cases follow by a similar method.

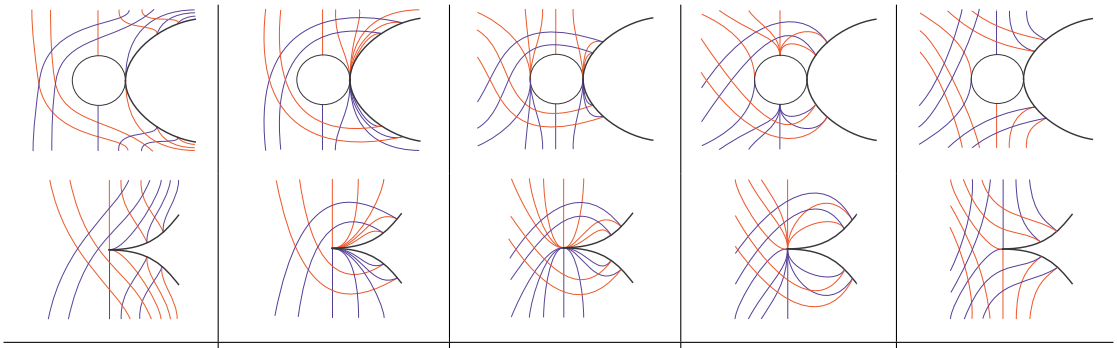

Figure 7.8: Polar blowing-up (top) and integral curves (bottom) of cusp type 2 BDEs.

We construct a homeomorphism as follows. Choose a neighbourhood U of the singularity of any BDE ω of cusp type 2 with $b_{11} \in (-3/2, -3/4)$ as shown in Figure 7.9, where all of the lines shown are integral curves, other than the discriminant, which is the thick black cusp AOE, and the thin black line segments AB and DE, which are everywhere transverse to both foliations. Note that it is always possible to choose them thus: if we choose a region containing B disjoint from the discriminant then the foliations are everywhere transverse to one another, so can be modelled by verticle and horizontal lines, and we can clearly construct a curve transverse to both segments. At A the unique solution direction is not tangent to the discriminant, so we can choose a direction that lies between the solution direction and the tangent to the discriminant, which by continuity is transverse to the solution curves nearby. We choose a similar neighbourhood U' of the singularity of any other BDE ω' of cusp type 2 with $b_{11} \in (-3/2, -3/4)$, with corresponding vertices on the boundary $O', A', B', C', D', E', F', G'$.

We give the boundary ∂U of U a positive orientation, and let

$$h : CDE \to C'D'E'$$

be any increasing homeomorphism of the section CDE of ∂U, sending vertices to vertices. It is clear that such a homeomorphism exists, since CDE is homeomorphic to any compact subset of the real line.

We divide U into 5 regions for the purposes of constructing the homeomorphism:

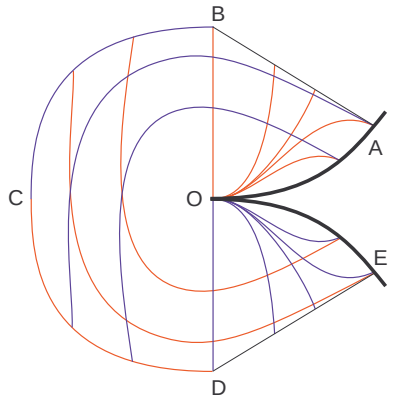

Figure 7.9: The neighbourhood U of the singularity.

R1: The region bounded by the segment of the discriminant OA and the red solution curve through A.

R2: The region bounded by the red solution curve through A and the segment of the separatrix OB.

R3: The region between the segments of the separatrices OB and OD.

R4: The region bounded by the blue solution curve through E and the segment of the separatrix OD.

R5: The region bounded by the segment of the discriminant OE and the blue solution curve through E.

We define similar regions R1′-R5′ in U'.

Choose a point $p \in$ R1. Slide along the red curve until it reaches the discriminant, then along the blue curve meeting the discriminant at that point until it reaches a point p_1 on the section of $CD \subset \partial U$. Now return to the original point p, and slide along the blue curve until it reaches a point p_2 on CD. Note that $p_2 \geq p_1$, with equality if and only if p lies on the discriminant, and that the pair (p_1, p_2) is different for each distinct $p \in$ R1. Now apply h, noting that $h(p_2) \geq h(p_1)$, and reverse the above process, sliding along the integral curves of ω to determine a point $p' \in$ R1′. We define H :R1$\rightarrow$ R1′ by $H(p) = p'$.

For a point $q \in$ R2 we determine the unique pair $(q_1, q_2) \in DE \subset \partial U$ by sliding along the red curve through q onto the segment AB, and from there along the blue curve to determine q_1, and sliding along the blue curve through q to determine q_1.

We then apply h and reverse the sliding process to determine q', and extend H to R2 by defining $H(q) = q'$. The homeomorphism extends to R4 and R5 in a similar way, by associating to each point a unique pair of points on BC.

In R3 we associate to each point r a pair (r_1, r_2) where r_1 lies on BC and is obtained by sliding along the red curve, and r_2 lies on CD and is obtained by sliding along the blue curve.

It can easily be checked that H is well defined on the boundary curves of the sectors, and is a homeomorphism taking the integral curves of the BDE ω to those of ω'.

(e) Normal forms.

We now have that the topological type depends only on the value of b_{11} (and on $c_{20} \neq 0$). We obtain the topological normal forms given in the statement of the Theorem by setting $c_{20} = 1$, choosing a value of b_{11} in each of the open regions determined by the values in the set $\{-3/2, -3/4, -1/2, 0\}$, and setting all other terms equal to zero. □

We consider now the exceptional values of b_{11} (note that when $b_{11} = -1/2$ the BDE is not of cusp type 2 and when $b_{11} = 0$ the discriminant has singularity worse than A_2). These BDEs have codimension ≥ 4.

Theorem 7.2.5 *A cusp type 2 BDE with codimension 4 is locally topologically equivalent to one of the following normal forms.*

$$(i) \quad (x, -\frac{3}{2}y + x^2, x^2) \quad \textit{Figure 7.10, left,}$$
$$(ii) \quad (x, -\frac{3}{4}y, x^2) \quad \textit{Figure 7.10, right,}$$

The topological type is determined by the 2-jets of the coefficients of the BDE.

Proof: We follow the notation of the proof of Theorem 7.2.4.

When $b_{11} = -3/2$, the vector fields $\bar{Y_1}$ and $\bar{Y_2}$ are both singular at the intersection of the exceptional fibre $t = 0$ and the blown-up discriminant. Following the method used in [64, 66], we change variables and set $w = t, z^2 = \bar{\delta}$, and restrict our attention to the region $z > 0$. Then

$$(w, z)^* \bar{Y_1} = \frac{9}{2c_{20}}(\frac{z}{2} + \frac{(c_{21} + 12b_{20})w}{8c_{20}} + h.o.t.)\frac{\partial}{\partial w} + (\frac{wz}{2c_{20}} + h.o.t.)\frac{\partial}{\partial z},$$

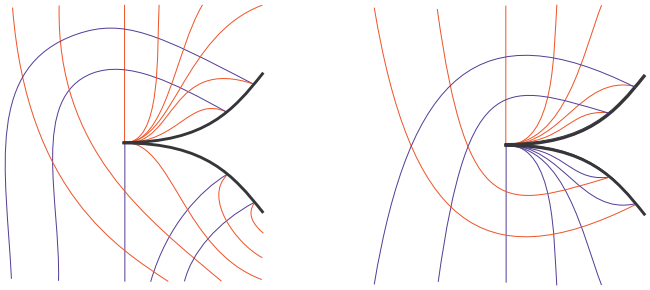

Figure 7.10: The integral curves of cusp type 2 BDEs with codimension 4.

which has a saddle-node at $w = 0, z = 0$ provided $c_{21} + 12b_{20} \neq 0$. The centre manifold is transverse to the exceptional fibre. The integral curves of $(w, z)^*\bar{Y}_2$ may be obtained from those of $(w, z)^*\bar{Y}_1$ via the change of variables $z \mapsto -z$. The integral curves of $(w, z)^*\bar{Y}_1$ and $(w, z)^*\bar{Y}_2$ are shown in Figure 7.11 (the solid parts are the the curves that are of interest).

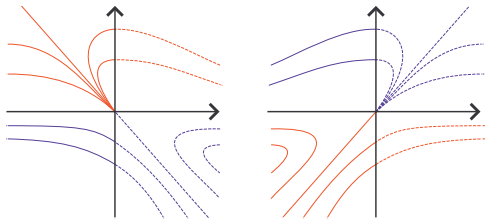

Figure 7.11: The integral curves of $(w, z)^*\bar{Y}_1$ (left) and $(w, z)^*\bar{Y}_2$ (right).

When $b_{11} = -3/4$, at $(s, t) = (0, 0)$ the vector field $\bar{Y}_1$ has a saddle-node singularity equivalent to

$$t\frac{\partial}{\partial t} + s^2\frac{\partial}{\partial s}$$

and $\bar{Y}_2$ has a saddle. Both $\bar{Y}_1$ and $\bar{Y}_2$ are regular elsewhere on $t = 0$. The integral curves of $\bar{Y}_1$ and $\bar{Y}_2$ are illustrated in Figure 7.12.

Blowing down gives the integral curves of Y_1 and Y_2. These are illustrated in Figure 7.13.

The blowing-up in the y-direction yields the same configuration of the integral curves of $\tilde{Y}_1$ and $\tilde{Y}_2$ as in the proof of Theorem 7.4 when $b_{11} < -1/2$, that is, as shown in Figure 7.7 (left). We combine the directional blowings-up into a polar blowing-up, and blow down to obtain the configuration. This is illustrated in Figure 7.14. □

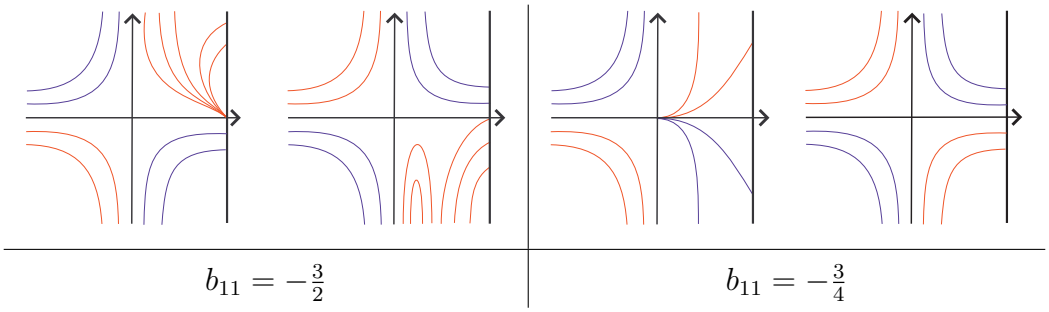

Figure 7.12: The integral curves of the vector fields $\bar{Y}_1$ and $\bar{Y}_2$ for cusp type 2 BDEs with codimension 4.

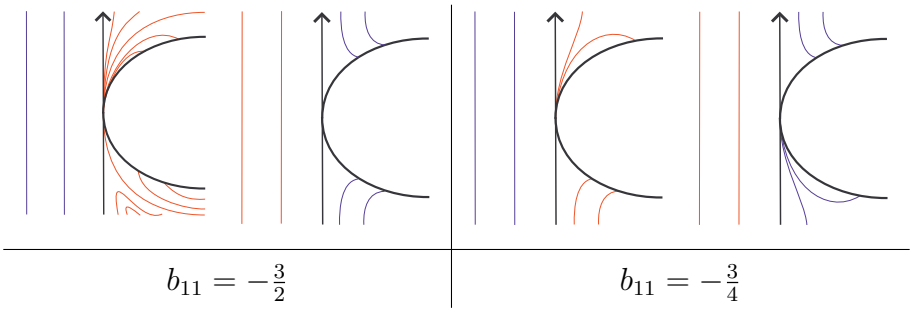

Figure 7.13: The integral curves of the vector fields Y_1 and Y_2 for cusp type 2 BDEs with codimension 4.

Remarks 7.2.6 *1. One may construct homeomorphisms using the method of* [13] *to show that the integral curves of a cusp type 2 BDE when* b_{11} *takes any value in* $(-\infty, -3/2)$ *are topologically equivalent to those when* b_{11} *takes any value in* $(0, \infty)$*, and that those when* b_{11} *takes any value in* $(-3/2, -1/2)$ *are topologically equivalent to those when* b_{11} *takes any value in* $(-1/2, 0)$*. No topological change occurs at* $b_{11} = -3/4$*. These topologically equivalent cases, however, may have topologically different deformations in generic families, as there are qualitative differences evident in their blowings-up.*

2. Furthermore, the integral curves of cusp type 2 BDEs are topologically equivalent to those of a BDE with a folded singularity (see [30]*): a folded saddle when* $b_{11} \in (-\infty, -3/2) \cup (0, \infty)$ *and a folded node when* $b_{11} \in (-3/2, 0) \setminus \{-1/2, 0\}$*. When* $b_{11} = -3/2$*, the lowest codimension case (Theorem 7.2.5 (i)) is topologically equivalent to a folded saddle-node.*

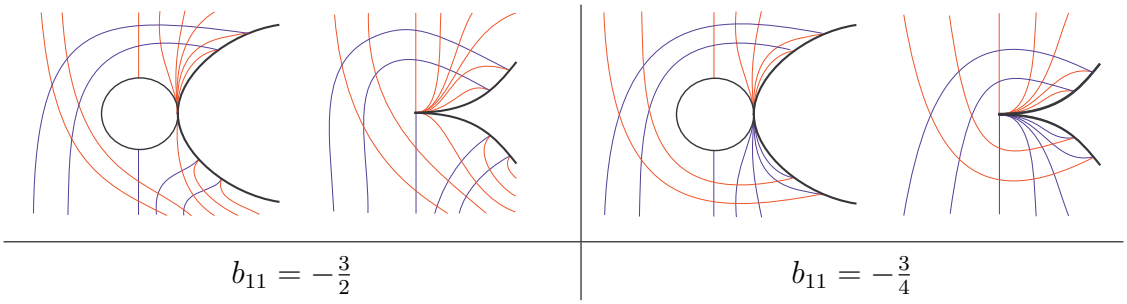

Figure 7.14: Polar blowing-up and integral curves of cusp type 2 BDEs with codimension 4.

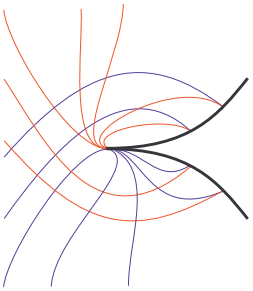

Figure 7.15: The integral curves of a cusp type 3 BDE.

7.2.3 Cusp type 3 BDEs

Theorem 7.2.7 *A BDE of cusp type 3 is topologically equivalent to*

$$(x+y)dy^2 - \frac{1}{2}ydxdy + x^2dx^2 = 0.$$

The topological type is determined by the 2-jet of the coefficients of the BDE. The configuration of the integral curves are as shown in Figure 7.15.

Proof: We use the notation of the proof of Theorem 7.2.4. In the second blowing-up, the vector fields $\bar{Y}_i$ are regular at all points on the exceptional fibre except for the point $s = 0, t = 0$ (the intersection of the two exceptional fibres). Here the vector field $\bar{Y}_2$ has a saddle singularity, and the vector field $\bar{Y}_1$ has a saddle-node singularity equivalent to

$$t^2\frac{\partial}{\partial t} - s\frac{\partial}{\partial s}.$$

These are illustrated in Figure 7.16. Blowing-down gives the integral curves of Y_1 and Y_2. These are illustrated in Figure 7.17. The y-direction blowing-up yields no singularities at the origin. Blowing down a second time we obtain the configuration in Figure 7.15. □

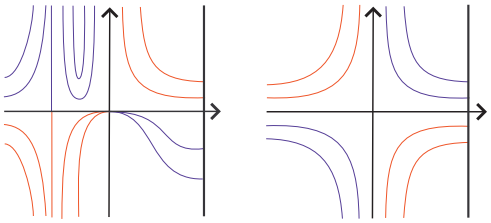

Figure 7.16: The integral curves of $\bar{Y}_1$ (left) and $\bar{Y}_2$ (right) for a cusp type 3 BDE.

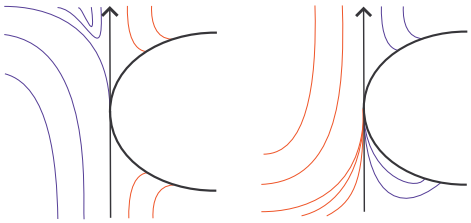

Figure 7.17: The integral curves of Y_1 (left) and Y_2 (right) for a cusp type 3 BDE.

7.3 Configurations of the separatrices

Blowing-up allows us to highlight further differences between the various types of cusp BDE. The observations below are immediate from the proofs of Theorem 7.2.2, Theorem 7.2.4 and Theorem 7.2.7, and we do not include proofs.

Recall Definition 1.3.2. The separatrix curves do not always separate distinct sectors, and there may be curves that do so which are not separatrices in the sense of Definition 1.3.2.

Proposition 7.3.1 *Let l be the limiting tangent line to the discriminant at the origin. A cusp type m BDE of lowest codimension has one or three separatrices, all transverse to l ($m = 1$); one separatrix transverse to l, and a cuspidal separatrix with limiting tangent line l ($m = 2$); one cuspidal separatrix with limiting tangent line l ($m = 3$). See Figure 7.18.*

The separatrices also highlight differences between those cusp type 2 BDEs that are topologically equivalent despite having different blowings-up (see Remark 7.2.6). In particular the cuspidal separatrix points in the same direction as the discriminant when $b_{11} < -3/4$ and in the opposite direction when $b_{11} > -3/4$. When $b_{11} = -3/4$ there is no cuspidal separatrix, although this case is topologically equivalent to those when $b_{11} \in (-3/2, -3/4) \cup (-3/4, -1/2) \cup (-1/2, 0)$ (the cuspidal separatrix does

not separate distinct sectors for such values of b_{11}).

Further differences are observed when one considers the foliation to which each separatrix belongs (see Figure 7.18).

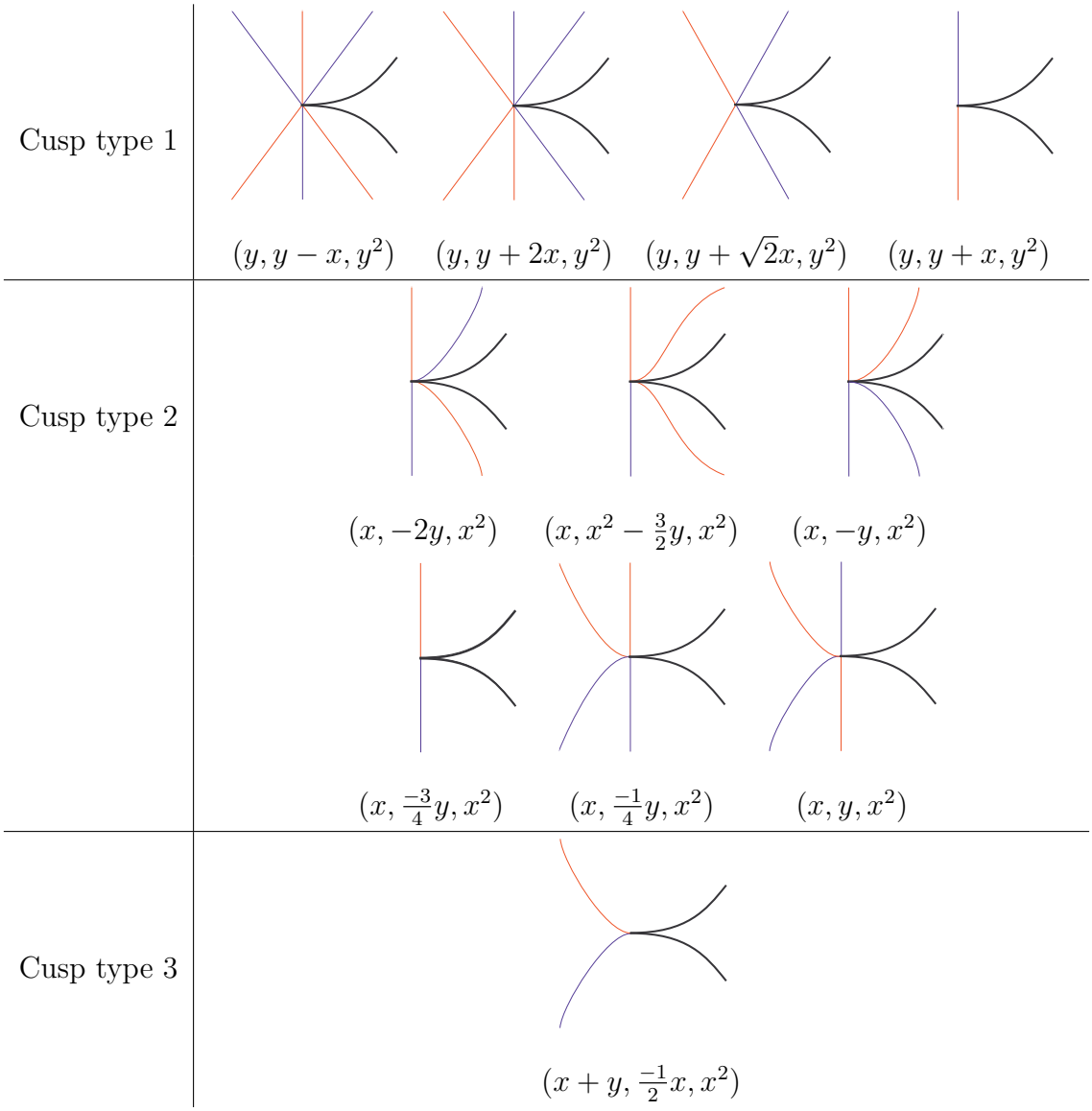

Figure 7.18: The separatrices of cusp BDEs.

7.4 Degenerate cusp BDEs

We consider now the degenerate case where the lifted field ϕ vanishes at all points of the exceptional fibre. Such BDEs have codimension ≥ 5. We establish the topological configurations of the integral curves in the least degenerate case. The

proof for Theorem 7.4.1 employs the same blowing-ups as those used in Theorem 7.2.4.

Theorem 7.4.1 *A cusp BDE with linear part equivalent to* $(x, -y/2, 0)$ *and with codimension 5 is topologically equivalent to*

$$(x + y^2, -\frac{1}{2}y, x^2).$$

The configuration of the integral curves of such BDEs are as shown in Figure 7.19.

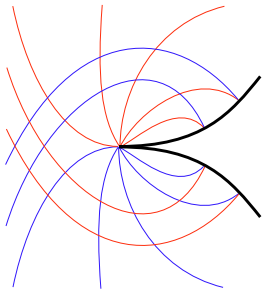

Figure 7.19: The integral curves of a cusp BDE equivalent to $(x + y^2, -y/2, x^2)$.

Proof: Consider the first x-direction and y-direction blowing-ups. In the notation of the proof of Theorem 7.2.4, the vector fields Y_i, $\tilde{Y}_i$, $i = 1, 2$ are singular along the whole of the exceptional fibre. We may, however, write $Y_i(u, v) = uZ_i(u, v)$, and $\tilde{Y}_i(\tilde{u}, \tilde{v}) = \tilde{v}\tilde{Z}_i(\tilde{u}, \tilde{v})$ for some smooth vector fields Z_i, $\tilde{Z}_i$, $i = 1, 2$. Away from the exceptional fibre the integral curves of Y_i (respectively $\tilde{Y}_i$) are the same as those of Z_i (respectively $\tilde{Z}_i$).

We consider a second blowing-up. The integral curves of $\bar{Y}_1$ and $\bar{Y}_2$ are illustrated in Figure 7.20. Blowing down gives the integral curves of Y_1 and Y_2. These are

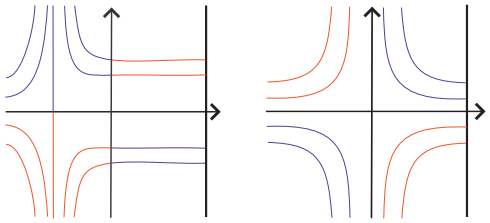

Figure 7.20: The integral curves of the vector fields $\bar{Y}_1$ (left) and $\bar{Y}_2$ (right) for degenerate cusp BDEs.

illustrated in Figure 7.21 (left). The integral curves obtained by the y-direction blowing-up are shown in Figure 7.21 (right).

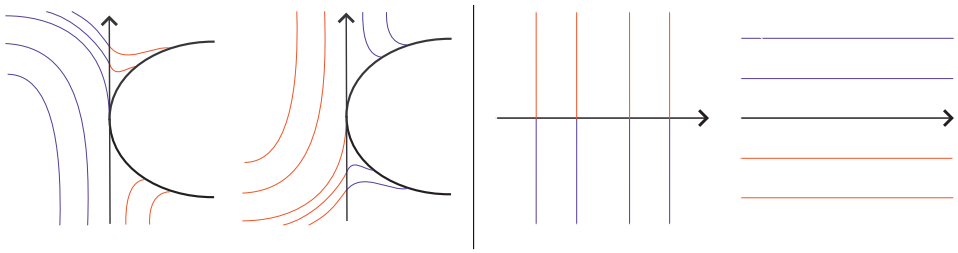

Figure 7.21: The integral curves of the vector fields Y_1 and Y_2 (left), and $\tilde{Y}_1$ and $\tilde{Y}_2$ and (right) for degenerate cusp BDEs.

We combine the x-and y-direction blowing-ups to obtain a polar blowing-up, and blow down to obtain the configuration. This is illustrated in Figure 7.22. □

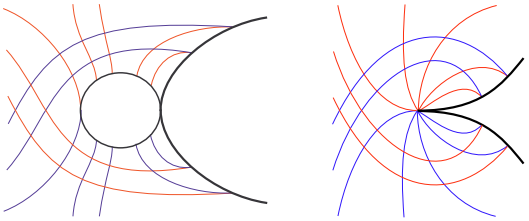

Figure 7.22: Polar blowing-up (left) and integral curves (right) of degenerate cusp BDEs.

7.5 Discriminant having a $Y^1_{1,2}$-singularity

We study BDEs with 2-jets equivalent to a $(x^2, -xy, 2y^2)$, and with the discriminant having a $Y^1_{1,2}$-singularity at the origin, (that is, a singularity that is $\mathcal{A}$-equivalent to $-x^2y^2 - x^5 - y^6$). Such BDEs arise in the study of the characteristic curves on a cross-cap (see Chapter 8).

Theorem 7.5.1 *A BDE with 2-jet equivalent to $(x^2, -xy, 2y^2)$ and a discriminant having a $Y^1_{1,2}$-singularity equivalent to $-x^2y^2 - x^5 - y^6$ then it is topologically equivalent to*

$$x^2dy^2 + 2(-xy - y^3)dxdy + (2y^2 - x^3)dx^2 = 0.$$

See Figure 7.23.

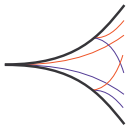

Figure 7.23: The integral curves of a $Y^1_{1,2}$-BDE.

Proof: We write $\omega = (a, b, c) = (x^2 + Q_a(x, y), -xy + Q_b(x, y), 2y^2 + Q_c(x, y))$, where Q_a, Q_b, Q_c are smooth functions with zero 2-jets at the origin. We write

$$j^3Q_a = a_{30}x^3 + a_{31}x^2y + a_{32}y^2x + a_{33}y^3,$$
$$j^3Q_b = b_{30}x^3 + b_{31}x^2y + b_{32}y^2x + b_{33}y^3,$$
$$j^3Q_c = c_{30}x^3 + c_{31}x^2y + c_{32}y^2x + c_{33}y^3,$$

The discriminant is $\delta = b^2 - ac$, which has a $Y^1_{1,2}$-singularity at the origin if $c_{20} \neq 0$ and $b^2_{33} - c_{33}a_{33} \neq 24a_{44}$, where

$$a_{44} = \frac{\partial^4 Q_a}{\partial y^4}(0, 0).$$

The discriminant is equivalent to

$$-x^2y^2 + sign(c_0)x^5 + sign(b^2_{33} - c_{33}a_{33} - a_{44})y^6.$$

We consider only the case $b^2_{33} - c_{33}a_{33} - 24a_{44} < 0$, and $c_{20} < 0$ (the case $c_{20} > 0$ gives topologically equivalent integral curves, up to a reflection in the y-axis).

The vector fields Y_1 an Y_2 studied in the first x-direction blowing-up are singular only at the origin, however they are not smooth there. After a second blowing-up, the discriminant is transverse to the exceptional fibre $t = 0$ at $s = -1/c_0$. The integral curves meet the discriminant transversally. The vector fields are both singular at $t = 0, s = 0$, but no integral curves exist in a neighbourhood of this point. The vector field $\bar{Y}_1$ has a saddle at $t = 0, s = -5/(4c_0)$ (see Figure 7.24.)

A first blowing-down gives the integral curves of the vector fields Y_1 and Y_2. These are shown in Figure 7.25 (left and centre).

A y-direction blowing-up is considered, but yields no extra information since there are no integral curves in a neighbourhood of the origin.

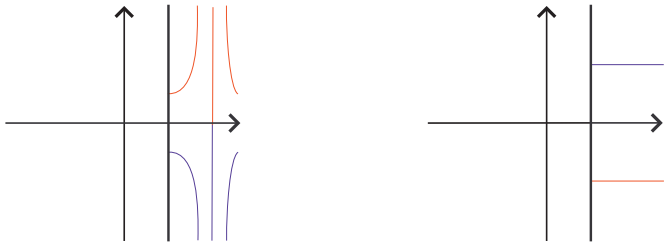

Figure 7.24: The integral curves of $\bar{Y}_1$, left and $\bar{Y}_2$, right for a $Y^1_{1,2}$-BDE.

The second blowing-down gives the configuration of the integral curves of the original BDE. These are shown in Figure 7.25 (right).

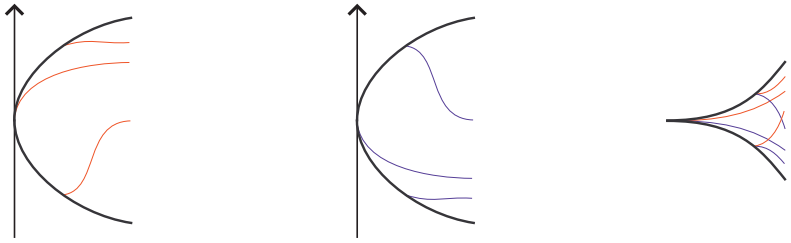

Figure 7.25: The integral curves of Y_1 (left) and Y_2 (centre), and the configuration at the singularity (right) for a $Y^1_{1,2}$-BDE.

□

Chapter 8

Pairs of foliations on a parabolic cross-cap

We turn our attention now to singular surfaces in $\mathbb{R}^3$. Given a surface patch parametrised by

$$\mathbf{r} : U \subset \mathbb{R}^2 \to \mathbb{R}^3,$$

Whitney ([75]) showed that $\mathbf{r}$ may have a singularity, known as a *cross-cap*, that is stable under smooth changes of coordinates in the source and target. As a cross-cap is a stable singular surface in $\mathbb{R}^3$ it is natural to seek understand its differential geometry.

The topological configurations of the asymptotic curves in the domain of a parametrisation of a hyperbolic cross-cap are established in [74], and the topological configurations of the asymptotic curves, characteristic curves and the lines of curvature on hyperbolic and elliptic cross-caps, in the domain and on the surface, are established in [64]. In this chapter we establish the configurations of the asymptotic and characteristic curves on a parabolic cross-cap.

The lines of curvature on a singular surface with a cross-cap singularity are studied in [64]. In the general the topological configurations of the lines of curvature on a cross-cap is independent of whether the cross-cap in hyperbolic, parabolic or elliptic, as the parameter ν in the parametrisation of the cross-cap (8.1.1) does not affect the topological normal form of the BDE of the principal directions so these curves are not considered in this chapter.

The results of this chapter and of Chapter 9 will appear in [55].

8.1 The cross-cap

It is shown in [75] that if

$$g : \mathbb{R}^2, 0 \to \mathbb{R}^3, 0$$

is a germ of a smooth mapping, then g has a local $\mathcal{A}$-stable singularity if and only if it is $\mathcal{A}$-equivalent to $f(x, y) = (x, xy, y^2)$.

Definition 8.1.1 *A* cross-cap *is the image of any map-germ*

$$\mathbf{r} : \mathbb{R}^2, 0 \to \mathbb{R}^3, 0$$

that is $\mathcal{A}$-equivalent to (x, xy, y^2).

As a cross-cap is a stable singular surface in $\mathbb{R}^3$, it is natural to seek to understand its differential geometry.

Cross-caps play a significant role in the study of other geometrical objects. For example, any immersion of the projective plane in $\mathbb{R}^3$ must have a cross-cap. The geometry of cross-caps also turns out to be significant in the study of the projections of smooth surfaces in $\mathbb{R}^4$ to 3-spaces (see [50]).

The differential geometry of the surface is preserved by isometries of $\mathbb{R}^3$ and enlargements of $\mathbb{R}^3$ of the form $(X, Y, Z) \mapsto t(X, Y, Z)$, so we must restrict ourselves to such changes of coordinates in the target. The parametrisation of a cross-cap in Proposition 8.1.1 is given in [74], we include here an outline of the proof.

Proposition 8.1.1 ([74]) *Any germ of a map $\mathcal{A}$-equivalent to f can be transformed by smooth changes of coordinates in the source and isometries and enlargements of the target to*

$$\mathbf{r}(x, y) = (x, xy + p(y), \nu x^2 + \mu xy + y^2 + q(x, y)), \tag{8.1}$$

where $p(y)$ and $q(x, y)$ are germs, at the origin, of functions with $j^2p = j^2q = 0$, and ν, μ are constants.

Proof: Let

$$\begin{aligned} g: \ \mathbb{R}^2,0 &\to \mathbb{R}^3,0 \\ (x,y) &\mapsto (g_1(x,y),g_2(x,y),g_3(x,y)). \end{aligned}$$

be a germ that is $\mathcal{A}$-equivalent to f. Then, by a rotation in the target if necessary, we may assume $j^1g_2 = j^1g_3 = 0$, as the Jacobian of g has rank one at the origin. We may then, by a diffeomorphism in the source if necessary, assume $g_1 = x$.

By a further rotation in the target and a linear change of coordinates in the source we may write

$$g(x,y) = (x, xy + p_1(x,y), d_1x^2 + d_2xy + d_3y^2 + q_1(x,y)),$$

where $d_1, d_2, d_3 \in \mathbb{R}$ and $j^2p_1 = j^2q_1 = 0$.

Any germ of the form $(x,y) \mapsto (x, xy + r_1(x,y))$ with $j^2r_1 = 0$ may be reduced to the form $(x,y) \mapsto (x, xy + r_2(y))$ where $j^2r_2 = 0$ by a smooth change of coordinates in the source (this result is given in [74] and is proved using tools from singularity theory). This is used to reduce the parametrisation of the cross-cap to the form

$$g(x,y) = (x, xy + p_2(y), d_1x^2 + d_2xy + d_3y^2 + q_2(x,y)).$$

The proof is completed by scaling the coordinates in the source and in the target. □

We will write

$$\begin{aligned} j^4p(y) = &\ p_3y^3 + p_4y^4, \\ j^3q(x,y) = &\ q_{30}x^3 + q_{31}x^2y + q_{32}xy^2 + q_{33}y^3. \end{aligned} \tag{8.2}$$

For a singular surface with a cross-cap singularity there is no well-defined unit normal to the surface at the cross-cap point as $||\mathbf{r}_x \times \mathbf{r}_y|| = 0$, so the coefficients of the second fundamental form are not defined. However the surface is smooth other than at the cross-cap, and the BDEs of the asymptotic and characteristic curves, lines of curvature and the families $\mathcal{C}_\alpha$ and $\mathcal{R}_\alpha$ are homogeneous in l, m, n, so we can multiply their coefficients by an appropriate power of $||\mathbf{r}_x \times \mathbf{r}_y||$, or equivalently replace l, m and n in each equation by

$$l_1 = \mathbf{r}_{xx} \cdot (\mathbf{r}_x \times \mathbf{r}_y), m_1 = \mathbf{r}_{xy} \cdot (\mathbf{r}_x \times \mathbf{r}_y), n_1 = \mathbf{r}_{yy} \cdot (\mathbf{r}_x \times \mathbf{r}_y).$$

Thus for a cross-cap we take the asymptotic BDE to be

$$n_1 dy^2 + 2m_1 dxdy + l_1 dx^2 = 0. \tag{8.3}$$

We take the characteristic BDE to be

$$\begin{aligned}(2m_1(Gm_1 - Fn_1) - n_1(Gl_1 - En_1))dy^2 \\ +2(m_1(Gl_1 + En_1) - 2Fl_1n_1)dxdy \\ +(l_1(Gl_1 - En_1) - 2m_1(Fl_1 - Em_1))dx^2 = 0.\end{aligned} \tag{8.4}$$

We take the principal BDE to be

$$(Gm_1 - Fn_1)dy^2 + (Gl_1 - En_1)dxdy + (Fl_1 - Em_1)dx^2 = 0. \tag{8.5}$$

The parabolic set is given by $m_1^2 - n_1 l_1 = 0$. If $\nu \neq 0$ in (8.1) then the parabolic set has a Morse singularity at the origin: A_1^+ if $\nu < 0$, in which case we have a hyperbolic cross-cap, and A_1^- if $\nu > 0$, in which case we have an elliptic cross-cap. If $\nu = 0$ the parabolic set has a more degenerate singularity. If $q_{30} \neq 0$, the parabolic set has an A_2-singularity (a cusp), and we label the surface a parabolic cross-cap. We take, without loss of generality, $q_{30} > 0$.

Remark 8.1.2 *If affine changes of coordinates in the target are permitted, we can simplify the parametrisation given in Proposition 8.1.1 to*

$$\mathbf{r}(x, y) = (x, xy + p(y), \epsilon x^2 + y^2 + q(x, y)), \tag{8.6}$$

where $\epsilon = 1, 0, -1$ for respectively elliptic, parabolic and hyperbolic cross-caps.

8.2 The asymptotic curves and the characteristic curves on a parabolic cross-cap

Establishing the configurations on the parabolic cross-cap of the asymptotic and characteristic curves is done in two stages. Firstly we establish the configurations in the domain by studying the appropriate BDE. Secondly we map the foliation to the surface. This is trivial for smooth surfaces, as the parametrisation is a diffeomorphism from the domain to the image. In the case of a cross-cap, however, we must analyse how the leaves of the foliations in the domain intersect the double point curve.

8.2.1 Configurations of the asymptotic curves

In [64] it is shown that there are two generically occurring topological configurations of the asymptotic curves in the domain of an elliptic cross-cap. The asymptotic BDE is topologically equivalent to

$$xdy^2 + 2(-y + x^2)dxdy + xdx^2 = 0$$

or to

$$xdy^2 + 2(-y + xy)dxdy + xdx^2 = 0.$$

In Figure 8.1 these are labelled case 1 and case 2 respectively.

It is shown in ([74]) that there is one topological configuration for hyperbolic cross-caps, and the BDE is topologically equivalent to

$$xdy^2 + 2ydxdy - xdx^2 = 0.$$

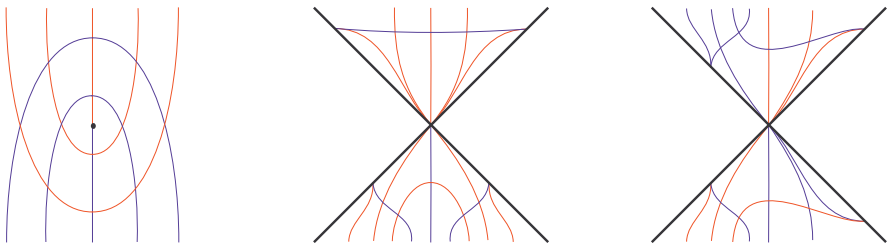

Figure 8.1: Configuration of the asymptotic curves in the domain of the parametrisation of a hyperbolic cross-cap (left), and an elliptic cross-cap, case 1 (centre), case 2 (right).

We adopt the parametrisation of a cross-cap given in Remark 8.1.2.

Proposition 8.2.1 *The asymptotic BDE in the domain of a parametrisation of a parabolic cross-cap is topologically equivalent to*

$$xdy^2 - 2ydxdy + x^2dy^2 = 0.$$

The topological type is completely determined by the 3*-jet of the parametrisation of the surface. See Figure 8.2.*

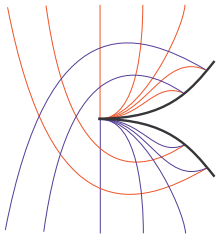

Figure 8.2: Configurations in the domain of the asymptotic curves at a parabolic cross-cap.

Proof: At a parabolic cross-cap we parametrise the surface as in (8.1.2) with $\epsilon = 0$. We calculate the coefficients of the second fundamental form. The coefficients of the asymptotic BDE may be written as

$$(x + H_1(x, y), -y + H_2(x, y), H_3(x, y))$$

where H_i, $(i = 1, 2, 3)$ are smooth functions, with

$$\begin{aligned} j^2 H_1 &= q_{32}x^2 + 3q_{33}xy - 3p_3y^2, \\ j^2 H_2 &= q_{31}x^2 - 3q_{33}y^2, \\ j^2 H_3 &= 3q_{30}x^2 + 3q_{31}xy. \end{aligned}$$

Since $q_{30} \neq 0$ we may apply Theorem 7.2.4 to establish the result. □

We seek now the configuration of the curves on the surface. If the cross-cap is parametrised as in (8.1), then the 3-jet at the origin of the double-point curve is

$$(-p_3y^2 - p_3(-\mu p_3 + q_{33})y^3, y).$$

If (x_1, y_1) and (x_2, y_2) are two points on the double-point curve with the same image under $\mathbf{r}$, then

$$y_2 = -y_1 - q_{30}y_1^2 + O(y_1^3). \tag{8.7}$$

The double-point curve is transverse to the limiting tangent to the parabolic set at the origin, and has a non-empty intersection with the hyperbolic region in a neighbourhood of the cross-cap. Thus we must take it into account when mapping the asymptotic curves to the surface.

In the case of the asymptotic curves we may take $\mu = 0$, so the 3-jet of the double-point curve is

$$(-p_3y^2 - p_3q_{33}y^3, y).$$

There is a single separatrix transverse to the limiting tangent to the parabolic set at the origin. The 3-jet at the origin of a parametrisation of this separatrix is

$$(-p_3y^2 - \frac{(3q_{33}p_3 - 8p_4)}{5}y^3, y).$$

Thus this separatrix and the double point curve have generically 3-point contact at the origin. The image of this separatrix under $\mathbf{r}$ has a cusp at the cross-cap point.

As shown in Figure 8.3, the double point curve (in dashed lines), in a neighbourhood of the origin, intersects one foliation only once, but intersects the other twice (which foliation depends on the sign of $p_4 - p_3q_{33}$). We need to establish whether or not these two intersection points map to the same point on the surface.

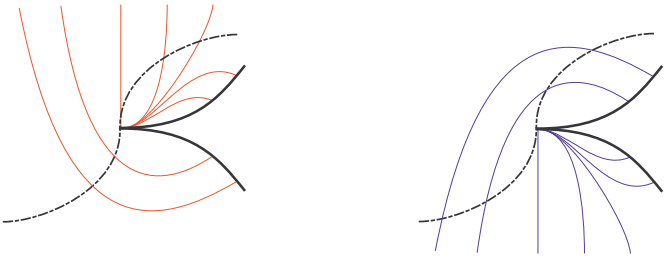

Figure 8.3: Configurations of the asymptotic curves with the double-point curve (shown in dashed lines).

There are two involutions on the double point curve: τ, which interchanges points of intersection of the double-point curve with a particular asymptotic curve, and σ, which interchanges points with the same image under $\mathbf{r}$.

Theorem 8.2.1 *For a generic parabolic cross-cap, $\tau(\beta) \neq \sigma(\beta)$ for any point β with $\beta \neq (0,0)$ on the double point curve in a neighbourhood of the origin. As a consequence, the configuration of the asymptotic curves on a parabolic cross-cap is as shown in Figure 8.4.*

Proof: We label the red and blue foliations $\mathcal{F}_1$ and $\mathcal{F}_2$ respectively. Without loss of generality we take $p_4 - p_3q_{33} > 0$. In a neighbourhood of the origin, each leaf of $\mathcal{F}_2$ intersects the double point curve twice. The case $p_4 - p_3q_{33} < 0$ follows by a similar argument on $\mathcal{F}_1$. The separatrix transverse to the limiting tangent to the parabolic set at the origin is given locally by the graph of a function $x = l(y)$,

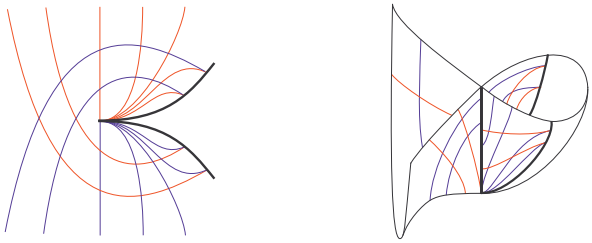

Figure 8.4: The asymptotic curves on a parabolic cross-cap.

where

$$j^3 l = -p_3 y^2 - \frac{(3q_{33}p_3 - 8p_4)}{5} y^3.$$

We make changes of coordinates $x = X + l(Y), y = Y$, so this separatrix is along the Y-axis, the separatrix being a curve of $\mathcal{F}_2$. The asymptotic BDE in this new system of coordinates is in the form

$$A(X,Y)dY^2 + 2B(X,Y)dXdY + C(X,Y)dx^2 = 0, \tag{8.8}$$

where

$$A(X,Y) = a(X + l(Y), Y) + 2b(X + l(Y), Y)l'(Y) + c(X + l(Y), Y)l'(Y)^2$$
$$B(X,Y) = b(X + l(Y), Y) + b(X + l(Y), Y)l'(Y)$$
$$C(X,Y) = c(X + l(Y), Y).$$

In the (X,Y) plane, the horizontal direction is a solution of the BDE (8.8) when $C(X,Y) = 0$. We have

$$j^2 C(X,Y) = 3q_{30}X^2 + q_{31}XY,$$

so if $q_{31} \neq 0$ this set has an A_1^--singularity at the origin, that is, it has two transversally intersecting branches. One branch is tangent to the Y-axis and the other to the line

$$3q_{30}X + q_{31}Y = 0.$$

We label these branches $\mathcal{C}_1$ and $\mathcal{C}_2$ respectively. A calculation shows that $\mathcal{C}_1$ is given by

$$X = p_3 Y^2 + h.o.t.$$

Further calculations show that in the region $Y > 0$, $\mathcal{C}_1$ and $\mathcal{C}_2$ are the loci of turning points of leaves of $\mathcal{F}_2$, and that if $q_{31} > 0$, $\mathcal{C}_1$ is the locus of local minima and $\mathcal{C}_2$ the locus of local maxima, the reverse being the case if $q_{31} < 0$.

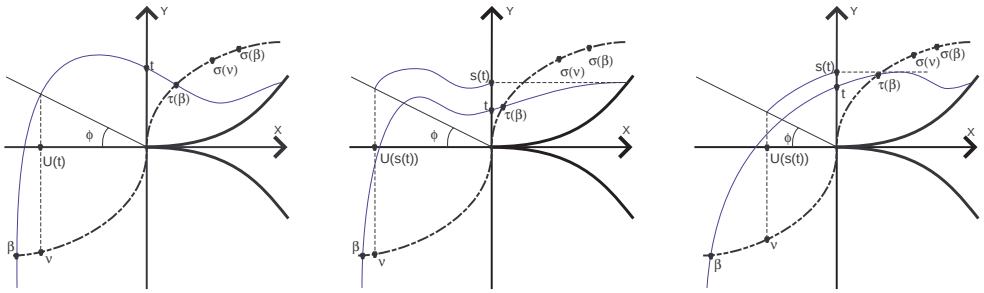

Figure 8.5: Involutions on the double point curve: (l-r) cases 1,2 and 3.

The vertical direction is a solution to the BDE if $A(X,Y) = 0$. This set is a smooth curve in a neighbourhood of the origin. So in such a neighbourhood, no leaf of either foliation has a vertical tangent other than the separatrix $X = 0$.

The double point curve is parametrised as $(\zeta(Y), Y)$, where $\zeta(Y)$ is a smooth function with

$$j^3\zeta = \frac{8(-q_{33}p_3 + p_4)}{5}Y^3.$$

There are three cases. If $p_3q_{31} > 0$, the turning points of the leaf of $\mathcal{F}_2$ lie on opposite sides of the double point curve. We label this case 1. If $p_3 < 0, q_{31} > 0$ (case 2), the turning points both lie on the opposite side of the double point curve from the point where leaf meets the discriminant. If $p_3 > 0, q_{31} < 0$ (case 3), both turning points lie between the discriminant and the double point curve. See Figure 8.5.

The leaves of $\mathcal{F}_2$ are tangent to

$$\xi_2 = A\frac{\partial}{\partial X} + (-B - \sqrt{B^2 - AC})\frac{\partial}{\partial Y}.$$

Choose a point on the Y-axis, $(0,t)$ where $t > 0$ is small. Denote the leaf of $\mathcal{F}_2$ through this point by γ_t. Choose a half-line h starting at the origin and making an angle ϕ with the negative X-axis. We write the intersection of h and γ_t as

$$U(t)(1, \tan\phi).$$

The polar blowing-up,

$$x = \rho\cos\theta, y = \rho\sin\theta$$

of ξ_2 yields a regular vector field η_2 for $(\theta, \rho) \in [\pi/2, \pi - \phi] \times [0, a)$, where a is a small positive real number. It follows that the map

$$k : \frac{\pi}{2} \times [0, a_1) \to (\pi - \phi) \times [0, a_2)$$

determined by the flow of η_2 is smooth and $k'(0) \neq 0$ (a_1, a_2 are appropriately chosen real numbers). Blowing down we have $U(t) = k(t)$, that is, that $U(t)$ is a smooth function of t, and that $U'(t) \neq 0$. It follows that we can write

$$U(t) = t(c + L(t))$$

for some (negative) non-zero scalar c and smooth function L vanishing at $t = 0$.

Denote by $\beta = (\beta_1, \beta_2)$ the intersection of γ_t and the double point curve in the region $X < 0$.

Case 1.

Denote by $\nu = (\nu_1, \nu_2)$ the point on the double point curve with $\nu_1 = U(t)$. We have $\beta_2 < \nu_2$. From (8.7), if

$$\sigma(\beta) = (\sigma_1(\beta), \sigma_2(\beta)),$$

then

$$\sigma_2(\beta) = -\beta_2(1 + \psi(\beta_2))$$

for some smooth function ψ vanishing at the origin. For small β_2 (that is, small t), we then have that $\sigma_2(\beta) > \sigma_2(\nu)$.

Since $U(t) = \nu_1 = \zeta(\nu_2)$, we have

$$t(c + L(t)) = \zeta(\nu_2).$$

The inverse function Theorem and the expression for the 3-jet of ζ yields

$$\eta_2 = t^{1/3}\alpha(t)$$

where α is some function, smooth off the origin, continuous at the origin and with $\alpha(0) < 0$. It follows that

$$\sigma_2(\nu) = -t^{1/3}\alpha(t)(1 + \psi(t^{1/3}\alpha(t))),$$

and so $\sigma_2(\nu) > t$ for small t. Since in this case γ_t is strictly decreasing between the positive Y-axis and the double point curve, $t > \tau_2(\beta)$, hence $\sigma_2(\beta) > \tau_2(\beta)$.

Case 3.

Define $s(t)$ the Y-coordinate of the local maximum of γ_t at the its intersection with $\mathcal{C}_1$. Note $s(t) > \tau_2(\beta)$. Denote by $\nu = (\nu_1, \nu_2)$ the point on the double point curve with $\nu_1 = U(s(t))$. We can, by choice of the half-line h, guarantee that $\beta_2 < \nu_2$. So by the argument used in the previous case, $\sigma_2(\beta) > \sigma_2(q\nu)$. Also by the argument used in the previous case, $\sigma_2(\nu) > s(t)$, and hence $\sigma_2(\beta) > \tau_2(\beta)$.

Case 2.

We define $s(t)$ to be the Y-coordinate of the point where γ_t meets the discriminant and follow the argument used in case 3 to show $\sigma_2(\beta) > \tau_2(\beta)$.

Hence we have proved that, provided $p_3 \neq 0$ and $p_4 - q_{33}p_3 \neq 0$ (we also need $q_{30} \neq 0$ for the configurations in the domain), $\sigma(\beta) \neq \tau(\beta)$. This is satisfied for an open and dense set of parabolic cross-caps. □

8.2.2 Configurations of the characteristic curves

It is shown in [64] that there are two generically occurring configurations of the characteristic curves at an elliptic cross-cap. The BDE is topologically equivalent to either

$$(x^2 + y^4)dy^2 - 2xydxdy + (-x^2 + 2y^2 + y^3)dx^2 = 0$$

(case 1), or to

$$(x^2 + y^4)dy^2 - 2xydxdy + (-x^2 + 2y^2 + xy^2)dx^2 = 0$$

(case 2). See Figure 8.6.

Proposition 8.2.2 *The equation of the characteristic curves in the domain of a parametrisation of a parabolic cross-cap is topologically equivalent to*

$$x^2dy^2 - 2xydxdy + (2y^2 - x^3)dx^2 = 0.$$

The topological type is completely determined by the 3*-jet of the parametrisation of the surface. See Figure 8.7 (left). The configuration on the surface is as shown in Figure 8.7 (right).*

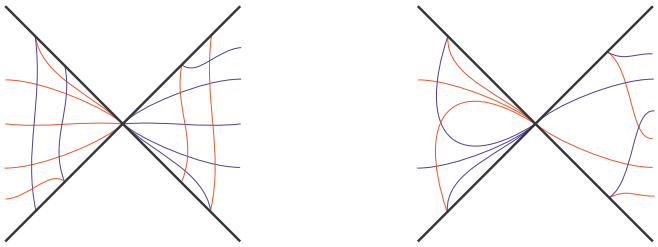

Figure 8.6: Configurations of the characteristic curves in the domain of an elliptic cross-cap, case 1 (left) and case 2 (right).

Proof: For a parabolic cross-cap parametrised as in (8.1.1), the coefficients of equation (8.4) are in the form

$$(a, b, c) = (x^2 + Q_1(x, y), -xy + Q_2(x, y), 2y^2 + Q_3(x, y)),$$

where Q_1, Q_2, Q_3 are smooth functions, with

$$\begin{aligned} j^3Q_1 &= 2q_{32}x^3 + 6(q_{33} - \mu p_3)yx^2 - 6p_3xy^2, \\ j^3Q_2 &= \tfrac{1}{2}q_{31}x^3 - yq_{32}x^2 + \frac{9}{2}(-q_{33} + \mu p_3)y^2x + 3p_3y^3, \\ j^3Q_3 &= -3q_{30}x^3 - 3q_{31}x^2y + 6(q_{33} - \mu p_3)y^3. \end{aligned}$$

If δ is the discriminant of equation (8.4) then

$$j^5\delta = x^2y^2 + 3q_{30}x^5 + 2q_{31}yx^4 - 2q_{32}y^2x^3 + 9(-q_{33} + \mu p_3)y^3x^2 + 6p_3xy^4.$$

This has a $Y^1_{1,2}$-singularity at the origin if $q_{30} \neq 0$. We apply Theorem 7.5.1 to establish the first assertion.

As noted, the intersection of the double point curve and the elliptic region is empty, so the characteristic curves can be mapped to the surface without problem. For the smooth part of the surface, the parametrisation is a diffeomorphism from the domain to the image. We therefore simply map each sector of the configuration in the parameter space to the surface in the appropriate way. □

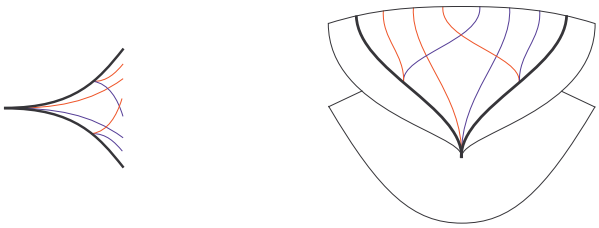

Figure 8.7: Configurations in the domain of the characteristic curves at a parabolic cross-cap (left), and their image on the surface (right).

Chapter 9

One-parameter families of cross-caps

It is natural to consider a one-parameter family of cross-caps in which the transition between the two generic (that is, the hyperbolic and elliptic) cross-caps is realised at a parabolic cross-cap. In this chapter we establish a parametrisation of this family and study the bifurcation of the asymptotic and characteristic curves in the family.

We adopt (following [33]) the notion of fibre topological equivalence, that is we shall consider two families of BDEs, ω_t and τ_t, equivalent if there exist neighbourhoods $U \subset \mathbb{R}^2$, $V \subset \mathbb{R}^r$ and $W \subset \mathbb{R}^3$, and a family of homeomorphisms h_t, for $t \in V$, all defined on U such that h_t is a topological equivalence between ω_t and $\tau_{\psi(t)}$, where ψ is a homeomorphism defined on W.

Although we are interested in the local configurations of the asymptotic and characteristic curves that appear in the bifurcation, we cannot rule out the possibility of semi-local phenomena emerging from the local singularity.

9.1 Generic families of cross-caps

Let $\Sigma_k \subset J^k(2,3)$ denote the set of k-jets of parametrisations of cross-caps where k is an integer greater than 2, that is, the set of k-jets germs of smooth maps $\mathbb{R}^2, 0 \to \mathbb{R}^3, 0$ that are $\mathcal{A}$-equivalent to (x, xy, y^2). This is a smooth variety of codimension 2 in $J^k(2,3)$.

To an r-parameter family of cross-caps

$$\mathbf{r}(x,y,t) = (\alpha_1, \alpha_2, \alpha_3)$$

depending smoothly on t, we associate the jet-extension map

$$\begin{aligned} \Phi : \mathbb{R}^2,(0,0)\times\mathbb{R}^r,0 &\to \Sigma_k \\ (x,y,t) &\mapsto j^k(\alpha_1,\alpha_2,\alpha_3)_t|_{(x,y)} \end{aligned}$$

where $j^k(\alpha_1,\alpha_2,\alpha_3)_t|_{(x,y)}$ is the k-jet of $(\alpha_1,\alpha_2,\alpha_3)$ at (x,y) with t fixed.

We say that a particular type of cross-cap is of codimension m if the conditions that define it yield a semi-algebraic set, R, of codimension m in Σ_k, that is invariant under the natural action of the $(k+1)$-jets of diffeomorphisms in (x,y), multiplication by non-zero functions in (x,y) and isometries of $\mathbb{R}^3$ in the target.

We say that an r-parameter family of cross-caps is *generic* if the map Φ is transverse to R. A necessary condition for genericity is $r \geq m$.

Proposition 9.1.1 *A generic $1-$parameter family of cross-caps, $\mathbf{r}_t$, can be written as*

$$(x, xy + p(x,y,t), y^2 + tx^2 + \mu(t)xy + q_t(x,y,t)), \tag{9.1}$$

where $\mu(0) = \mu_0$ and p_t, q are smooth functions with the following properties. For t fixed p and q have zero 2-jets at the origin and $p(x,y,0)$ has no dependency on x.

Proof: Suppose that the family is given by

$$\mathbf{r}_t = (g_1(x,y,t), g_2(x,y,t), g_3(x,y,t)),$$

with $\mathbf{r}_0$ as above. The cross-cap is $\mathcal{A}$-stable, so all members of the family $\mathbf{r}_t$ have a cross-cap singularity at some point near the origin.

At the cross-cap point the Jacobian of $\mathbf{r}_t$ has rank one. This occurs when

$$g_{1x}g_{2y} - g_{2x}g_{1y} = g_{1x}g_{3y} - g_{1x}g_{2y} = 0.$$

Define a map-germ

$$\begin{aligned} h : (\mathbb{R}^2\times\mathbb{R}),(0,0) &\to (\mathbb{R}^2,0) \\ (x,y,t) &\mapsto (g_{1x}g_{2y} - g_{2x}g_{1y}, g_{1x}g_{3y} - g_{3x}g_{1y}). \end{aligned}$$

We have

$$\left|Dh_{(x,y)}(0,0,0)\right| = \begin{vmatrix} 1 & \mu_0 \\ 0 & 1 \end{vmatrix} = 1,$$

so by the implicit function Theorem 1.1.6 $h^{-1}(0)$ is a smooth curve in the (x, y) plane parametrised by t, so by making a translation depending smoothly on t if necessary, we may assume that the cross-cap singularities of all members of the family $\mathbf{r}_t$ are at the origin.

Following the method of [74], for t fixed we may make a smooth change of coordinates in the source so that

$$g_1(x, y, t) = x,$$

and so that

$$j^1 g_2 = j^1 g_3 = 0$$

at the origin. We make a rotation in the target to set

$$j^2 g_2(x, y, t) = xy + c_1 x^2.$$

The cross-cap is at the origin so $c_1 = 0$ (we again use the implicit function Theorem 1.1.6 to show that these transformations depend smoothly on t).

We now have

$$j^2 g_3(x, y, t) = d_1 y^2 + d_2 xy + d_3 x^2$$

where d_i depend smoothly on t, and $d_1(0) \neq 0$. We scale coordinates in the source and dilate in the target to make $d_1 \equiv 1$, these changes being smooth since d_1 does not vanish.

The condition for a parabolic cross-cap is $d_3 = 0$, which is the case at $t = 0$. The jet-extension map is transverse to the subset of Σ_2 defining parabolic cross-caps provided $d_3'(0) \neq 0$. We take this to be the case, so we can make a smooth change of parameter t to give the parametrisation in the required form. □

In a generic family the parabolic cross-cap is the transition between a hyperbolic and elliptic cross-cap. It is shown in [50] that for each fixed t the parabolic set is a section of a Whitney umbrella. Thus the bifurcation of the parabolic set is as shown in Figure 9.1.

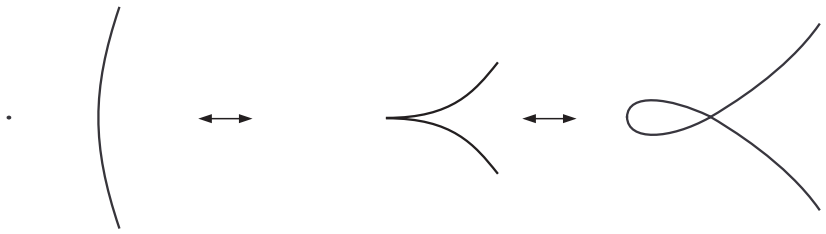

Figure 9.1: The bifurcation in the domain of the parabolic set at a parabolic cross-cap.

9.2 Bifurcations in the asymptotic curves

We require some preliminary results.

Proposition 9.2.1 *The cross-cap in* (9.1) *changes from hyperbolic ($t < 0$) to elliptic ($t > 0$) through a parabolic cross-cap $t = 0$. For the elliptic cross-cap, the asymptotic BDE is equivalent to*

$$xdy^2 + 2(-x + xy)dxdy + xdx^2 = 0.$$

The other configuration of the asymptotic curves on an elliptic cross-cap (see Figure 8.1) does not appear in the bifurcation.

Proof: We make affine changes of coordinates in the target in order to simplify the parametrisation in Proposition 9.1.1 to

$$\mathbf{r}_t = (x, xy + p(x, y, t), y^2 + tx^2 + q(x, y, t)). \tag{9.2}$$

We calculate the coefficients, L_1, M_1, N_1, of the asymptotic BDE on a cross-cap. The parabolic set is given by the discriminant $\delta = M_1^2 - L_1N_1$. We find that

$$j^2\delta = 4y^2 - 4tx^2$$

and the first assertion follows immediately.

It is shown in [64] that if the asymptotic BDE on an elliptic cross-cap is written as

$$(x + H_1(x, y))dy^2 + 2(-y + H_2)dxdy + (x + H_3(x, y))dx^2 = 0,$$

where H_i, $i = 1, 2, 3$, are smooth functions with zero 1-jets at the origin, and one sets

$$A(x, y) = j^2 H_1, B(x, y) = j^2 H_2, C(x, y) = j^2 H_3,$$

then the two generically occurring configurations of the asymptotic curves in the domain of a parametrisation of an elliptic cross-cap are distinguished by the sign of $\Lambda_1\Lambda_2$ where

$$\Lambda_1 = -\frac{1}{2}(C(1,1) + 4B(1,1) + 3A(1,1)),$$
$$\Lambda_2 = \frac{1}{2}(C(1,-1) + 4B(1,-1) + 3A(1,-1)).$$

The equation of the asymptotic curves in the domain of an elliptic cross-cap is topologically equivalent to

$$xdy^2 + 2(-y + x^2)dxdy + xdx^2 = 0$$

when $\Lambda_1\Lambda_2 > 0$, and to

$$xdy^2 + 2(-x + xy)dxdy + xdx^2 = 0$$

when $\Lambda_1\Lambda_2 < 0$ ([64]).

For t fixed we write

$$j^3 p_t = p_{30}x^3 + p_{31}x^2y + p_{32}xy^2 + p_{33}y^3,$$
$$j^3 q_t = q_{30}x^3 + q_{31}x^2y + q_{32}xy^2 + q_{33}y^3,$$

where the coefficients depend smoothly on t. When $t = 0$ we have the parabolic cross-cap parametrised by (8.1.1), so $p_{30} = p_{31} = p_{32} = 0$ at $t = 0$. We also have the genericity condition $q_{30} \neq 0$ at $t = 0$.

The 1-jet of the asymptotic BDE, when using the parametrisation (9.2) is

$$(x, -y, tx).$$

If we write the BDE as

$$(x + H_1(x, y, t))dy^2 + 2(-y + H_2(x, y, t))dxdy + (tx + H_3(x, y, t))dx^2 = 0$$

then we have

$$j^2 M_1 = (p_{31} + q_{32})x^2 + 3q_{33}xy - 3p_{33}y^2,$$
$$j^2 M_2 = \frac{1}{2}q_{31}x^2 - 2p_{31}xy - (\frac{3}{2}q_{33} + 2p_{32})y^2,$$
$$j^2 M_3 = (tp_{31} + 3q_{30})x^2 + (-6p_{30} + 2tp_{32} + q_{31})xy + (-2p_{31} + 3tp_{33})y^2.$$

We make the change of variables $(x, y) \mapsto (x/\sqrt{t}, y)$ in the source and multiply the equation by $\sqrt{t}$. We obtain a new BDE

$$(x + K_1(x, y, t))dy^2 + 2(-y + K_2(x, y, t))dxdy + (x + K_3(x, y, t))dx^2 = 0 \quad (9.3)$$

where

$$\begin{aligned} K_1(x, y, t) &= \sqrt{t}H_1(\frac{x}{\sqrt{t}}, y, t), \\ K_2(x, y, t) &= H_2(\frac{x}{\sqrt{t}}, y, t), \\ K_3(x, y, t) &= \frac{1}{\sqrt{t}}H_3(\frac{x}{\sqrt{t}}, y, t). \end{aligned}$$

We set

$$\begin{aligned} A(x, y, t) = j^2K_1 = \quad & \frac{(p_{31} + q_{32})}{\sqrt{t}}x^2 + 3q_{33}xy - 3\sqrt{t}p_{33}y^2 \\ B(x, y, t) = j^2K_2 = \quad & \frac{q_{31}}{2t}x^2 - \frac{2p_{31}}{\sqrt{t}}xy - \frac{3(q_{33} + 2p_{32})}{2}y^2 \\ C(x, y, t) = j^2K_3 = \quad & \frac{(tp_{31} + 3q_{30})}{t\sqrt{t}}x^2 + \frac{(-6p_{30} + 2tp_{32} + q_{31})}{t}xy \\ & + \frac{(-2p_{31} + 3tp_{33})}{\sqrt{t}}y^2. \end{aligned}$$

Then the configuration depends on the sign of $\Lambda_1(t)\Lambda_2(t)$ where

$$\begin{aligned} \Lambda_1(t) &= -\frac{1}{2}(C(1, 1, t) + 4B(1, 1, t) + 3A(1, 1, t)), \\ \Lambda_2(t) &= \frac{1}{2}(C(1, -1, t) + 4B(1, -1, t) + 3A(1, -1, t)). \end{aligned}$$

We have

$$\begin{aligned} \Lambda_1(t) &= \frac{-3(q_{30} + (q_{32} - 2p_{31})t - 2p_{33}t^2 + ((q_{31} - 2p_{30}) + (q_{33} - 2p_{32})t)\sqrt{t})}{2t\sqrt{t}} \\ \Lambda_2(t) &= \frac{3(q_{30} + (q_{32} - 2p_{31})t - 2p_{33}t^2 - ((q_{31} - 2p_{30}) + (q_{33} - 2p_{32})t)\sqrt{t})}{2t\sqrt{t}} \end{aligned}$$

Since $t > 0$ the sign of $\Lambda_1(t)\Lambda_2(t)$ is the same as that of

$$\frac{4}{9}t^{\frac{3}{2}}\Lambda_1(t)\Lambda_2(t) = -((q_{30} + (q_{32} - 2p_{31})t - 2p_{33}t^2)^2 - t((q_{31} - 2p_{30}) + (q_{33} - 2p_{32})t)^2).$$

Note that

$$\lim_{t\to 0}(\frac{4}{9}t^{\frac{3}{2}}\Lambda_1(t)\Lambda_2(t)) = -q_{30}^2(0) < 0.$$

Thus for small t, $\Lambda_1(t)\Lambda_2(t) < 0$, and by Theorem 3.1 of [64] the BDE is topologically equivalent to

$$xdy^2 + 2(-y + xy)dxdy + xdx^2 = 0.$$

□

Proposition 9.2.2 *The separatrix transverse to the limiting tangent to the discriminant does not bifurcate in the family.*

Proof: We write the BDE in the form

$$(x + H_1(x, y, t))dy^2 + 2(-y + H_2(x, y, t))dxdy + (tx + H_3(x, y, t))dx^2 = 0,$$

and take the affine chart $q = dx/dy$ for $\mathbb{R}P^1$. The surfaces M_t associated to the BDE are then given by $G(x, y, q) = 0$, where

$$G(x, y, q) = (x + H_1(x, y, t)) + 2(-y + H_2(x, y, t))q + (tx + H_3(x, y, t))q^2.$$

This surface is smooth on this chart for all values of t. We look for roots of the cubic

$$\phi(q) = (G_y + qG_x)(0, 0, q).$$

One root lies at $q = 0$. The lifted field has a saddle there, with one separatrix projecting to a curve transverse to the discriminant of the BDE. □

In [25, 74] the family of height functions (recall Definition 1.2.4) on a cross-cap is considered. It is shown that the height function in no direction at a parabolic cross-cap has worse than an A_2-singularity, provided the discriminant has a genuine A_2-singularity. Thus no cusps of Gauss appear in the bifurcation of a parabolic cross-cap.

This observation excludes the possibility of semi-local phenomena occurring in the bifurcation. Should any integral curve meet the discriminant at two distinct points, the foliation would necessarily have a singularity between them. As the discriminant is smooth away from the cross-cap, the singularity would be a cusp of Gauss.

We are now in a position to establish the following result.

Theorem 9.2.1 *The asymptotic BDE on a generic one-parameter family of surfaces parametrised by* $\mathbf{r}_t$*, with* $\mathbf{r}_0$ *having a parabolic cross-cap at the origin is fibre topologically equivalent to*

$$xdy^2 + 2(-y + txy)dxdy + (tx + (1 - t^2)x^2)dx^2 = 0.$$

The topological type is completely determined by the 3*-jet of the parametrisation of the surface. See Figure 9.2 (top pictures). The curves map to the surface as shown in Figure 9.2 (bottom pictures).*

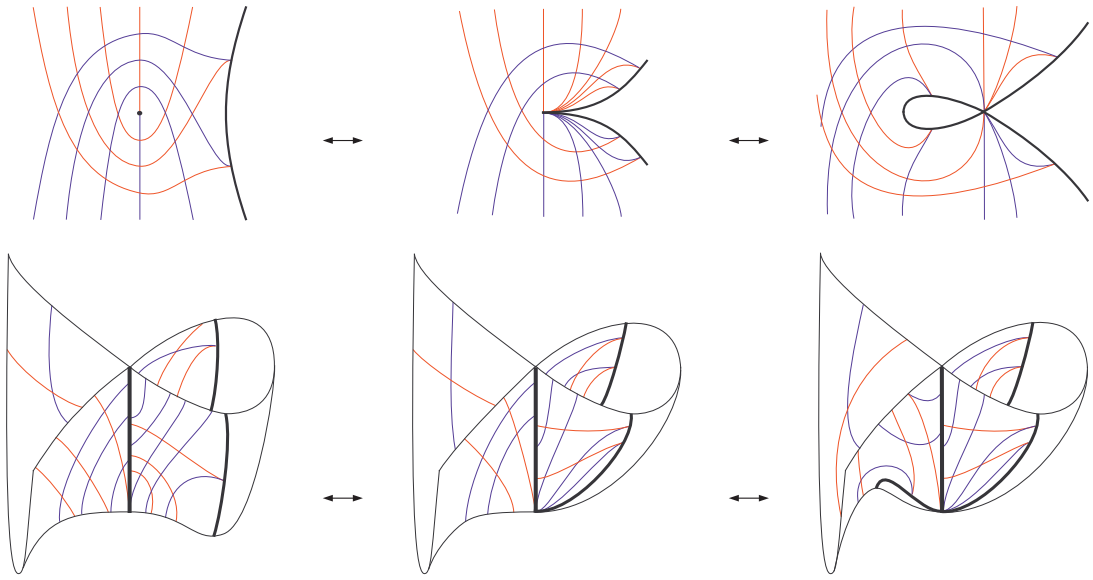

Figure 9.2: The bifurcations of the asymptotic curves at a parabolic cross-cap in the domain (top pictures) and on the surface (bottom pictures): $t < 0$ (left), $t = 0$ (centre) and $t > 0$ (right).

Proof: We must show that the configuration of the integral curves is constant in $t > 0$ and constant in $t < 0$ (the singularity of the surface that occurs when $t = 0$ is at infinity). This is done by choosing an appropriate neighbourhood of the discriminant and sliding along integral curves to construct the required homeomorphism (see [13, 63, 65, 66]). For fixed $t < 0$, the equation given in the statement is topologically equivalent to the normal form of the asymptotic BDE on a hyperbolic cross-cap established in [74]. For fixed $t > 0$ the equation given in the statement is topologically equivalent to the normal form of the asymptotic BDE on an elliptic cross-cap of the required type as given in Proposition 9.2.1. If the genericity conditions established in Section 8.2.1 that allow us to map the curves to the surface are satisfied when $t = 0$, they will, by continuity, be satisfied for t close to zero, so we can map the curves to the surface as shown. □

9.3 Bifurcations in the characteristic curves

We take the parametrisation as in (9.1). When $t < 0$, the cross-cap is hyperbolic and so no characteristic curves exist in a neighbourhood of the cross-cap.

Proposition 9.3.1 *In the family* $\mathbf{r}_t$ (9.1) *the characteristic BDE at the elliptic cross-cap (when* $t > 0$*) is equivalent to*

$$(x^2 + y^4)dy^2 - 2xydxdy + (-x^2 + 2y^2 + xy^2)dx^2 = 0.$$

The other type of elliptic cross-cap in Figure 8.6 does not appear in the bifurcation.

Proof: The proof is similar to that of Proposition 9.2.1 and is omitted. □

It is noted in [64] that the singularity of the BDE of the principal directions at a hyperbolic/parabolic/elliptic cross-cap is locally an isolated point, so there is no sequence of umbilic points converging to the cross-cap point, and no such points appear in the bifurcation. Since no cusps of Gauss appear in the bifurcation either, the characteristic curves form a family of cusps at the smooth part of the discriminant.

Theorem 9.3.1 *The characteristic BDE on a generic 1-parameter family of cross-caps is fibre topologically equivalent to*

$$(x^2 + y^4)dy^2 - 2xydxdy + (-tx^2 + 2y^2 + txy^2 - x^3)dx^2 = 0.$$

The topological type is completely determined by the 3*-jet of the parametrisation of the surface. The bifurcation is illustrated in Figure 9.3 (upper pictures).*

Proof: The proof is similar to that of Theorem 9.2.1. The characteristic curves can be mapped onto the surface without difficulty as the intersection of the elliptic region and the double point curve is empty. □

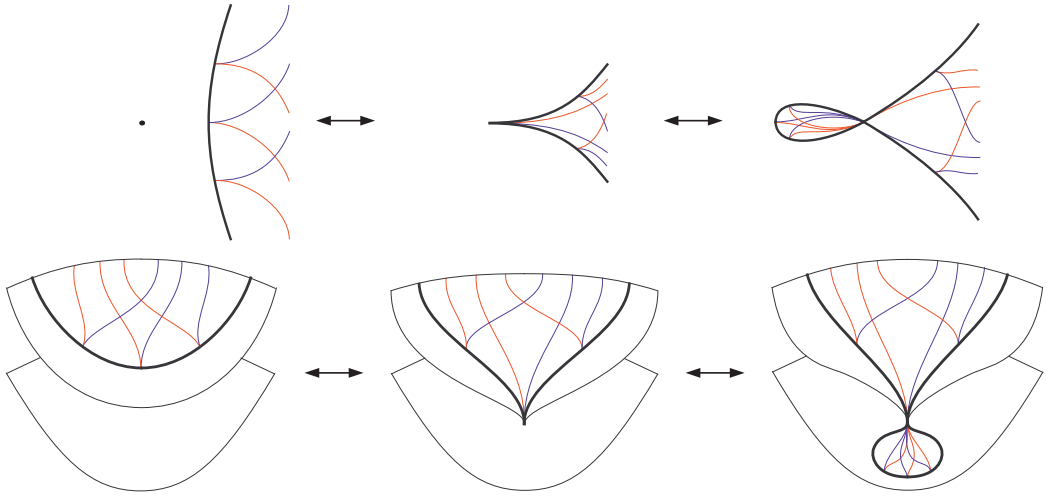

Figure 9.3: The bifurcation of the characteristic curves at a parabolic cross-cap in the domain (upper pictures) and on the surface (lower pictures): $t < 0$ (left), $t = 0$ (centre) and $t > 0$ (right).

Ideas for further work

The largest open problem in this area remains that of defining the characteristic curves via contact with a model submanifold. This would allow one, for example, to explain the significance of the characteristic locus of inflections, the characteristic bi-inflections and the special curves connected to the torsion of the characteristic curves that were defined in chapter 6.

On smooth surfaces, the characteristic curves on elliptic discs need further investigation. We saw in chapter 3 that the number and type of cusps of Gauss on the boundary of an elliptic disc is connected to the number of umbilic points within the disc. It may also be possible to adapt Uribe-Vargas' results ([71, 72]) concerning global properties of the flecnodal curve to the characteristic inflection curve. Of course, the proper context in which to study elliptic discs is within 1-parameter families of smooth surfaces.

West ([74]) considered the ridge curves on cross-cap, and also showed that there is no conodal curve in the neighbourhood of a cross-cap point. Other special curves, including the flecnodal curve, characteristic inflection curve, zero-torsion curves and sub-parabolic lines, should also be studied on singular surfaces. In the case of the flecnodal curve one may apply our results from chapter 7 on the configuration of the inflection sets of cusp BDEs. The families of curve congruences, $\mathcal{C}_\alpha$ and $\mathcal{R}_\alpha$, have also not yet been considered on cross-caps.

In chapter 4 we exhibited a natural one-to-one correspondance between BDEs at a point on a surface S and linear involutions of the projective line. The latter are the induced action on $\mathbb{R}P^1$ of real 2×2 matrices with vanishing trace. The set of such matrices is the Lie Algebra associated to the group $SL(2, \mathbb{R})$. Furthermore, the Jacobian of two any BDEs (that is, the polar of the line that joins them) corre-

sponds to the (induced action on $\mathbb{R}P^1$) of the Lie bracket (commutator) of the two corresponding matrices. In other words, the set of all binary quadratic forms is the projectivation of a real Lie Algebra. This gives rise naturally to several questions. Can the results of chapter 4 be reformulated in terms of Lie algebras? Is there a group of forms that corresponds to $SL(2,\mathbb{R})$? Can correspondances be established between other Lie algebras and forms on the tangent bundles to surfaces or higher dimensional manifolds?

Our work in chapter 4 on involutions on the real projective line showed that given two such involutions σ_1, σ_2, the composite maps $\sigma_1 \circ \sigma_2 \circ \sigma_1$ and $\sigma_2 \circ \sigma_1 \circ \sigma_2$ are also involutions. The self-polar triple comprising the asymptotic, principal and characteristic BDEs is constructed using two linear involutions, which we labelled C and O. In chapter 5 we considered quadratic forms constructed using the involution $C \circ O \circ C$, namely the third fundamental form and the BDE of the MOSI curves. The work in chapter 4 suggests that we should also consider BDEs constructed using the involution $O \circ C \circ O$. Preliminary calculations indicate that, following our methods one obtains a self-polar triple of BDEs comprising the principal BDE and two BDEs, analogous to the asymptotic and characteristic BDEs that have the parabolic set as their common discriminant and folded singularities at the point of intersection of the parabolic set and the sub-parabolic lines.

There is further work to be carried out concerning the MOSI curves defined in chapter 5, and the related one-parameter families of BDEs. In particular, the evolution of the configuration of the integral curves at the discriminants in these families should be studied, as it is for the families $\mathcal{C}_\alpha$ and $\mathcal{R}_\alpha$ in [14]. It is also clear, from the results proved here, that these BDEs have intrinsic meaning in terms of the geometry of the surface that has not yet been identified.

The asymptotic and characteristic curves and the lines of curvature, and hence all related geometry, are derived from the metric and the Weingarten map (or equivalently the first and second fundamental forms). The Weingarten map is a self adjoint linear operator. In [67] the properties of an arbitrary surface endowed with an arbitrary self-adjoint operator and a Riemmannian metric. These ideas have also been extended to surfaces in Lorentzian space, that is, a surface with a pseudo-

Riemmannian metric. It would be of interest to carry out similar work with the new BDEs and families of BDEs that were defined in chapter 5, since those BDEs are also derived purely from the metric and the Weingarten map.

Our work on cusp BDEs in chapter 7 is, to a certain extent, incomplete. Unstable singular BDEs are only properly understood by considering their bifurcations in generic families. Furthermore, there are BDEs that have discriminants with other types of singularities that have the same codimension as the cusp BDEs we studied, that should be considered when these generic families are studied.

Bibliography

[1] V. I. Arnold (1983), **Geometrical methods in the theory of differential equations**, Springer.

[2] V. I. Arnold (Ed.) (1994), **Dynamical systems 5: Bifurcation theory and catastrophe theory. Encyclopaedia of Mathematical Sciences**, Springer-Verlag.

[3] V. I. Arnold, S. M. Gusein-Zade, A. N. Varchenko (1985) **Singularities of differentiable maps Vol I.**, Birkhauser.

[4] D. K. Arrowsmith and C. M. Place (1990), **An Introduction to Dynamical Systems**, CUP.

[5] T. Banchoff, T. Gaffney & C. McCrory (1982), **Cusps of Gauss mappings: Research Notes in Mathematics 55**, Pitman (Advanced Publishing Program).

[6] D. Barden and C. Thomas (2002), **An Introduction to Differential Manifolds**, Imperial College Press.

[7] Th. Brocker, trans. L. Lander (1975), **Differentiable Germs and Catastrophes**, CUP.

[8] J. W. Bruce (1984), *A note on first order differential equations of degree greater than one and wavefront evolution*, Bull. London Math. Soc. **16**, pp 139-144.

[9] J. W. Bruce (1984), *Projections and Reflections of Generic Surfaces in* $\mathbb{R}^3$, Math. Scand. **54**, pp 262-278.

[10] J. W. Bruce (1989), *Geometry of singular sets*, Math. Proc. Camb. Phil. Soc. **106**, pp 495-509.

[11] J. W. Bruce (2003), *On families of symmetric matrices*, Moscow Math. J. **3**, pp 335-360.

[12] J. W. Bruce and D. Fidal (1989), *On binary differential equations and umbilics*, Proc. Roy. Soc. Edinburgh Sect. A **111**, pp 147-168.

[13] J. W. Bruce, G. J. Fletcher and F. Tari (2000), *Bifurcations of implicit differential equations*, Proc. Roy. Soc. Edinburgh Sect. A **130**, pp 485-506.

[14] J. W. Bruce, G. J. Fletcher and F. Tari (2004), *Zero curves of families of curve congruences*, **Real and complex singularities, Contemp. Math. 354**, pp 1-18, Amer. Math. Soc..

[15] J. W. Bruce and P. J. Giblin (1984), **Curves and Singularities**, CUP.

[16] J. W. Bruce, P. J. Giblin and F. Tari (1995), *Families of surfaces: height functions, Gauss maps and duals* Real and Complex Singularities, Pitman Research Notes in Mathematics 333 pp 148-178, Longman.

[17] J. W. Bruce, P. J. Giblin and F. Tari (1998), *Families of surfaces: height functions and projections to planes*, Math. Scan. **82**, pp 165-185.

[18] J. W. Bruce, P. J. Giblin and F. Tari (1999), *Families of surfaces: focal sets, ridges and umbilics*, Math. Proc. Camb. Phil. Soc. **125**, pp 243-268.

[19] J. W. Bruce and M. C. Romero-Fuster (1991), *Duality and projections of curves and surfaces in 3-space*, Quart. J. Math. Oxford Ser. (2), **42**, pp 433-441.

[20] J. W. Bruce and F. Tari (1995), *On binary differential equations*, Nonlinearity **8**, pp 255-271.

[21] J. W. Bruce and F. Tari (1997), *Generic one-parameter families of binary differential equations of Morse type*, Discrete Contin. Dynam. Systems **3**, pp 79-90.

[22] J. W. Bruce and F. Tari (1998), *On the multiplicity of implicit differential equations*, J. Differential Equations **148**, pp 122-147.

[23] J. W. Bruce and F. Tari (2000), *Duality and implicit differential equations*, Nonlinearity **13**, pp 791-811.

[24] J. W. Bruce and F. Tari (2004), *Dupin indicatrices and families of curve congruences*, Trans. Amer. Math. Soc. **357**, pp 267-285.

[25] J. W. Bruce and J. M. West (1998), *Functions on a cross-cap*, Math. Proc. Cambridge Philos. Soc. **123**, pp 19-39.

[26] M. Cibrario (1932), *Sulla reduzione a forma delle equatione linearialle derviate parziale di secondo ordine di tipo misto*, Accamdemia di Scienze e Lettrere, Instituto Lomardo Redicconti **65**, pp 889-906.

[27] L. Dara (1975), *Singularites generiques des equations differentielles multi-forms,* Bol. Soc. Dras. Mat., **No. 6**, pp 95-129.

[28] G. Darboux (1896), *Sur la forme des lignes de courbure dans las voisinage d'un ombilic, Note 07*, **Lecons sur la Theorie des Surfaces, vol IV**, Gauthier Villars.

[29] M. P. do Carmo (1976), **Differential Geometry of Curves and Surfaces**, Prentice Hall.

[30] A. A. Davydov (1985), *Normal forms of differential equations unresolved with respect to derivatives in a neighbourhood of its singular point*, Math. Functional Anal. Appl. **19**, pp 1-10.

[31] A. A. Davydov (1994), **Qualitative Control Theory: Translations of Mathematical Monographs vol. 142**, Amer. Math. Soc..

[32] A. A. du Plessis and L. Wilson (1985), *On right-equivalence*, Math. Z. **190**, pp 163-205.

[33] F. Dumortier (1993), *Techniques in the theory of local bifurcations: blow-Up, normal forms, nilpotent bifurcations, singular perturbations*, **Bifurcations**

and periodic orbits of direction fields, pp 19-73, NATO Adv. Sci. Inst. Ser. C Math. Phys. Sci., 408, Kluwer Acad. Publ.

[34] L. P. Eisenhart (1909), **A treatise on the differential geometry of curves and surfaces**, Ginn and Company.

[35] L. P. Eisenhart (1940), **An Introduction to Differential Geometry**, Princeton University Press.

[36] G. J. Fletcher (1996), *Geometrical problems in computer vision*, PhD. thesis, University of Liverpool.

[37] J. Gallier (2000), **Geometrical Methods and Applications, TAM Vol. 38**, Springer-Verlag.

[38] R. Garcia, J. Sotomayor and C. Guitierrez (2000), *Lines of principal curvature around umbilics and Whitney umbrellas*, Tohoku Math. J. (2) **52**, pp 163-172.

[39] R. Garcia and J. Sotomayor (2001), *Structurally stable confgurations of lines of mean curvature and umbilic points on surfaces immersed in* $\mathbb{R}^3$, Publ. Mathematiques **45**, pp 431-466.

[40] R. Garcia and J. Sotomayor (2002), *Geometric mean curvature lines on surfaces immersed in* $\mathbb{R}^3$, Annales de la faculte des sciences de Toulouse Ser. 6 **11** no. 3, pp 377-401.

[41] R. Garcia and J. Sotomayor (2003), *Harmonic mean curvature lines on surfaces immersed in* $\mathbb{R}^3$,Bull. Braz. Math. Soc. (N.S.) **34**, pp 303-331.

[42] R. Garcia and J. Sotomayor (2003), *Lines of mean curvature on surfaces immersed in* $\mathbb{R}^3$, Qual. Theory Dynam. Systems. **4**, pp 263-310.

[43] C. G. Gibson (1979), **Singular points of smooth mappings: Research Notes in Mathematics 25**, Pitman.

[44] V. Guíñez (1994), *Locally stable singularities for positive quadratic differential forms*, J. Differential Equations **110**, pp 1-37.

[45] P. Hartman and A. Wintner (1953), *On the third fundamental form of a surface*, Amer. J. Math. **75** pp 298-334.

[46] S. Izumiya (2007), *Singularity theory of smooth mappings and its applications: A survey for non-specialists*, Real and complex singularities: Proceedings of the Australian-Japanese Workshop, pp 124-175.

[47] J. Martinet, trans. Carl P. Simon (1982), **Singularities of Smooth Functions and Maps: London Math. Soc. Lecture Note Serties 58**, CUP.

[48] J. A. Montaldi (1986), **On contact between submanifolds**, Michigan Math. J. **33**, pp 195-199.

[49] J. A. Montaldi (1986), **Surfaces in 3-space and their contact with circles**, J. Differential Geometry **23**, pp 109-126.

[50] J. J. Nuño-Ballesteros and F. Tari (2007), *Surfaces in* $\mathbb{R}^4$ *and their projections to* 3*-spaces*, Proc. Roy. Soc. Edinburgh Sect. A **137**, pp 1313-1328.

[51] R. Occhipinti (1914), *Sur un systeme de lignes d'une surface*, L'enseignement Mathematiques **16**, pp 38-44.

[52] R. D. S. Oliveira and F. Tari (2002), *On pairs of regular foliations in the plane*, Hokkaido Math. J. **31** 3, pp 523-537.

[53] J. M. Oliver (2009) *Binary differential equations having a cusp singularity*, `http://maths.dur.ac.uk/~dma3jmo`, Preprint.

[54] J. M. Oliver (2009) *On the characteristic curves on a smooth surface*, `http://maths.dur.ac.uk/~dma3jmo`, Preprint.

[55] J. M. Oliver (2010) *On pairs of geometric foliations of a parabolic cross-cap*, to appear in Qual. Theory Dynam. Systems **8**.

[56] J. M. Oliver (2010) *On linear involutions on the real projective line*, `http://maths.dur.ac.uk/~dma3jmo`, Preprint.

[57] B. O'Neill (1997), **Elementary Differential Geometry (Second Edition)**, Academic Press.

[58] O. A. Platanova (1981), *Singularities of the relative position of a surface and a line*, Uspehhi Mt. Nauk **36**, pp 221-222.

[59] I. R. Porteous (1994), **Geometric Differentiation**, CUP.

[60] L. Raffy (1902), *Sur le reseau diagonal conjugue*, Bull. Soc. Math. France **30**, pp 226-233.

[61] L. P. Eisenhart (1927), **A treatise in analytic geometry of three dimensions**, Chelsea Publications.

[62] J. Sotomayor and C. Gutierrez (1982), *Structurally stable configurations of lines of principal curvature*, Bifuraction, ergodic theory and applications (Dijon, 1981) pp 195-215, Asterisque, 98-99, Soc. Math. France, Paris.

[63] F. Tari (2005), *Two parameter families of implicit differential equations*, Discrete Contin. Dynam. Systems **13**, pp 139-162.

[64] F. Tari (2007), *Pairs of geometric foliations on a cross-cap*, Tohoku Math. J. **59**, pp 233-258.

[65] F. Tari (2007), *Geometric properties of the integral curves of an implicit differential equation*, Discrete Contin. Dynam. Systems **17**, pp 349-364.

[66] F. Tari (2008), *Two parameter families of binary differential equations*, Discrete Contin. Dynam. Systems **22**, pp 759-789.

[67] F. Tari (2009), *Self-adjoint operators on surfaces in* $\mathbb{R}^n$, Differential Geometry and its Applications, **27**, pp 296-306.

[68] F.Tari (2009), Pairs of foliations on surfaces, http://maths.dur.ac.uk/ dma0ft, Preprint.

[69] R. Thom (1971), *Sur les équation différentielles multiformes et leurs intégrals singulières*, Bol. Soc. Brasil. Mat. **3** pp 1-11.

[70] E. R. Van Kampen (1939), *A Remark on Asymptotic Curves*, Amer. J. Math., pp 992-994.

[71] R. Uribe-Vargas (2006), *A projective invariant for swallowtails and godrons and global theorems on the flecnodal curve*, Mosc. Math. J. **6**, pp 731-768.

[72] R. Uribe-Vargas (2006), *Surface evolution, implicit differential equations and pairs of Legendrian fibrations*, Preprint, www.math.jussieu.fr/ uribe.

[73] C. T. C. Wall (1978), *Geometric properties of generic differentiable manifolds*, **Geometry and Topology: Lecture Notes in Math. vol 597** pp 707-774, Springer-Verlag.

[74] J. West (1995), *The differential geometry of the cross-cap*, Ph.D Thesis, University of Liverpool.

[75] H. Whitney (1944), *The singularities of a smooth $n-$manifold in $(2n-1)$-space*, The Annals of Mathematics **45**, pp 247-293.